Influence of nitrate availability and environmental stimuli on seed germination and stomatal behaviour

Joanna Landymore

A thesis submitted in full fulfilment of the requirements for the degree of Doctor of Philosophy

The University of Sheffield

Faculty of Science

School of Biosciences

February 2024

Acknowledgements

Firstly, I would like to thank my supervisors Professor Julie Gray and Dr Angela Hodge for giving me the opportunity to undertake my PhD. I would also like to thank Dr Stuart Casson, who along with Professor Julie Gray has provided support and guidance.

My journey has faced a number of challenges, from unforeseen and ongoing health issues, resulting in surgeries and time away, to an unexpected Covid-19 pandemic. Both Professor Julie Gray and Dr Stuart Casson have been supportive and enabled me to continue.

I would like to thank my scholarship funding body, the University of Sheffield who enabled me to pursue my dream.

I would like to thank Professor Mike Holdsworth for providing Arabidopsis seeds used in Chapters 3 and 4. I would also like to thank my collaborators Jess Dunn, Luke Fountain, and particularly Hanna Horak, who's support, friendship and source of knowledge has been invaluable. Hanna was involved in work in Chapter 4 and helped with compiling the initial list in Chapter 5, as well as helping me when I went to Estonia to perform whole plant gas exchange experiments (for which I obtained a grant to perform these experiments). I would also like to thank Robert Caine and Jen Sloane for information on the pilot experiment on rice in Chapter 4.

I would also like to thank members of C33 all for their support, motivational chats and guidance. All of which have kept me sane.

I would like to thank my friends and family for all their support, cups of coffee, walks and chats keeping me sane.

Lastly, I would like to thank my parents for their constant support and encouragement throughout my life and PhD. I would also like to thank Alex for his support and encouragement throughout.

COVID-19 Impact statement

This thesis reports research conducted during the Covid-19 pandemic and was significantly affected by the mandatory lockdown regulations imposed by the UK Government. Laboratories remained closed for around four months, with limited access to research facilities persisting for an extended period of time afterwards. The closure and restricted access led to the loss of numerous experiments, particularly those that involved plant growth detailed in chapters 3, 4 and 5. This resulted in: a) reduced available research funding, attributed to the lost experiments and associated resources, b) imposed significant time constraints on the subsequent research due to reduced laboratory availability, and c) reduced ability to undertake research due to both time constraints and reduced funding.

Abstract

An expanding global population is putting pressure on the world's climate and global food supply chain, with governments simultaneously restricting the use of nitrogen fertilisers. The implications for food security has never been more urgent. Plants need to adapt to rapidly changing environments and understanding how plants respond including levels of nitrogen and abiotic stresses is critical.

This thesis aimed to identify the effects of reduced nitrate assimilation on plants' health and growth, by utilising mutants deficient in nitrate reductase and observing their responses to abiotic stresses. Initial investigations suggested gene redundancy for the nitrate reductases *NIA1* and *NIA2*, indicating their involvement in different stress responses. Regulation of their transcription factors also appears to play a role in plant health and growth.

Secondly, how nitrate availability affects responses to abiotic stresses was explored. This was achieved by utilising dynamic thermal imaging, salt and a range of nitrate reductase and stomatal mutants. Studies showed that ABA induced stomatal closure is influenced by endogenous nitrate and remains unaffected by exogenous nitrate application.

Thirdly, identify novel stomatal regulators, focusing on post-transcriptional modifications, specifically kinases and phosphatases was explored. A literature review was undertaken to identify potential candidates; 10 were chosen for further study. Phenotypic analysis was undertaken on two of the identified candidates, using a range of techniques. The study showed that, potential stomatal regulators PSKR2 and GCK1 were identified, but further analysis is required.

Overall, whilst initial data indicate the existence of complex interactions between multiple pathways, signalling and developmental, determining the exact causes requires further investigation. This research enhances understanding of plant responses to environmental stresses, has developed and presented novel methods to study stress responses in whole crop plants, and provides new knowledge that can be used to enhance crop resilience and help ensure global food security.

List of abbreviations

%	Percent
°C	Degrees Celsius
µl	Microlitre
µM	Micromolar
μm^2	Micrometre squared
µmol	Micromole
α	Alpha
ABA	Abscisic acid
ABI1	Abscisic acid insensitive 1
ABI2	Abscisic acid insensitive 2
ABI5	Abscisic acid insensitive 5
ABRC	Arabidopsis Biological Resource Center
AGC	Protein kinase A, G and C
AKT1	Arabssinwardly-rectifying K^+ channel 1
AKT2	Arabssinwardly-rectifying K^+ channel 2
ANOVA	Analysis of variance
Arg	Arginine
ATE	Arginyltransferase
ATP	Adenosine triphosphate
ATPase	Enzymes that catalyse the decomposition of ATP
ATS	*Arabidopsis thaliana* salt
BAC	Bacterial artificial chromosome
BHP	BLUE LIGHT-DEPENDENT H^+ATPASE PHOSPHORYLATION
BLUS1	BLUE LIGHT SIGNALLING 1
bp	Base pair
C	Cysteine
$Ca(NO_3)_2$	Calcium nitrate
CA1	β-carbonic anhydrase 1
Ca^{2+}	Calcium ion
CA4	β-carbonic anhydrase 2
$CaCl_2$	Calcium chloride
CAMK	Calmodulin/Calcium regulated Kinase
CAS9	CRISPR associated immunological defence protein
CBC1	Convergence of blue light and CO_2 1
CBC2	Convergence of blue light and CO_2 2
CDK	Cyclin-dependent kinase
Ci	Concentration of intercellular CO_2
CK1	Casein/Cell Kinase 1
cm	Centimetre
CMGC	CMGC kinases (CDKs, MAPKs, GSKs and CLKs)
CO_2	Carbon dioxide
$CoCl_2$	Cobalt(II) chloride
Col-0	*Arabidopsis thaliana* ecotype
comp	Complement line

C^{ox}	Oxidase C
CPK	Calcium dependent protein kinase
CRISPR	Clustered regularly interspaced short palindromic repeats
$CuSO_4$	Copper sulphate
dATP	Deoxyadenosine triphosphate
DDT	Dichlorodiphenyltrichloroethane
dCTP	Deoxycytidine triphosphate
dGTP	Deoxyguanosine triphosphate
DNA	Deoxyribonucleic acid
dNTP	Deoxynucleotide triphosphate
dTTP	Deoxythymidine triphosphate
E3	Ubiquitin
EDTA	Ethylenediaminetetraacetic acid
eFP	Electronic fluorescent pictograph
EPF	Epidermal patterning factor
EPFL	Epidermal patterning factor like
EPFL9	Epidermal patterning factor like 9
ERF	Ethylene response factors
ERFVII	Group VII ethylene response factors
FeEDTA	Ethylenediaminetetraacetic acid ferric sodium salt
FIJI	Open source image processing package
FLIR	Forward looking infrared
Fm	Maximum fluorescence
Fv	Variable fluorescence
g	Grammes
g	Gravity
GAK	Glycogen synthase kinase
gck1	*guard cell kinase 1*
gDNA	Genomic deoxyribonucleic acid
GFP	Green fluorescent protein
GHR1	GUARD CELL HYDROGEN PEROXIDE-RESISTANT 1
GORK	Gated outwardly rectifying K^+ channel
gs	Stomatal conductance, which is used as a gas exchange capacity indicator
H^+	Hydrogen ion
H_3BO_4	Boric acid
HCl	Hydrochloric acid
HCO_3^-	Bicarbonate
HEPES	4-(2-hydroxyethyl)-1-piperazineethanesulfonic acid
His	Histidine
HSD	Honestly significant difference
HT1	High leaf temperature 1
ht1	mutant line in HT1
IR-64	Indian long grain rice (control)
IRGA	Infrared gas analyser
K^+	Potassium ions
K_2HPO_4	Dipotassium phosphate
kb	Kilobase

KCl	Potassium chloride
KD	Knock-down
KH_2PO_4	Monopotassium phosphate
KNO_3	Potassium nitrate
KO	Knockout
KOD	*Thermococcus kodakaraensis*
KOH	Potassium hydroxide
Ks	Kinases
L	Litre
LB	Luria-Bertani
Ler	*Landsberg erecta*
LRR-RLK	Leucine Rich Repeat Receptor-Like Kinase
Lys	Lysine
M	Molar
m^{-2}	Meters squared
MAP	Methionine aminopeptidase
MAPK	Mitogen-activated protein kinase
MC	Methionine cysteine
MES	2-(N-Morpholino) ethanesulfonic acid sodium salt
$MgSO_4$	Magnesium sulphate
ml	Millilitre
mM	Millimolar
mm^2	Millimetres squared
$MnCl_2$	Magnesium chloride
MPK12	Mitogen-activated protein kinase 12
MPK4	Mitogen-activated protein kinase 4
MS	Murashige & Skoog
N	Nitrogen
n	Number
NaCl	Sodium chloride
NADH	Nicotinamide adenine dinuleotide hydrogen
$NaMoO_4$	Sodium molybdate
NASC	Nottingham Arabidopsis Stock Centre
NCBI	National Center for Biotechnology Information
NEB	New England Bio lab
NH_4^+	Ammonium ions
NIA1	*Nitrate reductase 1*
NIA1	Nitrate reductase 1 Protein
nia1	Mutant line in *NIA1*
nia1-2	Mutant *NIA* line
nia1nia2	Mutant *NIA* line
NIA2	Nitrate reductase 2 Protein
nia2	Mutant *NIA* line
NIA2	*Nitrate reductase 2*
nia2-5	*Arabidopsis thaliana* mutant seed
NiR	Nitrate reductases
nM	Nanomolar

NO	Nitric oxide
NO_2^-	Nitrite ions
NO_3	Nitrate
NO_3^-	Nitrate ions
NOFNiR	Nitric oxide forming nitrite reductase subunit
NOS	Nitric oxide synthase
NR	Nitrate reductase
NRT	Nitrate transporter
ns	Not significant
NUE	Nitrogen use efficiency
O_2	Oxygen
OsEPF1oe	Rice overexpressor line in EPF1
OsEPF1oeS	Rice overexpressor line in EPF1 Strong phenotype
OsEPF1oeW	Rice overexpressor line in EPF1 Weak phenotype
OST1	Open stomata 1
ost1	Mutant line in OST1
PATROL	Proton ATPase translocation control 1
PCR	Polymerase chain reaction
PHOT1	Phototropin 1
PHOT2	Phototropin 2
PP1	Type 1 protein phosphatase
PP2C	Type 2C protein phosphatases
PP2CA	Clade A type 2C protein phosphatases
ppm	Parts per million
PRSL1	Regulatory subunit of PP1
PRT1	PROTEOLYSIS 1
prt1-1	Mutant of PRT1 in Col-0
PRT6	PROTEOLYSIS 6
prt6-1	Mutant line in PRT6
Ps	Phosphatases
PSII	Photosystem II
pskr2	Phytosylfokine-Alpha receptor 2
PVPP	Polyvinylpolypyrrolidone
PYL	Pyrabactin resistance 1-like
PYR	Pyrabactin resistance 1
RCAR	Regulator component of ABA receptor
RFP	Red fluorescent protein
RH	Relative humidity
RLK	Receptor-like kinase
RNA	Ribonucleic acid
RNAi	RNA interference
rpm	Revolutions per minute
s	Second
SAM	Shoot apical meristem
SD	Standard deviation
SDS	Sodium dodecyl-sulphate
SEM	Standard error of the mean

SLAC1	SLOW ANION CHANNEL-ASSOCIATED 1
SNAP	S-Nitroso-N-acetylpenicillamine
SOC	Super optimal broth with catabolite repression
START	Steroidogenic acute regulatory protein (StAR)-related lipid transfer
STE	Homologs of the yeast STE genes
SUMO	Small ubiquitin-like modifier
TAE	Tris-acetate-EDTA
TAIR	The Arabidopsis Information Resource
T-DNA	Transfer deoxyribonucleic acid
TKL	Tyrosine kinase-like
UBR	Ubiquitin ligase N-recognin
v	Volume
w	Weight
wt	Weight
WUE	Water use efficiency
$ZnSO_4$	Zinc sulphate

Table of Contents

List of Tables

List of Figures

Declaration

I, Joanna Landymore, confirm that the Thesis is my own work. I am aware of the University's Guidance on the Use of Unfair Means (www.sheffield.ac.uk/ssid/unfair-means). This work has not been previously been presented for an award at this, or any other, university.

Publications that have arisen from this thesis are as follows:

Hõrak H, Fountain L, Dunn JA, Landymore J, Gray JE (2020) Dynamic thermal imaging confirms local but not fast systemic ABA responses. Plant Cell Environ. doi: 10.1111/pce.13973

Hõrak H, Fountain L, Dunn JA, Landymore J, Gray JE (2021) Leaf temperature responses to ABA and dead bacteria in wheat and Arabidopsis. Plant Signal Behav 1899471

Chapter 1 – Introduction

The world's population is increasing and expected to reach just over 9 billion by 2050 (United Nations and Population Division, 2022). This rising population simultaneously increases pressure on the global food supply chain, whilst restricting the availability of arable farmland. If the challenge of increased future food production is going to be met, then sustainable land use and improved breeding strategies are critically important, and factors such as climate change and usage of fertilisers will need to be addressed (Ray et al., 2013).

Climate change directly influences the global water cycle. Rising temperatures increase the amount of water evaporation on a global scale, increasing drought and desertification in some areas of the world. A warmer atmosphere holds more moisture resulting in increased precipitation, which can ultimately lead to flooding. In areas of drought, this leads to an increase in heavy metal and salt concentrations, which stresses affected plants by restricting available water and nutrients (such as nitrogen, potassium and magnesium), and in turn impacts growth and desiccates plants. In flooded areas, plant roots become hypoxic, restricting the available oxygen resulting in death (Ciríaco *et al.*, 2010; Linkohr *et al.*, 2002; Khasanova, James and Drenovsky, 2013). Understanding the mechanisms that control plant stress responses in these environments, is imperative to improve crop yield and plant survival in these harsh conditions. This provides a long-term solution for increasing food demands (Sinclair and Rufty, 2012; Ray et al., 2013; Wheeler and von Braun, 2013; Misra et al., 2015). Plant growth and health is also dependent on nitrogen, obtained largely from soils in the form of nitrogen fertilisers, application of which has drastically increased in the last few decades. Due to both economical and more importantly environmental reasons there is a need to reduce nitrogen fertiliser use. In 2007, there was a recorded value of 110 million metric tons for global use. It has been estimated that by 2050 this could reach 125 – 236 million metric tons. Although a large amount of fertiliser is applied to arable land to aid in plant growth, only about 30 – 50 % of nitrogen is taken up by plants. The remainder largely leading to environmental pollution, mainly via leaching whereby the nitrate enters water systems (Savci, 2012; Rashmi et al., 2020). The added nitrogen causes algal blooms blue-green algae (cyanobacteria) and increased plant growth leading to eutrophication[1] (Chislock et al., 2013). Nitrogen fertilisers can also release ammonia which acts as a base for emissions of nitrous oxide which is a potent greenhouse gas. Nitrous oxide has a significantly higher global warming potential (GWP) of 298 compared to carbon dioxide which has a GWP of 1. In 2021 it was estimated that 57 % of the total UK

[1] Eutrophication is the term used when nutrients (largely from field run off from fertiliser application) amass in lakes or bodies of water. This results in increased growth of microorganisms, resulting in hypoxia (reduced oxygen levels) in the water effectively killing fish and other life within the body of water.

emissions of N_2O were from agricultural soils (fertilisers) (National Atmospheric Emissions Inventory, 2024).

1.1 – Nitrogen

Nitrogen (N) is a key growth limiting resource for plants; nitrate (NO_3^-) and ammonium (NH_4^+) are the two forms found in soil (Crawford, 1995; Sinclair and Rufty, 2012; Gruffman et al., 2014; Soltani et al., 2014). Plants obtain N mainly in the form of NO_3^-, which is a highly soluble molecule and able to be taken into plants via the transpiration stream, requiring nitrate transporters (NRTs) to cross membranes to where nitrate is needed. The nitrate is assimilated to make amino acids, proteins and chlorophyll. N is also used as a signalling molecule (mainly in the form of nitric oxide (NO)). Nitric oxide is a highly versatile signalling molecule which functions through interactions with cellular targets via reduction or oxidation (Lamattina et al., 2003; Delledonne, 2005; Palavan-Unsal and Arisan, 2009). Nitric oxide requires a nitric oxide synthase (NOS) for NO to be incorporated into the plant for signalling in particular during defence responses to stress, flowering and hormone signalling (Guo and Crawford, 2005). NO also plays a role in root development, branching, pollen tube growth, stomatal aperture changes, fruit maturation, cellulose biosynthesis and leaf senescence (Sanz et al., 2014; Sanz et al., 2015; Signorelli and Considine, 2018). NO signalling is also used to control stomatal movements (microscopic pores on a leaf's surface, which control gas/water exchange) (Hetherington and Woodward, 2003) and trigger stress responses in signalling pathways (such as abscisic acid (ABA) and the N-end rule pathway) to protect the plant (Desikan et al., 2004; Bright et al., 2006a; Neill et al., 2008).

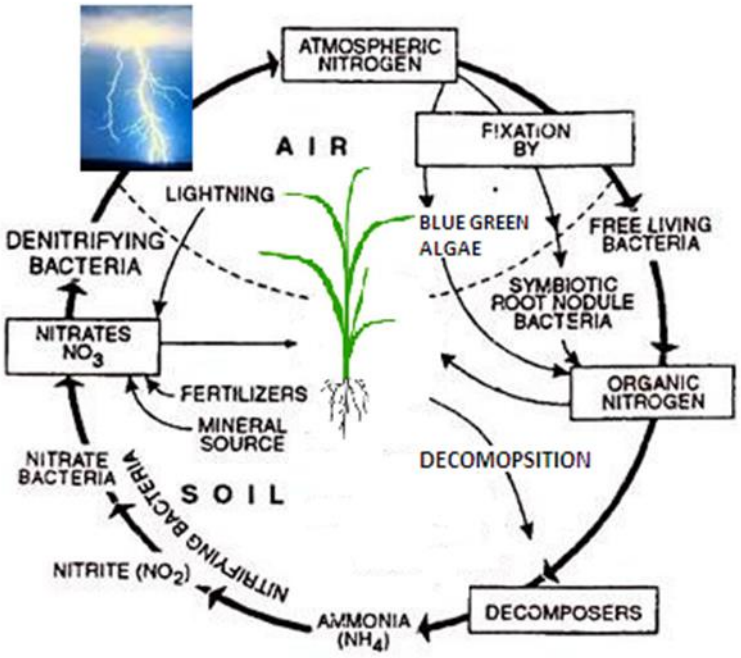

Figure 1.1 – The Nitrogen cycle for bacteria. Adapted from Shagun Khandelwal (2017), showing the routes by which NO_3^- and ammonia enter the plants from both atmospheric N and NO_3^- in the soil from fertilisers.

Endogenous NO is produced in mammalian cells due to their genome encoding nitric oxide synthase (NOS) enzymes. There is no evidence of NOS homologues in plant genomes and unlike some bacteria (in particular diazotrophs (Dixon and Kahn, 2004)), plants cannot fix N from atmospheric N_2 gas, instead rely on assimilation of NO_3^- into plants (Pike et al., 2002). Figure 1.1 demonstrates the routes by which nitrogen can enter plants using bacterial nitrogen fixation. It is estimated that ~80 % of nitrogen fixation in traditional agriculture is undertaken by diazotrophic bacteria involved in a mutualistic relationship with *Fabaceae* (legumes) (Peoples *et al*., 1995). Other microorganisms, such as *Pseudomonas spp*., *Azospirillum spp*. and *Azotobacter spp*. can also fix atmospheric N, if conditions are optimal (Giller et al., 1997; Bürgmann et al., 2004; Orr et al., 2011).

1.2 – Stomata

Stomata are microscopic pores on the epidermis of the leaves that enable gas exchange. They are surrounded by two guard cells that open and close in response to both abiotic and biotic stimuli, such as light, temperature, humidity, changes on CO_2, phytohormones and presence of pathogens (Bertolino et al., 2019). Changes in turgor pressure of the guard cells allow the opening and closure of stomata. During light induced stomatal opening, blue light is detected by phototropins (PHOTs) present in guard cells. PHOTs then activate the MAPKKK BLUS1. Then MAPKKK BHP is then activated by BLUS1 which leads to the activation of plasma membrane H^+-ATPases. This activity then causes

hyperpolarisation of the plasma membrane which in turn regulates the activity of ion channels. The change in polarisation is followed by the influx K^+ ions followed by water and osmolytes like chloride, nitrate, and malate to guard cells. The influx of water causes a change in turgor pressure leading to stomatal opening (Sussmilch et al., 2019; Lawson and Matthews, 2020; Yang et al., 2020). Closing of stomata triggered by darkness or other signals results from the opening of anion channels which temporarily depolarise the plasma membrane and alter ion channel activity to allow the release of K^+ ions and other osmolytes causing loss of water and cell turgor. Opening and closure of stomata affect water use efficiency (WUE), which is a measure of the amount of carbon fixed per unit of water lost. The maximum and minimum levels of carbon fixation and water loss are also affected by the size and density of stomata and these traits are also affected by environmental signals to reduce water loss and optimise WUE. In addition, stomata need to be properly spaced and patterned in the epidermal surface. If there is not enough spacing between stomata, their performance may be suboptimal as diffusion shells could overlap and decrease gas exchange efficiency, and adjacent cells may not be able to supply sufficient water to achieve guard cell turgor change. Many plant species appear to operate a one-cell spacing rule, whereby at least one epidermal cell is formed between two stomata. Mutant studies in Arabidopsis have identified numerous genes that affect the signalling pathways which regulate stomatal development and patterning. An early example was the *Too Many Mouths (TMM)* gene, which encodes a membrane protein that inhibits the development of stomata adjacent to each other (Nadeau and Sack, 2002). Mutations in the *TMM* gene can cause stomatal clustering. *TMM* encodes a *Leucine Rich Repeat Receptor Like Kinases (LRR-RLK*), that acts as a co-receptor for *ERECTA* and *ERECTA-LIKE* 1 and 2 receptor kinases to regulate stomatal development (Shpak et al., 2005). Other gene products that regulate stomatal development and clustering, include several *EPIDERMAL PATTERNING FACTOR (EPF)* signalling peptides. *EPF* mutants can have abnormally high or low stomatal densities which can cause changes in the level of plant transpiration (Hunt et al., 2010). The *TMM/ERECTA* family complexes act as receptors for peptide ligands that regulate stomatal spacing (*EPF1*) and stomatal density (*EPF2* inhibits entry to stomatal lineage whilst *EPFL9/STOMAGEN* promotes this) (Hara et al., 2007; Hara et al., 2009; Hunt and Gray, 2009; Lee et al., 2012; Torii, 2012). Stomatal development involves asymmetric division of stomatal precursor cells known as meristemoids in immature leaves. This is promoted by the transcription factor *SPEECHLESS (SPCH)* and the division plane orientated by *BREAKING OF ASYMMETRY IN THE STOMATAL LINEAGE (BASL)* (Franks and Casson, 2014; Torii, 2015; Gong et al., 2021). Formation of stomata is controlled by the presence of SPCH in meristemoids, followed by the activity of related basic helix loop helix proteins *MUTE* and *FAMA* in Guard Mother Cells (GMCs) and immature guard cells. Changes in any of these can affect stomatal formation (Zoulias et al., 2018; Zoulias et al., 2021). Environmental factors such as CO_2

concentration, water availability and light intensity can all affect stomatal density. High CO_2 levels reduce stomatal density by promoting epidermal cell formation and high light intensity promotes stomatal formation (Casson and Gray, 2008; Casson and Hetherington, 2010).

There are two major morphologies of guard cells: Kidney-shaped guard cells are present in most groups of land plants including eudicots, and elongated dumbbell-shaped guard cells are found in the monocot grasses (Nunes et al., 2020). It is widely reported that stomata with dumbbell-shaped guard cells have a rapid opening and closure response however, recent data has revealed that other species including a fern can open stomata just as rapidly (Pichaco et al., 2024). It is believed that the faster opening or closing of stomata could be advantageous under stress conditions to reduce unnecessary water loss and improve WUE. Rapid opening is attributed to the fast transport of osmolytes between guard cells and specialised subsidiary cells, representing a mechanical advantage to changes in ambient conditions (Lawson and Vialet-Chabrand, 2019). Several studies have also suggested that smaller stomata can close at a faster rate, potentially due to faster changes in osmolarity, affecting turgor pressure (Nadeau et al., 2002; Raven, 2014).

Changes in stomatal aperture are achieved by complex molecular pathways, resulting in alterations in ion concentration (MacRobbie, 1998) and these pathways are regulated by signalling molecules, such as NO (see Figure 1.2) (Balmant et al., 2016). Biochemical changes also play a role, of particular interest is guard cell starch metabolism, which releases sugars and increases osmotic potential. Within 30 minutes of exposure to blue light, the plasma membrane H^+-ATPase activity leads to activation downstream of β-AMYLASE1 (BAM1) and α-AMYLASE3 (AMY3) enzymes to degrade guard cell starches to glucose and promote stomatal opening. The presence of NUCLEOTIDE TRANSPORTER (NTT) proteins can import ATP into GC chloroplasts (GCCs) enabling starch degradation which in turn enables stomatal opening and aids in plant growth (Horrer et al., 2016; Flütsch et al., 2020; Flütsch and Santelia, 2021; Lim et al., 2022).

Under abiotic and biotic stress conditions guard cell signalling pathways are often triggered promote stress tolerance. For example, under drought stress stomata close in response to the stress-response phytohormone ABA, to prevent water loss and dehydration. Drought tolerance responses can also affect stomatal density and size in developing tissues to restrict future water loss (Doheny-Adams et al., 2012; Hepworth et al., 2015). A number of ways of manipulating guard cell signalling pathways or altering stomatal densities have been investigated with the aim of improving WUE (Kollist et al., 2014; Franks et al., 2015). Kusumi *et al.* (2012) demonstrated that rice (*Oryza sativa*) growth is limited by stomatal transpiration, indicating the importance of manipulating guard cell density and movement to reduce water loss. The ability to produce a more rapid stomatal response, is also proposed to affect

plant WUE and survival, for example, rapid stomatal closure under drought conditions (Lawson and Blatt, 2014).

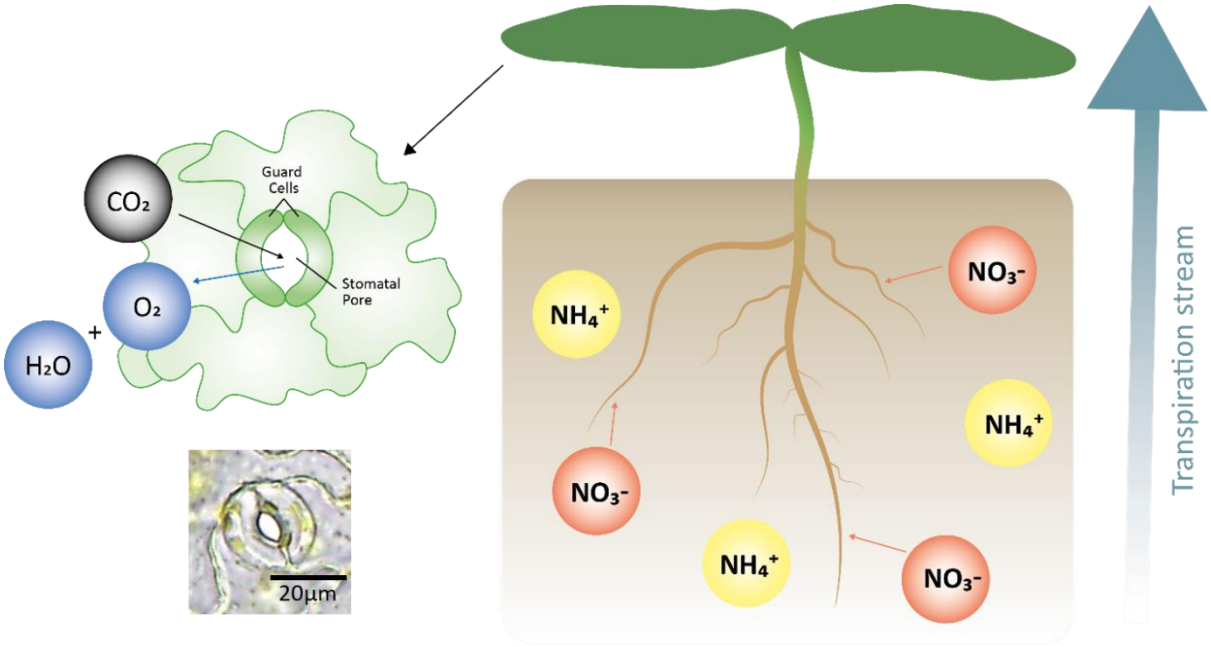

Figure 1.2 – A representation of the uptake of nitrogen ions into the plant. Nitrate is highly soluble and able to be taken up via the transpiration stream, which is dependent on stomatal pores being open to allow gas exchange and water vapour loss. A diagrammatic and actual representation of stomata are shown.

1.3 – Nitrate reductase

In some plant species, nitrogen is fixed from the atmosphere by bacteria in root nodules (as is the case of legumes) or through a symbiotic relationship with nitrogen fixing bacteria with their root system. These bacteria fix atmospheric nitrogen (N_2) by converting it into ammonia (NH_4^+) which is absorbed by the host plant. In plants without these advantages, the main way that nitrate is assimilated is via nitrate or ammonia uptake by the roots followed by nitrate reductase activity inside the plant. NR uses the reducing power of NAD(P)H to catalyse reduction of nitrate (NO_3^-) to nitrite (NO_2^-) that can be used in essential biosynthetic pathways (Desikan et al., 2002; Orr et al., 2011; Li et al., 2013).

Nitrogen is taken up into plant roots in two soluble forms – nitrate or ammonia. Nitrate is a highly soluble molecule, which is absorbed from the soil into the root epidermis and cortical cells and transported throughout the plant. This is via specialised proteins known as nitrate transporters (NRTs), nitrate is also transported to the shoots in xylem tissues using the transpiration stream as a result of evaporation at the stomata. In Arabidopsis, there are two main NRTs; NRT1 and NRT2. NRT1 is a low affinity transporter which can be switched to high affinity when phosphorylated. NRT2 is a high affinity transporter responsible for nitrate uptake when soil nitrate levels are low (Xu et al., 2024). Nitrate can be stored in the vacuoles of root and leaf tissues when not required. Nitrate is assimilated into organic

compounds such as amino acids and proteins via nitrate (NR) and nitrite (NiR) reductases, which require energy and all steps of nitrogen uptake determine nitrogen use efficiency (Forde, 1999; Krapp et al., 2014; Zhang et al., 2018a; Aluko et al., 2023). NH_4^+ is a larger molecule than nitrate and requires more energy to be taken into the plant where NH_4^+ is relocated via ammonium transporters before being assimilated. NO_3^- and NH_4^+ are the main forms of N present in agricultural soils and are obtained from synthetic fertilisers, the application of which is being reduced following government guidelines (DEFRA, 2022). This is due to detrimental downstream ecological effects such as leaching leading to eutrophication and overall impacting water quality, air quality, biodiversity, soil health and global climate. Nonetheless, nitrogen compounds are critical for plant survival and the reduction of nitrate by NR is a key step in nitrogen assimilation in plants.

Nitrate reductase forms part of a large protein complex with several other enzymes involved in nitrogen metabolism. The molecular structure of the NR complex illustrated in Figure 1.3 helps to demonstrate the mechanism by which nitrogen assimilation and metabolism occurs. In brief, a dimer heme containing NR subunits catalyse the reduction of NO_3^- to NO_2^-, which can be used by the plants. However, an associated nitrite reductase, NOFNiR, can catalyse the further reduction to NO (nitric oxide) and an associated NO dioxygenase THB1 can act on NO to catalyse the re-formation of NO_3^-.

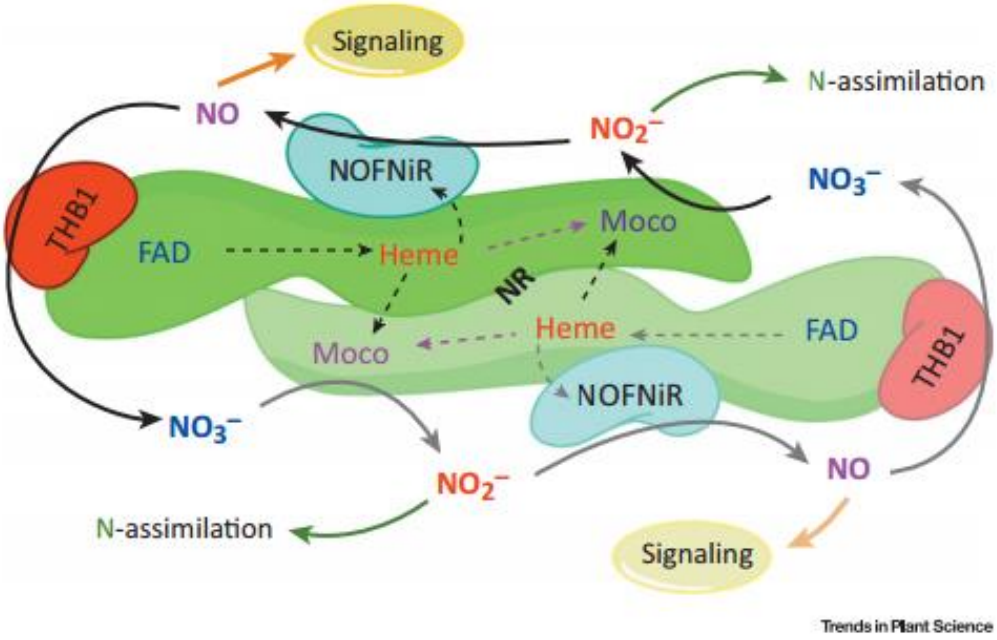

Figure 1.3 – An updated model of NR enzymatic activities taken from (Chamizo-Ampudia et al., 2017), showing its two subunits in green (making a dimer), each with 3 functional prosthetic groups: moco, Heme and FAD. Moco (molybdenum cofactor) catalyses the reduction of NO_3^- to NO_2^-, which is able to be taken up by plants. This uses electrons from NAD(P)H to reduce FAD, Heme and Moco, the dashed lines show movement of electrons. NOFNiR catalyses the production of NO from NO_2^- by the reduction of NO_3^-. The enzyme complex catalyses both NO production and its oxidation to NO_3^- by dioxygenase activity by the THB1, which uses electrons from NR. Thus, the complex catalyses NO_3^- reduction and controls levels of NO.

1.4 – Nitric Oxide and Abscisic Acid

Many changes in the environmental conditions are sensed by the plants and some environmental response pathways have been shown to be triggered by signalling cascades involving NO. NO signals are involved in the regulation of plant growth as well as in the response to both biotic and abiotic stresses. In plants, the activity of nitrate reductase, as a component of the NR complex described above, is the major source of NO. Thus, NO which is a byproduct of nitrate metabolism appears to play a role in linking plant nitrate status to stress responses. For example, several studies have implicated NO as a signalling intermediate in the ABA signalling pathway that triggers stomatal closure (Zhao et al.; Desikan et al., 2002; Bright et al., 2006b; WILSON et al., 2008).

Nitrate reductase is encoded by two genes in Arabidopsis. The NR double mutant *nia1nia2* is slow growing and chlorotic, presumably because of its inability to properly assimilate nitrogen. This mutant also has a reduced ability to produce NO. It is clear that in plants NR activity is a significant source of NO. In animals however, NO is also produced by nitric oxide synthase enzymes but evidence for the presence of this activity in plants is poor. In Arabidopsis Nitric Oxide-Associated1 (NOA1) was

previously believed to be involved in NO synthesis. More recent work indicates that it is not a nitric oxide synthase, although other unknown routes to NO synthesis may exist in plants. Lozano-Juste and Leon (2010) looked at the triple mutant *nia1nia2noa1* which produce significantly reduced levels of NO, but some NO was still produced. ABA-induced NO synthesis was only partially reduced in *nia1nia2noa1*, suggesting that there is another yet unidentified pathway involved. It should be noted that these experiments used a *nia1nia2* double mutant made from crossed ecotype backgrounds and lack a good control (as described later) which could have influenced the results observed. Most studies show that when NO is applied a stomatal closure response is stimulated. However, Sakihama *et al*. (2003) indicated that, when used at high concentrations, NO donors can cause stomatal opening.

Several signalling pathways interact in guard cells including ABA, ethylene and NO response pathways (Chater et al., 2014). When these signals are applied separately, they induce stomatal closure. It has been found that if ABA or NO are applied in the presence of ethylene, then stomatal closure is reduced (Desikan et al., 2006). These signalling pathways all interact in order to cause a response, but there is another route which uses NO to cause changes in stomatal aperture, known as the N-end rule pathway.

1.5 – Post-translational modifications in nitrogen signalling and stomatal regulation

The N-end rule pathway was first proposed by Varshavsky *et al*. in 1986. It describes how the half-life of each proteins dependent on the nature of its N-terminal amino acid residue and certain destabilising residues cause the half-life to be decreased (Bachmair et al., 1986). The N-end rule operates in all organisms including plants, mammals and bacteria, but the composition of the enzymes responsible, substrates and modes of action involved can vary. The N-end rule pathway for targeted proteolysis is highly conserved in eukaryotes and has been linked to many developmental processes. Most importantly for this project, the N-end rule pathway has been shown to regulate the stomatal closure response to ABA (Gibbs et al., 2014a; De Marchi et al., 2016; Mendiondo et al., 2016). The closure of stomata is regulated by a complex signalling network that provides a robust response and is now known to involve targeted proteolysis via the N-end rule pathway. The route by which proteins with destabilising N-terminal amino acid residues are targeted for degradation involves the presence of nitric oxide. The classic N-end rule pathway, also known as the arginine (Arg) branch, recognises particular residues to be ubiquitinated (Graciet and Wellmer, 2010; Gibbs et al., 2016). Figure 1.4 shows a simplified version of the N-end rule pathway, which targets proteins starting with methionine cysteine (MC) residues. The N-terminal methionine is cleaved from the peptide by methionine aminopeptidase (MAP) leaving the destabilising cysteine (C) residue exposed, which is readily oxidised by NO in the presence of oxygen. Oxidised C (C^{ox}) can then be arginylated by arginyltransferases (ATE)

resulting in RC^{ox}, which is then recognised by *PROTEOLYSIS 6* (*PRT6*) and targeted for degradation via the proteasome. *PRT6* is a 224 kDa N-recognin that contains a ubiquitin ligase N-recognin (UBR) box. *A. thaliana prt6* mutants are impaired in degradation of N-end rule substrates; which are type 1 degrons (destabilising N-terminal residues). Type 1 degrons are basic residues which *PRT6* recognises and include: arginine (Arg), lysine (Lys) and histidine (His) (Garzón et al., 2007). Group VII ethylene response factors (ERFVII) have been identified as substrates for this particular branch of the N-end rule pathway (Gibbs et al., 2014b; Gibbs et al., 2015; Papdi et al., 2015). ERFVII's are plant-specific transcriptional factors with conserved N-terminal domains (MC) which are dependent on NO and O_2 to be targeted for degradation via proteolysis. As discussed above, NO levels are regulated by NR activity and thus *nia1nia2* mutants that lack NR are defective in the ability to target N-end rule substrates for degradation and the ERFVII transcription factors are stabilised.

Proteolysis plays an important role in stomatal movements by regulating the levels of key proteins involved in the control of stomatal aperture signalling pathways. In particular the modulation of the ABA signalling pathway for stomatal closure under drought stress. The protein ABI5 (ABA Insensitive5) is a transcription factor that promotes ABA responses, including the expression of genes involved in stomatal closure. Group VII ERFs regulate NO/ABA crosstalk by promoting the expression of *ABI5* and ABA sensitivity. Proteolysis of ERFVIIs by the N-end rule pathway results in reduced ABI5 levels, preventing excessive stomatal closure, allowing plants to respond to environmental conditions. Group VII ERFs are destabilised in the presence of NO via the N-end rule pathway and stabilised in the absence. Through these mechanisms, proteolysis adjusts the guard cell's protein composition, enabling precise control over stomatal movements in response to environmental cues (Gibbs et al., 2014b; Sanz et al., 2015; Vicente et al., 2017). This work showed that NO promotes stomatal opening, in contrast to previous work by Desikan et al. using pharmacological agents that suggested that NO promotes stomatal closure. Thus the role of NO in stomatal aperture control requires further investigation.

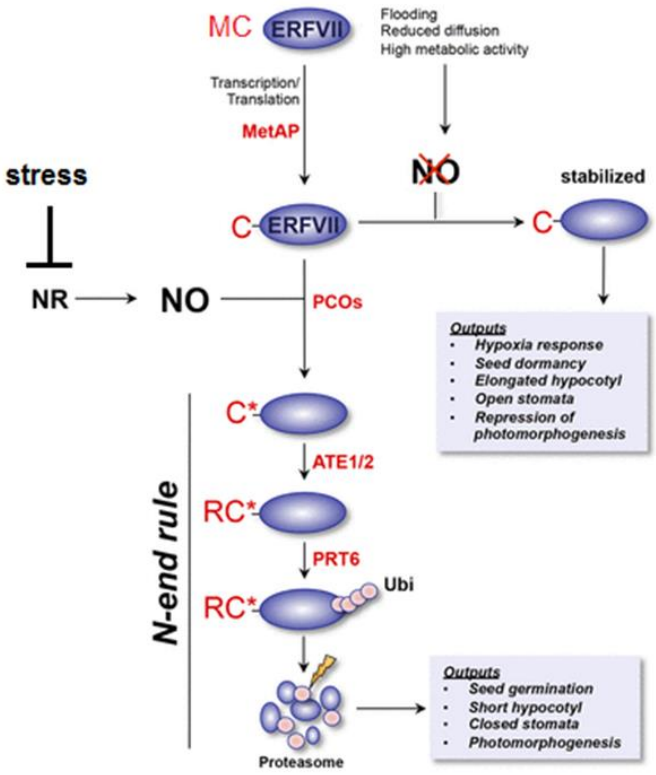

Figure 1.4 – Nitric oxide is required for degradation of MC proteins. A simplified version of the N-end rule pathway for targeted protein degradation, adapted from Gibbs *et al.* (2014). Any alterations in NR activity could affect degradation of the MC protein.

The N-end rule pathway is not the only route which affects protein stability and targets for degradation. Recently, a new mechanism has emerged called sumoylation. Sumoylation is a post translational modification. It is similar to the ubiquitination process in the N-end rule pathway, but it adds small ubiquitin like modifiers (SUMOs), which affect protein stability, structure and localisation. It is interesting to note that both *NIA1* and *NIA2* have potential sites for sumoylation and it has been suggested that these could regulate NR stability and activity and therefore affect levels of NO, resulting in a stomatal aperture response (Srivastava *et al.*, 2016; Soo Park *et al.*, 2011).

1.6 – Abiotic stresses

Plants have developed defence mechanisms in order to survive under certain conditions. Key challenges in this changing world are abiotic stresses, which include: high salinity (due to rising sea levels infiltrating water systems), drought and extreme temperatures.

1.6.1 – Salinity

High soil salt content negatively affects plant growth and reproduction with more than 20 % of cultivable land adversely affected (Hasanuzzaman and Fujita, 2022). Higher salt levels affect osmotic pressures of cells and can cause wilting, chlorosis and depending on the stage of growth, stress applied can affect root branching and growth (Negrão et al., 2017; Hasanuzzaman and Fujita, 2022). Ultimately, long exposure to these stresses causes plant death and even short-term exposure can affect plant health and subsequent grain yield and quality. Biochemical processes as well as biomass and morphology are affected. It has been suggested that salt and nitrogen are linked to each other and that an increase in salt levels up to a toxic amount increases the activity of NR (Ullrich W.R., 2002; Guo et al., 2017). Salt is involved in many biochemical pathways, the ones of greatest interest in this study are those affecting stomatal aperture changes. NR activity indicates that stomatal closure response is activated to reduce water loss.

1.6.2 – Drought

Rising temperatures are causing more widespread drought, which has effects on both water content and nitrogen nutrition within plants and subsequent grain / seed. ABA signalling pathway is involved in stomatal closure response due to drought to reduce water loss via evapotranspiration. Under drought, plants synthesise and accumulate ABA, which is transported to the guard cells. ABA binds to receptors in the guard cells, which initiates a signalling cascade that leads to the activation of protein kinases and inhibition of phosphatases (an example being ABI1 (ABA Insensitive 1). This results in the production of reactive oxygen species (ROS) and an increase in cytosolic calcium levels. The changes activate anion channels, leading to efflux of anions, chloride, malate and potassium ions. The loss of ions reduces the osmotic potential within the guard cells, which causes a loss of water and turgor pressure, which leads to stomatal closure. The process conserves water by reducing transpiration, helping plants to survive during periods of drought. Through these tightly regulated mechanisms, ABA signalling ensures that stomatal movements are responsive to drought conditions, thus optimising water use efficiency (Pei et al., 1997; Yoshida et al., 2006; Sirichandra et al., 2009; Cutler et al., 2010; Kim et al., 2011). As well as drought, high temperatures can have a drought-like effect and depending on the growth stage can affect fertility.

1.7 – Overall aims and objectives

This thesis seeks to understand the link of nitrate availability and environmental stimuli on plant responses and survivability. Mainly focusing on stomatal aperture changes and plant development. Improving Nutrient Use Efficiency (NUE) and Water Use Efficiency (WUE), whilst no or limited detrimental effect to yield, can help to address critical global challenges in food supply. It also seeks to make a significant contribution to the fields of plant biology and plant biochemistry through comprehensive investigations into a) nitrate assimilation, b) stomatal regulation and c) stress responses in plants.

There are three overall aims of this thesis to:

1. Understand how plants respond to changes in their environment including abiotic stresses and varying levels of nitrogen.
2. Explore the effect of salt stress on stomatal conductance, survivability and overall yield effects in both Arabidopsis and rice.
3. Assess the effect of nitrogen status on seed germination and growth.

Specifically, to:

1. See if reducing nitrate assimilation impacts plant growth and health:
    a. Utilising mutants in Arabidopsis deficient in NR to observe germination and growth differences as well as stomatal aperture changes due to stress.
    b. To see if adding exogenous nitrate can restore any potential loss of response from reduced nitrate assimilation.
2. Develop methods to view whole plant fast systemic responses and effects on stomatal aperture to abiotic stresses:
    a. Utilising a range of techniques (including thermal imaging, chlorophyll fluorescence, epidermal peel bioassays and media changes) and mutants in both Arabidopsis and crops.

Chapter 2 – Methods and materials

2.1 – Plant material

Arabidopsis thaliana ecotype Col-0 and mutant seeds (AT1G77760 (NIA1): (SALK_147807) and (SALK_148487) (referred to as *nia1 (1)* and *nia1 (2)* in this report). AT1G37130 (NIA2): *nia2-5*, SALK_088070 and SK_2486 (referred to as *nia2 (1)* and *nia2 (2)* in this report) were obtained from the Nottingham Arabidopsis Stock Centre (NASC).

Additional A. thaliana (Arabidopsis) mutant seeds (AT5G02310 (PRT6)) *prt6-1*, (AT3G24800 (PRT1)) *prt1-1* and complement line (comp), *NIA1SDM Line 1, NIA1SDM Line 2, nia1nia2*) were provided by the University of Nottingham (Professor M. J. Holdsworth).

Arabidopsis Epidermal Patterning Factor (EPF) mutant lines (AT2G20875 (EPF1)) *epf1-1*, (AT1G34245 (EPF2)) *epf2-1, epf1-1epf2-1, EPF2OE*, (AT4G12970 (EPFL9)) *EPF9OE*, Barley Golden Promise cultivar, Rice Indian long grain Rice (IR-64) and EPF mutant lines OsEPFoeW and OsEPFoeS were provided by the University of Sheffield (Professor J. E Gray).

2.2 – Growth conditions and media

Seeds were stratified (placed in the dark) in cold water for 72 hours at 4°C and subsequently propagated for 6 weeks (in a growth chamber), until the rosettes were completely expanded, but flowering had not commenced. Growth conditions were: 9 hours photoperiod, light intensity 180 µmol m^{-2} sec^{-1}, temperature 20/16 ˚C (day/night), relative humidity 67 % and ambient CO_2 (400 ppm). Mutants and their controls were grown simultaneously, using the same conditions, except for the *nia1nia2* mutant, which was sterilised a week before the controls. Plants in 5 cm small pots on Levington M3 compost and perlite (Sinclair (2.0 – 5.0 mm)) in a 3:1 ratio, were watered every two days with 200 to 400 ml of water per tray.

For experiments using nutrient media, sterile 0.5x Murashige & Skoog (MS) agar plates (2.2 g L^{-1} MS salts, pH 5.8, 1 % (w/v) agar) was prepared. *A. thaliana* seeds were surface sterilised by soaking in 1 ml of 70 % ethanol (v/v) solution for 2 minutes, followed by 10 minutes in 1 ml of a 3 % bleach (v/v) solution, containing 0.05 % Tween 20 and agitated throughout. Seeds were washed 5 times with sterile deionised water, to remove the bleach solution and then spread onto the MS agar plates, sealed with micropore tape and stratified in the dark at 4 °C for 72 hours (inverted to reduce damage from condensation). Seeds were placed vertically and incubated as above for 1 week or 2 weeks (depending on the mutant), to induce germination. Once germinated, seeds were transferred to either a) pots

containing a 3:1 mix of levington M3 peat compost to perlite or b) new MS plates for further experiments.

2.2.1 – Germination assay

0.5 X MS media with 0.8 % agar plates were made with the addition of 0, 1, 3, 5 or 10 µM ABA. Seeds were surface sterilised with 1 ml of 70 % ethanol (v/v) solution. Seeds then were placed onto sterilised filter paper and using sterilised toothpicks, in a flow cabinet, seeds were transferred onto plates. All genotypes were contained on each plate. All genotypes were placed in a row across the top of the plate in order (Col-0, *nia1 (1), nia1 (2), nia2-5, nia2 (1), nia2 (2)* and *old nia1nia2* (left to right)). This horizontal pattern continued vertically throughout the plate. Plates were sealed with micropore tape and then placed vertically into a sanyo vertical cabinet with short day conditions (9 hour photoperiod, light intensity 180 µmol m^{-2} sec^{-1}, temperature 20/16 ˚C (day/night), relative humidity 67 % and ambient CO_2 (400 ppm)). Plates were observed each day, images taken, and germinating seeds marked as shown in Figure 2.1.

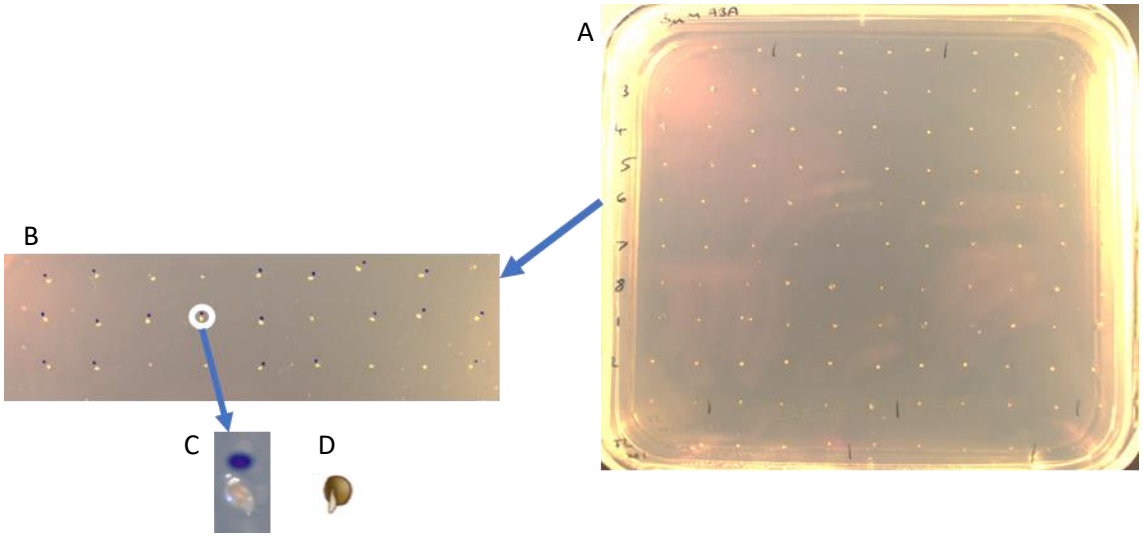

Figure 2.1 – Representative images of germination assay. A) Image of the initial germination assay set up. B) Marked germinated seeds. C) An enlarged image of a germinating seed. D) A diagram of a germinated seed.

2.2.2 – Drought assay

Six weeks after germination, plants were randomised into four trays; 2 trays were left to drought (watering was stopped), and the remaining 2 watered as normal (see Section 2.2). The weight of the pots was recorded and monitored every other day throughout the experiment, to compare water loss and infer biomass (through weight changes). Plants were incubated for 15 days as previously described (see Section 2.2). Images were taken daily, using a thermal imaging camera (FLIR SC660) mounted on a tripod 1 m above the chamber floor, until plants showed signs of extreme drought (wilted and curled

up leaves). Plants were then hydrated and images taken for a further 3 days. Images were taken every minute for 1 hour, commencing 2 hours after the start of the chamber's photoperiod; allowing the plants time to acclimatise to the lights. Analysis was performed using FLIR tools software (FLIR, USA) and digital images were taken for comparison using a Nikon AF-S DX digital camera. Differences between treatments were determined using a one-way ANOVA with multiple pairwise comparisons.

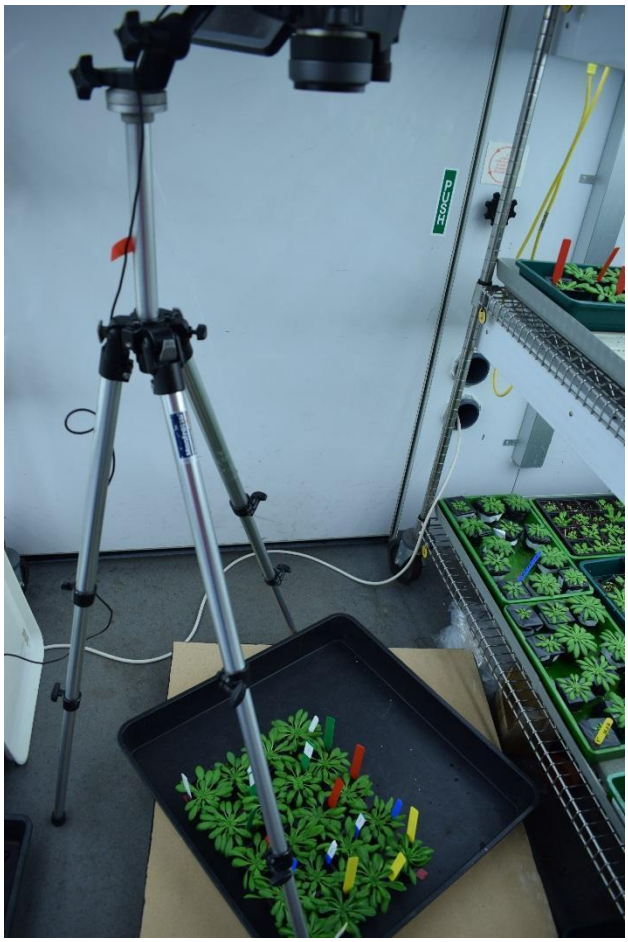

Figure 2.2 – FLIR SC660 thermal imaging camera set up and used to image *A. thaliana*. Camera was mounted on a tripod 1 m above the chamber floor and the chamber temperature was equilibrated during imaging by placing plants in a black tray, which was raised off the floor.

2.2.3 – Salt assay

Four days after germination (see Section 2.2), seedlings were transferred (under sterile conditions, using forceps) to 100 mm square petri dishes containing 50 ml ½ MS agar (2.2 g L^{-1}, pH 5.8, 1 % agar) and one of four NaCl concentrations (0, 100, 125 or 150 mM). Thirty seedlings from each genotype, were analysed per NaCl concentrations (see Section 2.1), except for the *nia1nia2* mutant. In total 780 of seedlings were analysed (120 seedlings from 3 genotypes, experiments (repeated twice) and 60 seedlings from *nia1nia2*).

The start point of each seedlings root tip was recorded, to analyse root growth and the seedlings subsequently placed vertically in the growth cabinet and incubated for 7 days. Images of the plates were then taken at the end of the experiment, using the NIKON AF-S DX digital camera (a ruler was included for scale), analysis of growth was performed using FIJI distribution of image J software (Schindelin, J. et al., 2012). Differences between treatments were determined using a one-way ANOVA with multiple pairwise comparisons.

2.2.4 – Arabidopsis thaliana salt solution

A. thaliana salt (ATS) solution was prepared as follows: 5 mM KNO_3, 2.5 mM KH_2PO_4, 2 mM $MgSO_4$, 2 mM $Ca(NO_3)_2$, 70 µM H_3BO_4, 50 µM FeEDTA, 14 µM $MnCl_2$, 10 µM NaCl, 1 µM $ZnSO_4$, 0.5 µM $CuSO_4$, 0.2 µM $NaMoO_4$, 0.01 µM $CoCl_2$ in one litre of sterile water or 0.8 % (w/v) agar (plant cell culture tested; Sigma, St. Louis) for plates, and filter sterilised. When using low NO_3^- concentrations, the KNO_3 and $Ca(NO_3)_2$ were replaced with the same concentration of KCl and $CaCl_2$ (Leyser and Furner, 1992; Linkohr et al., 2002; Weigel, D., & Glazebrook, 2002).

2.2.5 – Nitrate assay

ATS media was prepared with agar plates with or without 7 mM NO_3. Seedlings were germinated on 0.5 X MS, 0.8 % agar plates and transferred after seven days to ATS, 0.8 % plates with or without nitrate.

2.3 – Callus production

Callus production was measured using the method detailed in (Ellis 1993). Six week old leaf material was used for callus production and grown under long day conditions in Sanyo cabinets. 16 hour photoperiod, 180 $\mu mol^{-2}\ s^{-1}$, 400 ppm CO_2, 24°C day / 22°C night and 60-67 % humidity.

2.4 – Extraction of genomic DNA

DNA was extracted using the Edward's method (Edwards et al., 1991). Fresh leaf tissue (10 – 20 mg) was collected in 1.5 ml microcentrifuge tubes and ground for 10 seconds, using a plastic pestle. Four hundred µl of Edward's extraction buffer (200 mM Tris-HCl (pH 8), 250 mM NaCl, 25 mM EDTA (pH 8.0), 0.5 % (v/v) SDS) was added to the sample, which was ground for a further 10 seconds and then vortexed for 5 seconds. Samples were centrifuged for one minute at 14,000 x *g* and 300 µl of the supernatant transferred into a fresh microcentrifuge tube. Three hundred µl of isopropanol was added and mixed thoroughly (by pipetting) before incubating the samples at room temperature for two minutes. Samples were then centrifuged for 5 minutes at 14,000 x *g*, the supernatant was decanted and pellet left to air dry for 10-15 minutes, to remove the residual isopropanol. The DNA was then resuspended in 50 µl of sterile de-ionised water and frozen at -20 °C.

2.5 – Genotyping

To test whether plants were homozygous or segregating, specific primers were designed and PCRs performed on each genotype. Isolated DNA was used as a template in 10 µl reactions, containing 0.5 µl template DNA, 1x MyTaq Red Mix (Bioline, UK), 0.25 µl of both the forward or reverse primers (10 µM concentration) (see Table 2.1) and the remaining volume made up with nuclease-free water. Each set of PCR reactions also included positive controls (wild type DNA) and negative controls (nuclease-free water). A standard PCR cycle was performed with changes in the annealing temperature, extension time and cycle number, depending on the primer set and fragment length, specifically: 94 °C for 5 minutes initial denaturation; 25-30 cycles of denaturing at 94 °C for 30 seconds, annealing at 55-62 °C for 30 seconds and extension at 72 °C for 30 seconds; and a final extension of 72 °C for 5 minutes.

The genotyping for *prt6-1* varied slightly, due to detecting a single base pair change, specifically: 98 °C for 30 seconds initial denaturation; 30 cycles of denaturing at 98 °C for 20 seconds, annealing at 56 °C for 30 seconds and extension at 72 °C for 2 minutes; and a final extension of 72 °C for 5 minutes.

Product size was then checked for all amplicons using gel electrophoresis. Eight µl of the PCR product was then run on a 1 % (w/v) agarose gel with TAE buffer and 0.001 % of a 10 mg/ml ethidium bromide (Sigma-Aldrich, UK) solution. Two µl of Hyperladder I (Bioline, UK) was run alongside the samples to enable band size of fragments to be determined. Samples were run for 30 minutes at a 100 volts.

2.6 – qPCR

Mature leaf tissue was collected and ground under liquid nitrogen. RNA was extracted using and RNeasy kit with DNase treatment (Qiagen) according to the manufacturer's instructions. cDNA synthesis was performed using Reverse Transcriptase Superscript (Thermo Fischer Scientific). RT-qPCR was performed using QuantiNova SYBR green PCR kit (Qiagen). Reference genes Ubiquitin (UBC) and Actin (ACT). Results were analysed using 2-Delta C_t method.

Table 2.1 – Primer sets and specific reaction conditions for the PCR performed for each genotype

Genotype	Primer	Forward/Reverse	Annealing temperature (°C)	Extension time minutes : seconds
prt6-1	5' – GGAGTTTTCTATGTCCAGTGAGAGTTT – 3'	Forward (mutation specific)	56	02:00
prt6-1	5' – GTCTCCAATGACACGTTCACTTGTCT – 3'	Reverse	56	02:00
prt6-1	5' – GGAGTTTTCTATGTCCAGTGAGAGTTT – 3'	Forward (wild type)	56	02:00
NIA1SDM	5’ – CAAATTCCGAAGCTTGGTGGTATCGGCCTGA ATACATAATCAAC – 3’	Forward	67	01:00
NIA1SDM	5’ – GTTGATTATGTATTCAGGCCGATACCACCA AGCTTCGGAATTTG – 3’	Reverse	67	01:00
nia2 (1)	5’ – TACGACGACTCCTCAAGCGAC – 3’	Forward	61	01:00
nia2 (1)	5’ – GGCTATAGATCCCGCATCGAC – 3’	Reverse	61	01:00
nia2 (2)	5’ – CATCTACCGTGACCTCCACAC – 3’	Forward	61	01:00
nia2 (2)	5’ – TGGTACGTCTCACAGGGAAAC – 3’	Reverse	61	01:00
nia2-5	5’ – ACGGCGTGGTTCGTTCTTACA – 3’	Forward	63	01:20
nia2-5	5’ – ACCTTCTTCGTCGGCGAGTTC – 3’	Reverse	63	01:20
nia1 (1)	5’ – ACCAGCAATTGTTCATCATCC – 3’	Forward	58	00:40
nia1 (1)	5’ – ATCGAGTCCTTCCTTCTCTCG – 3’	Reverse	58	00:40
nia1 (2)	5’ – CAGTAGTTCCAACTTTGTAGGACG – 3’	Forward	58	00:40
nia1 (2)	5’ – GGAAAGGTATTCCGTTAAGCG – 3’	Reverse	58	00:40

2.7 – Stomatal impressions for density and index

Three mature (6 week old), fully expanded rosette leaves, from 3 different plants of each genotype were taken for impressions (9 leaves total per genotype). The abaxial side of the leaves were placed on top of high definition dental resin (Coltene Whaledent, Switzerland) and left to set. The leaf material was then removed to reveal an impression, which was coated in a thin layer of clear nail polish and was left to dry for ten minutes. The nail polish patches were then transferred onto a microscope slide and the epidermal and stomatal cell numbers from 4 different areas counted on each leaf, using a light microscope (Nikon LABOPHOT2, Japan) and images collected using a 40x magnification objective, with an eyepiece grid (0.065 mm^2 area). The average stomatal density and stomatal index[2] for each genotype were determined and converted to a 1 mm^2 area. Differences between genotypes and treatments were determined using a one-way ANOVA with multiple pairwise comparisons.

2.8 – Measurement of stomatal apertures

Epidermal strips were taken from fully expanded mature rosette leaves from the abaxial surface of six week old *A. thaliana* plants. Three independent replicates of the experiment were performed on 3 sequential days. On each day epidermal strips were taken from 3 leaves per plant, 3 plants of wild type and mutant, making n=9. The strips were then transferred into Petri dishes containing 10 ml of opening buffer (10 mM 2-(N-Morpholino) ethanesulfonic acid sodium salt (MES), 50 mM KCl, pH 6.2 (using KOH to adjust pH)), which were illuminated by two light boxes (fluorescent bulbs), at an intensity of 300 µmol m^{-2} s^{-1}. To ensure aeration of the opening buffer, ambient air was bubbled through, into the Petri dishes via manifold attached to air-tight rubber tubing and a syringe needle at 100 ml min^{-1} and incubated for one hour at room temperature. Flow rate was set separately for each experiment to make sure that aeration provided adequate mixing of the opening buffer and did not displace the epidermal peels. The opening buffer was then removed from the Petri dish, using a sterile 10 ml syringe and replaced with one of four treatments, either: a) opening buffer (control), b) 1 mM abscisic acid (ABA) (dissolved in ethanol) (Sigma Aldrich, USA) in opening buffer, c) 5 mM ABA in opening buffer or d) 100 mM S-Nitroso-N-acetylpenicillamine (SNAP) (Caymen Chemicals, USA) in opening buffer. Samples were then aerated for a further for 2 hours before imaging.

[2] Stomatal density is the amount of stomata within a region of 1 mm^2 and the stomatal index (see equation below) is the ratio of epidermal cells to stomata within 1 mm^2.

$$\text{Stomatal index} = \text{Stomatal density} (\text{Stomatal density} + \text{Epidermal cell density})$$

For imaging, epidermal peels were placed on a microscope slide (hydrated by their treatment solution) and a cover slip placed on top. Images were taken immediately using an Olympus BX51 optical light microscope and images collected using a 40x objective lens, with a camera mounted on the 10X eyepiece to record images with the light intensity set to the lowest setting. A minimum of 40 stomata were imaged for each treatment and analysed using the object J package on Image J. Four measurements were taken for each stomata: pore width, pore length, complex width and complex length. The experiment was repeated three days in a row, resulting in a total of 120 stomata imaged per genotype. Data was expressed as µm and aperture areas were calculated using the formula for an ellipse (π ½ (length) ½ (width)). Results were expressed as aperture mean ± SE. Differences between treatments were determined using a one-way ANOVA with multiple pairwise comparisons.

2.9 – Cloning

2.9.1 – Primer design

Specific primers to include 35S promoters and native promoters in order to be GFP tagged were designed for *NIA1* and *NIA2*.

To design the primers to be on a 35S promoter, the full-length coding sequence for *NIA1* and *NIA2* were downloaded from The Arabidopsis Information Resource (TAIR), *NIA1* (AT1G77760.1) and *NIA2* (AT1G37130.1). Internal restriction sites were checked using NEB cutter V2.0 (New England Bio lab, UK) using the pMDC83 vector (Arabidopsis Biological Resource Center (ABRC), USA). Forward primers were designed to be 20-30 bp in length. *NIA1* forward primer had four AAAA bases then the *pacI* restriction site of TTAATTAA and 20 bases from the start of the gene. For the reverse primer, the stop codon and one additional base pair was removed and then the restriction site *kpnI* was added along with four AAAA bases. *NIA2* was designed in the same way and had a forward restriction site of *pacI* and a reverse primer restriction site of *kpnI*.

To design the native promoter primers, the *NIA1* sequence was found in TAIR and then blasted (using National Center for Biotechnology Information (NCBI) database) against *A. thaliana* genomic DNA, which results in a variety of sequences. The matched sequence gb|AC012193.6 was selected and the reverse compliment strand was looked at, as the gene was in the opposite direction. Restriction sites were checked using NEB cutter and compared to restriction sites present in the vector PMDC 107. *SpeI* (ACTAGT) was selected as a restriction enzyme for this experimental programme, because there is an *xba1* restriction site on the vector. A primer was then designed using primer3 (Koressaar and Remm, 2007; Untergasser et al., 2012), to include the *SpeI* restriction site on the forward primer. The reverse primer was designed for the 35S promoter.

For the *NIA2* native promoter, the Bacterial artificial chromosome (BAC) result (56334) was used. The restriction sites were checked as above, however there were none available. Therefore, the *xba1* restriction site was used and a primer was designed using primer3, situated approximately 1 KB before the start codon. Four AAAA bases were added, then the restriction site TCTAGA before the start of the forward primer. The reverse primer was designed for the 35S promoter, as above.

2.9.2 – PCR

Genomic DNA was extracted as above (see Section 2.3) and was quantified a Nanodrop spectrophotometer (Thermo-Fisher, USA). The gene of interest was amplified out, using specific primers with restriction sites, to enable ligation into vectors. KOD Hot start, high proofreading DNA polymerase enzyme (Novagen, Germany) was used in 50 µl reactions containing: 100 ng template DNA, 1 µl KOD polymerase, 1x ammonium reaction buffer, 25 mM $MgSO_4$, 5 µl mixed dNTP (dATP, dCTP, dGTP and dTTP), 0.3 µM of each a) *NIA1*(PMDC83) forward primer (5'-AAAATTAATTAAAT GGCGACCTCCGTCGAT-3') or *NIA1*(PMDC107) forward primer (5'-GTCGCCGTGACACATTGATA-3') and *NIA1* reverse primer (5'-AAAAGGTACCAAGATTAAGAGATCCTCCTT-3') primers, or b) for *NIA2*(PMDC83) forward primer (5'-AAAATTAATTAAATGGCGGCCTCTGTAGATAA-3') or *NIA2*(PMDC107) forward primer (5'-AAAATCTAGAGTGCTGAATTGCCATTTGTG-3') and *NIA2* reverse primer (5'-AAAAGGT ACCAATATCAAGAAATCCTCCTT-3'). The remaining volume was made up with nuclease-free water. A negative control (nuclease-free water) was performed with each set of PCR reactions prepared. The *NIA1* on the 35S promoter was amplified used the following conditions: 95 °C for 2 minutes initial denaturation; 35 cycles of denaturing at 95 °C for 20 seconds, annealing at 60 °C for 15 seconds and extension at 70 °C for 1 minute; and a final extension of 70 °C for 5 minutes. All remaining amplifications used these conditions with the exception of *NIA2* on 35S promoter, which had an extension time of 1 minute. *NIA1* on native promoter where the extension time was 1 minute 40 seconds and *NIA2* on native promoter, which had an annealing temperature of 62 °C and an extension time of 2 minutes and 5 seconds. Five µl of PCR product was added to 2 µl of orange loading dye and 3 µl of water and run on a 1 % (w/v) agarose gel for 30 minutes at 100 V and alongside Hyperladder I (Bioline, UK) to confirm the product size.

2.9.3 – PCR product purification

NIA1 (on a native promoter) PCR product was purified using Monarch PCR and DNA clean up kit (New England Biolab, UK), directly following the manufactures instructions. One µl of the purified product was then used as a template to perform a second, 20 cycle PCR with KOD, as described above (see Section 2.7.2), to improve band intensity.

2.9.4 – Restriction enzyme digests

To prepare the samples for ligation reactions, two restriction enzyme digests were performed; one to obtain the *NIA1* gene of interest and one to prepare the PMDC 107 vector (Curtis vectors, TAIR, UK) to insert the gene. Firstly, 10 µl of *NIA1* PCR product was used as a templated in a 20 µl enzyme digest, containing 0.5 µl of both enzymes *SpeI* and *KpnI*, along with 2 µl of 10x restriction buffer and 7 µl nuclease free water. The mixture was gently homogenized via pipetting, incubated at 37 °C for 1 hour in a water bath and the product purified as described above (see Section 2.7.3) and the concentration of DNA determined using a Nanodrop spectrophotometer.

Secondly, 10 µl of PMDC 107 was used as a template in a 20 µl enzyme digest, containing 1 µl of both enzymes *XbaI* and *KpnI*, along with 2 µl of 10x restriction buffer and 6 µl of nuclease free water. The mixture was gently homogenized via pipetting, incubated for 1 hour at 37 °C in a water bath. Four µl of loading dye was then added to the reaction and the mixture run on a 1 % (w/v) agarose gel alongside Hyperladder I (Bioline, UK). The product obtained was between 8-10 Kb (as expected), the band was excised from the gel using a razor blade and 200 mg of the product gel purified (see Section 2.7.5).

2.9.5 – Gel purification

The excised band was placed in a 1.5 ml microcentrifuge tube and 800 µl of gel dissolving buffer (Sigma) was added per 200 mg of gel. Sample were then incubated between 37 °C and 55 °C for 5-10 minutes and periodically vortexed until the gel was dissolved. The purification was then performed using a Monarch PCR and DNA clean up kit (New England Biolab, UK) directly following the manufactures instructions and the DNA concentration quantified using a Nanodrop spectrophotometer.

2.9.6 – Ligation reactions

Ten µl ligation reactions were set up using a 3:1 molar ratio of gene of interest : vector. The reactions contained: 1 µl of 10x ligation buffer (New England Biolabs), 0.5 µl of T_4 DNA ligase, 3 µl of purified PMDC 107 vector and 5.5 µl of *pNIA1*:*NIA1*. A positive and negative control were also prepared for each set of reactions. Once mixed, the reaction was incubated at room temperature for 30 minutes.

2.9.7 – Transformation into *E. coli*

Twelve and a half µl of NEB 5-α competent *E. coli* high efficiency cells (New England Biolab, UK) were thawed on ice. Once thawed, 0.5 µl of the ligation reaction was added to cells and gently mixed by flicking the tube 4-5 times. Samples were incubated on ice for 10 minutes, heat shocked at 42 °C for 30 seconds and then incubated on ice for a further 5 minutes. One hundred µl of pre-warmed sterile SOC media (20 g L^{-1} tryptone, 5 g L^{-1} yeast extract, 4.8 g L^{-1} $MgSO_4$, 3.603 g L^{-1} dextrose, 0.5 g L^{-1} NaCl

and 0.186 g L^{-1} KCl) was added to the tube (in a laminar flow hood) and the solution incubated at 37 °C for 1 hour in a shaking incubator.

Luria Bertani (LB) agar plates (10 g L^{-1} tryptone, 5g L^{-1} yeast extract, 10 g L^{-1} NaCl, 15 g L^{-1} agar (pH 7.5)) containing 100 µg L^{-1} kanamycin were prepared and pre-warmed to 37 °C. Fifty six and a half µl of the liquid culture was then spread on to duplicate agar plates, allowed to dry (in a laminar flow hood) and incubated overnight at 37 °C.

2.9.8 – Colony PCR

Colonies were picked, added to 100 µl of nuclease free water and incubated in a heat block at 100 °C for 5 minutes to lyse the cells. One µl of the cell solution was then used as a template for a colony PCR. Reaction conditions were undertaken as outlined in Section 2.4, using 0.25 µl of an insertion specific forward primer (*NIA1*) (5'-GTCGCCGTGACACATTGATA-3') and 0.25 µl of a plasmid specific reverse primer (*GFP*) (5'-ATCCTGTTGACGAGGGTGTC-3'), however only 3.5 µl of nuclease free water was used. The PCR cycle was: 94 °C for a 5 minute initial denaturation; 30 cycles of denaturing at 94 °C for 30 seconds, annealing at 58 °C for 30 seconds and extension at 72 °C for 1 minute and 30 seconds; and a final extension of 72 °C for 5 minutes. The PCR product was then run on a 1 % (w/v) agarose gel, to confirm that the insertion had been successful. Once confirmed, the positive colony was picked and incubated (shaking continuously) overnight in 5 ml of LB broth containing 5 µl of kanamycin at 37 °C.

2.9.9 – Plasmid miniprep and purification

Three ml of the liquid culture was used to perform a plasmid miniprep, using a Monarch plasmid miniprep kit (New England Biolab, UK) directly following the manufacturer's instructions. The remaining liquid culture was mixed with 80 % (v/v) glycerol solution and vortex gently for 30 seconds, to produce 15% (v/v) glycerol stocks, which were stored at -80 °C.

2.9.10 – Sequencing

To ensure that the *NIA1* gene was inserted into the PMDC107 vector in the correct orientation, 15 µl of purified plasmid was sent to the Genewiz® Sanger sequencing service (Takeley Sanger Sequencing Laboratory, UK) for sequencing. The sample was analysed using an Applied Biosystems 3730 DNA analyser (Life Technologies Corporation, UK). Plasmid DNA was sequenced using the M13 reverse (5'-CAGGAAACAGCTATGAC-3') primer to check orientation. Sequencing data was analysed using Chromas Lite (Technelysium Pty Ltd., Australia), converted into .FASTA file format and uploaded to NCBI database to confirm that the *NIA1* gene was inserted.

2.9.11 – Transformation in Agrobacterium tumefaciens

Fifty µl of *Agrobacterium tumefaciens* competent cells (strain C58) were thawed on ice. Once thawed, 5 µl of purified plasmid DNA (between 1 and 5 µg per sample) (see Section 2.7.9) was added to the cells and then incubated on ice for 5 minutes. Samples were then incubated in liquid nitrogen for 5 minutes, and subsequently incubated at 37 °C in a water bath for 5 minutes. Five hundred µl of pre-warmed LB broth was added to each tube and placed on a shaking incubator at room temperature for 2 to 4 hours. LB agar plates containing 50 µg/ml kanamycin (introduced T-DNA vector resistance) and 50 µg/ml rifampicin (*A. tumefaciens* naturally resistant) were prepared and pre-warmed to 28 °C. After incubation, cells were collected by briefly spinning the liquid culture at 7,000 x *g* for 15 seconds in a microcentrifuge and 277 µl, spread onto duplicate LB agar plates, allowed to dry, in a laminar flow hood and incubated for 2 days at 28°C.

A colony PCR was performed as described in Section 2.7.8, using the same specific primers to confirm that the insertion had been successful. Once confirmed, the positive colony was picked and incubated (shaking continuously) in 5 ml of LB broth containing 50 µg/ml of kanamycin and 50 µg/ml rifampicin at 28 °C for 2 days. Glycerol stocks produced as previously described (see Section 2.7.9) and stored at -80 °C, in preparation to transform plants via floral dip.

2.10 – Nitrate Reductase Enzyme Activity

0.2 g fresh tissue was flash frozen using liquid nitrogen and homogenised by grinding with a pestle and mortar. One ml of extraction buffer (2 mM EDTA, 2 mM DDT, 1 % PVPP, in 10 ml of 100 mM HEPES, pH 7.5) was added per 0.2 g of sample and centrifuged for 20 minutes at 20,000 x *g* at 4°C. During centrifugation, 1 ml of reaction buffer (100 mM potassium nitrate, 10 mM cysteine, 2 mM NADH, 10 mM $MgCl_2$ or 2 mM EDTA, in 100mM HEPES, pH 7.5) was prepared per sample and decanted into 1.5 ml Eppendorf tubes. After centrifugation, 300 µl of the supernatant was transferred into the reaction buffer, gently mixed then and incubated for 30 minutes at 30 °C (for colour development). After incubation, 60 µl of 500 mM zinc acetate solution was added to stop the reaction. Samples were the centrifuged at 2,000 rpm for 15 minutes. Sixty-seven µl of the sample supernatant was then transferred into a 96-well plate and 67 µl of sulphanilamide solution (1 % in 1.5 M HCl solution) and 67 µl of NNEDA (0.02 % in 0.2 M HCl solution) were both added to the well (Jaworski, 1971). The sample was incubated for 10 minutes at room temperature in the dark(**A**).

A 25 ml stock solution of 10 mM $NaNO_2$ solution was produced and serially diluted to produce a 25 ml 0.029 mM $NaNO_2$ solution (**S**). One thousand µl 100 mM HEPES (pH 7.5) solution (**B**) was also prepared and the following standard curve produced:

- B: 1000 µl HEPES 100 mM (pH 7.5) (**B**)
- C_1: 160 µl **S** + 840 µl **B** → 0.0034 mg/ml
- C_2: 330 µl **S** + 670 µl **B** → 0.0068 mg/ml
- C_3: 500 µl **S** + 500 µl **B** → 0.01035 mg/ml
- C_4: 670 µl **S** + 330 µl **B** → 0.0137 mg/ml
- C_5: 840 µl **S** + 160 µl **B** → 0.0179 mg/ml
- C_6: 1000 µl **S** → 0.0207 mg/ml

Sixty-seven µl of the sample supernatant was then transferred into a 96-well plate and 67 µl of sulphanilamide solution and 67 µl of NNEDA were both added to the well, in the same manner as the samples. Samples and controls were read at 540 nm using a FLUOstar Omega microplate reader (BMG Lab Tech, Germany). NO_2^- accumulation was calculated in nmol NO_2^- mg protein^{-1} h^{-1} using the data obtain in the NR assay (**A** and **B**) and the total protein concentration calculated using the Bradford method (**C**) (Bradford, 1976) (see Figure 2.3).

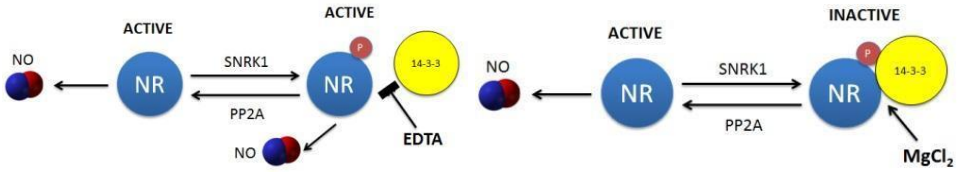

Figure 2.3 – Diagram of Active and inactive NR.

2.11 – Dynamic thermal imaging

Experiments were set up as described in (Hõrak et al., 2019). The difference being for barley grown (16 hour photoperiod, temperature 24 day / 20 night, light intensity 200 µmol^{-2} s^{-1}, 400ppm CO_2 and 60 – 67% relative humidity) with or without nitrate, barley (Golden Promise) seeds were surface sterilised and then placed into sterile tubes wrapped in foil, containing sterilised cotton wool and Hoagland's nutrient solution adapted to have with or without 5 mM KNO_3. Covered with parafilm until germination occurred and then slits cut in the top to allow seedlings to grow, nutrient solution was topped up periodically.

2.12 – Rice salt assay

Rice seeds (IR-64, *osEPF10eW* and *osEPF1oeS*) were germinated and seedlings frown for 7 days in a petri dish with 15 mls water in a Sanyo growth cabinet with a 12 hour photoperiod, 200 µmol m^{-2} s^{-1}

light intensity (PAR). Temperature 26 / 24 °C (Day / night), ambient CO_2 (400 ppm) and 60 – 67 % relative humidity. Plates were checked every 2 – 3 days for fungus growth, 7 day old seedlings were then transferred to 13D pots (0.881) (East Riding Horticulture, York, UK) containing soil consisting of 71 % Kettering Loam (Boughton, UK), 23.5 % Vitax John Innes No. 3 (Leicester, UK), 5 % silica sand and 0.5 % Osmocote Extract Standard 5 – 6 month slow release fertiliser (ICL, Ipswich, UK). Plants were placed into trays in batches containing water and placed into Conviron controlled environment growth cabinets (12 hour photoperiod, 30 °C day: 24 °C night, PAR 1000 $\mu mol^{-2}\ s^{-1}$ and 60 % relative humidity, ambient (400 ppm) CO_2. 13 day old seedlings were imaged and Fv/Fm measurements taken, all bar batch 5 were transferred to 50 mM salt, batch 5 remained in water. Measurements (images and Fv/Fm) were taken every 3 to 4 days, after one week of salt treatment batch 1 was returned to water, after 2 weeks batch 2 was returned to water, after 3 weeks batch 3 was returned to water and after 4 weeks batch 4 was returned to water from salt treatment. Plants were grown and measurements taken for a further 2 weeks. Tiller number was recorded and dry weight (Caine et al., 2019).

Chapter 3 – The roles of nitrate reductase in plant growth and as a source of nitric oxide in stomatal movements

3.1 – Introduction

Two important goals for crop improvement are Water Use Efficiency (WUE), to combat drought stress, and Nitrogen Use Efficiency (NUE) to allow growth in soils with lower nitrogen availability. In environments with limited nitrogen, plants with higher NUE can sustain better growth by optimising nitrogen uptake, assimilation, and remobilisation processes. This involves various physiological and biochemical adaptations, such as enhanced root architecture for better nitrogen acquisition, increased activity of nitrogen transporters, and efficient use of nitrogen in metabolic processes. Developing crop varieties with improved NUE is essential for sustainable agriculture, as it reduces the need for synthetic nitrogen fertilisers, lowers production costs, and minimises environmental impacts such as water pollution and greenhouse gas emissions. Genetic and biotechnological approaches, alongside traditional breeding methods, are being employed to enhance NUE in crops like rice, enabling them to thrive in nitrogen-deficient soils and contributing to food security in a resource-constrained world (Moll, R. H., Kamprath, E. J., & Jackson, 1982; Hirel, B., Le Gouis, J., Ney, B., & Gallais, 2007; Fageria, N. K., Baligar, V. C., & Li, 2008; Pathak, R. R., & Lochab, 2010; Xu, G., Fan, X., & Miller, 2012; Hawkesford, 2014). Plants use nitrogen to support a number of growth-related processes, for example, nitrogen is an essential component of chlorophyll, which captures energy from sunlight and via photosynthesis, enables plant growth and subsequent yield, and is a building block for amino acids and nucleic acids. Nitrate metabolism also generates signalling molecules related to stress responses. Nitrogen can enter plant roots in two main forms: ammonia and nitrate. Both are present in most fertilisers as ammonium nitrate. Urea is also a component of some fertilisers which through the action of the ubiquitous enzyme urease hydrolyse, provides plants with ammonia (Bucher and Kossmann, 2007). Certain plants (in particular legumes) have a symbiotic relationship with bacteria, called rhizobia, which inhabit small growths on roots called nodules and perform nitrogen fixation.

3.1.1 – Nitrate

Nitrate (NO_3) is an important nutrient for plants due to its mobility in soil. Nitrates are most commonly found in the soil in the form of fertilisers. The fertilisers contain both nitrate (NO_3^-) and ammonium (NH_4^+) ions. Due to the mobility of nitrate and its relatively small molecular size (62.01 daltons), it can be taken into the plant and transported via the transpiration stream. Nitrate transporters (NRTs, described in Chapter 1) are used for the uptake and transportation of NO_3 within the plant. Different forms of nitrogen have different purposes within the plant (ammonia and nitrate for amino acid and

subsequent protein formation, NO used as a signalling molecule and nitrate for growth and chlorophyll formation). NO, ammonium and nitrate are all crucial nitrogen-containing compounds involved in plant processes, each with distinct roles in plant physiology, metabolism and signalling. The balance between the three forms is important for optimal plant growth. Nitrate acts as a reservoir of nitrogen, which is reduced to ammonium ions which is assimilated into amino acids and proteins. NO acts as a regulator and is present in lower levels than nitrate but influences the efficiency of processes through signalling pathways. In particular, during exposure to stress, NO levels increase in order to mitigate the damage through signalling cascades, ammonium and nitrate availability influence the plant's ability to respond to the stress (Wang, Y., & Wu, 2013; Bloom, 2015). Both nitrate and ammonium are assimilated into the plant to make amino acids, proteins and chlorophyll. If plants are nitrogen deficient, growth, photosynthetic ability, appearance and subsequent grain and plant product quality are affected. When plants lack vital nutrients, their ability to respond to external stresses, for example drought, is affected. When plants start to struggle to obtain nitrogen, they can break down chlorophyll to release nitrogen and use it where it is most urgently needed; less chlorophyll leads to decreased photosynthetic ability and yellowing of leaves. Colour change can be due to other detrimental effects (not only a lack of nitrogen), such as high salt toxicity (which causes chlorosis), or lacking nutrients such as potassium (purple colour change). In older leaves, senescence also causes colour changes. Nitrate, after it is taken up via the roots, is primarily stored in the vacuoles in root, stem and leaf cells. Storage allows the plant to function when external nitrogen is low or in response to stress when there is a high biochemical demand. Nitrate is also stored to remove it from the cytoplasm to prevent toxicity. Nitrate stored in vacuoles also aids osmoregulation, maintaining osmotic balance within plant cells, helping to aid in cell turgor regulation (Hawkesford, M. J., & De Kok, 2006; Lea, P. J., & Azevedo, 2006; Krapp, 2015). An abundance of nitrate in the shoot apical meristem (SAM) can trigger flowering, conversely a decrease in nitrate availability can result in delayed flowering (Olas and Wahl, 2019). Nitrogen (mainly in the form of nitric oxide (NO)) is also used as a signalling molecule in stomatal aperture changes (Hetherington and Woodward, 2003). Stress responses are triggered via signalling pathways (such as abscisic acid (ABA) and the N-end rule pathway) to protect the plant (Desikan et al., 2004; Bright et al., 2006; Neill et al., 2008).

An example of a stress response is drought, where a plant may need to close its stomata to prevent water loss. It has been suggested that WUE could be modified through the manipulation of guard cell signalling pathways and stomatal density[3] (Kollist et al., 2014; Franks et al., 2015). In order for plants

[3] The number of stomata in a given area on a leaf's surface.

to respond, nitrate has to be assimilated into the plant, which is facilitated by the enzyme nitrate reductase (NR).

3.1.2 – Nitrate reductase (NR)

NR is a key enzyme in nitrate assimilation. It is the first enzyme of the nitrogen reduction pathway, which ultimately leads to the production of ammonia used for amino acid formation (see Figure 1.3 for the NR structure). Nitrate is first reduced to nitrite (NO_2^-) and then using the nitric oxide forming nitrite reductase (NOFNiR) subunit, nitrite is reduced to ammonium for assimilation into amino acids. Nitrite is also reduced to nitric oxide in plants. NO acts as a signalling molecule and can be transported to where it is required within the plant and is involved in various signalling pathways and stress responses. NO can be converted to other nitrogenous compounds or participate in signalling pathways before being removed or detoxified (Wendehenne et al., 2004; WILSON et al., 2008; Gupta et al., 2011). In Arabidopsis, NR is encoded by two genes, *NIA1* and *NIA2,* which are homologues/isoforms. NIA1 has a higher abundance / activity compared to NIA2. It has been suggested that the two different forms are involved in different stress responses and that they are regulated independently to assimilate nitrate, which is dependent on both stage and tissue type. (At the time of these experiments little was known about single mutant lines providing a gap in knowledge; most work had been performed on double mutant *nia1nia2*) (Salmi et al.; Tocquin et al., 2003; Zhao et al., 2016).

NR mutants serve as one of the enzymes to produce NO (through it's NOFNiR subunit) and play a role in the N-end rule pathway. They are used as an indicator for NO levels. Reduced NR activity lowers NO production, resulting in slower responses to stress stimuli. Previous studies (Zhao et al., 2009; Zhao et al., 2016) have focused on the *nia1nia2* double mutant. Growth observations from these studies indicated that some plants were smaller, whilst others were larger and resembled spinach plants. A literature review identified that the double mutant used in these studies was from a hybrid background, which could have influenced the observed growth response. (Plants were a cross between Col-0 and Ler. Control plants used were from the Col-0 strain. Ler, being a stomatal mutant).

3.1.3 – Nitric Oxide and N-end rule pathway

Post-translational modifications are important in both humans and plants, playing an important role in cellular functions. The N-end rule pathway for targeted protein degradation has been well documented as a part of the Ubiquitin-proteasome system (UPS). It relates to a proteins half life depending on the N-terminal residue. This pathway for targeted proteolysis has been linked to many developmental processes, most importantly for this project, the stomatal closure response, due to abiotic stresses (Gibbs et al., 2014a; De Marchi et al., 2016; Mendiondo et al., 2016). In plants, there

have been a group of Group VII ethylene response factors (ERFVII) that have been identified as substrates for this particular branch of the N-end rule pathway (Gibbs et al., 2014b; Gibbs et al., 2015; Papdi et al., 2015). ERFVII's are plant-specific transcriptional factors with conserved N-terminal domains (MC) which are dependent on NO and O_2 to be targeted for degradation via proteolysis. NR has been indicated by Gibbs et al. (2014b) to play a role in this pathway regarding the binding of ERFVII transcription factors and subsequent stomatal responses, based on the stabilisation of these transcription factors. NO is a signalling molecule in the N-end rule pathway for stomatal closure and NR is a way of viewing response / action of NO.

3.1.4 – SUMOylation

In plants there are different forms of post translational modifications which can affect a proteins activity and function SUMOylation is included in this. Small ubiquitin-like modifier (SUMO) proteins modify other proteins function by binding and detaching covalently to them, this process is known as SUMOylation. In most cases SUMOylation plays a negative role by repressing gene expression by affecting the interaction with DNA and chromatin.

With regards to NO and nitrate, SUMOylation plays a crucial role in the regulation of plant responses to these by modifying the activity and stability of key proteins involved in these pathways. This post-translational modification helps plants to adapt to environmental changes and efficiently utilises nitrogen resources. NO can influence the SUMOylation pathway modifying SUMO proteins or SUMO conjugation enzymes, altering their activity and stability. An example being NO-mediated S-nitrosylation of SUMO or SUMO ligases which can affect the SUMOylation of target proteins resulting in modulation of their function. Under stress conditions (e.g., salt, drought, pathogens), NO levels increase leading to changes in sumoylation patterns. The changes allow plants to adapt to the stress by altering the stability, localisation and activity of key regulatory proteins involved in stress responses. Nitrate uptake and assimilation involves several proteins whose activity is regulated by post-translational modifications including SUMOylation. Activity of enzymes nitrate and nitrite reductase can be affected. By modifying these enzymes, SUMOylation can fine-tune nitrate assimilation processes, ensuring efficient nitrogen use and adaptation to varying nitrogen availability. SUMOylation also plays a role in gene expression, particularly important for nitrate responsive genes, allowing plants to react to environmental changes in nitrate availability to survive and function (Gibbs et al., 2011b; Castro et al., 2012; Park, H. J., & Yun, 2013; Vosyka et al., 2020).SUMO sites can be predicted using bioinformatics tools (SUMOplot, GPS-SUMO and SUMOsp are all examples) which look for specific motifs in the protein sequence. In NIA1 there were three predicted sites, but one in particular was identified as the most likely site. Park et al., (2011) indicated that in Arabidopsis, the

lysine residue (K) in position 356 for NIA1 and K355 for NIA2 were the most likely predicted SUMO sites. Holdsworth group at the University of Nottingham used site directed mutagenesis to change K356 in NIA1 to an arginine (R) to disrupt SUMO site. This was expressed in Arabidopsis and lines created and nitrate reductase activity assessed (Miller and Vierstra, 2011; Park, H. J., & Yun, 2013; Elrouby, 2015).

3.2 – Aims and objectives

In this Chapter the overall aim was to identify the role of nitrate reductase in plant health, particularly in relation to abiotic stress responses in plants and more specifically in guard cell movements, focusing on the production of NO during nitrate assimilation.

Specifically to:

1. Investigate the impact of single mutant lines (nia1 and nia2) on plant growth and function:
    - Examine the phenotypic differences between nia1 and nia2 single mutants, particularly focusing on rosette leaf area, water loss and root architecture.
    - Determine whether these phenotypic changes are directly related to disruptions in NR activity.
2. Assess the effect of single mutant lines (*nia1* and *nia2*) on plant physiology and stress responses:
    - Analyse physiological changes, such as stomatal density, guard cell size and responses to ABA. This is to determine how these mutations affect overall plant stress responses, particularly drought tolerance.
3. Evaluate the ability of plants with reduced NR to survive under low nitrate conditions:
    - Test whether single and double mutant lines (nia1, nia2 and nia1nia2) exhibit differential growth, root architecture and survival under varying nitrate levels. To assess if reduced NR activity enables plants to adapt to low nitrate environments.
4. Show the role of SUMOylation in NR related plant growth and stress adaptation:
    - Investigate how disrupting SUMOylation of NIA1 affects NR enzyme activity, plant growth and stress resilience, particularly under drought conditions. This includes examining how changes in SUMOylation influence nitrate uptake and potentially distribution within the plant.

3.3 – Results

Previous studies have concentrated mainly on the nitrate reductase double mutant *nia1nia2*, which after research and initial experiments revealed that it was in a mixed ecotype background[4] (*nia1-2* from Columbia (Col-0) and *nia2-5* from Landsberg erecta (Ler)) (Tocquin et al., 2003; Lozano-Juste and León, 2010; Zhao et al., 2016). When focusing on stomatal responses a crossed background will give atypical results, especially as Ler[5] is a stomatal mutant. There has also been little characterisation of the single *nia1* or *nia2*, but it has been inferred that they are involved in responses to different stresses. The first steps were to characterise the single mutant lines and to create a double mutant in a Col-0 background.

The flow diagram shown in Figure 3.1 outlines the experimental analysis undertaken to assess the impact of mutations in the N-end rule pathway and the role of NO in regulating stomatal movements under abiotic stress conditions.

T-DNA insertion mutant lines were crossed to create double mutants (see Section 3.3.1 for results and more information). In order to view expression patterns with and without stress, *NIA1* and *NIA2* genes were isolated from Col-0 plants in order to tag the plants with GFP / RFP. However, whilst numerous attempts were made to isolate the *NIA* genes, sequencing confirmed that isolation was unsuccessful.

Experiments were also conducted on the single *nia1* and *nia2* mutants, whilst potential double mutant (*nia1nia2*) lines were propagated through generations. Limited literature is available on the characteristics of single mutants. However, in recent years it has been suggested that they may play distinct roles in various stress stimuli, notably salt stress (Rohilla and Yadav, 2019; Lee et al., 2021).

Method development was conducted to determine the optimal approach for testing both stress responses and the characteristics of the individual *nia* mutants compared to the wild type (Col-0). The plant's survival capacity was investigated by altering or eliminating the production of NR. Results in Section 3.3.4 showed that plants required both genes to be knocked out for a severe response to be observed.

T-DNA mutants in both *nia1* and *nia2* were ordered and crossed. Seeds were collected resulting in 2 successful crosses. Plants were grown from these crosses and the seeds were collected and germinated. Unfortunately, many did not germinate, and later generations were not found to be double mutants.

[4] A crossed background is when genes are taken from plants with different ecotypes which can have differences.
[5] Ler is a stomatal mutant, the erecta causes an increase in stomatal abundance.

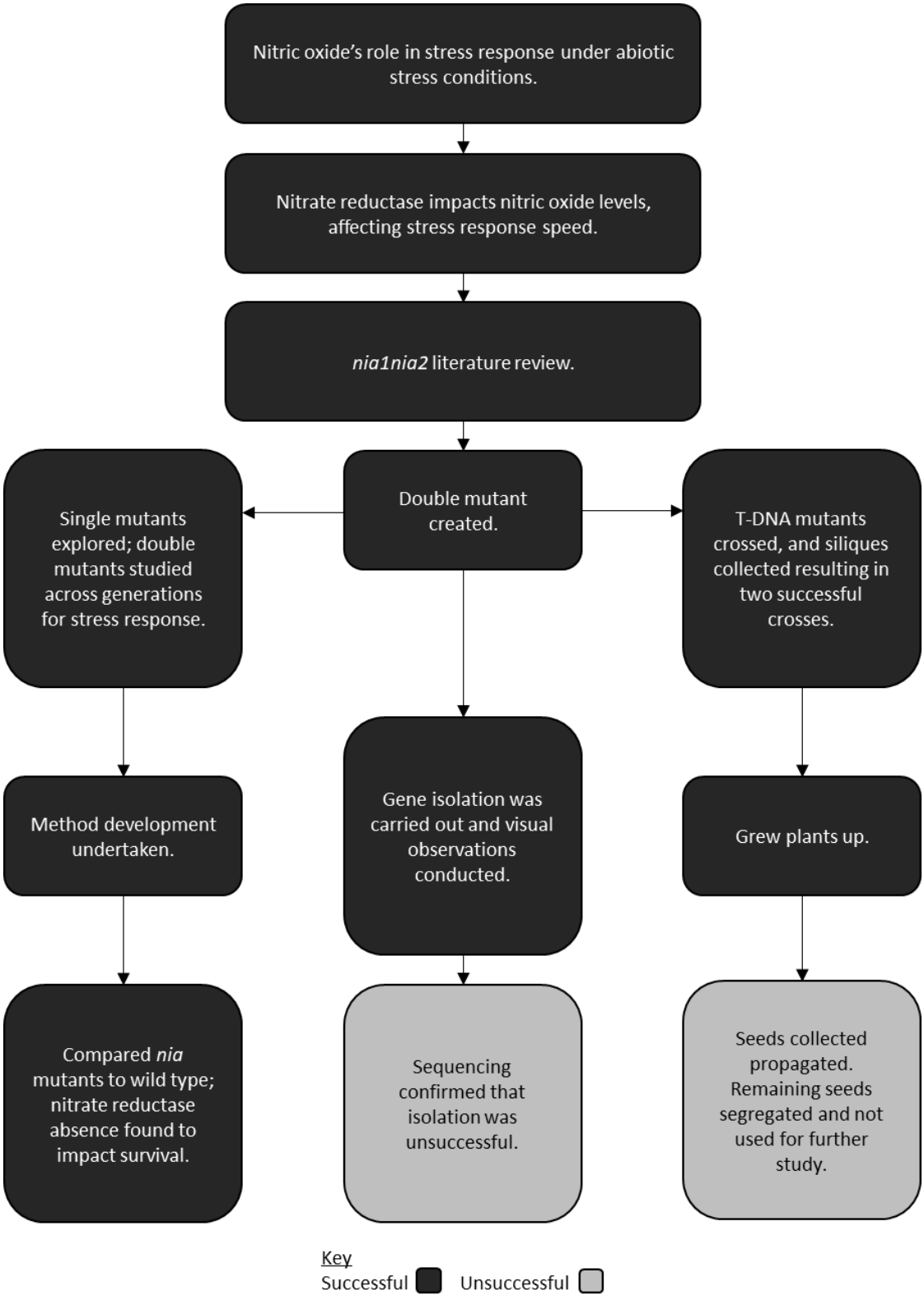

Figure 3.1 – Flow chart to show the workflow used to assess the impact of mutations in the N-end rule pathway and the role of nitric oxide (NO) in regulating stomatal movements under abiotic stress conditions. In particular NR which is important in the production of NO and response to stress.

3.3.1 – Generation of double mutants (*nia1nia2*)

Due to initial observations and a literature review, it was discovered that the double mutant *nia1nia2* (which had been used in previous work and supplied by Nottingham University) had been originally generated by the crossing of two mutants in different Arabidopsis ecotype backgrounds. This made it difficult to compare the double mutants to a relevant control. Having a mixed background could mean that any phenotypic changes or observations may not be due to the gene of interest, but instead due to the background. Therefore, a new double mutant was needed to allow for a proper control and investigation of the genes of interest. In order to create a double mutant, a range of single T-DNA insertion lines were ordered from the stock centre; two potential *nia1* and three *nia2* alleles were obtained. Plants were grown and then traditional crossing performed. A representative image is shown below (see Figure 3.2)

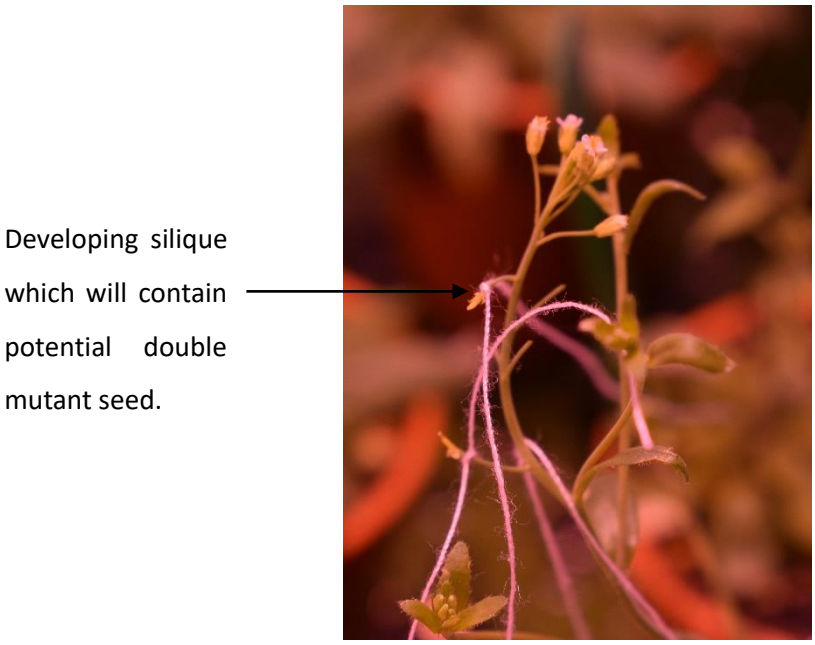

Figure 3.2 – A representative image of crossing method. Different coloured cotton was used to identify the different combinations for later genotyping. The plant shown is the mother; anthers, petals and sepals are removed making sure not to damage the stigma. Pollen from the male plant was used to pollinate the stigma. Pollination can either be done by eye or under a microscope.

The male or female recipient parent assignment depended on which plants were ready first. Anthers were removed to avoid self-fertilisation and stigmas cross pollinated. (see Figure 3.2). When siliques were mature, and before seed dehiscence, siliques were harvested and left to dry in Eppendorf tubes.

The siliques produced from crosses contained very few seeds. These were then germinated, plants genotyped, and seeds collected. It was noticed that the *nia1* mutants flowered slightly faster than the *nia2* mutants.

3.3.2 – Genotyping

Initially plants were genotyped using the male (father) specific primers, both wild type and mutant specific to identify plants. Female (mother) specific primers were then deployed to check for homozygous plants. Seeds from plants identified as homozygous mutant were collected. Figure 3.3 below shows an example result of genotyping. Leaf tissue was collected from homozygous plants and used for callus induction.

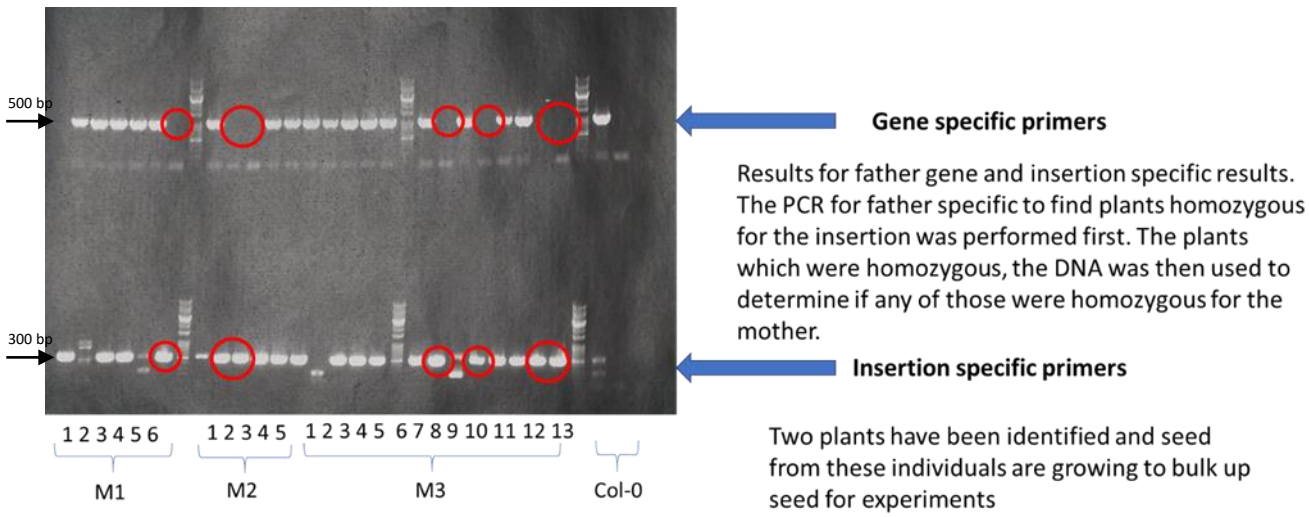

Figure 3.3 – An example of a genotyping gel for second generation seeds. M1 – M3 and numbers refer to individual plants and crosses between two T-DNA insertion parents compared to Col-0. The top line used gene specific primers and the bottom used the gene specific reverse primer with the left border primer to specifically amplify the insertion. The lines without a band in the top line but with a band in the bottom line are homozygous for the insertion and successful at least for single mutant lines. 1 kb ladder. PCR product of gene specific primers are approximately 500 bp in size. PCR product of insertion specific primers are approximately 300 bp in size.

3.3.3 – First generation confirmed double mutant plant material can be propagated via callus induction

Sometimes mutants are difficult to generate or can be sterile (this is gene dependent). Callus production can be used for newly generated double mutant plants for several reasons. It allows clonal propagation, ensures genetic stability, which enables the mutations to be preserved across generations. Callus tissue provides homogenous material for genetic and molecular analysis all under controlled environments. This allows gene expression studies, metabolic pathways and responses to

stress easier to examine. These advantages make callus production a powerful tool in plant biotechnology and genetic research (Hansen and Wright, 1999; Thorpe, 2007; Ikeuchi et al., 2013; Fehér, 2015). In order to make sure that any potential double mutant lines were not lost, callus production was performed on vegetative material (Ellis, 1993). Experiments can still be conducted on callus material as vegetative tissue and roots can be grown, but may not develop into whole plants. Root specific induction media was deployed and changed once a week under sterile conditions. Callus was grown from six week old leaf material, of confirmed double mutant plants, in petri dishes in controlled Sanyo cabinets under long day (16 hr photoperiod) conditions. The callus was grown until it reached a substantial size (at least 1 cm in diameter) and then some were transferred to shoot specific media for further callus development and the rest stayed on root specific media. Although callus production should lead to organ development both shoot and root depending on phytohormones present and growth conditions, there are limitations. It was suggested by Sugimoto and Meyerowitz (2013) that shoot regeneration depends on ecotype and under their conditions Col-0 and Ler were less efficient compared to other ecotypes. Roots form readily, but it is harder to produce shoots from leaf material. Unfortunately, due to unforeseen circumstances, the callus did not survive. Figure 3.4 represents an image of the callus' appearance. Underneath roots had started to form as well as on another callus produced. The roots started to embed in the media, which made it challenging to avoid transfer of previous media to fresh media.

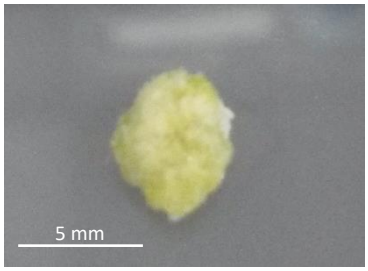

Figure 3.4 – An example of the callus produced from first generation confirmed leaf material. Callus was 5 mm in diameter. Underneath the callus roots had started to form penetrating the media.

3.3.4 – Characterisation of *nia1* and *nia2*

Most published work originally focused on the double mutant line, with little or no characterisation for the single lines. It has been suggested that *NIA1* and *NIA2* are involved in responses to different stresses and that they have different activity levels. It may be that single mutants do not have a clear phenotype and the double mutant does, as there may be gene redundancy, and possibly gene complementation. Characterising the single mutants will better help to understand the double mutant responses and the role of NR in plants and their responses to stress. Basic growth measurements will help to show if there are any differences between the two genes and can also see how this compares

to wild type (Col-0 in this experiment). Characterisation was mainly done via growth measurements from seed, leaf and root.

Previous work has suggested that *nia1nia2* is hypersensitive to ABA and therefore it was expected that the single mutant lines would also show hypersensitivity (Lozano-Juste and León, 2010; Zhao et al., 2016). NR is an important enzyme in the production of NO. NO is an important signalling molecule which plays a role in many processes, including germination. Plants with less NR should have less NO and therefore under higher ABA concentrations germination should be delayed. ABA is well known to induce seed dormancy and NO has been shown to inhibit ABA signalling (Signorelli and Considine, 2018). The role of NO in germination is crucial, by breaking dormancy, modulating the balance between gibberellins and abscisic acid, enhancing antioxidant defences, and regulating cell wall modification and gene expression. NO acts as a signalling molecule, interacting with reactive oxygen species and other compounds to facilitate the germination process (Bethke et al., 2007; Liu et al., 2010; Arc et al., 2013).

Previous work has suggested that in the absence of NO generation, the transcription factor Abscisic Acid Insensitive 5 (ABI5) ensures that seeds stay in the dormant state by controlling the expression of relevant genes. ABI5 expression in the double nia1nia2 mutant line may be indirectly affected due to alterations in nitric oxide (NO) production, which impacts the N-end rule pathway and the stability of Group VII Ethylene Response Factors (ERFs). These ERFs are regulated by the N-end rule pathway, which is sensitive to NO levels and can lead to proteolytic degradation of ERFs in the presence of NO. Since Group VII ERFs play a role in various stress responses and hormonal signaling, including interactions with the abscisic acid (ABA) pathway, changes in their stability can influence the expression of ABI5. ABI5 is a crucial transcription factor in ABA signaling, particularly in regulating seed germination and early seedling development under stress conditions. Therefore, the reduced NO production in the nia1nia2 mutant can lead to alterations in the N-end rule pathway, affecting Group VII ERFs and subsequently impacting ABI5 expression and activity. (Lopez-Molina et al., 2001; Gibbs et al., 2014b; Signorelli and Considine, 2018).

In Figure 3.5, when no exogenous ABA was applied, all genotypes germinated, and *nia1nia2* was the slowest. As the concentration of exogenous ABA increased, the speed of germination decreased. Viewing the graphs from left to right in Figure 3.5, as ABA concentration was increased it took longer for seeds to germinate. At 5 μM ABA Col-0 and old *nia1nia2* (mixed background) both had slightly slower germination rates than single mutants and this was more pronounced at 10 μM ABA. All single *nia* mutants appeared to be less sensitive to ABA compared to Col-0 and *nia1nia2*. After 8 days, at the end of the experiment, there appeared to be no effect of increased ABA on the germination efficiency

of both *nia1* mutants and *nia2 (2),* as all seeds germinated. This germination assay was repeated twice and showed similar results. NO and ethylene have both been shown to reduce seed dormancy, allowing seed to germinate by inhibiting ABA signalling. In this experiment, the double mutant *nia1nia2*, which has little or no NO production (from previous studies by Gibbs et al., (2014)), had reduced germination at higher ABA concentrations, and was more sensitive to ABA than Col-0. Because of problems with germination and growth, as well as the lack of a proper control (due to the two crossed backgrounds), it was decided not to include *nia1nia2* in further experiments in this Chapter.

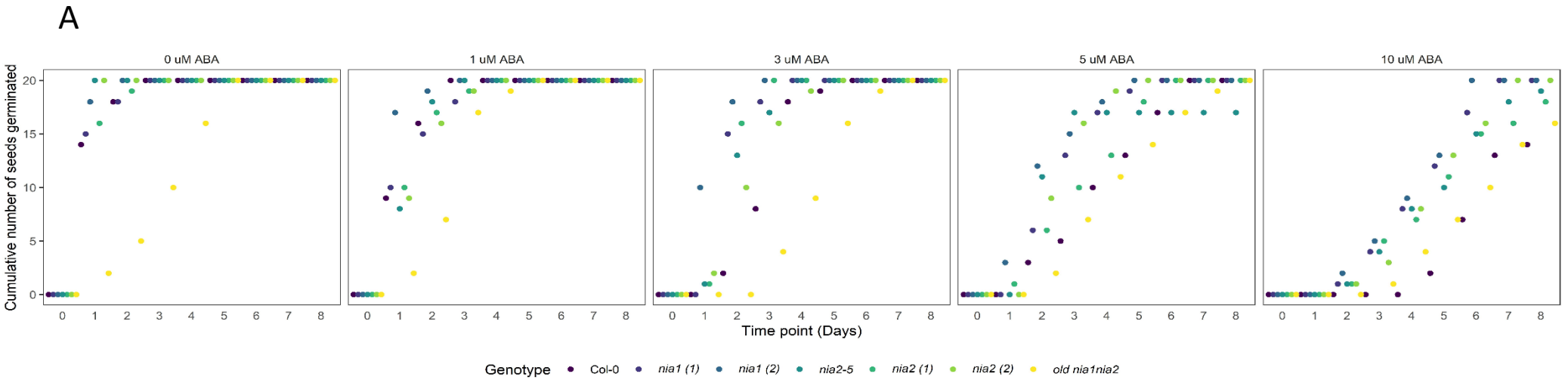

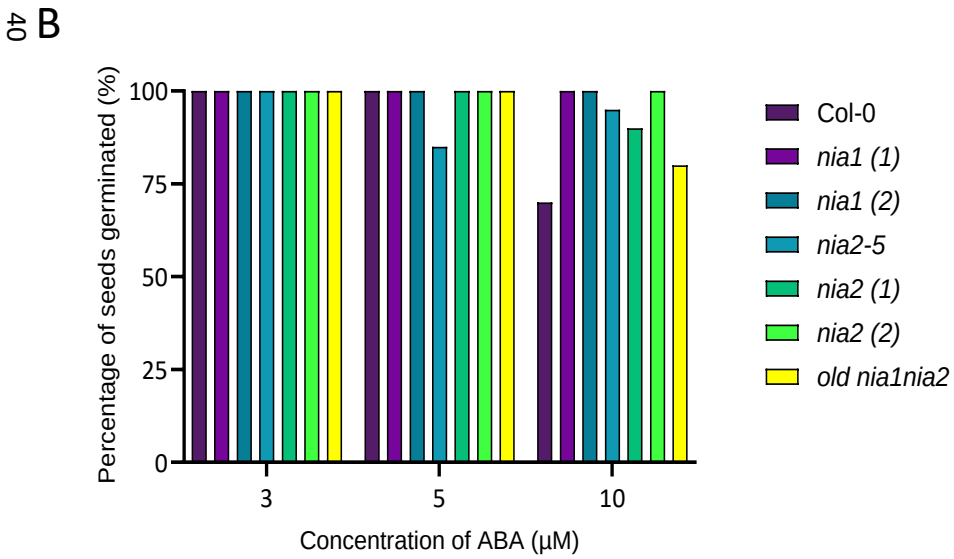

Figure 3.5 – Germination assay using increasing concentrations of ABA. (A) Cumulative number of seeds germinated out of a possible 20 seeds over a period of 8 days post sterilisation and plating. Left to right the ABA increases in concentration (0, 1, 3, 5 and 10 µM ABA). (B) Percentage of seeds germinated at the end point for 3, 5 and 10 µM ABA at 8 days.

When expression of *NIA1* was examined by RT-PCR in Figure 3.6 A, it appeared to be extremely low for *nia1 (1)* and higher in *nia1 (2)*, and at similar levels in the *nia2* mutants. These results suggested that for *NIA1*, only *nia1 (1)* allele was a gene KO line and *nia1 (2)* was not. Figure 3.6 A showed that when *NIA2* was potentially knocked out that expression of *NIA1* was significantly increased. When *NIA2* gene expression of mutant lines was performed, *nia1 (1)* had increased expression compared to Col-0 and *nia2* mutant lines. The results suggested that there would potentially be no significant impact on growth when a single gene was knocked out. Double mutant lines would most probably be required for severe phenotypes to be observed due to potential redundancy. Results seen could be influenced by the stage of leaf taken, but patterns seen could explain results further on in this report. Figure 3.6 B shows the expression levels of *NIA2* across the mutant alleles. *NIA2* expression appeared to be generally lower than for *NIA1*, and results showed that *nia2 (2)* had very low expression levels and was most likely a KO. Reduced expression was also seen in *nia2-5* which suggested a KD as opposed to a KO line. *nia2 (1)* had similar expression levels to Col-0 is most likely not a *nia2* KO or KD line. Thus, any effects seen in subsequent experiments are most likely due to off target T-DNA insertion effects. The literature suggests that NIA2 protein is the more abundant isoform and that it has a higher activity than NIA1. This is in contrast to the relative gene expression shown in Figure 3.6 which indicated that NIA1 had the higher expression levels – although as different primer pairs were used the reactions are not directly comparable, and transcript levels do not necessarily reflect protein or enzyme activity levels.

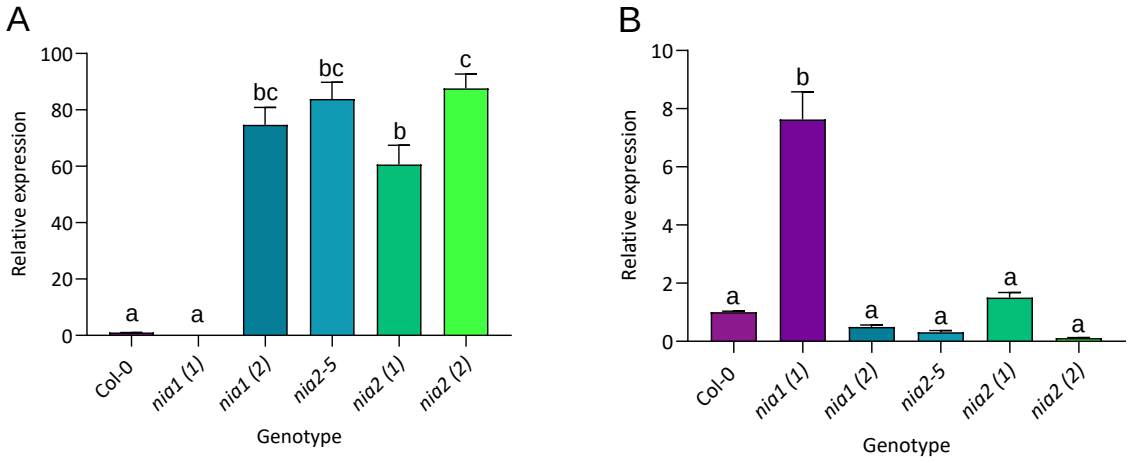

Figure 3.6 – Expression data for genes of interest *NIA1* and *NIA2* for single mutant lines compared to wild type (Col-0) using quantitative RT-PCR analysis. A) is expression levels of *NIA1* and B) is expression levels of *NIA2*, normalised to Col-0. One Way ANOVA performed followed by post hoc Tukey test. Letters denoted significant differences, $P < 0.0001$.

Once seeds germinate and begin to grow there are other traits which affect the ability of the plant to photosynthesise. One of these measures is the rosette leaf area of mature plants. The larger the leaf area potentially the larger area for light absorption and a higher stomata number per leaf, and the potential for more water loss from the larger surface area (Lawson and Blatt, 2014). Nitrate plays an important role in plant growth and therefore plants with less NR, might be expected to have reduced assimilation of nitrate with slower growth. This could cause effects not only on above ground parts but also on root growth. NR is most highly expressed in root tissue (*NIA1* had absolute gene expression of 1433.75 compared to *NIA2* which was lower at 674.98) and expressed in mature leaves (*NIA1* had absolute values of 898.98-1197.02, which was lower than *NIA2* which was 3124.23-3306.07). The gene expression values were taken from data displayed in the eFP browser available at arabidopsis.org. These data also indicate that expression levels of both genes decrease in leaves after flowering and that *NIA2* gene expression is relatively higher in cotyledons and the hypocotyl compared to *NIA1*. Nitrate is mainly obtained from fertilisers in the soil, in crops, which then can be transported to where it is needed via NRTs. NO is a molecule which can easily be transported to where it is required. Figure 3.7 is the area estimation of rosette leaves using imageJ of 6 week old plants. As can be seen, *nia1 (1)* was significantly smaller than Col-0 but not significantly different to any of the other *nia* mutants tested.

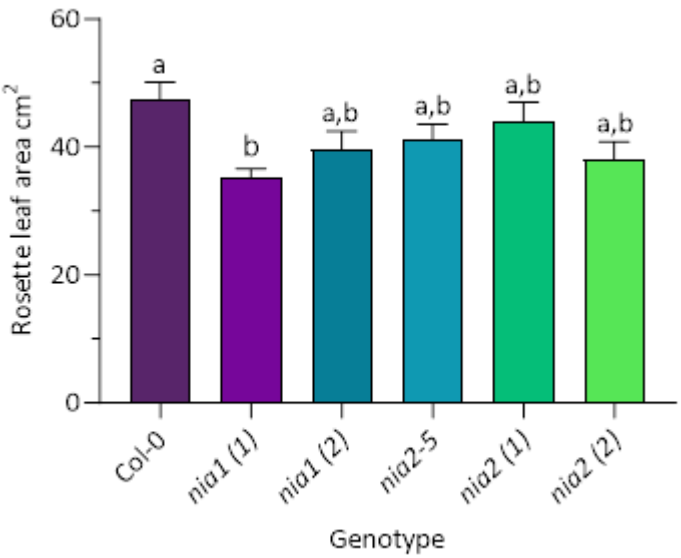

Figure 3.7 – Rosette leaf area of 6 week post germination mature plants. Mean values plotted and error bars were ± SEM. One way ANOVA followed by post Hoc Tukey tests were performed, letters denoted significant differences $P < 0.05$ ($n = 18$), samples which share a letter are not statistically different.

As there was a difference in rosette leaf area, this can influence processes such as transpiration and photosynthesis and affect responses to stresses such as drought. Smaller leaves in principle should lose water slower under drought conditions than larger leaves due to the smaller surface area. Due to *nia1 (1)* having a significantly lower rosette leaf area compared to Col-0, it was necessary to see if there was a correlation with leaf size and water loss, therefore a water loss assay was performed, which can infer a drought response. Also, of interest was *nia2 (2)* (confirmed KO line) which although had a reduced rosette leaf area compared to Col-0 it was not statistically significantly different. In Figure 3.8 three leaves of similar size from each plant were taken and placed into pre-weighed petri dishes. The fresh weight loss assay was a crude way to perform a drought experiment. It was seen that *nia1 (1)* lost water faster than the other genotypes in the first 9 hours and then levelled off. After 24 hours all mutant lines lost more water than Col-0 but there was no difference between the mutant lines. As this result was different to the expected (single lines expected to lose water faster), stomatal densities were viewed to determine if the higher water loss was due to a higher stomatal density.

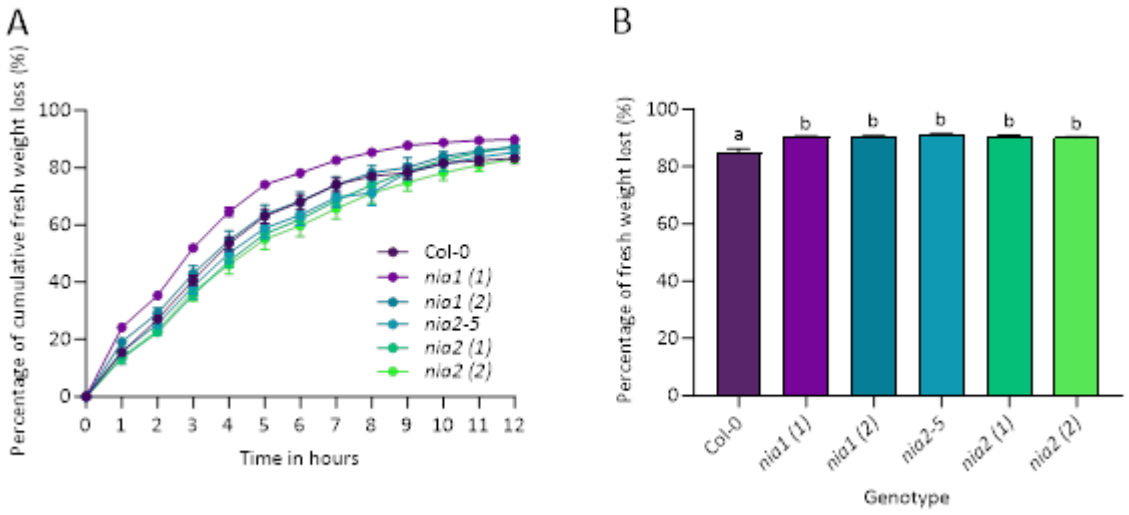

Figure 3.8 – There is a difference in cumulative fresh weight loss between genotypes. (A) The percentage of cumulative fresh weight lost over a period of 12 hours. Mean values plotted and error bars ± SEM, n = 10. (B) Percentage of fresh weight lost after 24 hours. Error bars ± SEM, one way ANOVA followed by post hoc Tukey tests performed. Letters denoted significant differences, $P < 0.05$ (n = 10). Samples which share a letter are not statistically different.

Due to the result from the fresh weight loss assay, stomatal densities were investigated as a higher stomatal density can result in a higher water loss. Figure 3.9 shows the stomatal densities from leaf 6 from 6 week old plants. There was no difference in stomatal densities or stomatal index between any

of the genotypes or between abaxial or adaxial sides of the leaf. Smaller leaves are sometimes correlated with a higher stomatal density and smaller stomatal complex size. This did not appear to be the case. The rosette leaf area difference in *nia1 (1)* was only slight and no difference was detected in stomatal densities.

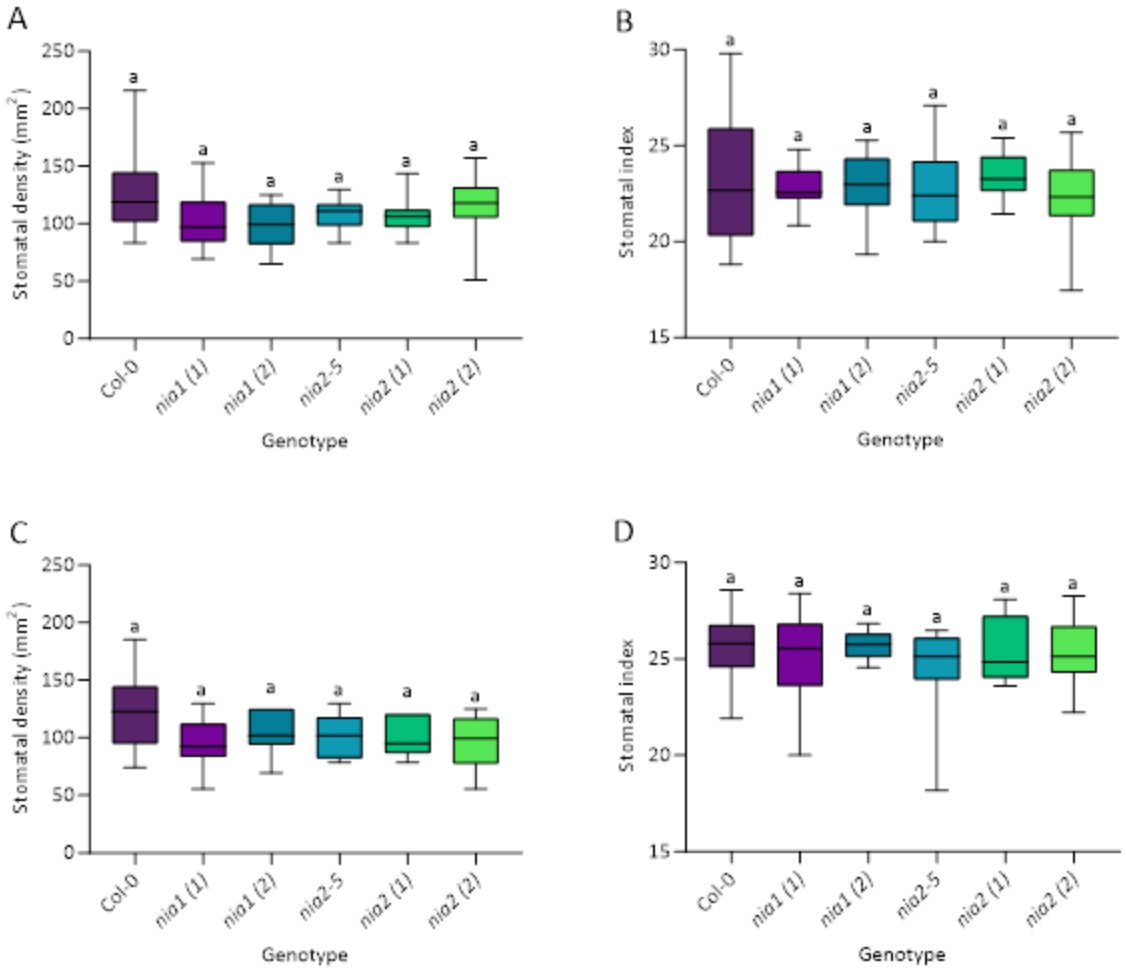

Figure 3.9 – There was no difference in stomatal densities between Col-0 and *nia* mutant lines. Leaf 6 impression data from 6 week old leaves of Col-0 and *nia* mutants. Stomatal density (A) abaxial and (C) adaxial. Stomatal index (B) abaxial and (D) adaxial. A one way ANOVA was performed. Letters denoted significant differences. There was no significant differences between any genotype for stomatal density or index on either abaxial or adaxial side (n = 40).

Along with stomatal densities, stomatal complex sizes have an impact on transpiration and therefore water loss. Smaller stomata will have smaller pores and therefore lose less water than larger stomata. They may also be able to close faster than larger stomata, which is a benefit under drought like conditions. The transpiration stream is also important to pull nutrients up through the roots and stem and be transported to where they are required. Figure 3.10 shows that there were differences in

stomatal complex sizes, which may have an impact on results and may indicate an alteration in development process, leading to slight complex size changes. The spread of data is wide and therefore may not impact overall when plants are put under stress conditions and observations seen may be due to control mechanisms as opposed to structure and size. Although *nia1 (1)* has smaller stomata, which may be due to smaller rosette leaf area, the leaves lost water at a faster rate compared to the other mutants, which suggests that the effect could be due to stomatal aperture. If stomata cannot close as much, then they may lose more water than more closed stomata.

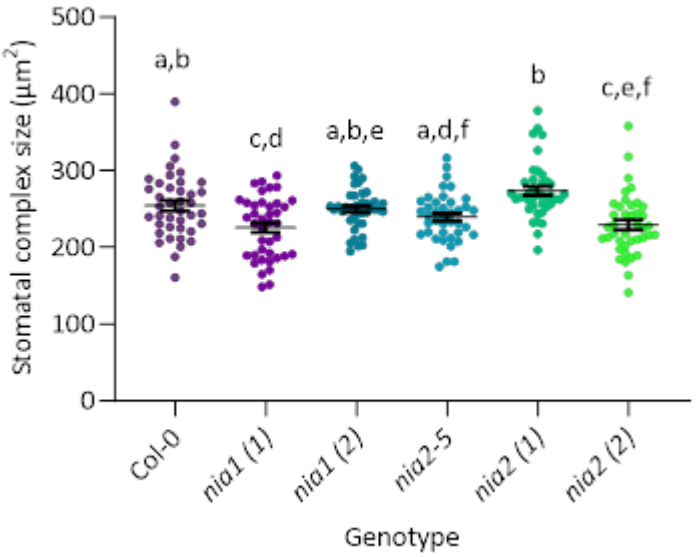

Figure 3.10 – There are differences in stomatal complex sizes between Col-0 and *nia* mutant lines. Stomatal complex size of Col-0 and *nia* mutants. Means plotted, error bars were ± SEM. One way ANOVA followed by post hoc Tukey tests performed. Letters denoted significant differences $P < 0.0001$ to $P < 0.05$ ($n = 40$). Samples which share a letter are not statistically different.

Stomatal aperture and response to stress involves many signalling pathways and in particular stomatal closure involves ABA as well as the N-end rule pathway involving NR. Reduced NR and therefore NO could result in less closed stomata. Work by Zhao (et al., 2016) suggested that the potential of certain genes in *nia2nia2* are being downregulated, such as GORK (K^+ moves out of guard cells) and AKT2 (K^+ moves into guard cells) with an upregulation of AKT1 (K^+ moves into cells). An increase in K^+ into cells would cause a movement of water into cells increasing turgor pressure and therefore result in more open stomata. Based on this, differences in a double mutant line would be expected, but due to the potential redundancy of the genes the same might not be seen in single mutant lines. Figure 3.11 overall showed that there was a response to increased ABA concentration. Increasing ABA concentration caused stomata to be more closed. In some experiments there appeared to be

significant differences between the genotypes, but it was not reproducible between experiments and therefore unlikely to be true and probably not the reason for the increased water loss.

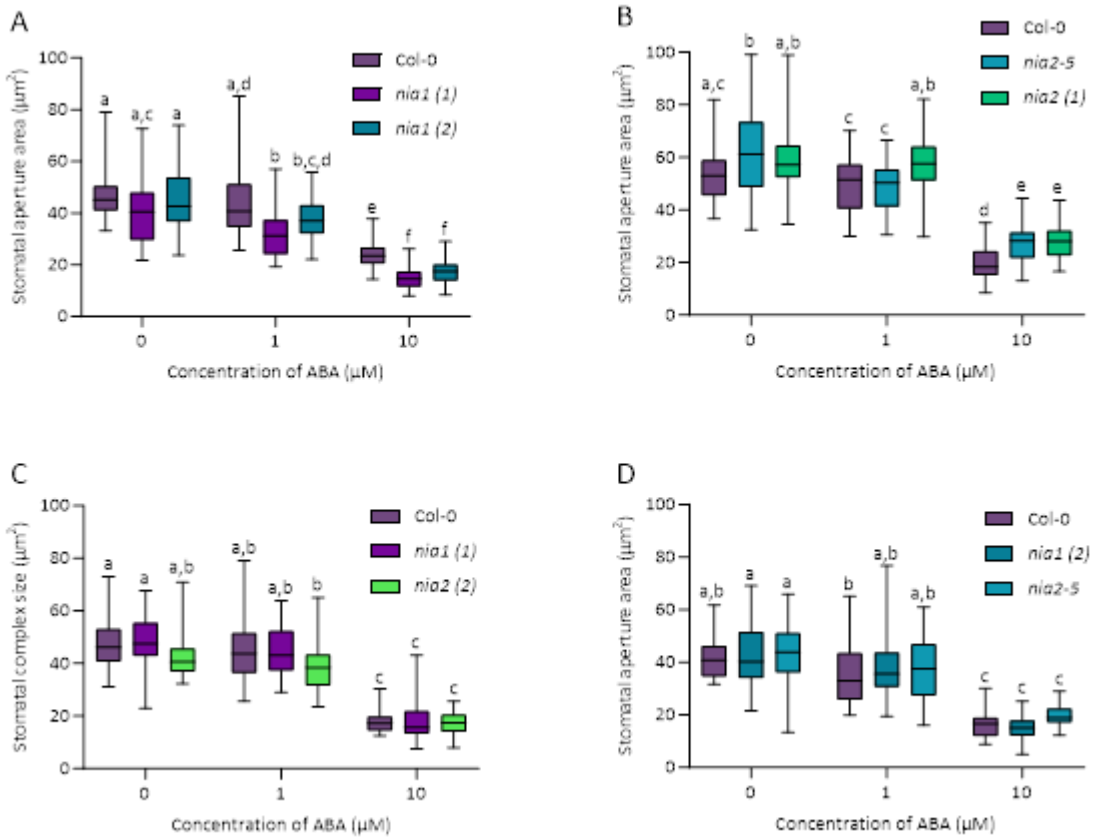

Figure 3.11 – Epidermal peel bioassay for Col-0 and *nia* mutants under ABA concentrations. (A – D) combinations of Col-0 and *nia* mutants used under application of increasing ABA concentrations (0, 1 and 10 µM) for epidermal peel bioassays. Standard box plot and whisker diagram, where boxes represent interquartile range and whiskers were minimum and maximum values. Two-way ANOVA performed with Geisser – Greenhouse correction followed by multiple comparison Tukey tests. Letters denoted significant differences. Samples which share a letter are not statistically different. $P < 0.05$.

Plants have many control mechanisms to keep healthy and grow, which can falter when exposed to stresses. Any stress which involves a loss in nitrogen can affect chlorophyll levels. Chlorophyll fluorescence measurement can be used as an early indication of stress. Plants lacking in nitrogen tend to have more yellow leaves and will not grow as large as healthy plants and will flower early as a survival mechanism. The nitrate available will move to the sink tissues via NRTs and an increase at the SAM can trigger flowering (Olas and Wahl, 2019). This was seen in old *nia1nia2* double mutants.

When plants lack nitrogen, they can break down chlorophyll for nitrogen use elsewhere; this usually results in chlorosis which is extreme stress. Chlorophyll fluorescence is not limited to nitrogen stress, it is also used to measure responses to environmental stresses, which reduce plants' ability to metabolise normally. The measurements are a ratio of Fv/Fm (Variable fluorescence / maximum fluorescence, a ratio representing the maximum potential quantum efficiency of Photosystem II (PSII) if all capable reaction centres are open in plants. This indicates the potential for photochemical energy conversion in photosynthesis and commonly used as a measure of plant stress or health. (Sánchez-Moreiras et al., 2020). Figure 3.12 showed the Fv/Fm measurements of plants grown under normal conditions, to see the effect of *NIA* gene on chlorophyll fluorescence. Although visually the bars are apart, there is no significant difference between most of the lines, in particular *nia1 (1)*. There is however, a significant difference between *nia2 (2)* and Col-0 suggesting that reduced *NIA2* gene expression affects nitrate content and subsequent chlorophyll content in *nia2* mutant line. The result corresponds to gene expression levels in mature leaves, *NIA2* was substantially higher in mature leaves compared to other tissues and *NIA1*.

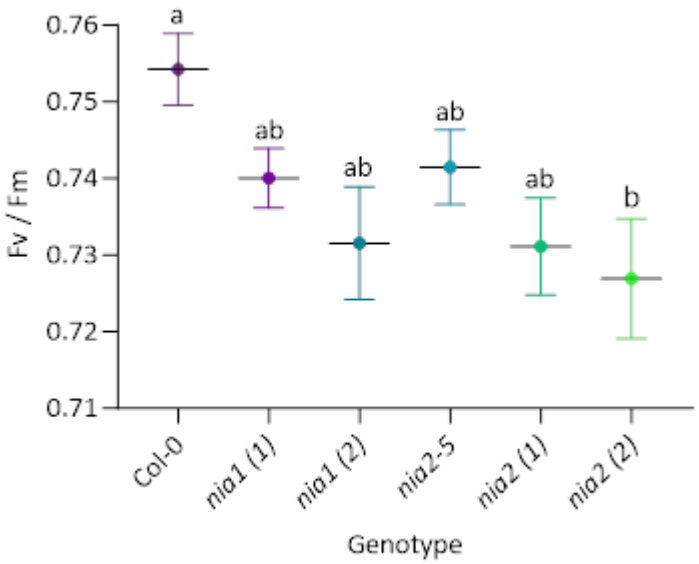

Figure 3.12 – Chlorophyll fluorescence values from 6-week-old leaves. 3 points per leaf were taken and averages per plant used (n= 15). One way ANOVA followed by post hoc Tukey tests were performed. Letters denoted significant differences, $P < 0.05$. Samples which share a letter were not statistically different.

3.3.5 – Methods for viewing responses to changes in nitrate levels

Most previous work utilising NO_3 involved root systems and aimed to determine if it is feasible to grow plants on plates where nitrate levels could be controlled, and for how long it is feasible to grow them.

Tests were performed ranging from low (0.1 nM, 0.1, 1 and 5 mM) normal (7 mM) and high (10, 50 and 100 mM) nitrate concentrations using Col-0 to begin with (If Col-0 does not survive, *nia* mutants are unlikely to) (Linkohr et al., 2002). A more effective approach is to study single mutant lines to establish optimal nitrate concentrations, ATS solution was chosen, which has been used in previous studies (Dharmasiri et al., 2005; Terrile et al., 2012; Waldie and Leyser, 2018). To ascertain the best way to view effects of nutrient deficiency and if plants lacking in NR can better survive compared to Col-0, plate growth experiments were undertaken at various concentrations and the root growth for Col-0 observed. From the plate work, concentrations to use for plant watering were determined. Initial experiments were carried out on agar plates. The results showed that Col-0 seeds could germinate well on concentrations of nitrate ranging from 10 nM to 100 mM. However, seedling growth establishment was less successful at lower nitrate concentrations (see Figure 3.13). Lower nitrate concentrations resulted in longer root growth, a higher number of root hairs and smaller cotyledons, which were lighter in colour (Figure 3.13). This suggested that the plants were sacrificing shoot development for root development, in an attempt to obtain higher levels of nitrate. Seedlings on higher nitrate appeared healthier, with shorter root growth, less root hairs and green healthy cotyledons.

Alongside these experiments, differing ways of growing plants on solid media with ATS solution were tested. It was found that sand with terragreen in a mix of 3:1 was better for growing plants than a mix of sand with vermiculite (3:1). Vermiculite caused the plants to become too waterlogged and stressed, resulting in early bolting; 5 weeks after germination (see Figure 3.14).

Overall, observational (qualitative) results inferred that a robust method of growing plants had been developed (whilst controlling nitrate concentrations). However, growth of mutant line was affected and when tested, survivability was poor. Therefore, this methodology was not used further for these mutant lines.

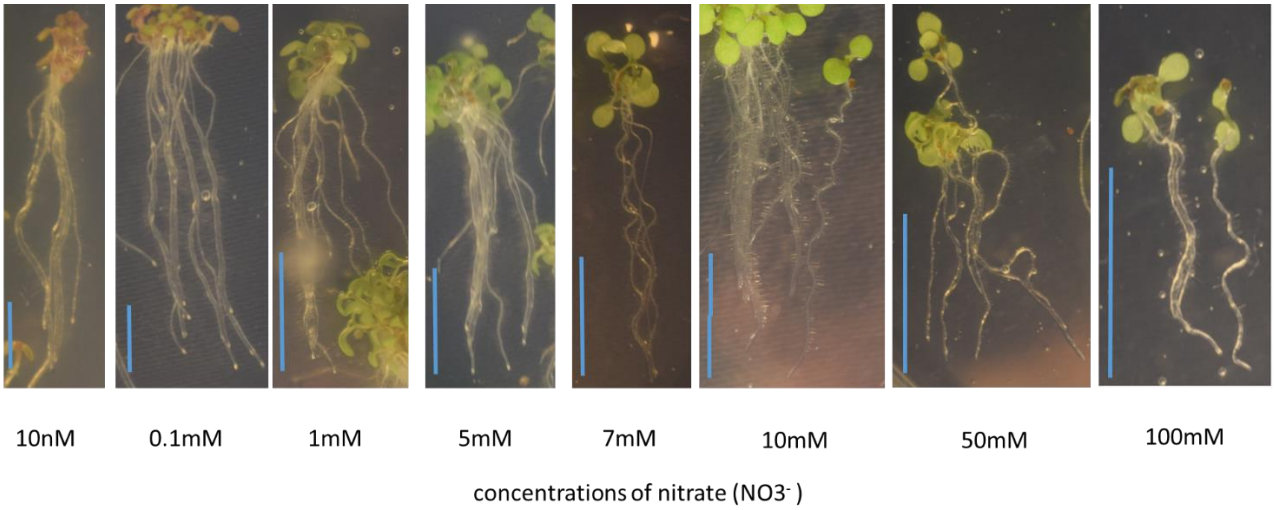

Figure 3.13 – Germination of Col-0 seedlings on varying concentrations of nitrate. Images from one week after germination, taken with Nikon AF-S DX digital camera. Scale bars represent 1 cm.

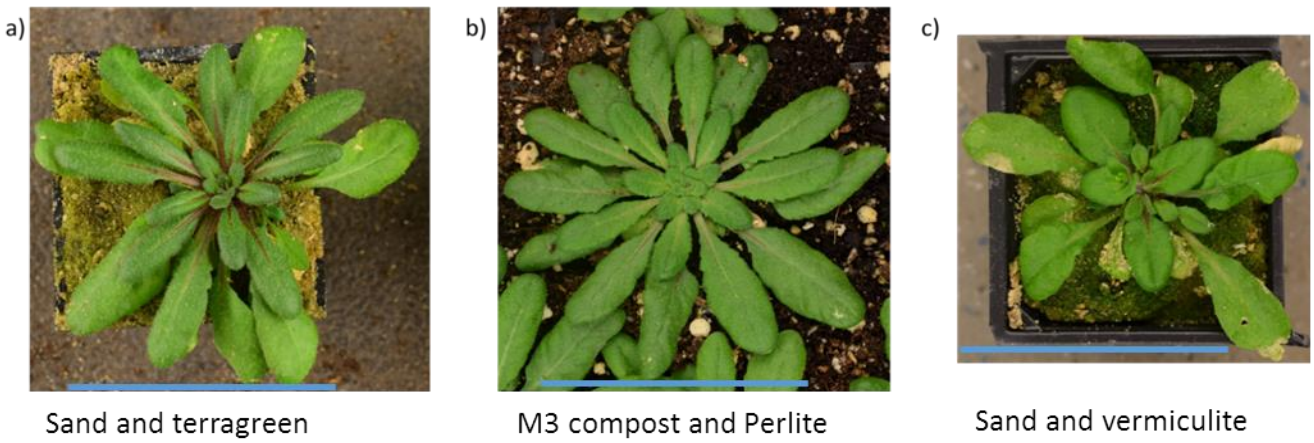

Figure 3.14 – Growth of Col-0 on different solid media with nitrate. Col-0 plants imaged 5 weeks after being germinated on plates and transferred to pots containing either, a) sand and terragreen (3:1 mix) fed with 7 mM NO_3^- ATS solution, b) M3 levington peat compost and perlite (3:1 mix) or c) sand and vermiculite (3:1 mix) fed with 7 mM NO_3^- ATS solution. Scale bars represent 5 cm.

In order to get an initial idea on the differences between the mutant lines and Col-0 with and without NO_3 seedlings were germinated on media containing nitrate and then were transferred to plates with or without nitrate. Root length difference observed after 7 days. The results in Figure 3.15 showed that root growth for plants without nitrate was not longer than with, which was unexpected.

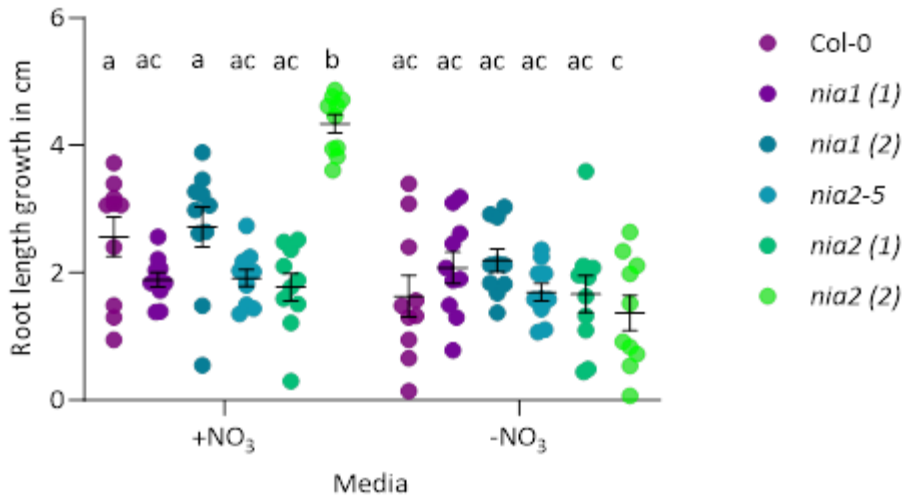

Figure 3.15 – There are variances in root length of plants grown with and without NO_3. The graph represents the difference in growth of seedling roots after 7 days exposure to media containing or omitting NO_3 after germination and growth for 7 days on normal media. Individual points are shown and bars represent mean ± SEM. n = 10 and letters denote significant differences. Samples which share a letter are not statistically different. Two – way ANOVA was performed followed by post hoc Tukey tests.

Root growth is important for plant survival (nutrients are obtained from the soil and roots provide anchorage). When looking at roots utilising media on plates, work can only be deployed for early seedling growth due to growth space limitations including the size of the plates, a set amount of nutrients and high humidity which affects growth. There have been lots of previous studies on nitrate which involve looking at roots and in particular split plates between nitrate and ammonia or with and without nitrate (Thirkell et al., 2016).

This investigation depended on larger more established plants (due to the need of controlling nutrient levels), so a hydroponic system was developed (modified from (Conn et al., 2013)). Unfortunately for Arabidopsis the nia mutants did not survive once transferred from the initial germination tub to the larger growth tubs.

To compare nitrate response and expression levels, it was decided to perform a nitrate reductase enzyme assay on mature leaf tissue and seedlings on the lines. The higher the activity of NR, the more NO_2^- would be produced overall (comparing active and inactive forms normalising to protein content) . Figure 3.16 showed that *nia1 (1)* and *nia2-5* have less activity compared to Col-0 and provided more interesting mutants to study responses. There was still NO_2 accumulation in *nia1nia2* suggesting another control mechanism.

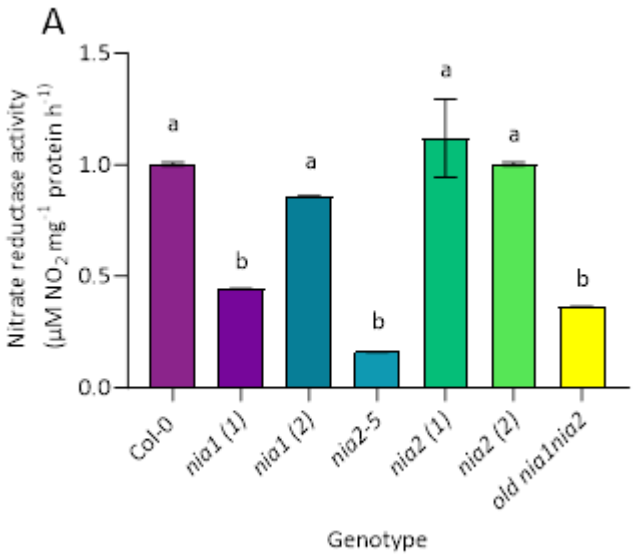

Figure 3.16 – Activity of NR is reduced in some lines compared to Col-0. Nitrate reductase enzyme assay. One-way ANOVA performed followed by post hoc Tukey test. Letters denoted significant differences, $P < 0.0001$.

3.3.6 – Disrupting sumoylation in NIA1 enables plants to recover from short term drought

As sumoylation negatively regulates gene transcription, it was hypothesised that disrupting sumoylation could cause gene overexpression. It was therefore of interest to investigate whether the impact of overexpression compared to gene expression knockout or knockdown differed from wild type (Col-0). Sumoylation is considered to be a diverse function, used in many ways to help control seed dormancy, growth, flowering and responses to stress such as drought and salt. In Arabidopsis there are many isoforms but only two have been shown to be conjugated onto target proteins upon various types of stress (AtSUMO1 and AtSUMO2) (Srivastava et al., 2016; Clark et al., 2022).

Potential SUMO sites were identified in *NIA1* and *NIA2*. Park et al., (2011) indicated that although there were more (3 for *NIA1* and more for *NIA2*) potential sites of SUMO conjugation in Arabidopsis, the lysine residue (amino acid code K) in position 356 for NIA1 and the lysine residue in position 353 for NIA2 were the most likely predicted sites (See Section 1.5). It was also revealed that K356 is not present in some lower land plants. Based on this, a sumoylation defective mutant for NIA1 was obtained which had been created by a targeted point mutation at the University of Nottingham. K356 was changed to an arginine (R). When more than one SUMO site was KO plants were not viable (sterile). Only *NIA1* was chosen for creation of a *NIA1 sumoylation defective mutant* (*NIA1 SDM*), partly due to research and the literature indicating that NIA1 protein is involved in environmental stress responses. It has been suggested that a balance between adaptation to stress and maintaining normal growth balance is via *NIA1*. NIA2 protein is involved in the regulation of plant growth and maintaining

the nitrogen source required for normal plant growth. To begin with it was prudent to see if there were any initial phenotypic changes by disrupting a potential sumoylation site. Germination was observed when growing plants with NIA1SDM lines germinating faster than Col-0. The potential increase in NR could cause an increase in NO which would help to offset the effect of seed dormancy by ABA.

Rosette leaf area is also a good indication of how healthy a plant is, larger leaves indicating more resources for growth. Higher availability of nitrogen can allow more vegetative growth. Figure 3.17 showed that mutant lines were significantly larger than Col-0.

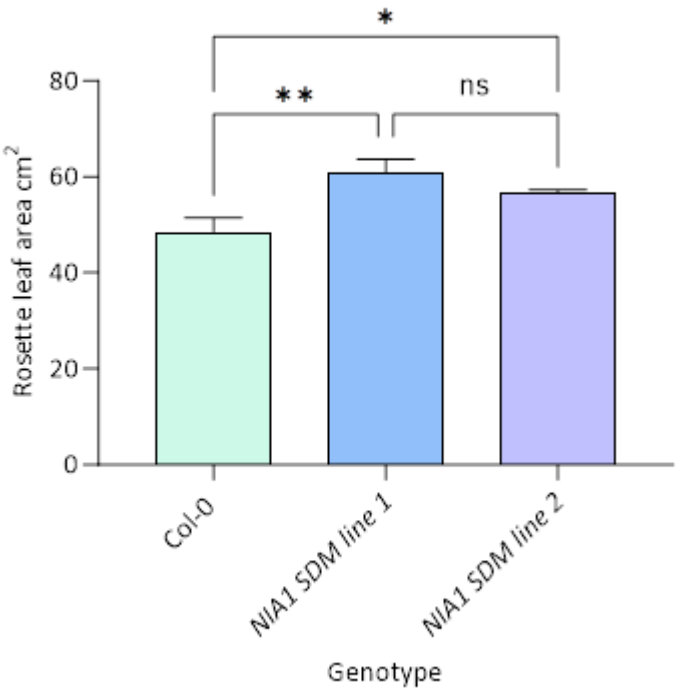

Figure 3.17 – *NIA1 SDM lines* had a larger rosette leaf area than Col-0. Rosette leaf area of 6 week old plants post germination. Rosette leaf area estimated using imageJ (Abràmoff et al., 2004). n = 13 and error bars were ± SEM, asterisks (* = P < 0.5 and ** = P < 0.05) denoted significant differences and ns was no significant difference.

As rosette leaf area of mutant lines was slightly significantly larger than wild type (Col-0), it was decided to perform a drought experiment. Intact whole plant was used rather than a detached leaf fresh weight loss assay. The reason is that the plants had larger leaves and it was interesting to see whether they drought faster or slower or if they could recover from exposure to short term drought. The results suggested that *NIA1* might play an important role in response to drought, at least in recovery (from thermal imaging observations). Plants were able to rehydrate and continue growing after being rewatered unlike Col-0.

It was decided to view the whole plants (as they were larger), over a period of 15 days drought and then ascertain if they could recover after rewatering. Pots were weighed and thermal images taken of both well-watered and droughted plants to see how the whole plant responded. Previous experiments have studied responses via stomatal bioassays and detached leaves, which only show snapshots. It was preferable to have a method that could not only view long term effects but also compare fast systemic responses, which other methods were not as sensitive to. In this study, overall effect including variations of nitrate were investigated. It is advantageous to study responses in whole plants as overall they have better survival rates compared with detached leaves that are subject to wounding responses, although the latter give insights into mechanisms and responses detached from the main plant (see Figure 3.18).

A new method was developed in collaboration with Horak. H, Dunn. J and Fountain. L, more details found in Chapter 4, and was published (papers in supplementary data) (Hõrak et al., 2020; Hõrak et al., 2021).

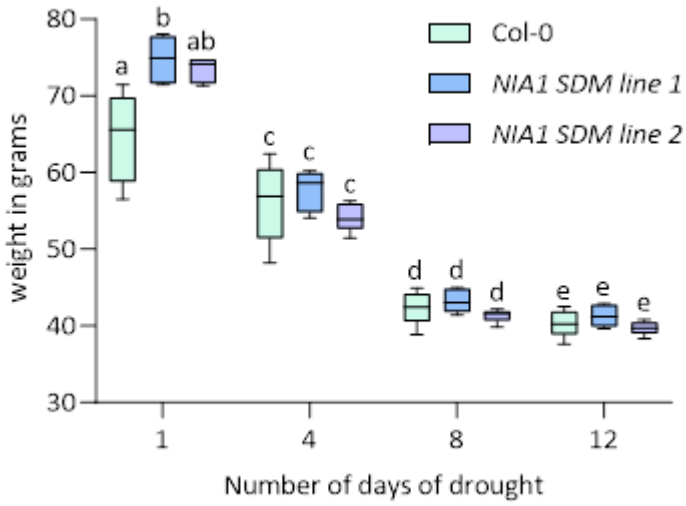

Figure 3.18 – Overall, no significant differences between lines and pot weights during drought. Two-way ANOVA followed by post hoc Tukey tests performed. Significant differences denoted by different letters (a – b, $P < 0.5$ and c – e, $P < 0.01$). Fresh weight of pots measured (n = 8).

As *NIA1 SDM lines* appeared to be more drought resistant, and can recover from short term drought easier than Col-0 (data observed via thermal imaging, not shown). It was decided to investigate stomatal densities to see if there was a difference that could impact water loss. Although *NIA1SDM* lines had larger plants, the pot weights across all three lines were similar suggesting that there might be slightly higher water loss from larger plants which could be due to a) a higher stomatal density (Figure 3.19) or b) larger stomatal complex sizes in the rosette leaf area (Figure 3.20).

Figure 3.19 showed that there were differences between *NIA1 SDM line 2* and the other lines for abaxial stomatal density and stomatal index but no differences between lines for adaxial stomatal density and stomatal index. As the phenotype was only observed in one line and not the other, it may not be a true result. More independent lines would need to be tested to verify.

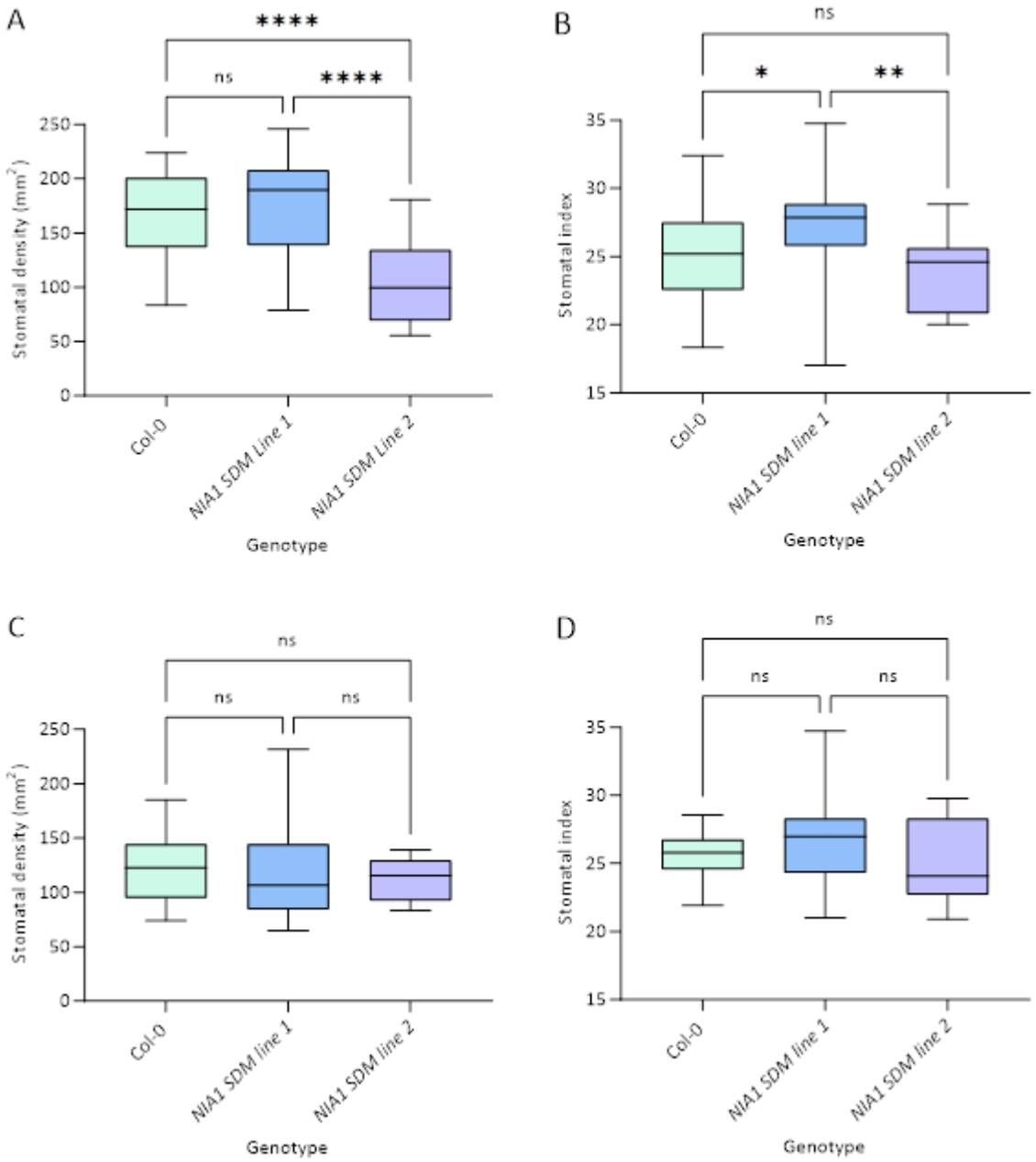

Figure 3.19 – There are abaxial side differences in stomatal density with *NIA1 SDM Line 2* compared to *Line 1* and Col-0. Leaf 6 impression data from 6-week-old leaves of Col-0 and *nia* mutants. Stomatal density (A) abaxial and (C) adaxial. Stomatal index (B) abaxial and (D) adaxial. A one-way ANOVA was performed. Letters denoted significant differences. There were no significant differences between any genotype for stomatal density or index on either abaxial or adaxial side (n = 40).

Rosette leaf area for *NIA1 SDM mutant lines 1* and *2* was significantly larger than Col-0, but in terms of drought there was no difference in pot weights. However, a difference was observed in recovery from drought utilising thermal imaging (as a snapshot). This suggested that the mutant lines lost water at the same rate as Col-0 even though the plants had a larger surface area. This was attributable to a

significant difference in abaxial stomatal density for only one mutant line, which does not account for drought phenotype.

The differences observed could have also been due to larger stomata (Figure 3.21). The results showed that overall, there were no large significant differences in stomatal sizes, mutant *line 2* was slightly larger than Col-0.

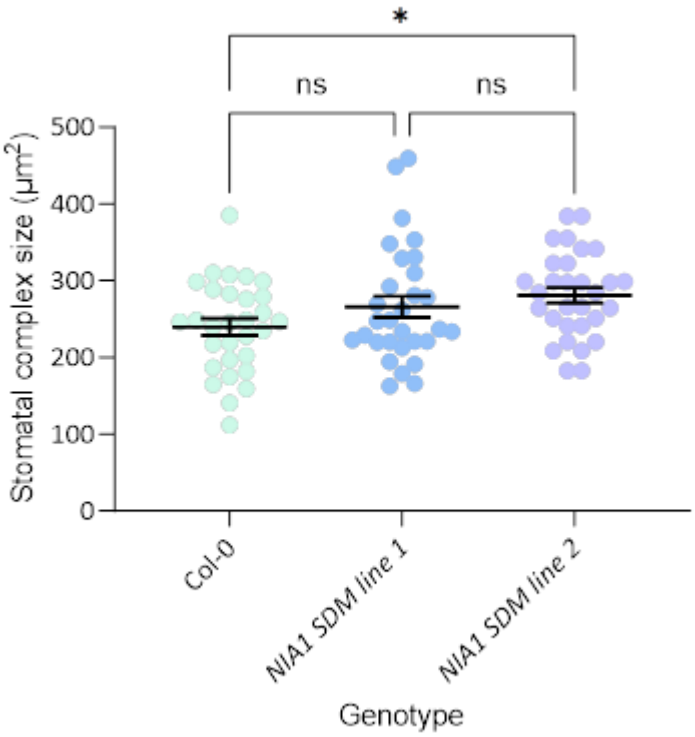

Figure 3.20 – Stomatal complex size has no large significant differences. Scatter plot of stomatal complex areas from X 40 stomatal impressions. n = 30 and Line is at mean and error bars are ± SEM.

Post translational modifications can affect expression levels and subsequent activity of in this case, NR enzyme. To test whether sumoylation (which negatively affects proteins and enzyme activity states) was affected or a higher activity of NR caused, a nitrate reductase enzyme assay was performed. The results in Figure 3.21 showed that there was increased activity which was to be expected. When sumoylation is defective it essentially causes an overexpression of the gene response, compared to single nia lines (in particular *nia1 (1)* and *nia 2-5*) which had lower activity than Col-0 when KO or KD.

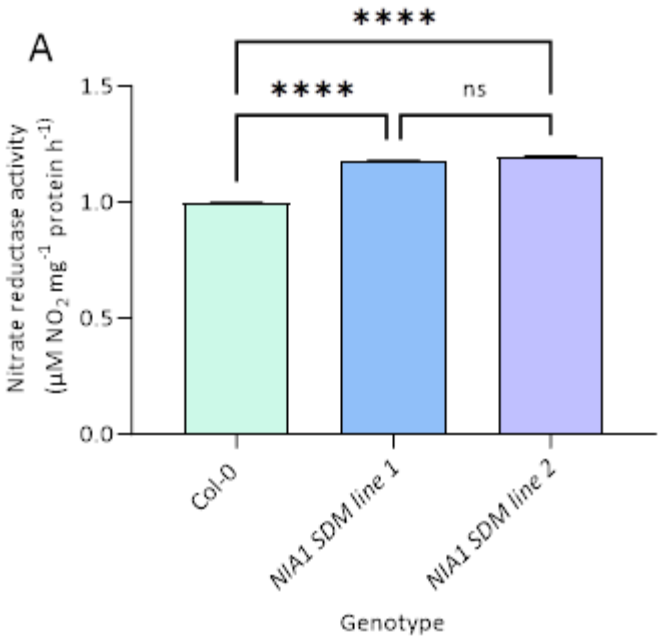

Figure 3.21 – NIA1 sumoylation defective mutants have higher overall NR activity than Col-0. NR enzyme activity from six week old mature leaves. One-way ANOVA performed followed by post hoc Tukey tests. Significant differences indicated by asterixis $P < 0.0001$. n = 3.

3.4 – Discussion

Overall, the two NR genes proved difficult to isolate and work with and the attempt to produce new double mutants was ultimately unsuccessful. It was not possible to retain the double mutant genotype into a second generation, but material could be kept alive via callus production. Nonetheless, another group has recently successfully created a double mutant for *nia1nia2* in a Columbia (Col-0) background (Tocquin et al., 2003; Lozano-Juste and León, 2010; Zhao et al., 2016). Unfortunately, the attempts to make promoter / protein fusions for NIA1 and NIA2 were also unsuccessful. It is not clear why *NIA1* and *NIA2* proved difficult to manipulate as the genes are not particularly large (1.8kb NIA1 and 1.9kb NIA2 promoter regions) and different approaches were tried. Nonetheless, a number of new *nia1* and *nia2* alleles were isolated and studied alongside the previously reported double and single mutant. Although the gene products are well characterised in terms of roots and enzyme activity and abundance, the single mutants have not been phenotypically characterised previously.

3.4.1 – Single mutations in *NIA* genes do produce phenotypes under certain conditions

An initial aims was to determine if single mutant lines (*nia1* and *nia2*) would have an effect on plant growth or function. The single mutants appeared to have a reduced sensitivity to the inhibitory effects of ABA during germination, which was different from expected. Figure 3.5 did not give the expected results, but there are many factors involved. The lack of ABA sensitivity in *nia1nia2* could be due to factors such as the positioning of the T-DNA insertion or gene expression levels. Positioning can determine if the gene of interest is completely disrupted creating a knockout (KO) line, partially disrupted (knock-down (KD)) or not disrupted at all. To check if effects seen were potentially due to T-DNA insertion positioning as opposed to the gene of interest, gene expression levels of mature leaves were investigated. The mutant line *nia1 (1)* has a T-DNA insertion in the exon and the disruption in *nia1 (2)* is in the intron (which could be spliced out and therefore may not disrupt gene expression). When multiple forms of a gene are present in plants, they can have different functions and provide a failsafe by creating redundancy. When one gene is missing if the other gene present increases in expression levels it may suggest redundancy (Nowak et al., 1997). Less availability of NO should increase seed dormancy. The previously published double mutant *nia1nia2* did show a slower germination rate, perhaps suggesting that when one gene is disrupted then the other gene overcompensates for the loss by causing more NO availability and therefore produces an opposite response. Potential redundancy was shown in Figure 3.6 of gene expression values. RT-PCR indicated that one KO line was isolated for each gene and for *NIA2* there was also a KD line. The discussion focuses on results from these lines.

3.4.1.1 – *nia1 (1)* has a smaller rosette leaf area and higher water loss but no difference in stomatal density

The mutation in *nia1 (1)* disrupts an exon, unlike in *nia1 (2)* where an intron is disrupted which may be expected to lead to a less severe phenotype. Indeed, only *nia1 (1)* showed a significant reduction in rosette size, suggesting that *NIA1* is associated with vegetative size. However as only one KO line was investigated, it cannot be ruled out that any observed phenotype is due to a different mutation. Studies with more independent lines or a complemented line would be needed to draw any strong conclusions. The same potential KO mutant line *nia1 (1)* also lost water more readily. As stomata are linked to ABA responses and water loss, it was decided to look for stomatal phenotypes. The stomatal experiments showed that there was no difference in stomatal density, but *nia1 (1)* had a reduced guard cell complex size but no difference in pavement cell density, suggesting that the complex size may be related to the smaller rosette leaf area (and therefore slightly smaller leaves). The reduced plant and guard cell size do not appear to provide a simple explanation for the enhanced water loss phenotype. There has been recent evidence to suggest that plants that exhibit drought tolerance, have lower NR gene expression, indicating that decreased NR activity could improve drought tolerance (Liu et al., 2022). Genes implicated in stomatal responses, such as GORK and AKT1 have also been shown to be down regulated and upregulated respectively in the *nia1nia2* double mutant. However, the expression of these genes was not investigated in the *nia1 (1)* mutant in this study.

NIA1 was more highly expressed in plants compared to *NIA2* and *NIA1* had a higher NR activity. This suggested that *NIA1* could be more involved in plant responses than *NIA2,* depending on responses. Indicating, *NIA2* may be redundant. This result differed from published data on NIA1 and NIA2 (Yu et al., 1998; Vazquez et al., 2019).

3.4.2 – No difference was observed in stomatal responses to ABA

Direct pore aperture measurements taken from epidermal peel bioassays investigated the stomatal aperture response to ABA. Some differences were seen in the mutants at some ABA concentrations, but these were not consistent between experiments, and it appeared unlikely that there was a major effect on guard cell ABA signalling. The NR genes are not highly expressed in guard cells. Stomatal analyses suggested that water loss was unlikely due to defective stomata and could therefore be related to mesophyll layer or the cuticle or a decreased number of trichomes. Leaves can also lose water through hydathodes, which are usually found at leaf edges.

3.4.3 – Plants with reduced NR can survive on media with less nitrate

Roots are essential for obtaining water and nutrients from the soil and for anchorage but they must adapt to environmental conditions such as drought, flooding, salinity or heavy metal toxicity which all cause stress responses in plants (Hirt and Shinozaki, 2004; Vazquez et al., 2019). The roots are the first point of contact for many stresses; and may activate signalling pathways throughout the plant (in particular ABA responses) (Kollist et al., 2014; Muhammad Aslam et al., 2022). The length and intensity of the exposure to stress will also affect the response and subsequently plant health and growth. Stomatal apertures close in response to several different stresses, stopping the transpiration stream, reducing the uptake of toxins and reducing water loss. If stressful conditions persist, plants still need to be able to function and therefore adapt. Root architecture is a good indication of plant health and soil conditions. Nutrients present can affect root architecture and subsequent plant health or stability, for example under low nitrate conditions plant roots have more branching compared to higher nitrate levels.

In this study, measurements of root length with and without nitrate provided interesting results. It was expected that roots on media without nitrate would be longer. However, plants on media without nitrate in this study had low root growth and no significant differences were observed between genotypes. However, when grown with nitrate in the medium, there was a significant difference observed for *nia2 (2)* which produced a longer root. The result is in line with published studies performed using ɗ ^{15}N to investigate root vs shoot differences; NIA1 had an increase of nitrogen assimilation in roots and NIA2 had an increase in leaves. This corresponds to what was seen in the *nia2 (2)* mutant line; when *NIA2* was knocked out it resulted in higher expression of *NIA1* which enabled more assimilation of nitrate in roots (Kalcsits and Guy, 2013). It is also known that the *NIA1* gene has a 3' flanking sequence that is required for nitrate inducible transcription of *NIA1*, whereas *NIA2* expression is not nitrate inducible (Konishi and Yanagisawa, 2011). However, in the experiment here plate grown seedlings could only be grown for short periods of time. Results shown were for 14 day old seedlings and therefore plants may not have been large enough for differences in root growth to be seen (but expression levels from eFP browser suggest high expression in hypocotyl and seedling roots).

3.4.4 – Removal of *NIA* genes reduces levels of NR enzyme activity

With NR enzyme assay, there may be differences in activity for the double mutant as it has been shown that when *nia1nia2* is KO, nitrogen metabolism genes Glu and Gln are upregulated (Zhao et al., 2016). There is also conflicting evidence that NOS and NOA are involved as alternative pathways resulting in

activity still made possible by the formation of NO_2. NR also contains a THB1 subunit which may still be active and can result in NO present turned into NO_2.

3.4.5 – Disrupting SUMOylation of *NIA1* impacts growth

When regulation of transcription is altered, allowing more to occur, there is a potential build-up of NIA1. Although this depends on protein turnover. Results in this chapter have shown that the potential increased transcription impacts growth and response to stress (in this Chapter drought, in Chapter 4 salt will be tested). Plants can grow larger, faster and recover from short term drought easier than Col-0 (observations, data not shown). Plants also had increased NR enzyme activity, as these results were observed in two independent lines, it is more likely to be a true result, however, more independent lines and replications would be needed to confirm this (Soo Park et al., 2011; Castro, P. H., Tavares, R. M., Bejarano, E. R., & Azevedo, 2012; Park, H. J., & Yun, 2013). If there is higher NR enzyme activity, which can lead to increased growth and survivability/ recovery from drought, there could be the potential for increase nitrate uptake from the soil. Increased uptake could reduce amount of nitrogen fertiliser in fields lost, potentially reducing damaging environmental effects. There were abaxial but not adaxial stomatal density differences. It has been shown that there are different regulatory pathways linked to abaxial and adaxial stomatal densities, such as CO_2 signalling and ABA. There was a study of mutants which had differing densities for abaxial and adaxial leaf surfaces (Lake et al., 2002). Stress can have a large effect on a plant growth and flowering. If stress occurs during the developmental stage, stomata formation can also be affected, and results seen from those experiments may be due to environmental factors as opposed to the gene of interest.

3.5 – Future work

Future research should build on the findings of this study by exploring several key areas related to the roles of *NIA1* and *NIA2* in plant growth, stress responses, and nitrate metabolism. One promising direction is to conduct phenotypic analyses on the newly published double *nia1nia2* mutant and compare these results to the phenotypes observed in the single mutant lines isolated here. This comparison could provide valuable insights into the potential redundancies and interactions between the *NIA1* and *NIA2* genes, helping to clarify their respective roles in plant physiology. This would involve identifying more single mutant lines to study, especially for *NIA1*, given the interesting phenotypic differences observed in the KO *nia1 (1)* mutant line. Investigating a second allele of *NIA1* could help confirm whether the observed changes in growth and water loss are indeed related to NR function or are due to another mutation. This approach would strengthen the understanding of how *NIA1* specifically contributes to these phenotypes (Seligman et al., 2008; Tang et al., 2022).

It would be good to examine changes in NR enzyme activity in the single mutant lines under multiple stress conditions to view how plants react in order survive under the interactions. This could provide new insights into the regulatory mechanisms which influence NR activity and its role the plants ability to adapt to changing environments (Liu et al., 2022).

An important area of future work involves exploring the role of SUMOylation in *NIA* genes. The disruption of SUMOylation in this study showed potential effects on plant growth, but it remains unclear which other cellular or physiological processes might be influenced. Further investigation into these pathways could involve manipulating more potential SUMOylation sites to assess its broader impact on plant stress responses and development (Miller and Vierstra, 2011; Soo Park et al., 2011; Castro, P. H., Tavares, R. M., Bejarano, E. R., & Azevedo, 2012).

Therefore, a significant focus for future research should be on the *NIA1SDM* lines, which exhibited increased NR enzyme activity, larger plant size and could recover from short term drought. These lines provide an opportunity to study how enhanced NR activity affects overall plant physiology. One approach would be to use radio isotope labelled N, to determine how much nitrate is taken up in the mutant lines compared to Col-0. This could help to determine if increased enzyme activity correlates with a higher nitrate uptake from the soil. This could potentially reduce the amount of fertiliser application and consequently the amount leached into the environment. Labelled N can also be used to track where the absorbed is stored, in roots or shoots, which could reveal if whole plant is involved in the observed phenotypic differences (Thirkell et al., 2016).

Finally, it would also be interesting to view the growth of these plants with varying levels of nitrate to see how low and high nitrate affect growth, enzyme activity and uptake. This research could help to identify optimal conditions for improving plant growth and NUE, with potential applications in agriculture to enhance crop performance and sustainability.

Chapter 4 – Detecting and assessing plant physiological responses to abiotic stress and or nitrate application

4.1 – Introduction

Abiotic stresses have consistently posed significant challenges for plants, but recent changes in climate, and forecast future changes in climate, are particularly concerning. IPCC reports detail climate changes such as temperature rises and areas of increased flooding. Rising sea levels leading to higher salinity and flooding are forecast, as are increasingly severe droughts (IPCC, 2023). The stages of when stresses occur, and for how long, can determine if plants can withstand their environment and survive or not (Zhang et al., 2020). If large quantities of our vital crops are ruined, or their growth stunted, the corresponding lower yields could lead to food shortages, particularly as populations continue to increase.

Stomatal regulation of gaseous exchanges is critical for stress responsiveness, with stomatal numbers influenced by environmental conditions and often controlled by Epidermal patterning factors (EPFs) (Hepworth et al., 2015; Hepworth et al., 2016; Bertolino et al., 2019) and aperture largely by ABA (also mediated by NO, derived from nitrate). Both potassium and chloride ions are important for stomatal opening as they enter the guard cell cytoplasm and vacuole, which drives turgor pressure by changing the osmotic gradient. This results in water entering guard cells, causing them to swell and the stomatal pore to increase in size. The interaction is also affected by blue light signalling (Dietrich and Hedrich, 1998). In grasses, stomata are dumbbell shaped and have subsidiary cells compared to Arabidopsis, which have kidney shaped cells (Hepworth et al., 2015; Bertolino et al., 2022). Despite these morphological differences, it has been shown that the EPF family of genes is highly conserved and that grasses have a similar developmental pathway. This made EPFs a good choice for observing responses in crops as well as how they compared to Arabidopsis. Nitrate accumulation also influenced by nitrate transporters which can subsequently affect stomatal apertures (Guo et al., 2003). Nitrate accumulation can affect stomatal apertures through several mechanisms such as: regulation of hormones in particular ABA, and cytokinins (higher nitrate availability can led to increased cytokinin levels which promotes stomatal closure). The production of NO, signalling molecules, ion balance and osmotic pressure (nitrate transporters can affect the ionic balance and osmotic pressure within guard cells, the change in nitrate levels can alter the osmotic gradient causing influx or efflux of water affecting stomatal aperture). Finally, NRT1.1 acts as both a sensor for nitrate levels as well as a transporter of nitrate, regulating responses using hormonal and environmental cues (Wilkinson and Davies, 2002; Guo et al., 2003; Desikan et al., 2006). It would be expected that different stomatal

numbers and apertures lead to different evaporative demand and nutrient uptake (potentially also altering salt uptake, and thus salt tolerance) (Hepworth et al., 2016; Zhao et al., 2021; Bertolino et al., 2022; Liu et al., 2022; Caine et al., 2023). Recent studies have indicated that in rice, there is a histone modification which can regulate stomatal responses positively by altering gene expression patterns, to enable them to be more drought and salt tolerant (Zhao et al., 2021). Drought and salt tolerance are linked with stomatal aperture changes; when stomata are less open, less water is lost through transpiration, and less salt is passively taken up via the transpiration stream (Zhao et al., 2021). It is therefore important to analyse how stomatal traits affect nitrate responses, and how nitrate and N-end rule pathway status (analysed via respective mutants) influence stomatal responses. There have also been recent links in rice looking at nitrate responsive genes (e.g. OsNRT1.1, OsNRT2.1, OsNIA1, OsNIA2, OsNIR1) which can affect responses to stress as well as affect traits such as tillering and stomatal density (Medrano et al., 2015; Fan et al., 2016; Zhou et al., 2020; Kumari et al., 2021; Mandal et al., 2022).

Historical methods to view stomatal responses to ABA have used isolated leaf fragments of epidermal peels placed in ABA containing solution, with air and with or without CO_2 (Mcainsh et al., 1991; Kuhn et al., 2006; Uraji et al., 2012; Yamamoto et al., 2015; Medeiros et al., 2018). Other methods include chlorophyll fluorescence, gas exchange analysis of ABA petiole fed detached leaves, gravimetry and thermal imaging. These methods have generally involved detached leaves or single leaves as opposed to whole plant responses (Meyer and Genty; Rasehke, 1975; Büntgen et al., 2011; Shatil-Cohen et al., 2011; Pantin et al., 2013a; Pantin et al., 2013b; Viger et al., 2013; M€uller et al., 2017; Schäfer et al., 2018; Tõldsepp et al., 2018). Gas exchange analysis was performed using a custom-built system to look at the effects of ABA spraying on whole plants, which is described in Chapter 5 (Merilo et al., 2013; Hõrak et al., 2017).

Nitric oxide (NO) has been linked to many processes such as: seed germination, photomorphogenesis, shoot and leaf development, stomatal closure, leaf senescence, pathogen response and submergence response(Holman et al., 2009; Graciet and Wellmer, 2010; Gibbs et al., 2011a; Licausi et al., 2011; Gibbs et al., 2014b; Gibbs et al., 2014a; Holdsworth et al., 2015; Xu et al., 2015; De Marchi et al., 2016). It has been suggested that NIA1 and NIA2 (which encode NR) are involved in stress responses. *NIA1* has been linked to cold tolerance responses (Zhao et al., 2009). It was shown that in decreased temperatures there was upregulation of *NIA1* gene expression and NO production in Col-0 (Zhao et al., 2009). It was also inferred using expression patterns in eFP browser and experiments performed in the literature, that levels of *NIA1* were higher than *NIA2* in the guard cells and that *NIA2* was not involved in the stress response (Bright et al., 2006b; Neill et al., 2007; Zhao et al., 2009). Previous studies on salt stress indicated that *NIA2*, rather than *NIA1*, plays a significant role in the stress

response. In crops with elevated sensitivity to nitrate uptake and subsequent reduction, this sensitivity was associated with improved growth under stress conditions (Flores et al., 2004; Debouba et al., 2007). If there is less nitrate available, there will be reduced NR enzyme activity, leading to decreased nitrate assimilation and potentially less available NO for signalling responses. NO is produced as a minor by-product of nitrate assimilation (Wang et al.; Crawford, 1995; Neill et al., 2003; Wang et al., 2010). The *nia* mutants have proved to be temperamental (germination problems in later generations and difficult to isolate) leading to the selection of some other mutants in these experiments for comparison. In particular, mutants in PRT1 (part of the N-end rule pathway involved in protein degradation before the introduction of NO, where nitrate reductase regulation comes in) and EPF (Stomatal density mutants) can help to establish links between drought tolerance and nitrate availability and responses. PRT1 mutants should exhibit similar responses to reduced NR activity due to their role in the N-end rule pathway (Rockel et al.; Hara et al., 2009; Dissmeyer and Schnittger, 2011).

Factors that influence stomatal closure responses play a crucial role in a plant's ability to respond to abiotic stresses, such as drought or high salinity. The N-end rule pathway, which was discovered by Varshavsky et al. in 1986 (discussed in detail in Chapter 1), is integral to this process, as it regulates the stability of proteins involved in nitric oxide (NO) production and signalling. NO is a key mediator of stomatal closure, and its levels are controlled by nitrate reductase, whose activity is influenced by the N-end rule pathway. Therefore, this pathway indirectly affects stomatal responses by modulating NO levels and other stress-related signalling molecules (Gibbs et al., 2014a).

4.2 – Aims and objectives

The overall aim was to develop and optimise methods for observing and understanding plant responses to abiotic stresses, particularly in relation to nitrate interactions and stomatal density, with the ultimate aim of applying these findings to improve crop resilience.

To achieve this aim, the following was undertaken:

1. Literature review:
    - Conduct a comprehensive review of existing methods previously used to observe both local and fast systemic responses to abiotic stresses over time.
2. Method development:
    - Evaluate and compare various techniques for monitoring whole plant responses to abiotic stress, focusing on efficacy of ABA signalling and its interaction with nitrate as key indicators.
3. Validate using model organisms:
    - Utilise both Arabidopsis and barley as model organisms to validate the novel method for assessing rapid systemic responses to abiotic stress.
4. Nitrate interaction:
    - Investigate the role of exogenous nitrate in enhancing ABA signalling responses and overall plant resilience under stress conditions.
5. Analysis of mutants:
    - Apply the developed method to mutants related to the N-end rule pathway, particularly those with reduced NR enzyme activity, to assess their impact on plant responses to abiotic stresses.
6. Pilot study on stomatal density mutants:
    - Conduct a pilot study using Arabidopsis grown on plates, to assess the relationship between stomatal density and salt tolerance, providing insights into potential mechanisms of stress adaptation.
7. Whole plant studies on rice:
    - Perform studies on rice to validate the findings from Arabidopsis, to examine the potential benefits of decreased stomatal density in improving salt tolerance in crop plants.
8. Integrated analysis:
    - Utilise the results of previous experiments to inform and refine the investigation into the relationship between stomatal density and salt tolerance, with a view to its applications in crop plant improvement.

4.3 – Results

4.3.1 – Dynamic thermal imaging aids in the detection of responses to stress in Arabidopsis

To develop a new method for assessing abiotic stress responsiveness, Arabidopsis and crops (specifically barley, wheat and rice) were studied to see if fast systemic responses could be captured. These responses were compared to directly observed stomatal responses and detached leaf analysis. The method for viewing fast systemic responses on whole plants and comparison to detached leaves was developed in collaboration and our results published, papers in supplementary data (Hõrak et al., 2020; Hõrak et al., 2021). ABA is involved in stomatal closure response, which would be the plant's response to drought to reduce their water loss (Park et al., 2010). The effect of closing stomata would be an increase in temperature over time, which can be viewed using thermal imaging. The earlier a temperature increase is detected, the faster a response / closure of stomata. Whole plant gas exchange measurements were less efficient and had lower potential throughput compared to dynamic thermal imaging. Therefore, concentrations of ABA (0, 1, 5, and 10 µM) were trialled (by spraying whole plants and observing temperature changes using thermal imaging) to determine if the responses corresponded with data from detached leaves and to observe if fast systemic responses could be detected (Jones, 1999; Lefebvre et al., 2002).

By assessing (using dynamic thermal imaging) Arabidopsis Col-0, Figure 4.1 shows a concentration-dependent response to ABA (0, 1, 5, and 10 µM) sprayed onto plants. Specifically, 5 µM and 10 µM ABA treatments resulted in similar temperature increases, with 10 µM causing a slightly higher, but not significantly different, temperature rise. These images and results were published in Horak et al. (2019), and Figure 4.1 provides representative images and data. The 10 µM ABA treatment led to the largest temperature change when comparing the images taken 1 hour after treatment and the 1 hour subtracted image. However, analysing the change in leaf temperature from before to 1 hour after treatment revealed no significant difference between the 5 µM and 10 µM ABA treatments (Jones, 1999; Bahrun et al., 2002; Lefebvre et al., 2002).

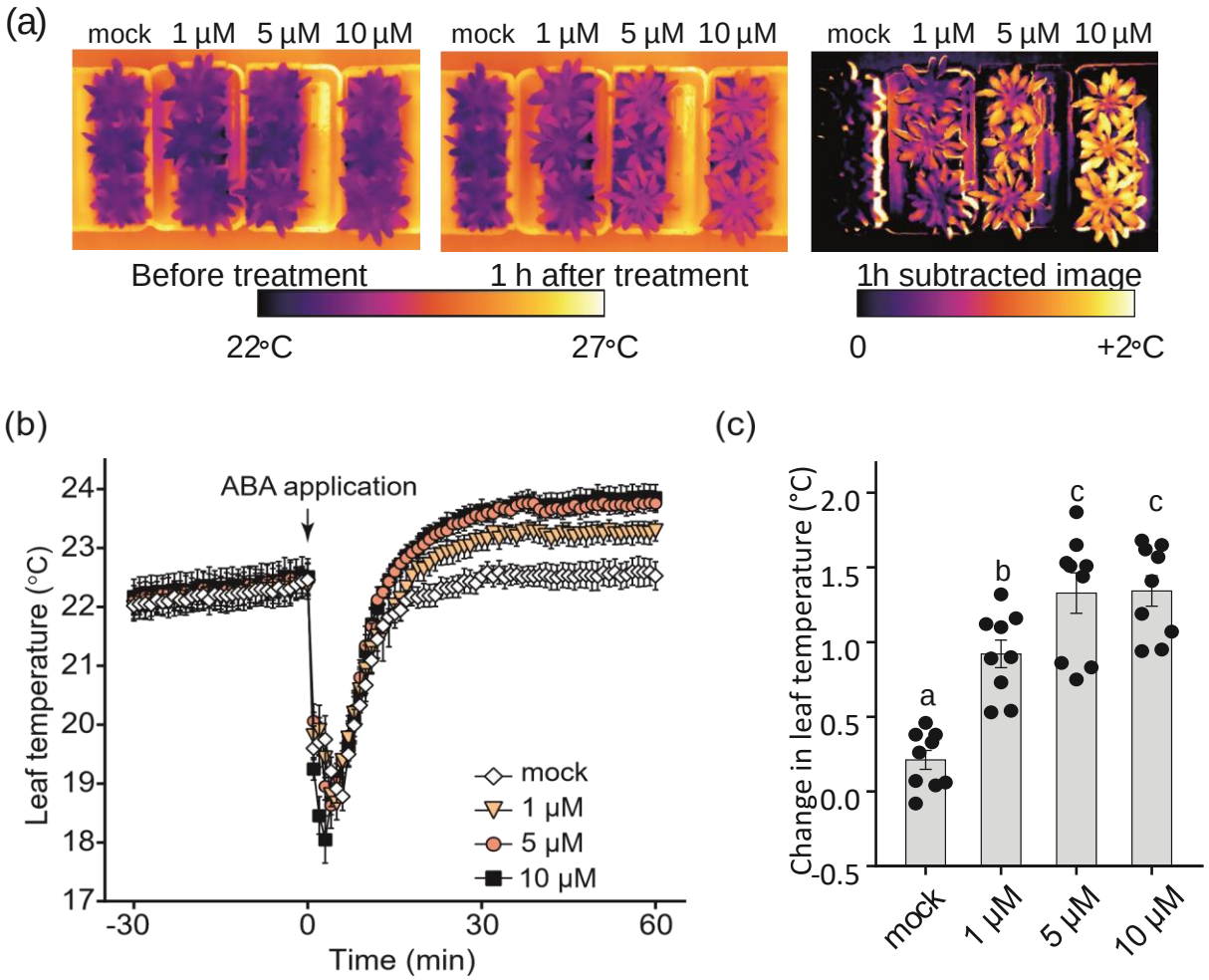

Figure 4.1 – ABA induces a concentration-dependent increase in leaf temperature. (a) Representative thermal images of Col-0 before and after 1 hour of treatment with either a control solution (mock (0.012% Silwet L-77, 0.05% ethanol) or different concentrations of ABA. The subtracted image showing the temperature change in °C. (b) Leaf temperature change over time before and after ABA application. Mean is plotted and error bars are ± SEM. (c) Change in leaf temperature from before treatment compared to 1 hour after treatment. Bars plotted are means ± SEM error bars. Dots represent individual points. One-way ANOVA was performed with Tukey HSD post hoc test and letters represent significant differences. (b) and (c) data was pooled from 3 independent batches. n = 9.

Differences between young and mature leaves were also investigated (results in supplementary data) and it was observed that in mature leaves there was a significantly higher change in temperature after treatment compared to young leaves. Mature Arabidopsis plants were used for the following experiments and leaf temperatures were taken from mature leaves. Due to the results, concentrations of 0, 1 and 5 µM ABA were selected for spraying Arabidopsis. The presence of fast systemic responses were also investigated by locally applying ABA to individual leaves and temperature changes observed in both treated and systemic leaves (results shown in supplementary data). Treated leaves had a response whereas systemic leaves did not appear to have any response (stomatal closure and increase

in temperature). The ABA spraying method and dynamic thermal imaging were used to assess the whole plant response.

The *nia* mutants posed several challenges, such as, inconsistent germinated and increased susceptibility to pests. Additionally, gene isolation for promoter fusions was unsuccessful and observed traits were also not reproducible, viewed once and then did not occur again. Therefore, other n-end rule pathway mutants, *prt6-1* and *prt1-1* were selected for further analysis. In the N-end rule pathway (also known as N-degron pathway), the E3 ligases PRT1 and PRT6 are upstream of NO (Figure 1.4), using mutants *prt1-1* or *prt6-1* should reduce the requirement for NO (Potuschak et al., 1998; Holman et al., 2009; Mendiondo et al., 2016). Published results indicate that PRT1 influences the immune response in Arabidopsis (Till et al., 2019). Although drought experiments and stomatal bioassays were performed on *prt6-1*, but the data contradicted published work and previous experiments (Garzón et al., 2007; Holman et al., 2009). Therefore, it was decided to use *prt1-1* as a comparison.

Using a wildtype plant as a control to assess a mutant line, can highlight how a given gene ordinarily contributes to plant form and physiology. By also using complementation of the gene in the mutant line, it is possible to more confidently determine if observed differences (between wildtype and mutant) are due to the mutation rather than an artefact. It was hypothesised that as PRT1 is involved in the stomatal closure response, the mutant line (*prt1-1*) would be less sensitive to ABA, have more open stomata and therefore display a lower temperature.

Seeds provided by the Holdsworth group at the University of Nottingham were grown under normal conditions in growth cabinets until 6 weeks post germination. Plants were imaged in batches of 12, left to acclimatise and then sprayed with either a mock solution (0.012% Silwet, 0.05% ethanol), 1 μM ABA or 5 μM ABA solution. Images of plants were taken every five minutes. Figure 4.2 shows representative images of the plants both digitally and thermally before, during, and after treatment with ABA.

The results in Figure 4.3 showed that under 1 μM ABA spraying, all genotypes reduce their temperature after being sprayed. After 30 minutes Col-0 had a higher leaf temperature than both *prt1-1* and its complement line. Under 5 μM ABA, there appeared to be no difference under mock treatment for any of the samples, but when ABA was applied, after the initial dip in temperature due to spraying, all samples increased in temperature. There were no significant differences ($P > 0.05$) between any genotype under 5 μM ABA, but there were significant differences under 1 μM ABA. The temperature differences in 1 μM ABA treatments, after 30 minutes post application were highlighted in Figure 4.3C and the bottom right panel of Figure 4.2. Before application, all genotypes were steady

in temperature and relatively similar (top left thermal, Figure 4.2), but after application, ABA treated leaves are lighter in colour (thermal image) with a higher temperature suggesting more closed stomata (bottom right thermal, Figure 4.2).

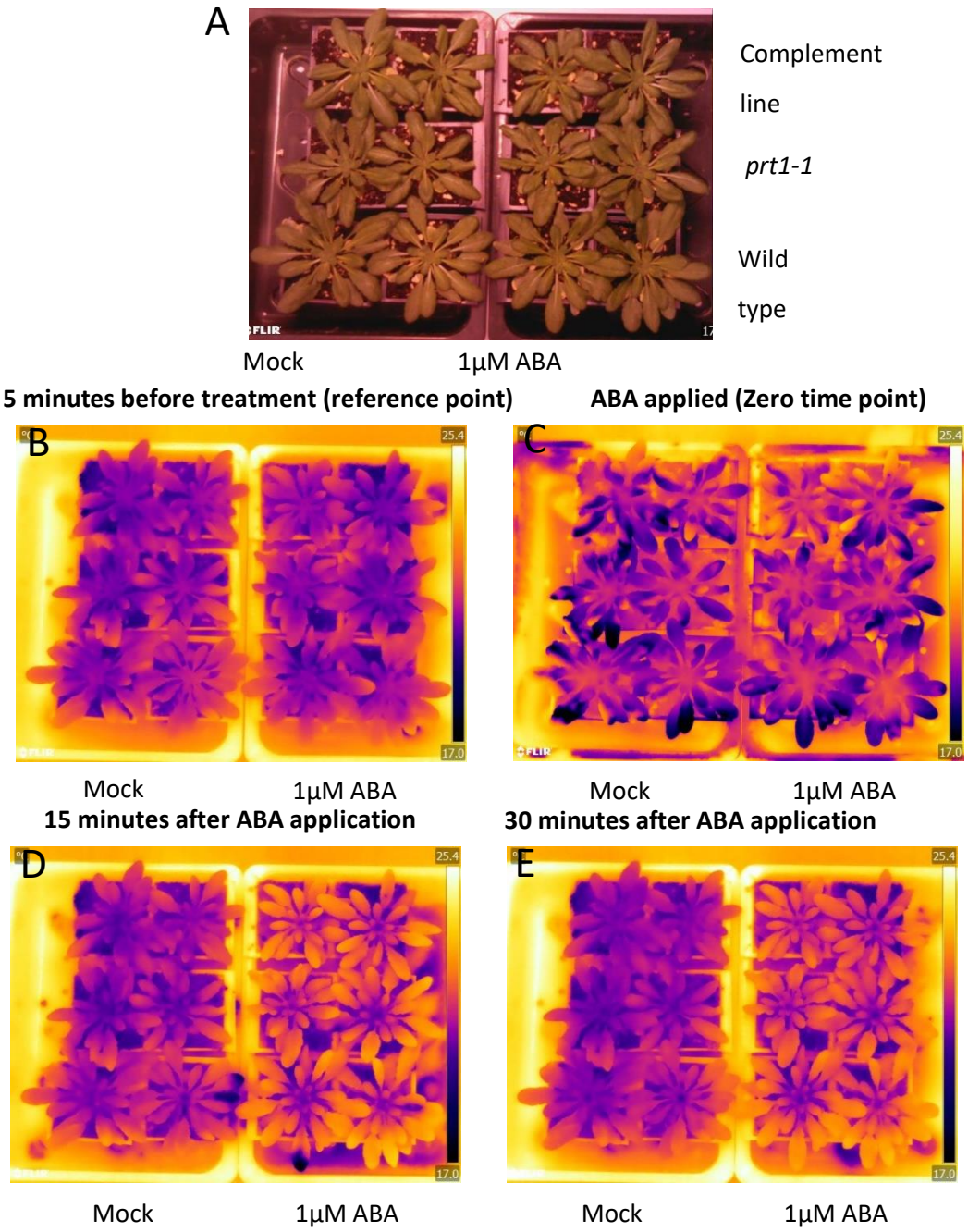

Figure 4.2 – ABA causes *prt1-1* to have reduced stomatal conductance. A) Representative plant images of Col-0 (wild type), *prt1-1* and its complement line. Digital image followed by thermal images B) 5 minutes before treatment, C) before treatment (zero time point), which was used as the refence point and when 1 µM ABA was applied. Then change in temperature thermal images for D) 15 and E) 30 minutes post application. The temperature scale bars range from 17 to 25.4 °C.

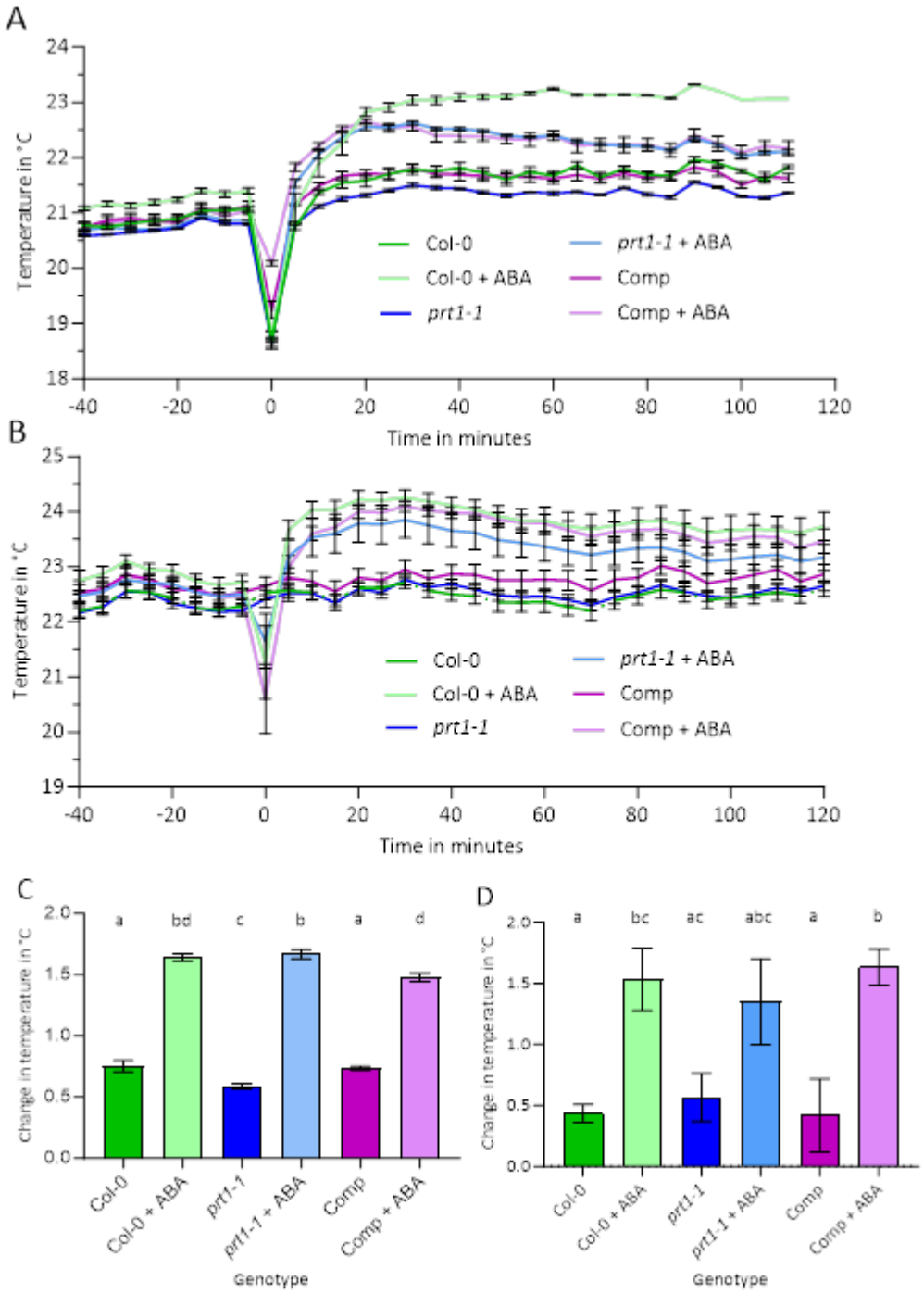

Figure 4.3 – *prt1* is less sensitive to 5 µM ABA compared to Col-0. A and B are time course experiments, ABA was applied at time point 0. A) Application of 1 µM ABA or mock solution and B) Application of 5 µM ABA or mock solution. Images taken every 5 minutes. Bars represent mean ± SEM, n = 6. Data pooled from 3 consecutive days of thermal imaging. Images taken every 5 minutes. C (1 µM) and D (5 µM) are change in temperature 30 minutes post application compared to before treatment. Bars represent the mean and error bars are ± SEM. One way ANOVA followed by post hoc Tukey tests resulted in significant differences denoted by letters. Treatments that share a letter are not significantly different.

4.3.2 – Responses to application of exogenous nitrate and ABA can be viewed using dynamic thermal imaging

The overarching aim of this section of research, has been to view differential nitrate application responses in crops, so to potentially reduce their future dependency on nitrate fertilisers, whilst not harming yield or plant health. To achieve this aim, two experiments were undertaken. Firstly, the efficiency of utilising thermal imaging on crop plants was trialled on the young barley (*Hordeum vulgare*) cultivar Golden Promise. Secondly, ABA induced stomatal closure in barley was assessed for its impact on drought phenotyping, similar to the experiments demonstrated above in Arabidopsis. These studies are relevant because stomatal behaviour significantly influences nitrate uptake and utilisation. Efficient stomatal closure can affect the transpiration stream, thereby influencing nitrate transport and assimilation in plants (Wilkinson and Davies, 2002; Bista et al., 2018). Barley is a robust, annual grass crop, which is largely grown in the UK, along with wheat (*Triticum aestivum*). Although grass stomata are morphologically different from Arabidopsis, they still respond to certain stimuli, including ABA for stomatal closure. It has been implied, that in cereals such as barley and wheat, nitrate is required for SLOW ANION CHANNEL-ASSOCIATED 1 (SLAC1) anion channel activation, as well as fast and efficient ABA responses (Schäfer et al., 2018). Figure 4.4 shows the results for Golden Promise treated with and without KNO_3, and with and without ABA. From graph (a), both ABA and ABA with nitrate, caused significant leaf temperature increases, whereas the addition of just KNO_3 did not cause such a high temperature increase. Actual values and changes in temperature are shown in (b) and (c). The results did not show the fast systemic responses indicated by Schäfer (et al., 2018), under these experimental conditions. To determine if the temperature response was cultivar based, the cultivar Barke was used as a control (data published and shown in appendix). Barke showed similar results to Golden Promise. Approximately one hour after treatment, leaves treated with both nitrate and ABA had a slightly higher temperature compared to leaves treated with just ABA. However, this difference was not significant. Additionally, leaves treated with just 5 mM KNO_3 did not show a significant temperature difference compared to the control mock treatment (data shown in appendix).

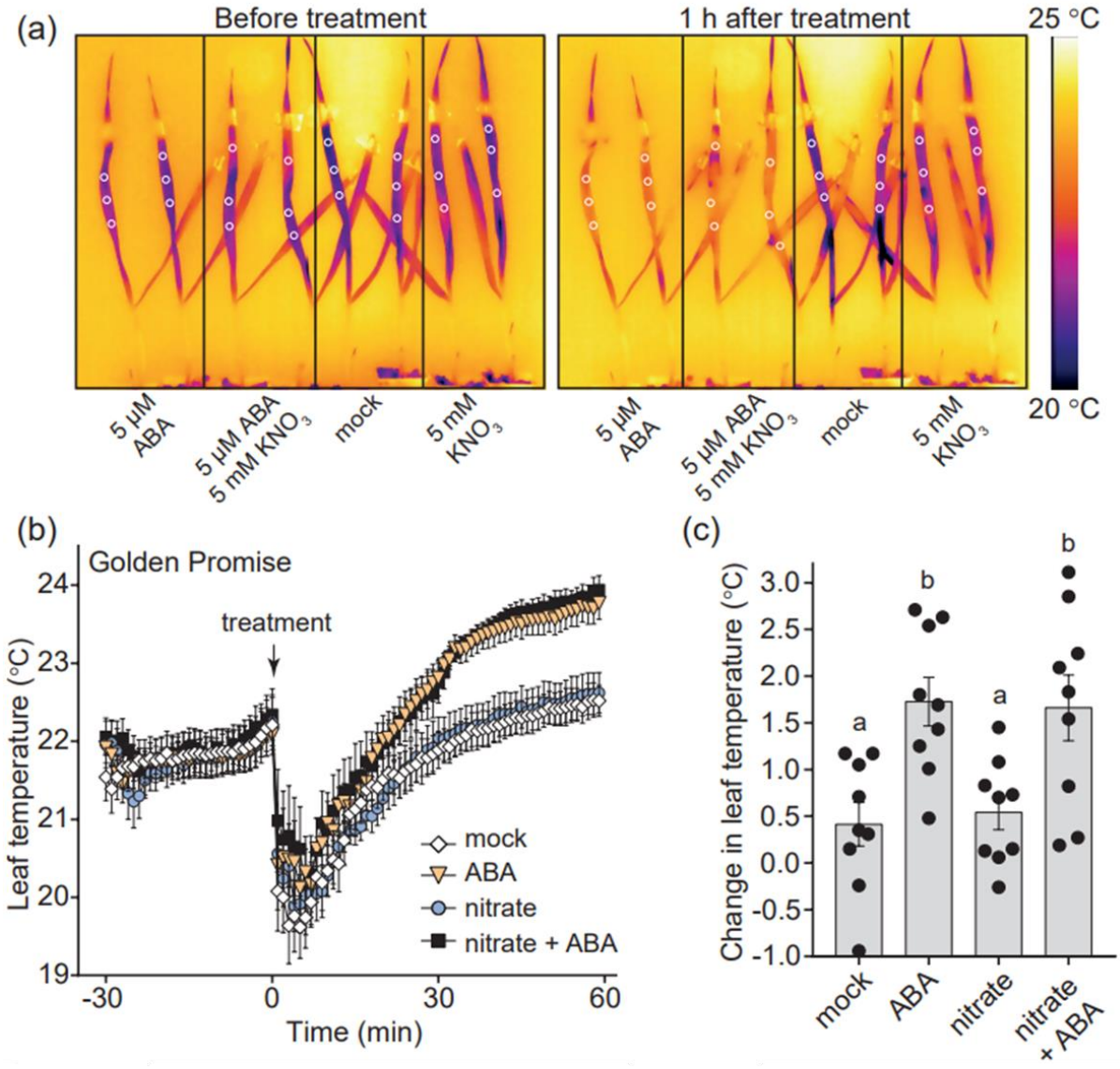

Figure 4.4 – ABA induces exogenous nitrate independent stomatal closure in barley. (a) Representative thermal images of ABA response in barley. Three points were sampled per plant on leaf 2, demonstrated by the white circles. (b) Golden Promise and its leaf temperature response to ± 5 µM ABA, ± 5 mM KNO_3 or mock (0.012% Silwet, 0.05% ethanol) (c) Temperature changes 1 hour after treatment. In (b) and (c) mean values are plotted ± SEM, n = 9. (c) Dots represent individual data points, one-way ANOVA with Tukey HSD post hoc test, letters denoted significant differences.

This system used intact plants, whereas previous studies used detached leaves and the transpiration stream to apply ABA (Meyer and Genty; Rasehke, 1975; Büntgen et al., 2011; Pantin et al., 2013b; Schäfer et al., 2018). Detached leaves can survive for up to a day in water and nutrient solutions using the transpiration stream to maintain turgor pressure and prevent wilting (Yarwood, 1946). Use of solid media and the application of specific growth hormones that promote both root and shoot growth were also trialled in Chapter 3 (Callus production) (Ellis, 1993; Sugimoto and Meyerowitz, 2013).

However, sterile conditions for this type of growth were not feasible for these experiments due to the potential upscaling.

To compare results, detached leaves were also used to detect changes in leaf temperature. Higher leaf temperatures indicate more closed stomata and reduced transpiration. When using detached leaves it must be considered that they have been cut from the main plant, which can cause wounding responses and also affect signalling pathways. However, as all leaves were handled similarly, these wounding responses should be consistent across treatments.

Barke barley was grown, and leaves were detached and placed in solutions containing ABA, nitrate, ABA with nitrate or a control solution and left to incubate. An hour after treatment, results were similar to those shown in Figure 4.3. Leaves treated with just nitrate did not exhibit significant changes in temperature, indicating no effect on the transpiration stream and stomatal aperture. However, treatments with ABA and ABA with nitrate did affect leaf temperature, with ABA alone resulting in a slightly higher temperature. These results are shown in Figure 4.4 (results are from published paper in appendix).

Results suggest that barley for ABA-induced stomatal closure had no requirement for exogenous nitrate. This was due proposed to be due to endogenous levels of nitrate present in the barley. To determine if plants starting with or without nitrate are then affected by application of ABA and nitrate, barley was germinated with and without 5 mM KNO_3. Nitrate is one of the main sources for NO production via NR. Hoaglands solution was chosen as the preferred nutrient solution as it has been well used in research with regards to crops and nitrate, as well as ammonia treatment (Hoagland and Arnon, 1950). Nitrate can easily be substituted out, in this case potassium chloride replaced potassium nitrate to avoid a drop in potassium. Once the seedlings had germinated, either with or without nitrate, a second leaf was detached and placed into Eppendorf tubes containing Hoaglands solution. The leaves were left to acclimatise in this solution. Leaves were then transferred into new tubes containing the nutrient solution with or without ABA and nitrate. The drop in temperature in the graphs in Figures 4.5 A and B indicated when solution was changed.

The results were similar to published but with a smaller difference in temperature compared to published data (Schafer et al 2018, Horak et al 2020). After treated with ABA (with or without nitrate), the leaf temperatures increase to a higher temperature than the mock or nitrate alone. Due to the spread of data resulting in large error bars it is difficult to determine significant differences. Seeds germinated with or without nitrate did not influence the plant's ability to respond more to ABA under the influence of exogenous nitrate. The drop towards the end of the graphs was due to the door being opened, affecting the ambient temperature.

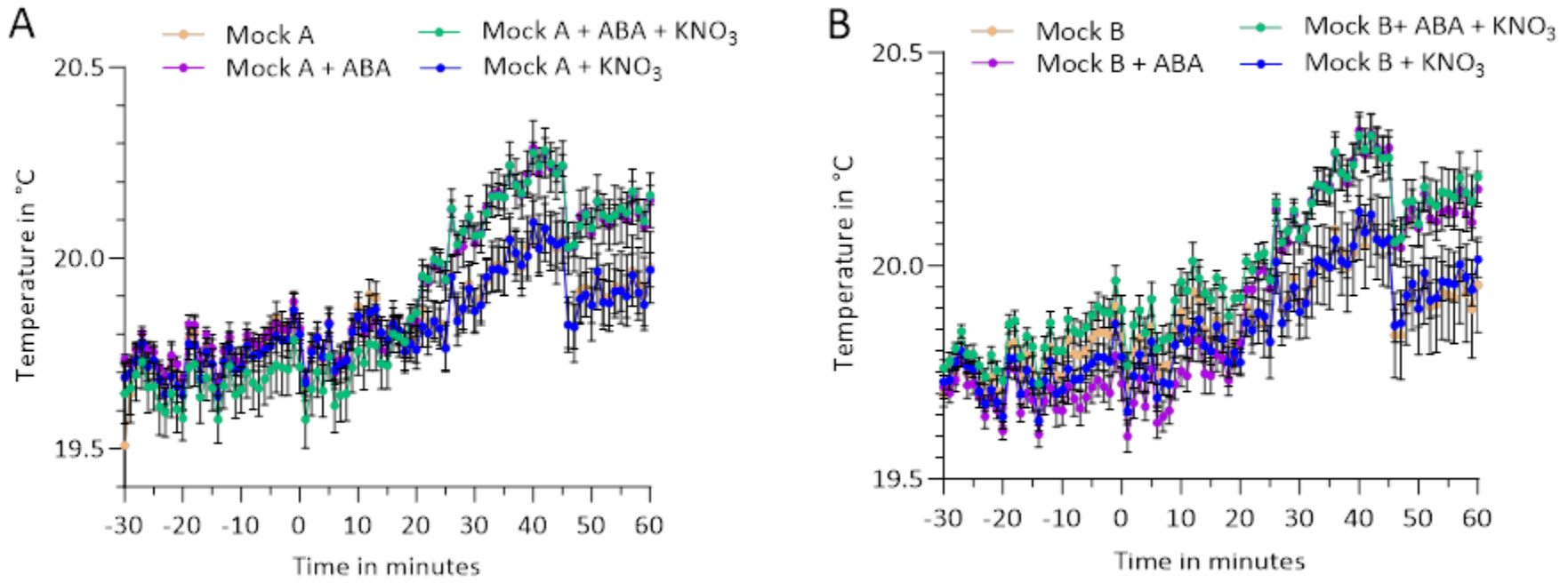

Figure 4.5 – 14-17 day old barley germinated without nitrate still responds to external ABA application in detached leaves. Barley seeds germinated and grown in nutrient solution with nitrate (A) or without nitrate (B) for 3 weeks. Graphs showed the response of leaf temperature to sheath fed with 5 μM ABA with or without nitrate. Mean points plotted and bars were ± SEM, n = 6.

4.3.3 – Effect of increased salt concentrations on seedling root growth

Increased salination is a growing problem due to rising sea levels. Sea water has entered river systems and during periods of flooding, can enter fields. An amount of salt is needed for normal plant development, but too much can lead to detrimental effects. Salt enters the plant via its roots. High levels of salt cause stunted growth and depending on length of exposure, as well as growth stage of exposure (Hepworth et al., 2015; Hepworth et al., 2016; Caine et al., 2023).

To further investigate the role of nitrate and NR activity in plant stress responses, a salt tolerance assay was performed using agar plates. This assay aimed to provide a snapshot of how NR activity, influenced by nitrate treatments, affects the plant's ability to withstand salt stress. This builds on the previous experiments that examined NR's role in stomatal responses and temperature changes under various conditions, including nitrate and ABA treatments. The salt tolerance assay complements our earlier findings by exploring how nitrate availability and NR activity contribute to the plant's overall stress tolerance, particularly under salt stress conditions. The results show the root length growth after 7 days on media containing 0-, 100-, 125- or 150-mM salt (Sodium chloride (NaCl) was used). As there had been an inference that NIA (Tang et al., 2022) and in particular NIA1 may be linked with salt tolerance responses, the nia mutant lines were looked at first. Unfortunately, due to germination and some infection problems, *nia2 (1)* was omitted from the results. In Figure 4.6, the graphs show responses to increasing concentrations of salt. Different concentrations were tried to ascertain the optimal concentrations. The trend from the graphs shows that initially as salt concentration increases, root length increases slightly and then as the concentrations increase higher, the levels become detrimental and root length growth decreases. Under the 125 and 150 mM salt chlorosis was also seen on all plants after 7 days. The graphs also show that *nia2* mutant lines seem to be slightly more affected by salt compared to *nia1* and Col-0, especially *nia2 (2)*. There are significant differences from 25 mM salt onwards for nia2 (2) compared to Col-0 and *nia1 (1)*.

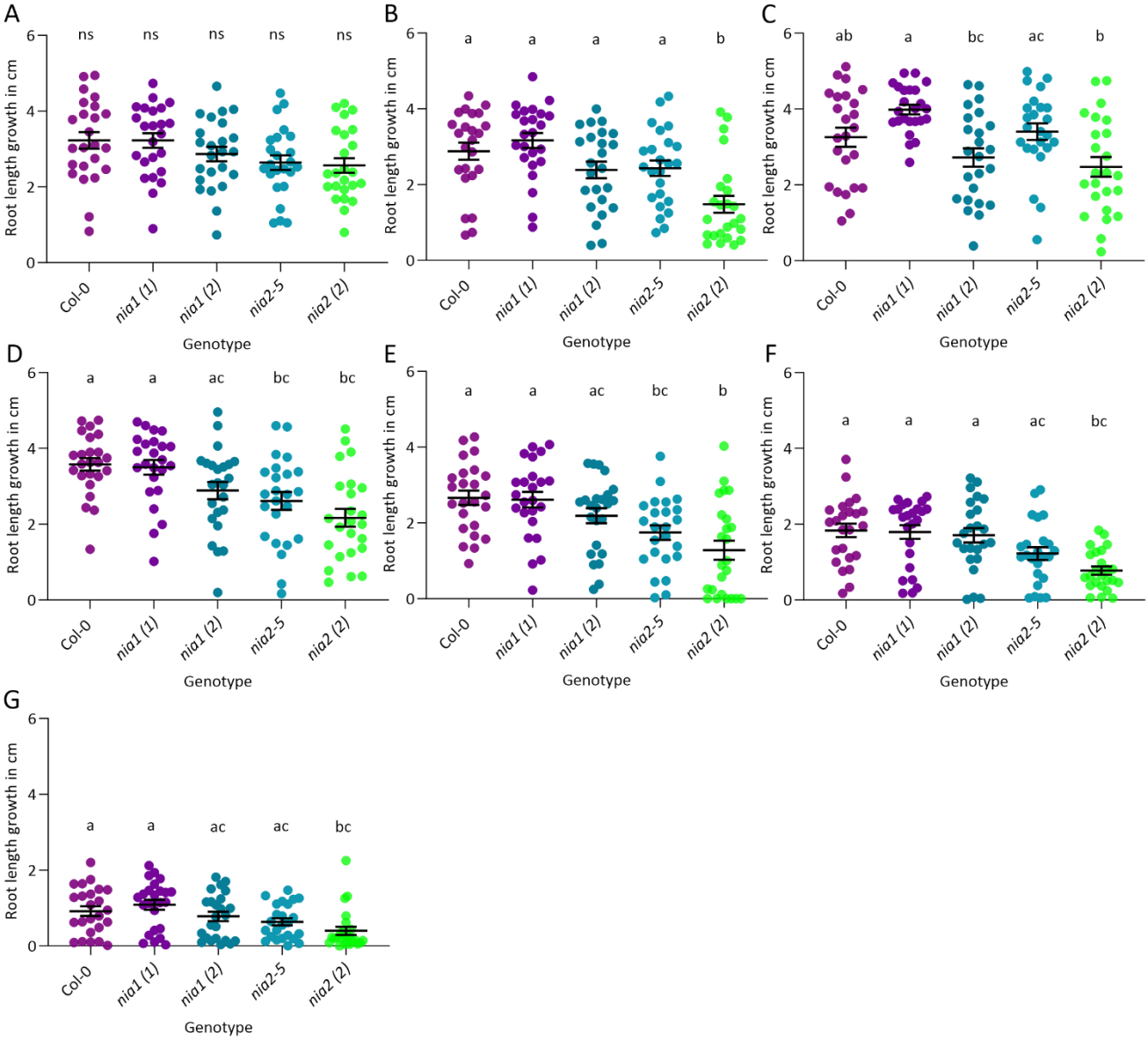

Figure 4.6 – There are slight differences between nia mutants under increasing salt concentrations. A-G represent increasing salt concentrations: 0, 25, 50, 75, 100, 125 and 150 mM salt. A-G show pooled data for root growth length after 7 days, post transfer to salt plates. n = 24 with individual points plotted. Bars represent mean ± SEM. A one-way ANOVA on each graph was performed and B-E post hoc Tukey tests, letters denoted significant differences. Root growth lengths that share a letter are not significantly different.

After looking at mutants with decreased expression, responses of NIA1 sumoylation defective mutants, which potentially (needs confirming) had increased gene expression were observed. The results are shown in Figure 4.7. Under 100 and 125 mM salt there are significant differences, the two mutant lines have significantly longer roots compared to Col-0. Under no added salt and 150 mM there are no significant differences between the genotypes, and all had reduced growth. Samples under high salt also had chlorosis.

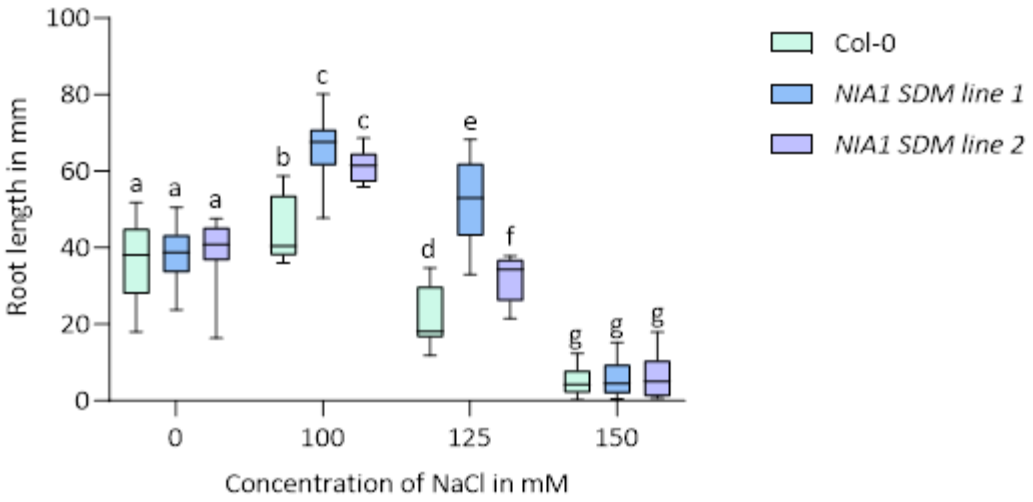

Figure 4.7 – Under certain salt concentrations NIA1 SDM lines have significantly longer roots than Col-0. Box and whisker diagram showing the root length growth of seedlings after 7 days post transfer to media plates containing salt. Middle line shows median, and whiskers show spread of the data. One way ANOVA was performed followed by a post-hoc Tukey test. Letters denoted significant differences. Root lengths that share a letter are not significantly different. n = 24.

Arabidopsis *epf* mutants, which have homologues in crop plants, were selected for experimentation because the ultimate goal is to enhance NUE and WUE in crops. Interactions between stresses and certain traits, such as flowering and root length were observed to see if they could aid in survivability or stresses. Ultimately aiming to enhance both NUE and WUE. Mutants were selected based on availability: these were EPFs (epidermal patterning factors). EPFs are small cysteine – rich peptides, which are important in signalling pathways. In particular, they control how many stomata develop and ensure that the one cell spacing[6] rule is upheld (Mohamed et al., 2023). The EPF and EPF like (EPFL) genes have also been linked to other developmental pathways, other than epidermal cell patterning, such as lateral shoot organ patterning, root architecture and inflorescence architecture (Bemis et al., 2013; Han and Torii, 2016; Tameshige et al., 2017; Torii, 2021) . EPFL9 has also been linked to a nitrate starvation response (Hamiditabar Z 2022). Therefore, these mutants were used to see if the amount of stomata present affects the plant's ability to survive on media containing increasing amounts of salt.

Images were taken on day 0 of transfer, 2 and 7 days post transfer. The results showed that as the concentration of salt increases, the overall root length growth decreases. The data spread is variable,

[6] One cell spacing refers to the separation of developing stomatal cells by one pavement cell.

as indicated by the individual data points and no significant differences between any of the mutant lines and wild type were observed. Results shown in Figure 4.8.

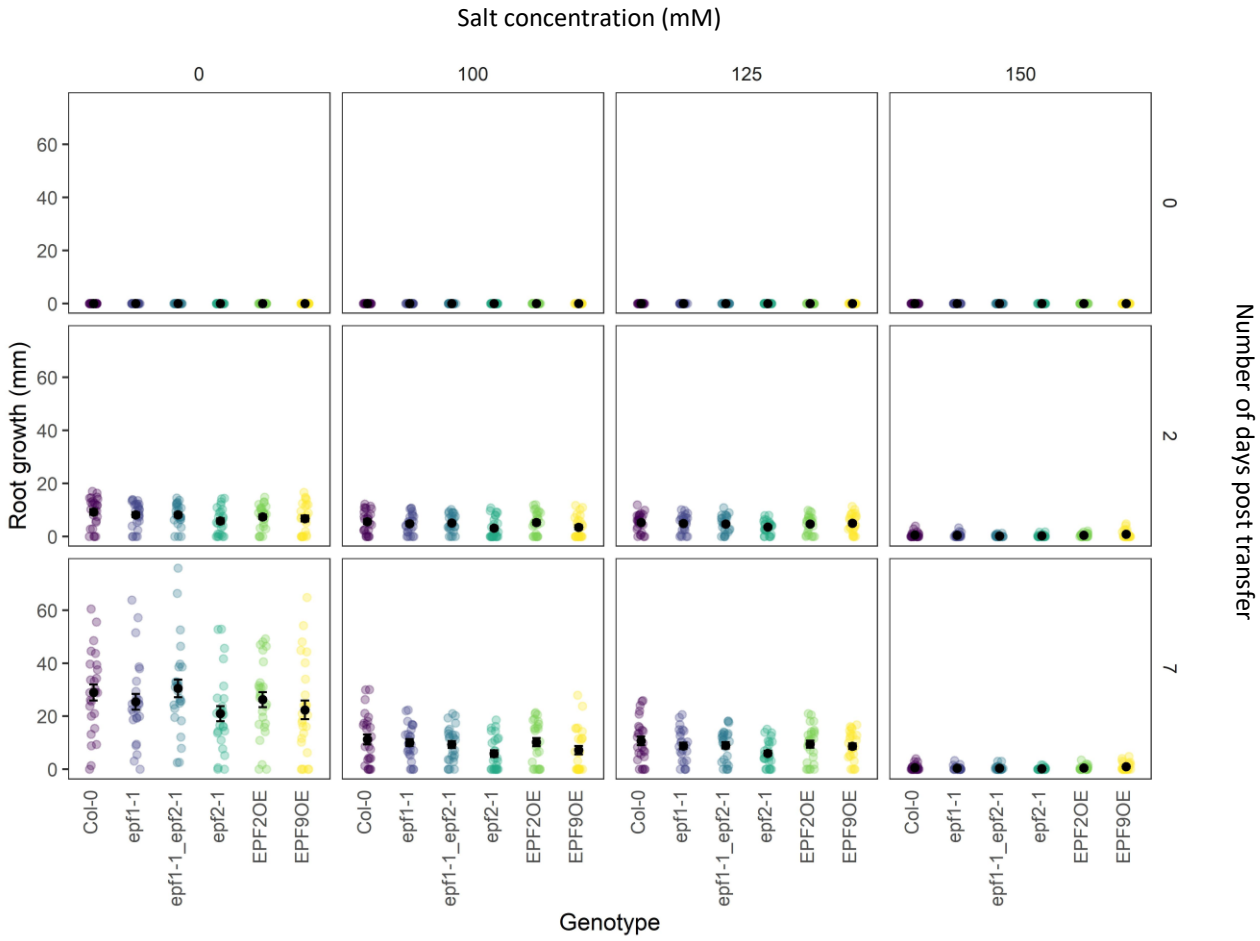

Figure 4.8 – Increasing salt concentration decreases root growth. Individual points were plotted and data was pooled from plates. Error bars, points at the mean and ± SEM. One Way ANOVA was performed and no significant differences were observed ($p > 0.05$). n = 24.

4.3.4 – Reducing stomatal density in rice promotes increased salt tolerance

To allow experimentation on crop plants, salt watering of rice (*Oryza sativa*) plants with differences in *EPF1* expression was conducted. Rice was chosen as resources were available that had different levels of *EPF1* over-expression with a weak (*OsEPF1oeW*) and strong phenotype (*OsEPF1oeS*). When the gene is overexpressed, it leads to a reduction in stomatal density, *OsEPF1oeW* had a 58 % reduction and *OsEPF1oeS* had an 88 % reduction compared to IR-64 control (Bertolino et al., 2019; Caine et al., 2023). It was hypothesised that a greater stomatal reduction (*OsEPF1oeS*) would result in less salt uptake and therefore such plants would be able to withstand salt stress for longer than control plants (or weak phenotype *OsEPF1oeW* plants). A pilot experiment (performed by Caine R and Sloane J) was performed. It was suggested that there were differences between the *EPF1* mutant lines compared to

the wild type. A variety of salt concentrations were trialled. Twenty mM NaCl was determined to be the best concentration for experimentation. It was suggested that *OsEPF1oe* plants have the potential to be able to tolerate salt stress for longer time periods, when compared to IR-64. Fv/Fm readings confirmed that IR-64 showed signs of stress earlier than *OsEPF1oe* lines. It was also noted that, as hypothesised, salt treated plants used less water than well-watered plants. Figure 4.7 shows the summary of results obtained from the pilot experiment; graphs provided by Sloane J and Caine R. It was shown that, salt concentrations increase, both water lost and dry weight decrease. Results from the 10 mM salt treatment are between 0 mM and 20 mM in terms of response but has a variable response when water loss is compared to plant biomass. Therefore, under these experimental conditions, two distinct groups are observed: 1) the 20 mM salt treatment, which had less water loss and lower plant biomass, and 2) the well-watered treatment, which had higher water loss and higher plant biomass.

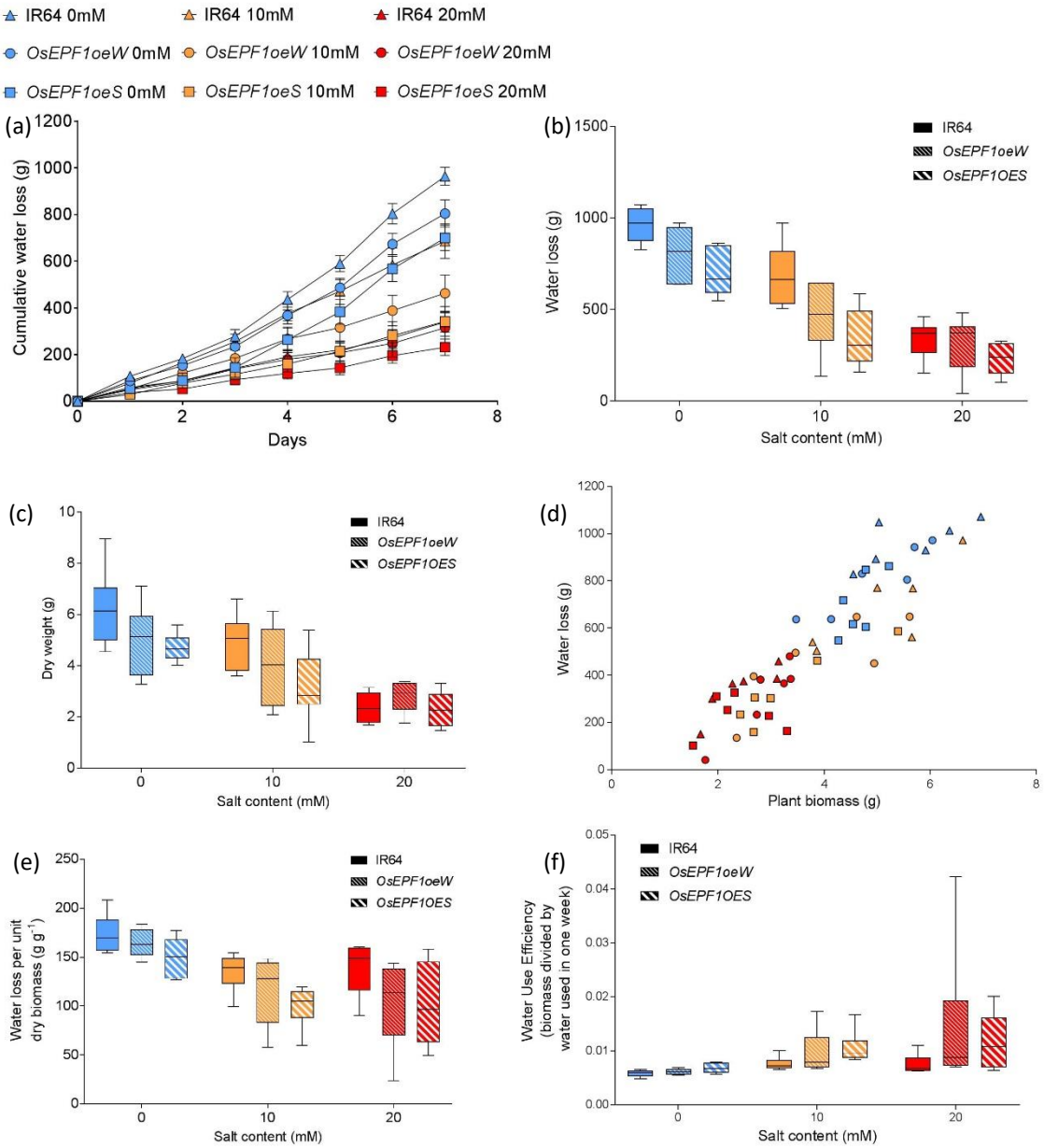

Figure 4.9 – Pilot experiment assessing salt tolerance in rice with reduced stomatal density. (a) Cumulative water loss over 7 days of control (IR-64), *OsEPF1oeW* and *OsEPF1oeS* treated with 0, 10 or 20 mM NaCl treatment. (b) Total water loss. (c) Dry weight. (d) Cumulative water loss regressed against dry biomass. (e) Water loss per unit biomass. (f) Water-use efficiency. n = 6. Salt treatment decreases water loss and dry weight. Summary data from pilot experiment provided by Caine, R and Sloan, J.

Due to these results, it was decided that, to analyse the differences between the mutant lines, a more severe stress would be needed, to see if they could survive the salt stress. Plants were grown in batches and 13 day old seedlings were transferred to 50 mM salt water for 1-4 weeks and then returned to water. Figures 4.10, 4.11 and 4.12 represent the results of Fv / Fm measurements for the tip, middle and base of plants. This was done so that severe stress could be quantified at the base of

plants once apical leaves had died due to high salt uptake. In treatments, of 2, 3 or 4 weeks exposure to 50 mM salt *OsEPF1oe* lines have higher chlorophyll fluorescence (inferred using ΦPSII measurements) compared to wild type. Four weeks of salt treatment shows a large drop in chlorophyll fluorescence IR-64 and OsEPF1oeS, but less for OsEPF1oeW. All values start considerably lower than the expected values of 0.79 – 0.84 for healthy plants, then all drop considerably after 4 weeks of salt treatment.

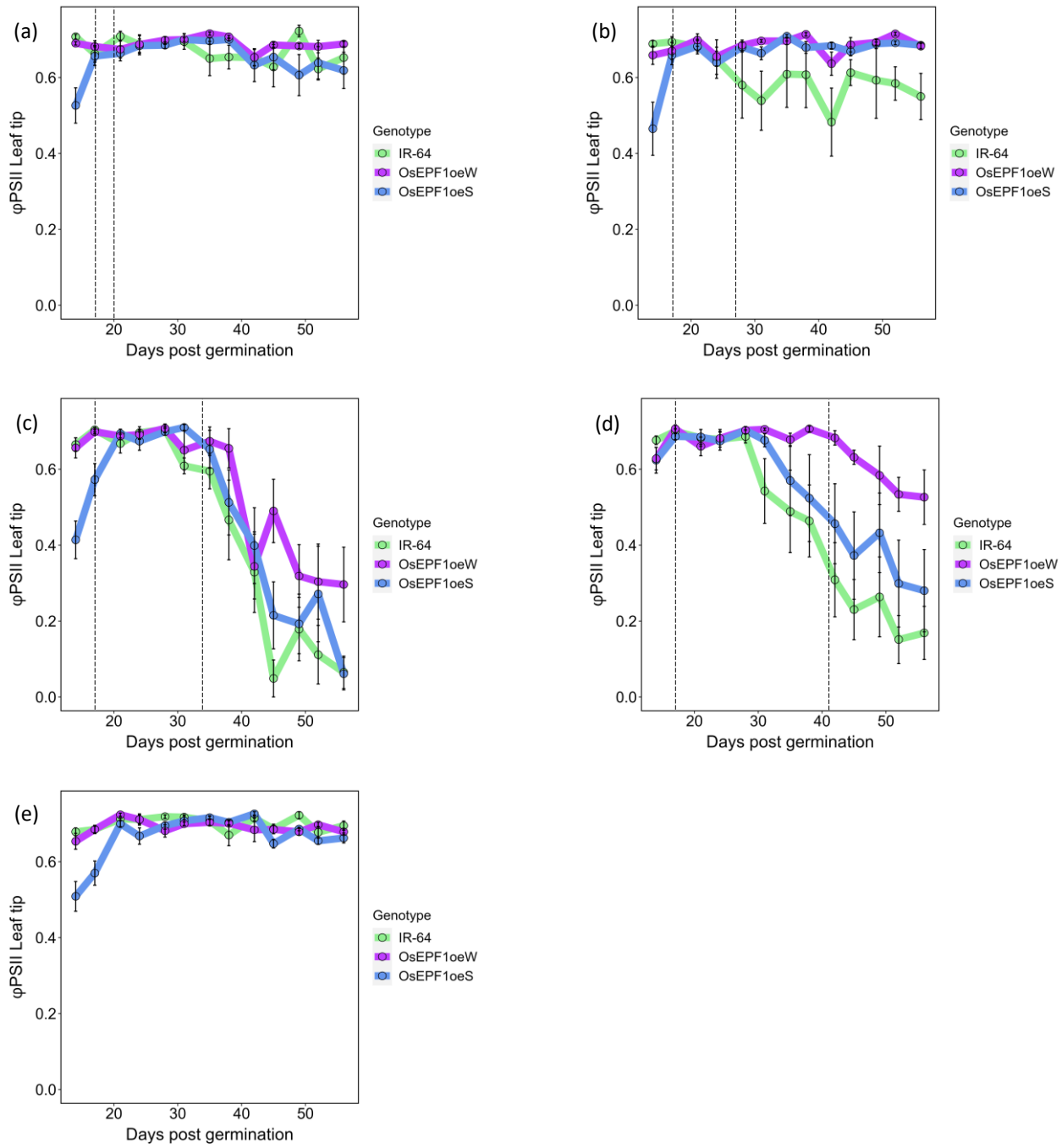

Figure 4.10 – Prolonged exposure to salt causes a reduction in chlorophyll fluorescence in the tip of the leaf. ΦPSII measurements for the leaf tip. A) One week in 50 mM salt. B) Two weeks in 50 mM salt. C) Three weeks in 50 mM salt. D) Four weeks in 50 mM salt. A) to D) After salt treatment plants returned to water. E) Plants grown under well-watered conditions. Vertical dotted lines represent time period under salt treatment. Mean values were plotted and error bars were ± SEM. n = 8.

In Figure 4.11, the middle of the plant at the sheath apex, the results are slightly different to those at the tip. IR-64 has a higher starting fluorescence, which it maintains under 1 and 2 weeks of salt treatment. After 3 weeks there are differences starting to show, with *OsEPF1oeW* not being as affected compared to *OsEPF1oeS* and IR-64. After 4 weeks of salt treatment all lines are affected, but OsEPF1oeW has a higher chlorophyll fluorescence compared to the other 2 lines.

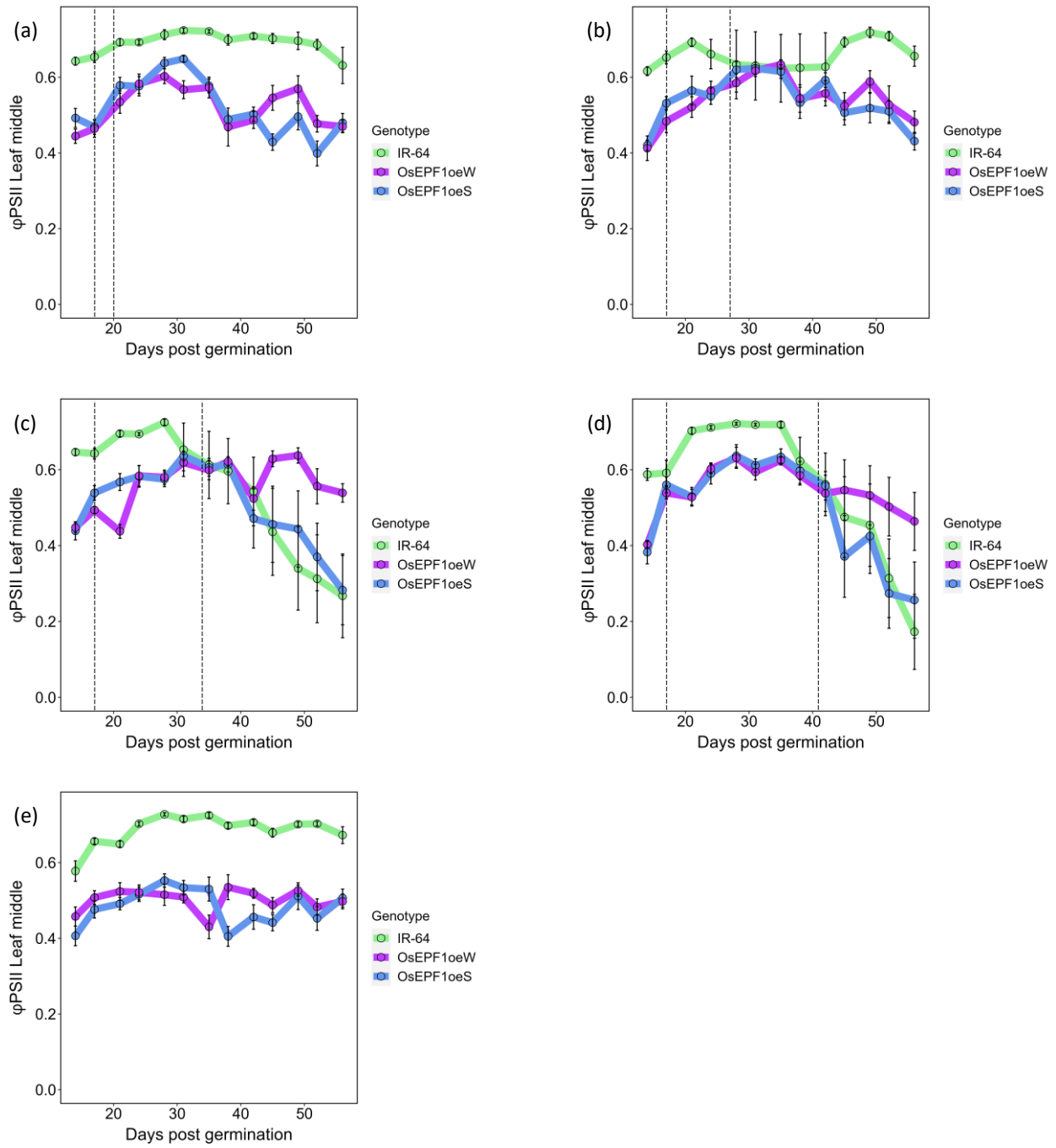

Figure 4.11 – Prolonged exposure to salt causes a reduction in chlorophyll fluorescence on the upper portion of the tiller sheath. ΦPSII measurements for the leaf tip. A) One week in 50 mM salt. B) Two weeks in 50 mM salt. C) Three weeks in 50 mM salt. D) Four weeks in 50 mM salt., A) to D) After salt treatment plants returned to water. E) Plants grown under well-watered conditions. Vertical dotted lines represent time period under salt treatment. Mean values were plotted and error bars were ± SEM. n = 8.

Tiller base measurements in Figure 4.12 showed that there was very little difference between the genotypes after 1 or 2 weeks of salt treatment, with Fv / Fm values still being reasonably high. Under 3 weeks of salt treatment all genotypes decreased, with both mutant lines having slightly higher fluorescence values compared to IR-64. Under 4 weeks of salt treatment, fluorescence values for all

genotypes decreased, but there was a larger difference for *OsEPF1oeW* compared to IR-64 and *OsEPF1oeS*. The weak phenotype had a higher value towards the end of the experiment and started to increase again, whereas IR-64 and *OsEPF1oeS* both were still declining in their values. Figure 4.13 shows representative images of rice seedlings under experimental conditions.

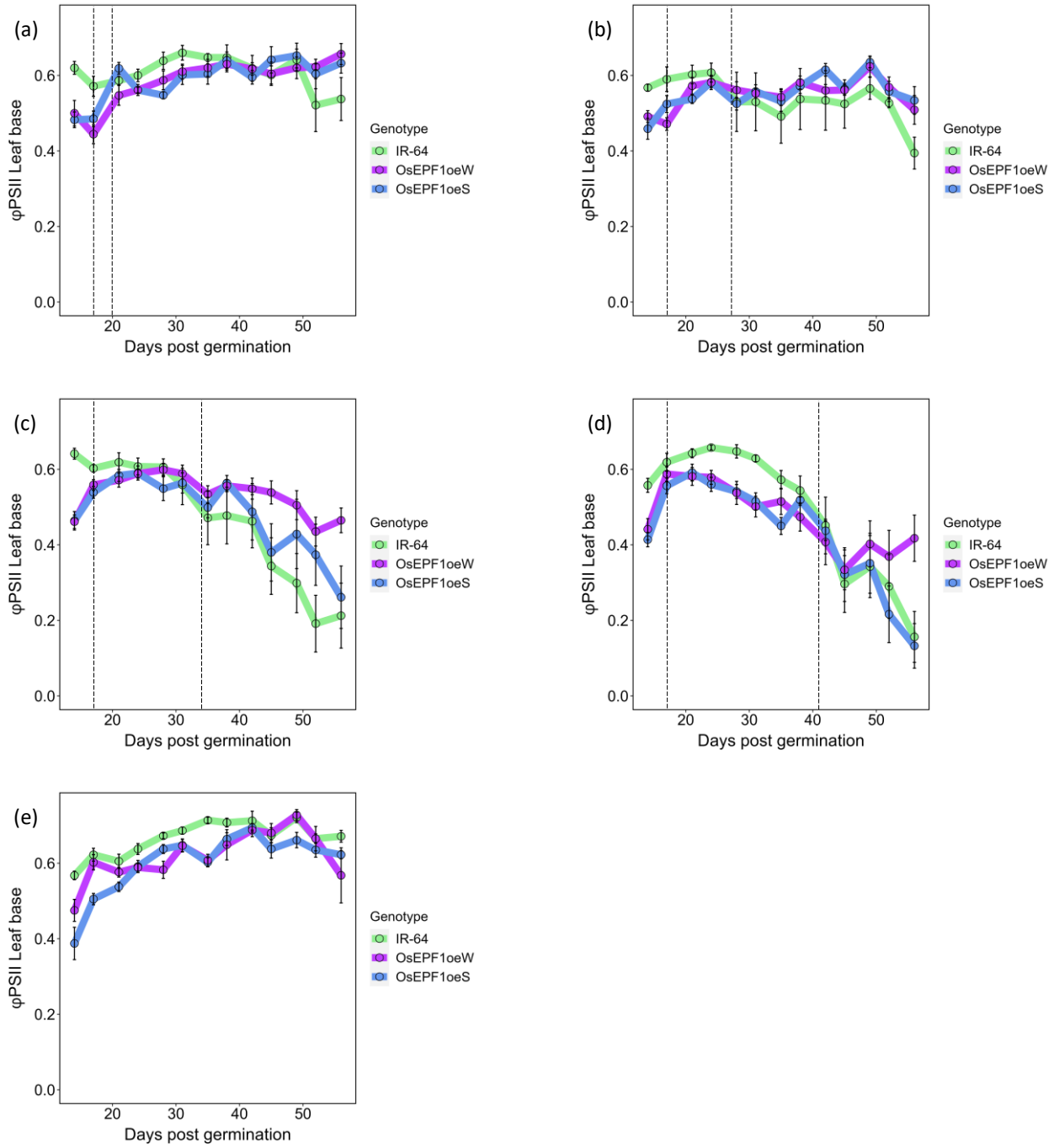

Figure 4.12 – Prolonged exposure to salt causes a reduction in chlorophyll fluorescence in the base of the leaf. ΦPSII measurements for the leaf tip. A) One week in 50 mM salt. B) Two weeks in 50 mM salt. C) Three weeks in 50 mM salt. D) Four weeks in 50 mM salt. A) to D) After salt treatment plants returned to water. E) Plants grown under well-watered conditions. Vertical dotted lines represent time period under salt treatment. Mean values were plotted and error bars were ± SEM. n = 8.

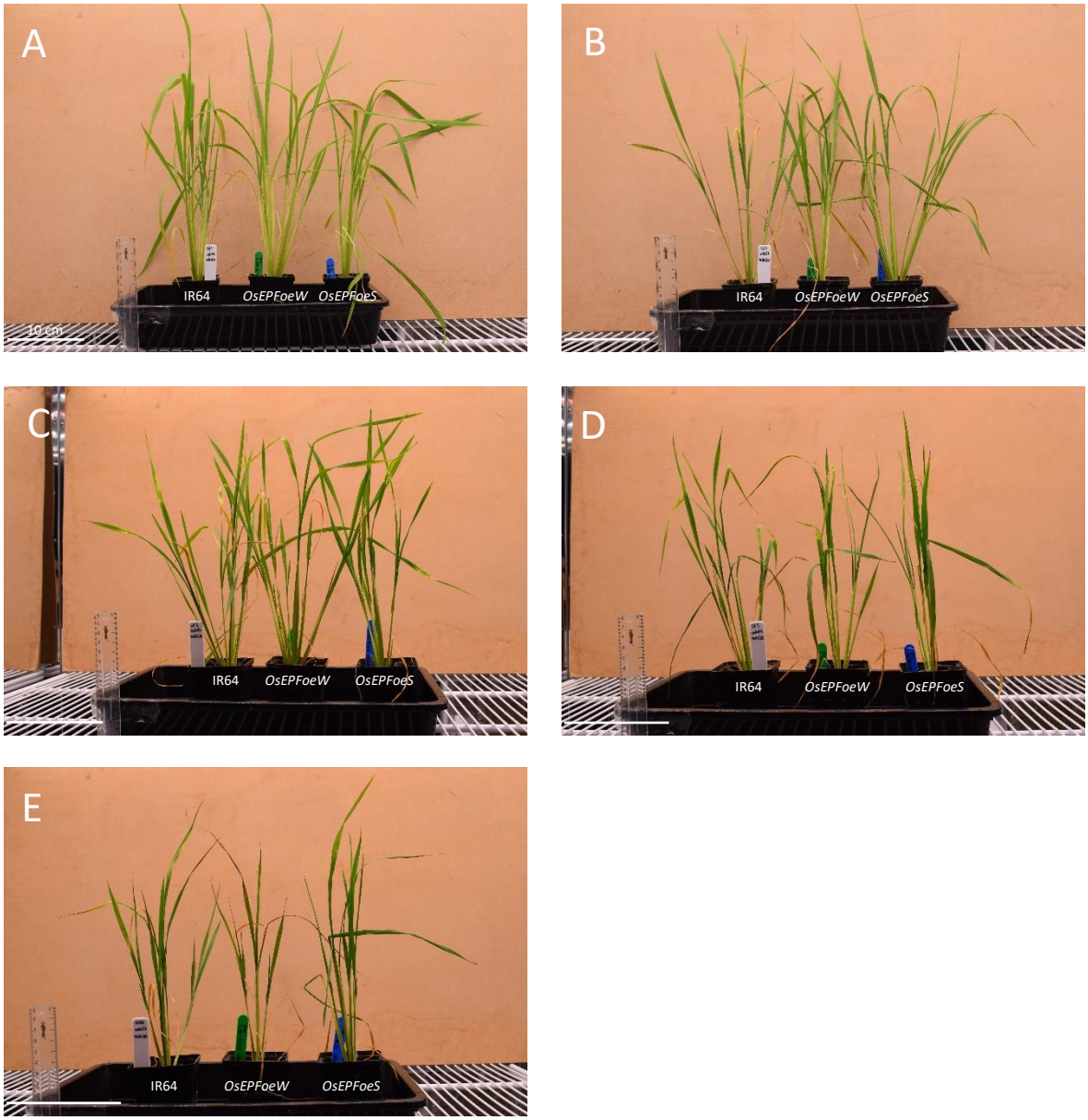

Figure 4.13 – Representative images of rice seedlings subjected to salt stress. Seedlings are 34 days old and have spent between 1 to 4 weeks in 50 mM salt solution. A) One week in 50 mM salt. B) Two weeks in 50 mM salt. C) Three weeks in 50 mM salt. D) Four weeks in 50 mM salt. Seedlings labelled with a white label are IR-64, green are *OsEPFoeW* and blue *OsEPFoeS*. Scale bars are 10 cm.

4.3.5 – The longer plants are exposed to high salt concentrations, the more the impact on growth and performance

Plants were returned to well-watered conditions after the salt treatment had finished and recovery and survivability were observed. All plants survived and produced tillers. When plants are stressed, early flowering and production of tillers can result in order for plants to survive. If there is reduced nutrient availability, then less tillers are produced. Stress causes normal growth development to stop and therefore fewer new leaves will be produced, and nutrients diverted to where they are most

needed. This can lead to colour changes in leaves and in some cases senescence. Once the experiment was completed, the number of tillers were counted for all genotypes and treatments and the dry weight was also measured.

Figure 4.14 showed the number of tillers produced for each genotype under increasing length of exposure to salt treatment. There were no significant differences between genotypes or treatments for number of tillers produced.

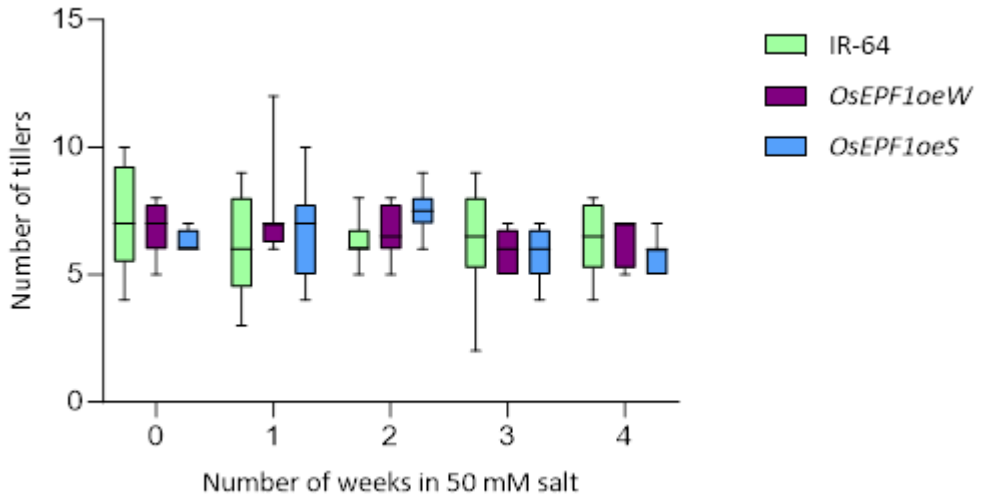

Figure 4.14 – Overall there is no significant difference in tiller number after salt treatment. Box and whisker diagram where median is plotted. Whiskers are minimum and maximum values. Two-way ANOVA was performed using Geisser-Greenhouse correction. No significant differences were found. n = 8.

Once the plants had stopped growing, the above ground material was collected, weighed and then left to dry. The dry weights are shown in Figure 4.15. There is a general trend that as time exposed to 50 mM salt increases, dry weight decreases. Initially under well-watered *OsEPF1oeW* has a slightly higher weight compared to the other two genotypes. Under 1 and 2 weeks of salt, *OsEPF1oeS* and *OsEPF1oeW* both have slightly higher dry weights compared to IR-64.

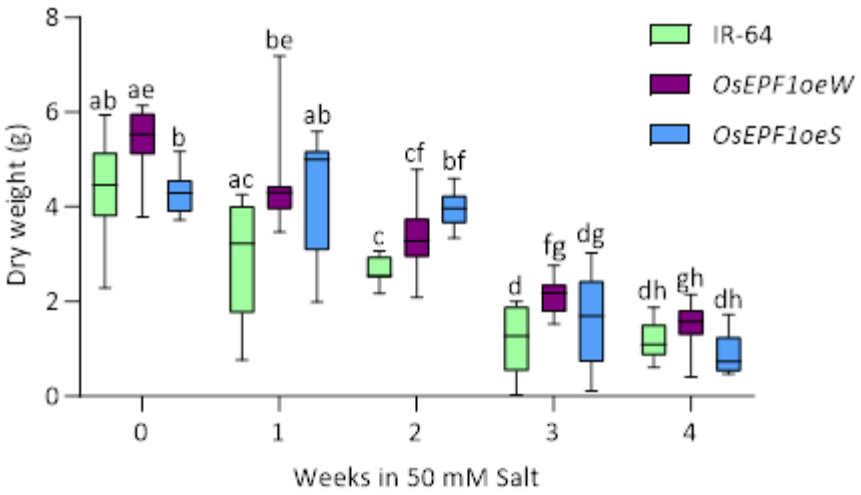

Figure 4.15 – As length exposure to salt treatment increases, dry weight decreases for all genotypes. Box and whisker plot, where line is the media and whiskers are minimum and maximum values. Two-way ANOVA was performed using Geisser-Greenhouse correction followed by post hoc Tukey tests. Letters denote significance. n = 8.

4.4 – Discussion

4.4.1 – Dynamic thermal imaging can view responses in whole plants

The purpose of the dynamic thermal imaging experiments was to observe how intact plants respond to the application of ABA. ABA was selected as a test mechanism for thermal properties because increasing levels of ABA cause stomatal closure, which reduces transpiration and consequently results in higher leaf temperatures.

Examining detached leaves can induce wounding responses and using epidermal peels, can also cause guard cells to be dead or unresponsive (Konstantis et al., 2022). Therefore, dynamic thermal imaging of whole plants, as well as localised ABA application provides a more accurate representation of the plant's response (Hõrak et al., 2020; Hõrak et al., 2021).

Localised thermal imaging can be important when investigating stresses such as wounding or bacterial infection and their effects on adjacent leaves. These observations can assist in identifying potential gene signalling pathways. Results in this chapter were published in Horak et al., (2020; 2021) and the confirmed method was then used for *prt1* mutant line.

4.4.2 – *prt1-1* is less sensitive to ABA signalling

PRT1 has been linked with the ABA signalling pathway, but there are conflicting results (experiments performed and literature) regarding sensitivity to ABA, particularly in relation to stomatal responses. There has been considerable work on PRT6, but less on PRT1, especially regarding stomatal movements (Holman et al., 2009; Zhang et al., 2018b).

ABA regulates various signalling pathways, including Ca^{2+} signalling, which plays a crucial role in plant responses to environmental stimuli. Specifically, ABA influences Ca^{2+} signalling pathways and any impairment in Ca^{2+} signalling can alter overall plant physiology. If Ca^{2+} signalling is compromised, plants may exhibit reduced sensitivity to ABA, resulting in less stomatal closure and consequently higher transpiration rates and cooler leaf temperatures (De Silva et al., 1985; Kim et al., 2011; Brandt et al., 2016).

Ca^{2+} ions act as secondary messengers in ABA signalling. The binding of ABA to its receptors triggers a cascade of intracellular events, including the release of Ca^{2+} from internal stores or the influx of Ca^{2+} from the external environment. This increase in intracellular Ca^{2+} concentration activates various protein kinases and other signalling molecules that mediate ABA's effects, such as stomatal closure. Impairments in this signalling pathway can disrupt these processes, leading to reduced stomatal responsiveness and altered water balance (Webb et al., 2001; Li et al., 2018; Wang et al., 2020).

Recent studies have provided new insights into the role of Ca^{2+} in ABA signalling, highlighting its importance in regulating stomatal movement and overall plant water management. For example, research has shown that specific Ca^{2+} sensors and signalling components are crucial for optimal ABA responses (Chater et al., 2014; Manik et al., 2015). These findings suggest, that *prt1-1's* reduced sensitivity to ABA could be linked to disruptions in Ca^{2+} signalling pathways, impacting its ability to close stomata effectively and maintain water homeostasis.

Interestingly, the experiments in this chapter revealed an unexpected result: there appeared to be less of a response under 5 μM ABA compared to 1 μM when ABA was applied through spraying. It was hypothesised that a higher ABA concentrations would result in a larger effect. From Hõrak (et al., 2020), Col-0 stomata should close earlier under 5 μM ABA, leading to higher leaf temperatures. However, the starting temperature for samples treated with 5 μM ABA was significantly higher than for the samples treated with 1 μM, which may have influenced the observed temperature differences (Movahedi et al., 2021).

4.4.3 – Barley germinated with or without nitrate does not effect ABA signalling

Follow-up work from the published material confirmed that there was no requirement for exogenous nitrate to improve ABA responsiveness. Leaf temperature measurements of plants grown with or without nitrate produced similar results (Figure 4.5). Previous studies had suggested that nitrate transporters play a role in guard cell movements and signalling, implying that higher nitrate availability potentially enhances guard cells reactivity. However, this study found no significant differences in ABA responses regardless of nitrate presence.

Nitrate transporters and their influence on guard cell behaviour have had conflicting views. NO, a byproduct of nitrate metabolism, is known to aid in both stomatal closure and opening, adding complexity to the relationship between nitrate and ABA signalling. Nitrate levels can significantly influence the presence and activity of transcription factors in plants. As a crucial nutrient and signalling molecule, nitrate activates specific signalling pathways that regulate the expression and function of transcription factors which in turn modulate the expression of genes involved in nitrate uptake, assimilation, and metabolism. This regulatory mechanism enables plants to adjust their physiological processes to optimize nitrogen use and adapting to varying nitrate availability in their environment (Konishi and Yanagisawa, 2013; Medici and Krouk, 2014; Canales et al., 2017).

Work also indicated a decrease in nitrogen assimilation under drought stress, which could affect NO production and subsequently influence ABA signalling and stomatal responses (Guo et al., 2003; Han et al., 2022). This finding suggests that environmental factors such as drought stress might have a more significant impact on ABA responsiveness than the availability of nitrate alone.

4.4.4 – Plate grown seedlings on increasing salt concentrations stunts root growth

There is evidence suggesting that *NIA2*, plays a more significant role in the response to salt stress response as compared to *NIA1* (Flores et al., 2004; Debouba et al., 2007; Debouba et al., 2013). In this study, the results indicated that mutant line *nia2 (2)* was more impacted by the addition of salt compared to the other genotypes. However, the large variability within the data suggests that this may not represent a true phenotype and further replication with independent mutant alleles would be required to confirm or refute findings.

Differences were observed in *NIA1SDM* mutant lines compared to Col-0 under 100 and 125 mM salt. At 150 mM, the salt levels were too high for all genotypes, leading to growth inhibition. There have been links to suggest that nitrate uptake under salt stress is decreased, but ammonium can accumulate within the roots (Debouba et al., 2007). Interestingly sumoylation defective mutants might tolerate slightly more salt due to increased nitrate production and uptake. This is consistent with findings in rice, where SUMO is a critical regulator for salt stress responses. In Arabidopsis, SUMO is known to regulate NIA, which is essential for nitrate assimilation (Soo Park et al., 2011; Srivastava et al., 2016). NIA2 has been linked to a salt stress response but has no predicted sumoylation sites. This might suggest that removing sumoylation enables plants to assimilate more nitrate, improving salt tolerance and enabling plants to grow roots deeper to find areas of less toxicity.

Finally, the EPF mutants did not respond as expected based on published data (Hepworth et al., 2015), there were no significant differences between the genotypes. This contrasts with previous findings that suggest EPF genes play a role in regulating stomatal density and, in turn, stress responses. One possible explanation is that the seedlings were too small or immature to exhibit distinct root phenotypes. Young plants may not have fully developed the mechanisms necessary to show noticeable differences in response to salt stress, particularly in their root systems. High humidity levels in plate growth environments also play a role in reduced responses and can affect development and responses(Casson and Gray, 2008; Hara et al., 2009; Doheny-Adams et al., 2012; Hughes et al., 2017; Caine et al., 2023).

The results suggest that the phenotypic differences associated with EPF mutations might be more pronounced in the aerial parts of the plant rather than the roots. EPF proteins primarily regulate stomatal patterning on the leaf surface, suggesting that root responses may be lower than the impact on WUE and transpiration. There could also be other mechanisms which mitigate the effects of salt stress on root growth, particularly in young developing seedlings. The findings suggest a potentially more complex role for EPF genes in responses to salt stress, which could potentially involve

interactions between root and shoot systems but requires further investigations (Hepworth et al., 2016; Caine et al., 2023).

Overall, while the data suggests a role for NIA2 in salt stress response, the variability and unexpected results, particularly with the EPF mutants, infers the complexity of salt stress responses in plants and further research is needed to fully understand the underlying mechanisms.

4.4.5 – *nia2* is slightly more susceptible to salt than *nia1*

During salt assays on plates, as salt concentrations increased, root length growth decreased, which was expected. Plants require a certain level of salt to survive and for various functions, but excessive salt becomes detrimental, leading to reduced growth, chlorosis and eventually death. Results from these assays showed that *nia2* mutants were more impacted by salt treatment than *nia1* mutants and Col-0. In particular, *nia2 (2)* which had significantly reduced root growth compared to Col-0 under nearly all salt treatments. This observation fits with the literature which suggests that *NIA2* might be more crucial in managing salt, however, the high humidity environments of the plats grown seedlings might impact growth and therefore results (Hirt and Shinozaki, 2004; Kolbert et al., 2010; Negrão et al., 2017; Liu et al., 2023).

Interestingly, previous results in Chapter 3 (Figure 3.6) indicated no significant differences between stomatal densities or aperture changes (in response to ABA) between the genotypes. This suggests that the observed differences seen in salt stress response are not likely to be related to stomatal movements / function. The variability in response, a strong effect was observed in only one of the nia2 mutant lines, indicating that the response could be due to an artefact caused by the positional effects of the T-DNA insertion. To determine if there is a genuine phenotype, more lines would need to be tested, as well as to use mature plants and salt watering. CRISPR Cas 9 technology could also be used to specifically target and investigate the regions altered in the *nia2* mutants, which would provide deeper insights into gene function (Bertolino et al., 2019; Dellero, 2020).

These results were unexpected given that in previous studies (Guo et al., 2017; Tang et al., 2022) it was suggested that NIA1 was involved in salt stress responses and is important for responses to stresses in general. However, NIA2 is more abundant and has a higher activity in plants than NIA1, suggesting that general plant health and growth are more linked to NIA2 than NIA1. No firm conclusions can be drawn, as significant differences were found in only one mutant line, but it is an interesting observation (Wilkinson and Crawford, 1991; Debouba et al., 2013; Le et al., 2023).

4.4.6 – *NIA1 SDM* lines are more salt tolerant than Col-0

The results for root growth of *NIA1 SDM* lines under increasing salt concentrations showed that the mutant lines were more salt tolerant than Col-0 under 100 and 125 mM salt. However, at 150 mM salt, all genotypes were affected, which is expected as 150 mM is a very high salt concentration and typically detrimental to plant health. The enhanced salt tolerance in *NIA1 SDM* lines may be linked to alterations in sumoylation, a post-translational modification known to negatively affect the regulation of proteins and gene expression. *NIA1* has been identified in having 3 potential sumoylation sites and in these mutants the predicted main site was knocked out by an amino acid change, potentially leading to the overexpression of *NIA1* and improved stress responses (Soo Park et al., 2011; Costa-Broseta et al., 2021).

Interestingly, mature plants had slightly larger rosette leaf areas compared to Col-0. However, at seedling stage this was not a large difference and therefore suggesting minimal impacts on root growth results. One line, *NIA1 SDM line 2*, had significantly lower abaxial stomatal density compared to Col-0 and *NIA1 SDM line 1*, but no significant differences on the adaxial side. These differences are unlikely to account for the responses observed, especially as *NIA1 SDM line 1* has a slightly longer root growth compared to the other 2 genotypes (LU et al., 1993; Lake et al., 2002).

To confirm that *NIA1* is involved in a salt response, *NIA1* overexpression lines could be used. It would also be interesting to view mature plants and salt watering. Unfortunately, plants do no survive well on sand and terragreen. Hydroponics would be a better method, as the interaction between salt and nitrate could also be investigated and viewed. A hydroponics system was set up and trialled with Col-0, *nia* mutant lines and EPF mutant lines, unfortunately under the conditions none of the plants survived and therefore that method for Arabidopsis was abandoned (Ullrich W.R., 2002; Tocquin et al., 2003; Conn et al., 2013).

4.4.7 – Duration of salt watering on rice affects its chlorophyll fluorescence

The experiment examining the effects of salt watering on rice revealed that leaf tips did not recover from salt stress, which was expected, as leaf tips are the first parts to senesce and lose nutrients. The leaf tips had started to turn yellow and in some cases brown by the end of the experiment, which corresponded to the decrease in chlorophyll fluorescence values. This reduction in chlorophyll content indicates a decrease in photosynthesis, resulting in lower chlorophyll fluorescence readings. The results from all parts of the leaves suggested that *OsEPF1oeW* was slightly more salt tolerant than *OsEPF1oeS*, which was slightly more tolerant than IR-64. Treatment of two weeks in salt treatment biomass data suggest that extreme reduction of stomatal density is beneficial up to a point and then after that point it can be detrimental. This is different from what was expected. Typically, reduced

stomatal density would result in less water lost and therefore less salt being taken into the plant roots via the transpiration stream. However, when there was an 88 % reduction in stomatal density, although WUE improved and the plants were visibly no different from IR-64, the plants were more affected by salt, when compared to the weaker phenotype, resulting in a 58 % reduction for leaf base after 1 or 2 weeks in salt treatment (Hepworth et al., 2015; Hepworth et al., 2016).

The small size of the seedlings used in this experiment may have affected the accuracy of chlorophyll fluorescence measurements. The fluorpen used to measure fluorescence requires full coverage of the measurement hole, and in some cases, the small leaves may not have completely covered this area, leading to variability in the data (observed in Figures 4.8 – 4.10). Increasing the number of replicates and repeating the experiment with more mature plants could help reduce this variability and provide more reliable results (Chaves et al., 2009; Medrano et al., 2015).

Furthermore, the method of salt application may have caused variability, as larger, healthier plants may have taken up water and thus salt faster than their smaller, less healthy counterparts. Therefore, there is the potential that the healthier plants were exposed to a higher salt concentration. To see if this occurred, future experiments could utilise sacrificial plants, to view the initial salt concentrations and observe how this changed over the course of the experiment (Medrano et al., 2015; Negrão et al., 2017).

The comparison between rice and Arabidopsis in terms of chlorophyll fluorescence highlighted that rice plants generally exhibited lower fluorescence values, suggesting lower photosynthetic efficiency and overall health in rice under similar conditions. This observation could be linked to differences in species-specific responses to salt stress, as well as variations in experimental conditions, such as pot size and environmental controls. The smaller pot size used in this study may have constrained root growth, leading to stress and reduced vegetative growth, which could further complicate the interpretation of the results (Munns and Tester, 2008; Chaves et al., 2009).

Finally, the experimental setup, including the need to open growth chambers for data collection and the effects of fan-induced airflow, likely contributed to the observed variability. Plants closer to the fans would potentially lose more water through their stomata compared to those further away, due to increased wind speed. Regularly changing plant positions within the chamber was an attempt to mitigate these effects, but the variability observed in chlorophyll fluorescence data suggests that these factors still influenced the results. Chlorophyll fluorescence measurements are a snapshot of plant health and measurements were taken from one leaf. Using IRGA equipment such as a LiCor, can allow the photosynthesis of one leaf to be viewed. However, with whole plant gas exchange, analysing the plant as a whole, in relation to photosynthesis would be interesting, as it would mitigate some of

the variances from leaf positioning. However, due to the number of plants in this experiment the LiCor was not a viable option (Munns and Tester, 2008; Ashraf and Harris, 2013; Medrano et al., 2015). As a result, the findings from this study are preliminary, and further research using more refined methods and larger-scale experiments is needed to draw more definitive conclusions.

4.4.8 – Tiller number is not affected by length of salt treatment but dry weight is

Tiller number was counted with no differences found. Yield was not counted, as dry weight was required.

4.5 – Future work

In future studies for *PRT1* it would be advantageous to expand and refine the experimental approach to develop a greater understanding of its role in ABA signalling and stomatal regulation. First, incorporating more than one independent mutant line which would help to confirm the mild phenotype observed and to rule out any inference of potential artefacts or positional effects of T-DNA insertions. Increasing the number of replicates in experiments would help to reduce effects of variability and increase confidence in statistical differences. This is especially important in complex pathways like ABA signalling, where subtle phenotypic differences are hard to detect. To better understand the dose dependent effects of ABA, future experiments should include lower concentrations of ABA, for example 0.5 and 1 μM. The lower concentrations could reveal more pronounced phenotypic differences which may not be present at higher concentrations. In order to gain more of a developmental insight, more long term studies under various environmental conditions, such as drought or osmotic stress would be able to provide insights into *PRT1*'s role in stress responses (MacRobbie, 1998; Bright et al., 2006b; Till et al., 2019).

The *EPF* mutants, did not show the expected phenotypic differences under salt stress. Further experiments are therefore needed to clarify their role in salt stress responses. Focusing on more mature plants in future studies could help determine whether the lack of root phenotypes observed in seedlings was due to their developmental stage. Mature plants might exhibit more distinct differences in root and shoot responses to salt stress, offering clearer insights into the role of *EPF* genes. Adding more detailed measurements of transpiration rates, stomatal density and WUE in both roots and shoots is important, especially as *EPF* mutations may only have effects on aerial tissue. Hydroponics for investigating salt stress could help to minimise variability and provide a more controlled and uniform salt treatment and easier to observe root growth changes under the stress (Doheny-Adams et al., 2012; Franks et al., 2015; Hepworth et al., 2015).

With regards to chlorophyll fluorescence measurements in rice under salt stress, using older larger leaves could mitigate the full leaf coverage problems during data collection. Increased sample size and replication number would also help to improve reliability of findings. Huge differences between genotypes were not observed, extending the exposure to salt and using larger pots or a hydroponic growth system could help to mitigate some of the variability. These experiments would help to provide more detailed insights into the roles of *PRT1* and *EPF* mutants in plant stress responses, in particular on chlorophyll fluorescence (Sánchez-Moreiras et al., 2020).

Chapter 5 – Identification of novel stomatal regulators

5.1 – Introduction

Changes in stomatal aperture in response to both environmental and endogenous signals, control plant water loss through transpiration and thus affect drought tolerance. Many previous studies, particularly those using *Arabidopsis* mutants, have identified components of the complex signalling pathways which regulate this system, such as the guard cell-expressed cytoplasmic serine-threonine kinases OST1 (Open Stomata 1) and HT1 (High Leaf Temperature 1), which are required for ABA- and CO_2-induced stomatal closure (Chater et al., 2015a; Tian et al., 2015; Hõrak et al., 2016; Ma and Bai, 2021). The *ost1* and *ht1* mutants were both identified by thermal screens from their cool and hot phenotypes respectively, suggesting impaired control of leaf water loss (Lefebvre et al., 2002). HT1 protein kinase was identified by a microarray expression analysis of *Arabidopsis* guard cells (Leonhardt et al., 2004). Despite many mutants being characterised, there are still important gaps in the guard cell signalling network to be filled. As kinases (Ks) and phosphatases (Ps) play key roles in almost all signal transduction pathways it is likely that there are additional phosphoregulatory components to be identified. As discussed in the introduction and nitrate chapters, the N-end rule pathway, and the post-translational modification of nitrate reductase via sumoylation are both examples of signalling cascades that involve the activity of Ks and Ps. In plant genomes, protein kinases constitute one of the largest gene families[7]. Activity of target proteins are regulated by these enzymes which catalyse the reversible phosphorylation of specific amino acids (serine, threonine and tyrosine). There are different classifications of both Ks and Ps. There are nine main groups used in mammalian, plants and fungi, and Ks are put into these groups based on their catalytic domain[8] which is comprised of 250-300 amino acid residues (Champion et al., 2004; Lehti-Shiu and Shiu, 2012; Zulawski et al., 2014). These groups are:

1. Protein Kinase A, G and C (AGC);
2. Receptor-Like Kinase (RLK) (there are also Leucine Rich Repeat RLKs (LRR-RLK)), Calmodulin/Calcium regulated Kinase (CAMK);
3. CMGC group (named after cyclin-dependent kinases (CDKs);
4. Mitogen-Activated Protein Kinases (MAPKs);
5. Glycogen Synthase Kinases (GAK) and CDK-like kinases);
6. Homologs of the yeast STE genes (STE);

[7] In *Arabidopsis thaliana* protein kinases account for about 4% of genes encoded. Genes encoding kinases are known as the *Arabidopsis* kinome (Champion et al., 2004; Zulawski et al., 2014).
[8] Catalytic domain is the region of an enzyme which interacts with its substrate causing an enzymatic reaction.

7. Casein/Cell Kinase 1 (CK1);
8. Tyrosine Kinase-Like (TKL);
9. Two general groups called Plant-specific and Others (Lehti-Shiu and Shiu, 2012; Romero-Hernandez and Martinez, 2022).

Protein phosphatases have two major classifications: protein tyrosine and serine – threonine phosphatases.

5.2 – Background

Specifically, in the light-induced stomatal opening signalling pathway there is a gap in our understanding between blue light perception and H^+ ATPase phosphorylation; the direct activators of which are unclear (Hõrak, 2021). Several components of this pathway have been identified: BLUE LIGHT SIGNALLING 1 (BLUS1), BLUE LIGHT-DEPENDENT H^+ATPASE PHOSPHORYLATION (BHP), type 1 protein phosphatase (PP1) and its regulatory subunit PRSL1 (Inoue and Kinoshita, 2017a). It is known that phototropins phosphorylate BLUS1 which leads to the activation of H^+ ATPase, (see Figure 5.1), although the direct activators of H^+ ATPase are not clear. There are further gaps in our understanding in the red light induced stomatal opening pathway, in particular those which do not respond to a change in Ci[9]. With regards to the CO_2-induced stomatal signalling pathway, several CO_2 / bicarbonate receptors have been suggested and recent work indicates that the HT1-MPK12 complex acts as a receptor for CO_2 signalling (Takahashi et al., 2022; Yeh et al., 2023). Previous studies and research have identified several components involved in stomatal regulation in response to different stimuli. These signalling pathways regulate stomatal development and aperture size in response to both environmental cues and internal signals. For plants to compete successfully in a changing environment, they are required to be efficient at sensing and reacting to these signals. In particular for WUE[10] and hence survival under conditions such as drought, stomata need to close in order to reduce the water loss through transpiration. The interacting guard cell pathways that regulate these aperture responses form a signalling network as illustrated (see Figures 5.1 and 5.2).

5.2.1 – Stomatal opening signalling network

The core guard cell ABA-signalling pathway is well studied. ABA is perceived by fourteen START-family receptors in *Arabidopsis* named the PYR/PYL/RCAR proteins (Yue et al., 2009; Park et al., 2010). In the absence of ABA, stomata are open. This is due to the activation of the central guard cell anion efflux channel SLAC1 by its activating kinases, OST1. Also, various calcium-dependent kinases are suppressed

[9] Ci is the concentration of intercellular CO_2 used in estimating photosynthetic rates in plants.
[10] Water Use Efficiency.

by protein phosphatases of class 2C (PP2Cs, ABI1, ABI2 and PP2CA) that dephosphorylate SLAC1 and its activating kinases (Negi et al., 2008; Vahisalu et al., 2008; Geiger et al., 2009; Lee et al., 2009b; Umezawa et al., 2009; Vlad et al., 2009; Geiger et al., 2010; Vahisalu et al., 2010; Brandt et al., 2012; Ye et al., 2013; Tobias et al., 2014; Brandt et al., 2015). Upon ABA binding, the receptor binds to a PP2C, releasing the SLAC1-activating kinases from inhibition and allowing them to activate and phosphorylate SLAC1 to trigger stomatal closure (Geiger et al., 2009; Lee et al., 2009a; Vahisalu et al., 2010; Brandt et al., 2012; Ye et al., 2013; Brandt et al., 2015) Fujii *et al* 2009). This core ABA signalling pathway is also involved in stomatal closure in response to elevated CO_2 levels, darkness and low air humidity, although the extent of its importance has been debated (Figure 5.1) (Merilo et al., 2013; Chater et al., 2015b; Dittrich et al., 2019).

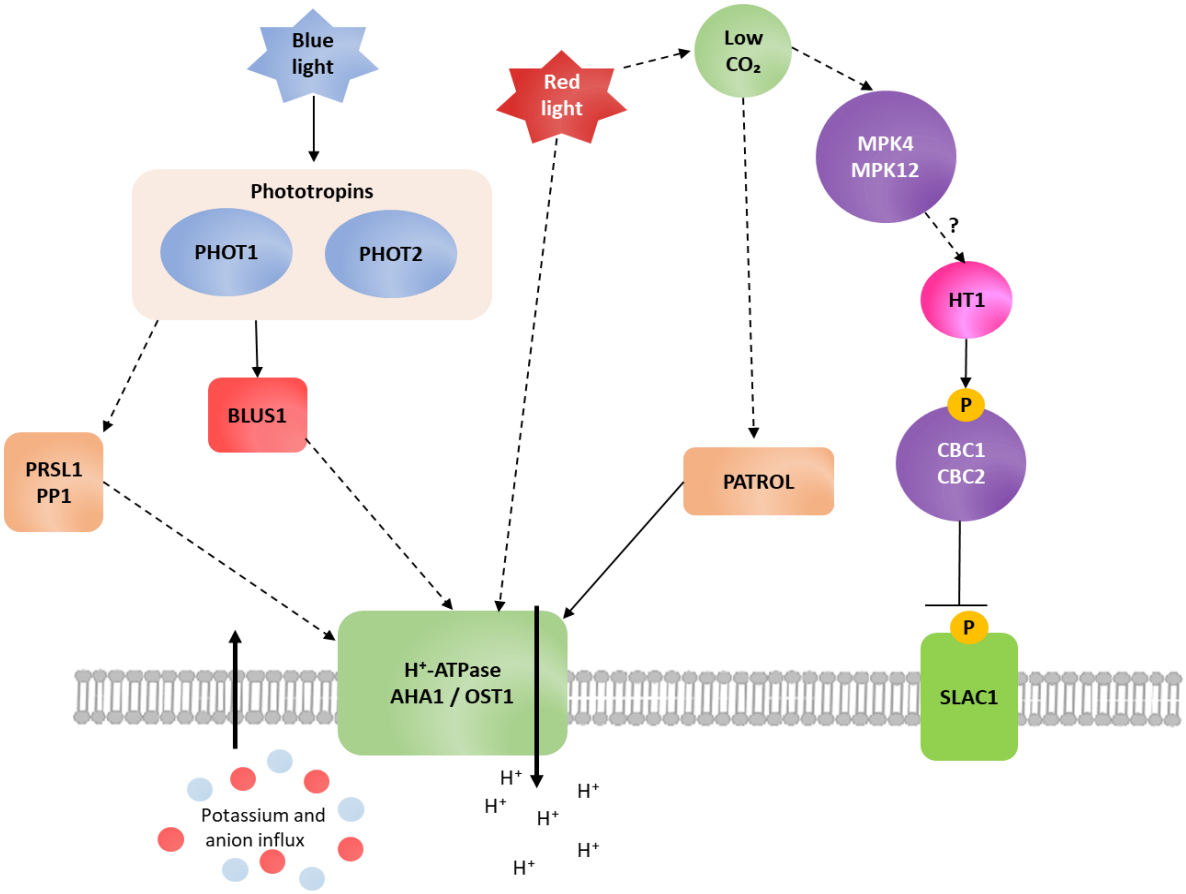

Figure 5.1 – Opening in response to environmental stimuli. Blue light is detected by Phototropins (PHOT1 and PHOT2), which transmit a signal to BLUS1 kinase, a key step in stomatal opening. ATPase is then activated, protons are expelled from the membrane leading to potassium and anion influx causing stomatal opening. Phosphatase PP1 and its regulatory subunit PRSL1 are also required for blue light activation of ATPase. Low CO_2 inhibits the phosphorylation of CBC1 and CBC2 by HT1, which inhibits the phosphorylation of SLAC1, leading to suppression of stomatal closure. Less is known about the red light signalling pathway, but it is linked to low CO_2 signalling, which also involves MPK4, MPK12 and PATROL. Solid black lines indicate known interactions, dashed lines and question marks indicate unknown mechanisms with possible multiple steps.

5.2.2 – Stomata closing signalling network

Elevated CO_2 levels also trigger SLAC1 activation through a recently identified alternative pathway that is specific to CO_2 and not involved in ABA-induced stomatal closure (Hõrak et al., 2016; Jakobson et al., 2016; Sierla et al., 2018). In this pathway, CO_2 is converted to bicarbonate (HCO_3^-) in cells with the aid of β-carbonic anhydrases CA1, CA4 and CA7 (Hu et al., 2010, 2015). Bicarbonate triggers the activation of mitogen-activated protein kinases MPK12 and MPK4 by currently unknown mechanisms. This leads to the suppression of the activity of the key negative regulator of CO_2 signalling, the HT1 kinase (Hashimoto et al., 2006; Hõrak et al., 2016; Jakobson et al., 2016). HT1, which at ambient CO_2 levels suppresses SLAC1 activation by the OST1 and by LRR-RLK GUARD CELL HYDROGEN PEROXIDE-RESISTANT 1 (GHR1) proteins, is inhibited by MPKs 12 and 4 at elevated CO_2 levels. This leads to SLAC1 activation and stomatal closure (Figure 5.2) (Tian et al., 2015; Hõrak et al., 2016; Sierla et al., 2018).

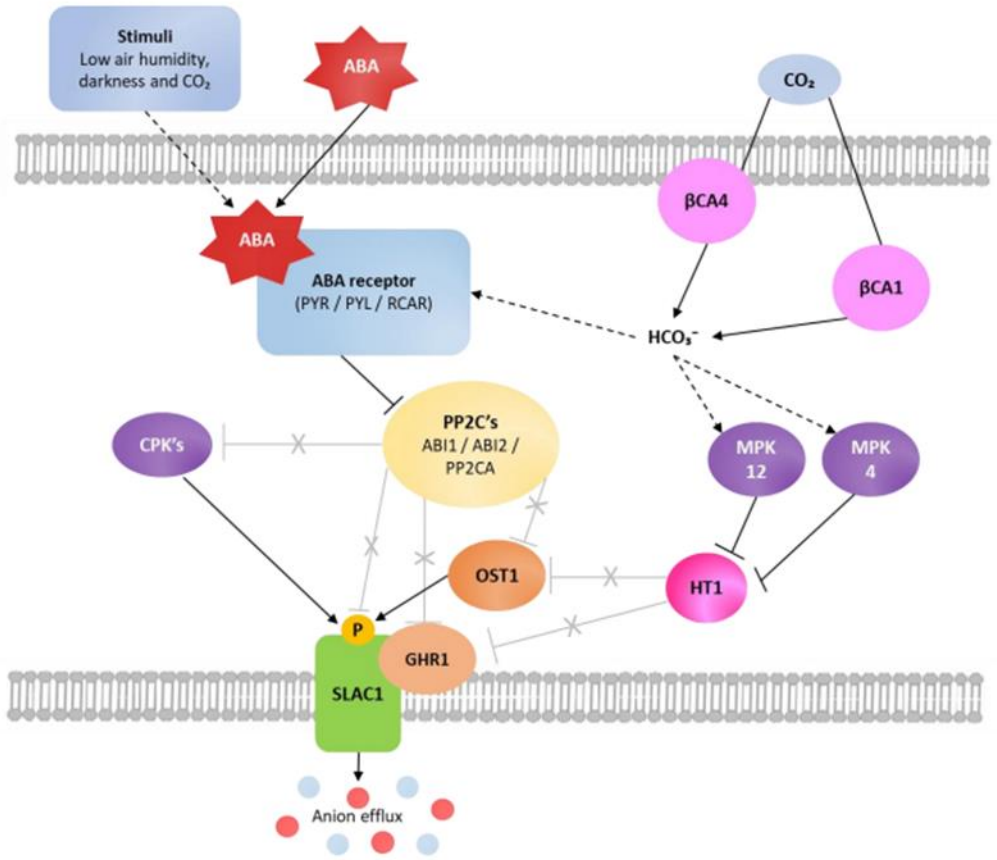

Figure 5.2 – Closing in response to environmental stimuli. Molecular mechanism of stomatal aperture closure in response to abiotic stimuli. Environmental stimuli (low air humidity, darkness and elevated CO_2) are detected, leading to higher ABA levels in cells. ABA binds to its receptor to form a complex, which inhibits the PP2C's. The inhibition allows calcium dependent (CPK's) and calcium independent (for example OST1 SLAC1-activating kinases to phosphorylate and activate SLAC1 anion channels), which leads to channel activation, anion efflux and stomatal closure. CO_2 is converted to bicarbonate (HCO_3^-) by β-carbonic anhydrases CA1 and CA4. When CO_2 levels are high, this activates mitogen-activated protein kinases (MPK4 and MPK12), which inhibit the activity of HT1 kinase. SLAC1 can then be activated by phosphorylation by OST1 and through GHR1. Solid black lines indicate known interactions, dashed lines indicate unknown mechanisms and grey are supressed interactions in the presence of ABA or CO_2 (Xie et al., 2006; Hu et al., 2010; Bauer et al., 2013; Tian et al., 2015; Hõrak et al., 2016; Jakobson et al., 2016; Pantin and Blatt, 2018; Sierla et al., 2018).

5.3 – Aims and Objectives

The experiments described in this Chapter aim to identify novel guard cell abiotic stress regulators. Systematic analysis of plants deficient in specific predicted kinase or phosphatase gene products, known to be preferentially expressed in guard cells was initiated. The signalling components identified have potential utility as targets in crop breeding programmes for drought tolerance.

Aims:

1. To ascertain if PSKR2 and GCK1 are expressed in guard cells.
2. To determine whether *pskr2* and *gck1* mutants affect stomatal movement under abiotic stress conditions.

Objectives:

1. Identify potential guard cell abiotic stress regulators:
    - Screen microarray data to identify novel gene candidates involved in guard cell regulation under abiotic stress conditions.
2. Analyse the effect of guard cell regulators on stomatal conductance:
    - Investigate whether the identified guard cell regulators affect stomatal conductance in response to various abiotic stresses, such as drought and high CO_2 levels.
3. Link responses to specific abiotic stress pathways:
    - Determine if the observed responses in stomatal conductance are linked to specific abiotic stress pathways, indicating a potential mechanistic link.
4. Examine stomatal density, index and size:
    - Assess if the identified guard cell regulators alter stomatal density, index or size, which could contribute to the overall regulation of stomatal function.
5. Compare epidermal peel bioassays with whole plant responses:
    - Compare the responses observed in epidermal peel bioassays with those observed in whole plant responses to validate the relevance of the findings in a more physiological context.
6. Investigate germination sensitivity to ABA:
    - Analyse germination sensitivity to ABA in *pskr2* and *gck1* compared to Col-0 to determine if these genes play a role in early developmental stages under stress conditions.

5.4 – Methods

5.4.1 – Plant growth

5.4.1.1 – Seedling growth for identifying homozygous lines

Seeds stratified for 72 hours on compost in trays covered with cloches were transferred to a growth chamber with a 9-hour photoperiod 200 µmol m^{-2} s^{-1}, 23 /19 °C day /night temperatures. Once seedlings had germinated to 4 to 5 true leaves, leaves were taken for genotypic analysis. Plants identified as homozygous were then transferred to individual pots in 3:1 M3 compost : perlite. Seeds harvested from these plants were used in subsequent experiments.

5.4.1.2 – Plants for whole plant gas exchange analysis

Seeds were stratified in cold water at 4-10 °C for 72 hours before transfer to plastic tubs (10 x 10 cm) filled with 2:1 peat : Vermiculite mix and covered with a glass slide with a central hole. Seeds were planted through the hole and tubs were placed into a growth chamber with a 10-hour photoperiod, light 250 µmol m^{-2} s^{-1}, 23 /19 °C day /night temperatures and 60 / 80 % day/night relative humidity. Petri dishes were placed over the seeds initially to keep humidity high and protect seedlings (see Figure 5.3). Three batches of plants were grown in a staggered experiment. Plants were analysed when they were 25-32 days old.

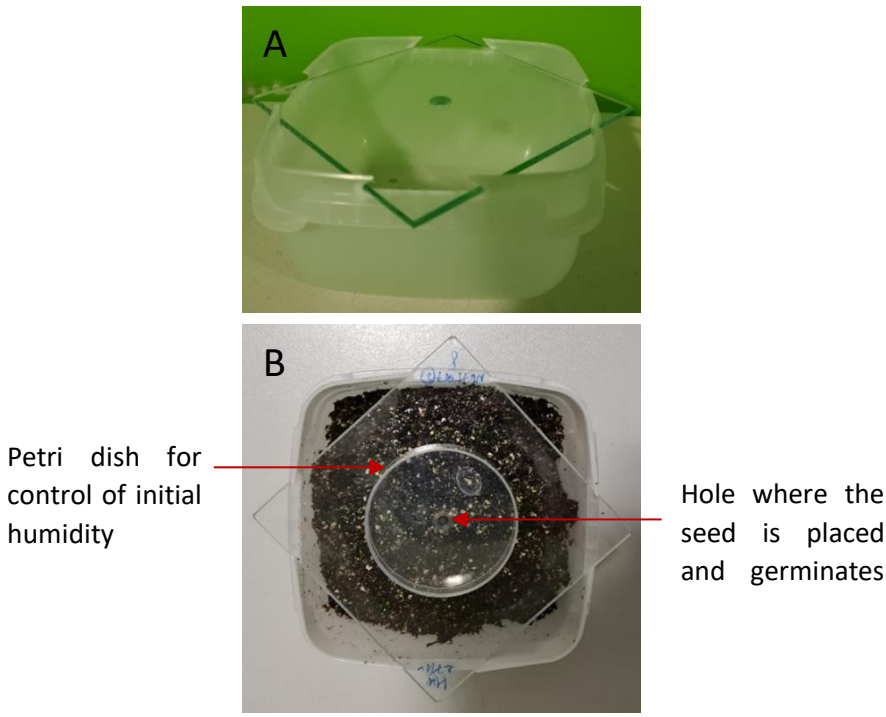

Figure 5.3 – Representative images of pots and initial set up for plant growth. A) Representation of the pot and glass slide in which seedlings were grown in. B) Contains both seedling and soil under experimental conditions. White plastic pots are 10 x 10 x 6 cm.

5.4.2 – Genotyping (conditions and primers)

5.4.2.1 – DNA extraction for identifying homozygous lines

Edward's buffer was used for genomic DNA extraction as described in methods Chapter 2 (see Section 2.3). PCR reaction conditions were the same as shown in Table 2.1 with exception of the primers (see Table 5.1).

5.4.2.2 – Genotyping for gas exchange analysis

Homozygous plants had already been identified and isolated using the genotyping method in the methods section and specific primers detailed in Table 5.1. Seed from these plants was collected and used in the experiments described in this Chapter. In each experiment plant genotypes were verified. Isolated DNA from leaf tissue was used as template in 20.2 µl reactions containing, 2 µl template DNA, 10 µl nuclease-free water, 2 µl Solis Biodyne reaction buffer B (10X), 2 µl 25 mM Magnesium Chloride, 2 µl of 2 mM DNTPs, 1 µl of 10 µM forward primer, 1 µl of 10 µM reverse primer and 0.2 µl FIREPol DNA polymerase (Solis Biodyne, solisbiodyne.com).

Each set of PCR reactions also included positive controls (in this case (Col-0) DNA) and negative controls (nuclease-free water). A standard PCR cycle consisted of denaturation at 95 °C for 3 minutes followed by 35 cycles of denaturing at 95 °C for 15 seconds, annealing at 53 °C for 20 seconds and extension at 72 °C for 90 seconds, and a final extension of 72 °C for 7 minutes.

5.4.2.3 – Primers

Table 5.1 – Primer sequences and product sizes for genotyping top 10 kinase T-DNA lines ordered. Highlighted in yellow are the two genes taken forward for experiments in this chapter. At1g11340 was currently unnamed and will be referred to as Guard Cell Kinase 1 (GCK1) for this Chapter.

AGI code	Gene name	T-DNA Line	NASC no	(Forward) primer	(Reverse) primer	WT product (bp)	Mutant product (bp)
At4g24480		SALK_025685	N525685	CTCCACTTGTGGACTTTCAGG	TGAAACCTACTGATCCATGCC	1092	554-854
At4g24480		SAIL_835_E09	N877222	TTAAATAGGATGGCACGATGC	GATTCGGCTAGGACGGTTAAC	1003	491-791
At1g60630		SALK_114666	N614666	AGATTCCTAGCTCGTTGCTCC	CGTGAGACAGGACTCGAAGTC	1110	568-868
At1g11410		SALK_116075	N616075	GTTTTGCTCCTCTGTATCCCC	TCATCAGTTTGATTGCAGTCG	1217	576-876
At1g56140		SALK_005808C	N658501	AATGATACAGGTAATCCCCCG	GCCAGTGTTCTCGACTCAAAC	1039	439-739
At4g23190	At-RLK3	SALK_013983C	N661560	TTTCATCCATCTGGTAGACGC	CCCACTGTTATTGCCATCTTG	1138	486-786
At5g43020		SALK_035437C	N665759	ACCTCCTGCTCTCTTCACCTC	CACTCTCTTGTTCTATCGCCG	1113	440-740
At1g11340	GCK1	SALK_050988C	N675057	ACAAGAACCATGGTGAACGAG	ATAAACAGGTCCGAAACCACC	1077	437-737
At1g11300	EGM1	SALK_058300C	N682396	TATGTTCCAACGACCCTTCTG	GATCGGTACAATATTGGCAGG	958	445-745
At1g56130		SALK_074874C	N686342	TCCGCTCCAATTTATGATCAG	AATCTTGCATCCTTTTGGAGG	1182	594-894
At5g53890	AtPSKR2	SALK_024464	N800006	GAGAACTTGTTGGAGCTCACG	TTTTGGGATGTGAGCGTTTAG	1112	474-774

5.4.3 – Whole plant gas exchange analysis

Twenty-four hours before whole plant gas exchange analysis, the hole surrounding the plant, on the glass slide was sealed using a Vaseline mix (100 g Vaseline, 5 g Beeswax and 5 g Parafilm).

After the 24-hour period had elapsed, plants were imaged (see Figure 5.4) and the area of the leaf rosette was estimated as shown by the dotted line in A. The digital image was then compared to a 3 cm scale for area estimation (Abràmoff et al., 2004). The estimated areas were then input into an Infrared Gas Analyser (IRGA) software before calibration and data collection began.

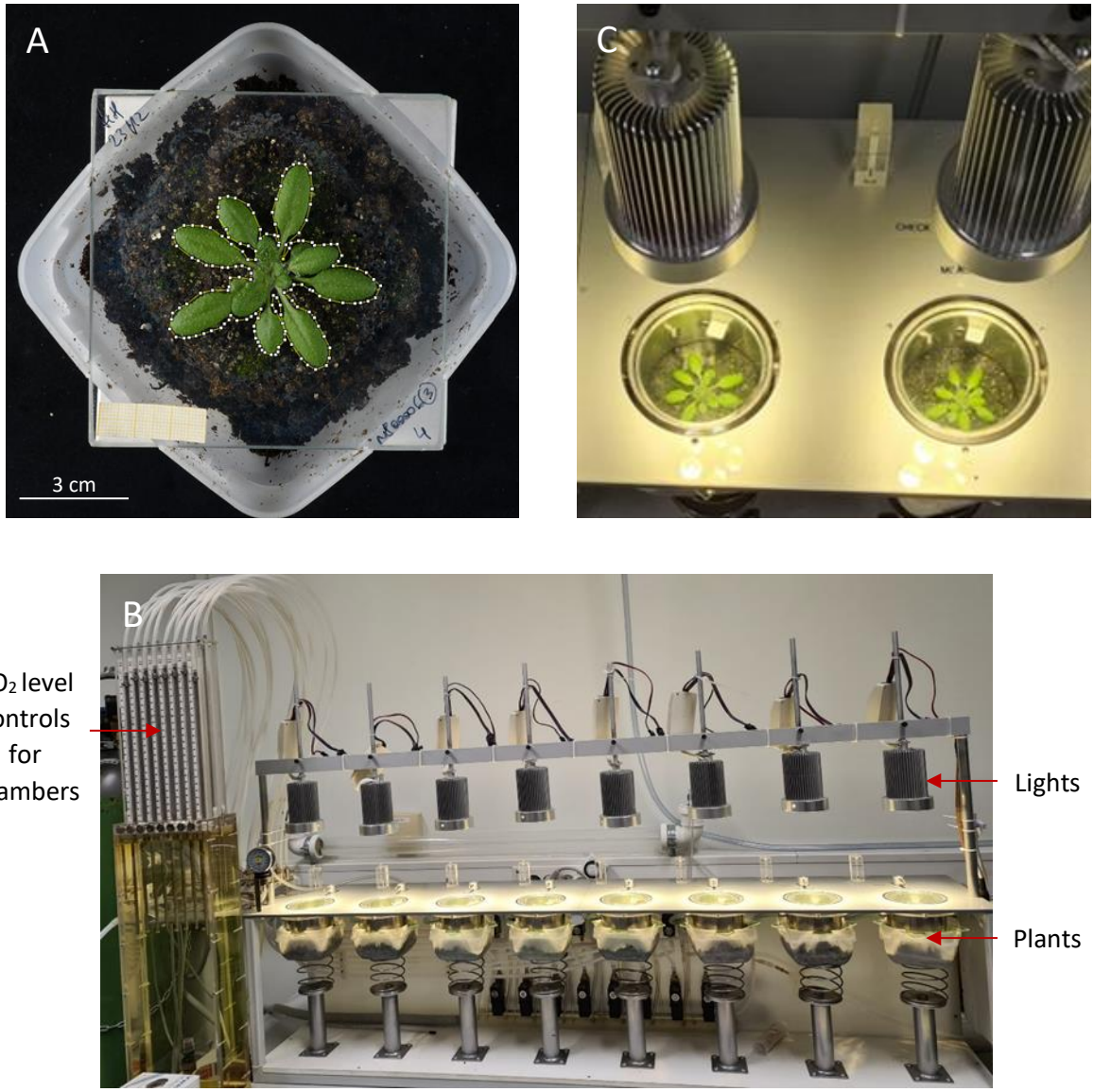

Figure 5.4 – Representative images of A) plants used for gas exchange analysis and of images used for leaf area estimation. Scale bar: 3 cm. B) The eight-chamber IRGA used to monitor the effect of ABA application. Height between lights and plants: 20 cm. C) A top-down view of plants whilst impact of stress, including ABA and high or low CO_2, application was being monitored in the IRGA.

The set up for the whole plant gas analysis was as described in Hõrak (*et al* 2017), using a custom built eight-chamber, temperature controlled IRGA. Experiments to monitor the effect of ABA application and changes in CO_2 concentration were performed on the analogous device mentioned. Plants were measured in batches of 8 at constant 150 µmol m^{-2} s^{-1} light, 24-25°C air temperature, 400 ppm CO_2 and ~70% RH. Measurements were taken sequentially every minute for each chamber (30 seconds reference and 30 seconds plant measurement).

5.4.3.1 – Response to high CO_2

Plants were placed into the first 4 chambers, checking to ensure that they were all sealed and no gas leakages apparent, by using the control switch on top, when it was switched to check, it sent gas into the chamber. If there were no leakages then a plastic pellet moved up, if there were leakages the plastic pellet did not move (see Figure 5.4 C). Confident that the chambers were sealed, the switch was then returned to 0 before measuring the setting for experiments. Plants were acclimatised at 400 ppm CO_2 (equivalent to ambient using a gas cylinder), for at least 20 minutes until stomatal conductance had stabilised. The concentration of CO_2 was then increased to 800 ppm and measurements were taken every 4 minutes for an hour. Plants were then left to reacclimatise at ambient CO_2.

5.4.3.2 – Response to low CO_2

The experimental set up was similar to above except low CO_2 experiments were performed after high CO_2 experiments (midday to afternoon). CO_2 levels were changed from (ambient) 400 ppm to 100 ppm (using a gas cylinder). The removal of CO_2 was carried out using a potassium hydroxide (KOH) pump. Plants were monitored for an hour with measurements for each chamber taken every minute sequentially in low CO_2.

5.4.3.3 – Response to ABA

ABA experiments were performed on same set of plants as the above experiments but after they had received other treatments. After the acclimation period to CO_2 levels 400 ppm, 24-25 °C air temperature and approximately 70 % RH plants were removed from the chamber individually in order of chamber number. Plants were sprayed with 0.42 ± 0.04 µl cm^{-2} ABA (Sigma, https://www.sigmaaldrich.com; 5 µM ABA, 0.012 % Silwet L77 (De Sangosse, http://www.desangosse.com), 0.025 % ethanol) (mock was without ABA). Plants were then placed back into the chambers and seal checked. Droplets were allowed to dry before gas exchange monitoring commenced. Once sprayed, plants were measured for an hour every minute sequentially.

5.4.3.4 – Response to Red/Blue light and Darkness

The experiment was set up as described in (Hosotani et al., 2021). Plants were measured in batches of 7 with one chamber blank as a reference and control. Plants were first acclimatised to 400 ppm CO_2, 24-25 °C and approximately 70 % RH. 300 µmol m^{-2} s^{-1} (640 nm) red light was used to begin with for acclimatisation, plants were left for 30 minutes to acclimatise then recalibrated using the blank chamber. Measurements were taken for 30 minutes and then exposed to 10 µmol m^{-2} s^{-1} (450 nm) blue light. Measurements continued for 2 hours after the blue light treatment. Plants were then put into darkness for one hour. Measurements were taken sequentially every 30 seconds for each chamber, which differs slightly to the data collection for ABA, High and Low CO_2.

5.4.4 – Leaf epidermal impressions for stomatal density and stomatal index measurements

On completion of the experiments, leaf 6 was identified and used for both abaxial and adaxial impressions (leaf was sliced in half down the mid vein), dental resin (Zhermack Oranwash L (Orange) (https://www.zhermack.com/en/) and Coltene speedex light body (Blue) (http://nam.coltene.com)) was then applied and left to set into an impression of the epidermal surface. Clear nail varnish was applied to the set impression after leaf removal and mounted on a glass slide. Z-stack images captured at X20 magnification on a Brunel n300-M microscope equipped with a prior ES10ZE Focus Controller and Moticam 5 camera. ImageJ was used for stomata and epidermal cell counting with statistical analysis performed using GraphPad Prism (Zoulias et al., 2021)

5.4.5 – Fresh weight loss assay

The three largest leaves of similar size from each plant were excised and placed in pre weighed Petri dishes. Once excised the leaves were weighed immediately and were re-weighed every 30 minutes for 8 hours at room temperature and humidity (23-27 °C and 20-30 % respectively)(Higher temperature and lower relative air humidity than expected, but outside of my control).

5.5 – Results

5.5.1 – Identification of putative guard cell expressed kinase and phosphatase genes

In order to identify possible guard cell kinases (Ks) and phosphatases (Ps) for study, a survey of prior publications was carried out to identify a gene list of potential Ks and Ps. Available microarray data sets (from literature as had access compared to RNA-seq data) were then queried to check if respective genes were guard cell enriched. 780 potentially interesting Ks and 67 Ps were identified, however this list may not be fully comprehensive (Leonhardt et al., 2004; Jammes et al., 2009; Hachez et al., 2011). Relative expression levels for these selected genes were obtained using the eFP browser by applying the guard cell enrichment setting, with values of mean (expression levels) and standard deviation extracted for guard cell enriched tissue (epidermal peels) and whole leaves treated with and without ABA (Pandey et al., 2010). Experiments identified genes that expressed at a high level in guard cells, and more frequently, that were preferentially expressed in guard cells relative to other leaf cells. See Figures 5.6 and 5.7 for two examples of the genes chosen for further investigation. Similarly, relative guard cell and mesophyll cell expression levels were examined in the eFP browser using data from an experiment comparing stomatal development mutants (Yang et al., 2008). Finally, guard cell and meristemoid expression levels were examined utilising the values obtained in (Adrian et al., 2015) using mature guard cells and epidermis leaves. (See Supplementary data 3 for the expression levels for all genes (Ks and Ps) including whole leaf, mesophyll cell and meristemoid.) Some genes of interest were not represented on the Affymetrix microarray chip used to create the database. Therefore, these genes were omitted from potential candidates. Ratios were then calculated to determine guard cell enrichment, thresholds set and candidates ranked in order of highest value to lowest enrichment using values (from Pandey which was the most informative study) for guard cell enrichment, and the one with the highest number of replications for both biological samples and technical reps)[11]. Threshold 1 was for 10-fold or greater level of guard cell relative expression compared to whole leaf expression level, and threshold 2 was for 4-fold enrichment and above. The magnitude of gene expression levels was then examined to determine their suitability for investigation, and thresholds of higher than 1000 and higher than 500 were set (arbitrary expression levels as described on eFP browser). Table 5.2 shows the 77 genes out of a potential 780 kinases which met the thresholds, both *PSKR2* and *GCK1*[12] met threshold 1. *PSKR2* and *GCK1* had both 22-fold higher expression levels in GC enriched compared to whole leaf tissue. Genes that had potentially high expression and enrichment in guard cells, and that had T-DNA insertion mutant lines available were selected for further study (highlighted in blue in

[11] In these experiments a sample number of 3 was used.

[12] At1g11340 currently unnamed on TAIR which from this point on will be called *Guard Cell Kinase 1 (GCK1)* for identification purposes.

Table 5.2). Those genes which were already well-characterised elsewhere were not selected for further investigation, for example *HT1*.

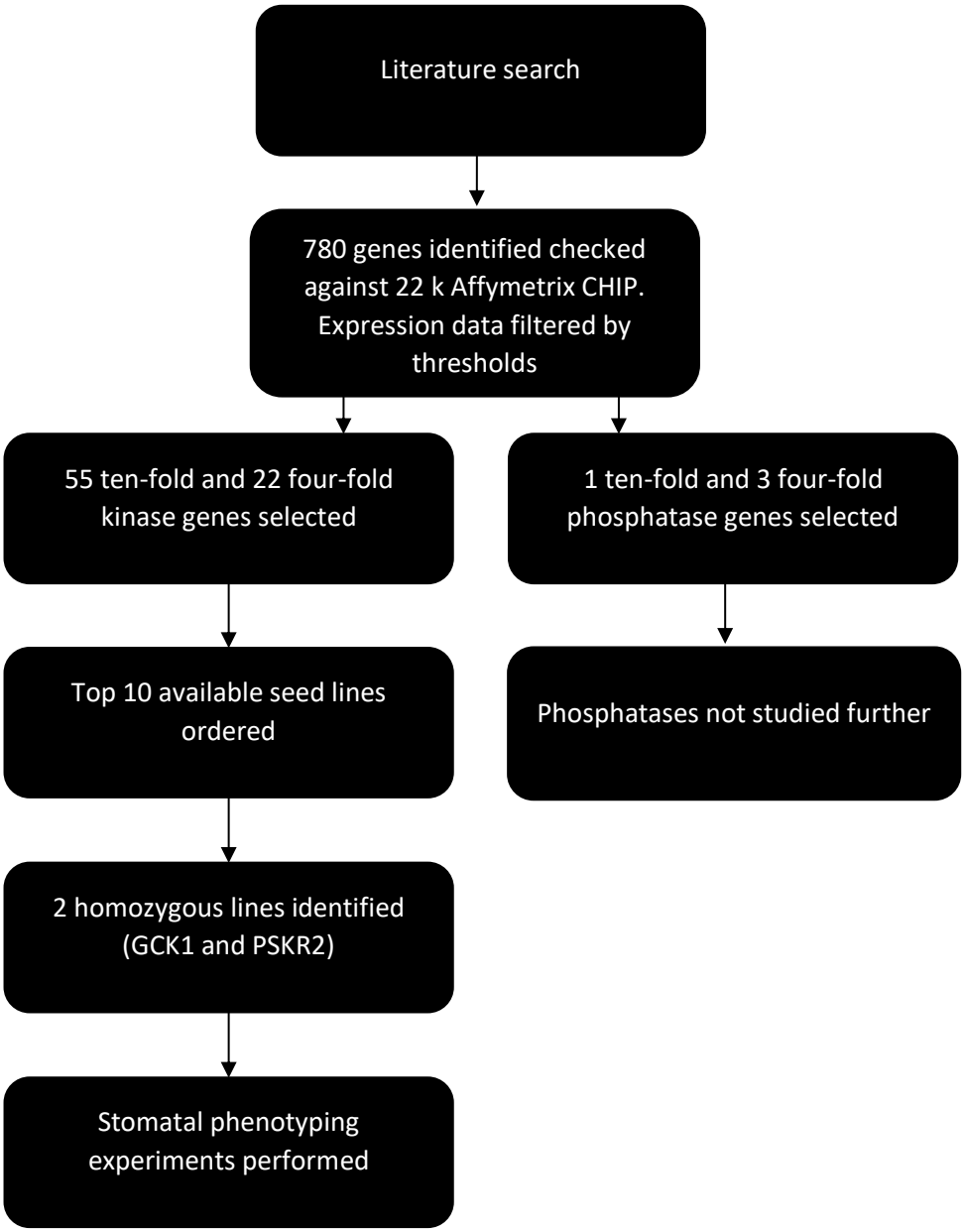

Figure 5.5 – Workflow chart used to identify potential guard cell expressed kinase and phosphatase genes for experimental analysis.

Table 5.2 – Expression data for selected subset of kinase genes preferentially expressed in guard cells. 77 kinase genes which met thresholds 1 (red shaded cells) and 2 (yellow shaded cells) using expression data from eFP browser and experiments according to Pandey et al. (2010). The 10 blue shaded AGI codes are the 10 lines seed was obtained for and initial genotyping experiments performed on and the two genes in bold (GCK1 and PSKR2) were taken forward for experiments.

AGI	Gene name	Epidermal peel (GC) expression	Whole leaf expression	ABA treated GC expression	ABA treated whole leaf expression	GC fold enrichment	ABA treated GC fold enrichment
At1G62400	*HT1*	*2861.95*	*20.07*	*2080.19*	*2.84*	*142.60*	*732.46*
AT1G05100	*MAPKKK18*	*141.75*	*1.05*	*2690.58*	*239.11*	*135.00*	*11.25*
AT3G25250	AGC2	553.45	5.82	458.72	7.72	95.09	59.42
AT5g37450		43.83	0.94	4.41	1.62	46.63	2.72
At4G18950	*BHP*	*5551.37*	*156.11*	*5792.7*	*271.25*	*35.56*	*21.36*
At4G24480		510.26	16.04	646.49	13.18	31.81	49.05
At1g11410		507.49	16.8	272.43	7.45	30.21	36.57
AT5g06740	LecRK-S.5	18.97	0.64	13.8	0.48	29.64	28.75
At1g60630		229.28	8.74	34.31	4.21	26.23	8.15
At1g11340	**GCK1**	**424.49**	**19.05**	**17.99**	**2.37**	**22.28**	**7.59**
AT5g53890	**AtPSKR2**	**1082.06**	**49.21**	**332.45**	**8.05**	**21.99**	**41.30**
At1g70530	CRK3	2267.22	129.7	1863.94	38.15	17.48	48.86
/AT5g07280	EMS1	178.78	11.42	59.07	4.69	15.65	12.59
At1g78530		85.7	5.98	81	8.58	14.33	9.44
At1g11300	EGM1	51.73	3.68	32.01	1.56	14.06	20.52
AT2G34650	ABR	177.05	12.61	224.59	2.36	14.04	95.17
AT4G14480	*BLUS1*	*299.35*	*23.01*	*43.13*	*5.53*	*13.01*	*7.80*
AT2G30040	MAPKKK14	587.01	51.11	1071.69	120.55	11.49	8.89
AT4g35030		75.93	6.78	71.01	6.73	11.20	10.55
At1g74490		11.87	1.15	16.58	6.39	10.32	2.59
At2g33580	*AtLYK5*	*468.88*	*45.71*	*349.16*	*43.91*	*10.26*	*7.95*
AT3g01840	LYK2	40.75	4.01	21.81	8.13	10.16	2.68

AGI	Gene name	Epidermal peel (GC) expression	Whole leaf expression	ABA treated GC expression	ABA treated whole leaf expression	GC fold enrichment	ABA treated GC fold enrichment
AT4g02410	AtLPK1	1015.47	101.94	1000.83	85.02	9.96	11.77
AT3g59420	ACR4	49.46	5.17	9.64	0.39	9.57	24.72
At1g78940		15.36	1.61	30.47	1.2	9.54	25.39
AT3g53810	LecRK-IV.2	628.43	69.64	401.72	50.8	9.02	7.91
At1g56140		1754.65	205.08	736.35	49.23	8.56	14.96
At1g56130		1754.65	205.08	736.35	49.23	8.56	14.96
At1g56120		1754.65	205.08	736.35	49.23	8.56	14.96
At1g56140		1754.65	205.08	736.35	49.23	8.56	14.96
AT5g25930	HSL3	1291.24	151.18	1191.79	75.34	8.54	15.82
AT5g18610	*PBL27*	*12.73*	*1.5*	*5.31*	*0.89*	*8.49*	*5.97*
AT4g39110	BUPS1	10.02	1.2	8.35	3.02	8.35	2.76
AT5g43020		108.58	13.77	22.72	4.64	7.89	4.90
AT5g59270	LecRK-II.2	3.86	0.52	6.07	0.93	7.42	6.53
AT4g23190	At-RLK3	865.2	117.53	751.87	38.5	7.36	19.53
At3G24715	HCR1	59.62	8.11	51.43	10.81	7.35	4.76
AT5g47850	CCR4	36.45	5.18	30.07	5.53	7.04	5.44
AT5g01950		771.62	111.66	271.79	20.6	6.91	13.19
AT5g51270		5.17	0.75	1.85	2.64	6.89	0.70
At5G50000		843.35	123.42	128.03	36.78	6.83	3.48
At1g70740		205.25	30.14	230.8	20.38	6.81	11.32
AT1G70430		30.02	4.48	19.22	1.6	6.70	12.01
At1g16150	WAKL4	45.87	7.06	94.02	4.14	6.50	22.71
At5g57610		384.61	60.12	1099.24	69.7	6.40	15.77
At1g19090	CRK1	4.13	0.66	4.33	2.35	6.26	1.84
At2g28930	APK1B	1261.63	209.82	736.38	31.38	6.01	23.47
AT5g58540		60.84	10.44	25.18	4.02	5.83	6.26
AT4g23180	CRK10	1193.19	205.48	917.92	85.02	5.81	10.80

AGI	Gene name	Epidermal peel (GC) expression	Whole leaf expression	ABA treated GC expression	ABA treated whole leaf expression	GC fold enrichment	ABA treated GC fold enrichment
At3G46930	Raf43	338.37	58.32	290.77	47.03	5.80	6.18
At1g17230		433.54	74.76	128.11	13.08	5.80	9.79
At1g61460		6.83	1.23	5.56	3.58	5.55	1.55
AT4g32300	SD2-5	675.09	124.65	433.76	54.75	5.42	7.92
At1g06840		426.32	79.65	233.81	20.52	5.35	11.39
At2g02800	APK2B	1709.04	319.41	1334.33	105.94	5.35	12.60
AT3g09010		296.38	55.88	353.16	33.54	5.30	10.53
At4G08500	ARAKIN	460.26	87.04	372.73	80.18	5.29	4.65
At2g19130		520.94	101.22	314.78	63.54	5.15	4.95
At5G40540		330.5	64.36	487.52	119.92	5.14	4.07
AT5g65240		151.34	29.95	330.44	9.47	5.05	34.89
AT5g46080		130.2	26.03	138.48	88.69	5.00	1.56
AT3g20530		4.72	0.97	2.43	3.92	4.87	0.62
At1g07570	APK1	1215.93	254.23	478.41	149.07	4.78	3.21
At1g07870		145.48	30.63	1271.95	55.55	4.75	22.90
AT4g31100		2.27	0.48	2.05	3.46	4.73	0.59
At1g48480	RKL1	161.57	35.04	59.55	42	4.61	1.42
AT5g61560		569.55	126.21	481.07	46.18	4.51	10.42
At1g79620		3.82	0.85	3.69	1.17	4.49	3.15
At2g48010	RKF3	592.33	133.06	440.93	106.3	4.45	4.15
AT5G55090	MAPKKK15	12.22	2.81	71.77	19.63	4.35	3.66
At1g09440		54.02	12.92	12.53	2.74	4.18	4.57
At1g77280		81.88	19.91	712.02	16.34	4.11	43.58
At1g15530	LecRK-S.1	7	1.71	1.96	3.38	4.09	0.58
At2g02220	AtPSKR1	564.52	138.95	373.17	29.97	4.06	12.45
AT4g28350	LecRK-VII.2	321.31	79.4	225.07	59	4.05	3.81
At1g50610	PRK5	2.75	0.68	3	0.64	4.04	4.69

AGI	Gene name	Epidermal peel (GC) expression	Whole leaf expression	ABA treated GC expression	ABA treated whole leaf expression	GC fold enrichment	ABA treated GC fold enrichment
AT1G79640		77.46	19.34	53.82	7.55	4.01	7.13

A table of 847 potential guard cell expressed protein kinase (780) and phosphatase (67) genes was assembled. The 77 most highly guard cell expressed kinases (according to Pandey et al. (2010) dataset) are shown in Table 5.2. Candidate knock-out mutants in 10 of these genes were identified (based on high differential expression data and had not been thoroughly studied/ well known and were available to order as a T-DNA line) from available collections and ordered from stock centres (unfortunately only 1 allele from each gene was obtained. Of these, several lines did not germinate and on PCR screening several did not appear to contain a T-DNA insert. As a result of these preliminary experiments two mutant lines (*pskr2* and *gck1*) were selected for further study. Whole plant IRGA experiments were carried out to determine whether there was a defect in guard cell function. The workflow chart to select the two genes is shown in Figure 5.5.

Phytosulfokines have been linked with regulating growth in Arabidopsis as well as promoting cell proliferation and are involved in responses to wounding and protein phosphorylation. Phytosylfokine-Alpha receptor 2 (PSKR2) encodes a leucine-rich repeat receptor kinase (LRR-RK), which is involved in the perception of the sulphated peptide hormone Phytosylfokine (PSK) (see Figure 5.6). PSKR2 has serine/threonine (Ser/Thr) protein kinase activity (Amano et al., 2007; Ladwig et al., 2015). There has been little research to date into PSKR2. More is known about PSKR1 which has been linked to root elongation in Arabidopsis. It has been determined that the homologous receptor PSKR2 plays a redundant role in root growth compared to PSKR1 (Amano et al., 2007; Kutschmar et al., 2009).

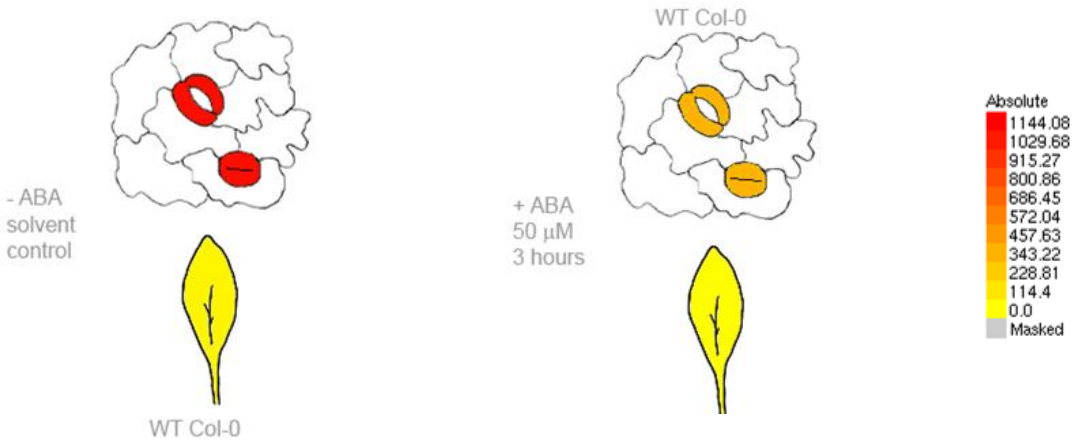

	Expression level	SD
Guard cell enriched without ABA	1082.06	25.2
Whole leaf tissue without ABA	49.21	3.25
Guard cell enriched with 50 µM ABA	332.45	22.86
Whole leaf tissue with 50 µM ABA	8.05	2.21

Figure 5.6 – *AtPSKR2* expression values for guard cell enriched and whole leaf samples. Wild type (Col-0) plants had whole leaf tissue and epidermal peels which were treated with cellulase, then treated with either (high) 50 µM ABA or Ethanol (mock) for 3 hours and RNA extracted from these samples (Images and data taken from Arabidopsis eFP browser, accessed 10/1/22). Table of values extracted from images (Expression levels and standard deviation (SD)). The colour represents the expression level within the guard cell tissue, the darker the colour the more highly expressed.

Recent studies have indicated that PSK can maintain growth and delay leaf senescence under drought conditions. It has been suggested that it can also affect the transpiration stream by mediating stomatal closure, preventing water loss via a pathway involving reactive oxygen species (personal communication H. Horak). All of these are good indications that *PSKR2* has the potential to be involved in regulation of stomatal movement. However, there are multiple *PSKR* genes, and there may be some redundancy within the family.

GCK1 also has a Ser/Thr protein kinase domain (see Figure 5.7). It is potentially involved in the recognition of pollen as it is an S-receptor like kinase (Leonhardt et al., 2004; Mondal et al., 2021). At present the gene has not been assayed for PK activity.

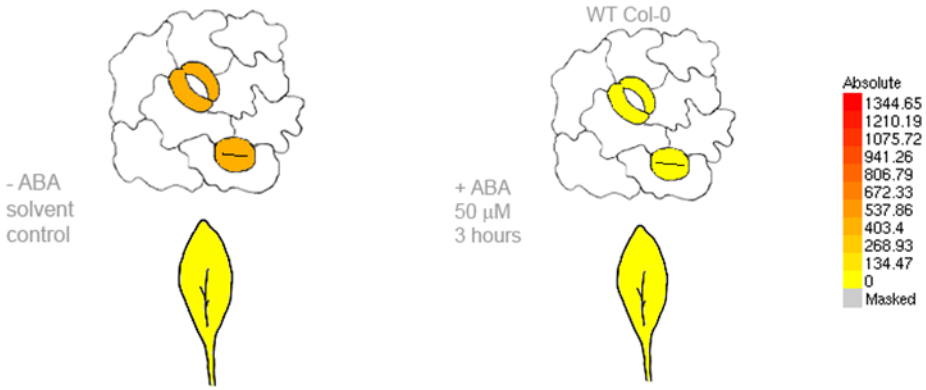

	Expression level	SD
Guard cell without ABA	424.49	61.05
Leaf tissue without ABA	19.05	6.42
Guard cell with 50 µM ABA	17.99	7.22
Leaf tissue with 50 µM ABA	2.37	0.51

Figure 5.7 – *GCK1* expression values for guard cell enriched and whole leaf samples. Wild type (Col-0) plants had whole leaf tissue and epidermal peels which were treated with cellulase, then treated with either 50 µM ABA or Ethanol (mock) for 3 hours and RNA extracted from these samples (Images and data taken from Arabidopsis eFP browser, accessed 10/1/22). A table of values was extracted from images (Expression levels and standard deviation (SD)). The colour represents the expression level within the guard cell tissue, the darker the colour the more highly expressed.

5.5.2 – Identification of homozygous lines

To initially identify homozygous for insertion mutants and to check that plants used in subsequent experiments were mutant lines containing the T-DNA insertion, genotyping was performed. Figure 5.8 is an example of a genotyping gel for *pskr2* plants to identify if they contain the T-DNA insertion (band in a) but not in b)) or if they contain no T-DNA insertion (band in a) but not in b)). If bands are present in both, samples are heterozygous and segregating for the insertion.

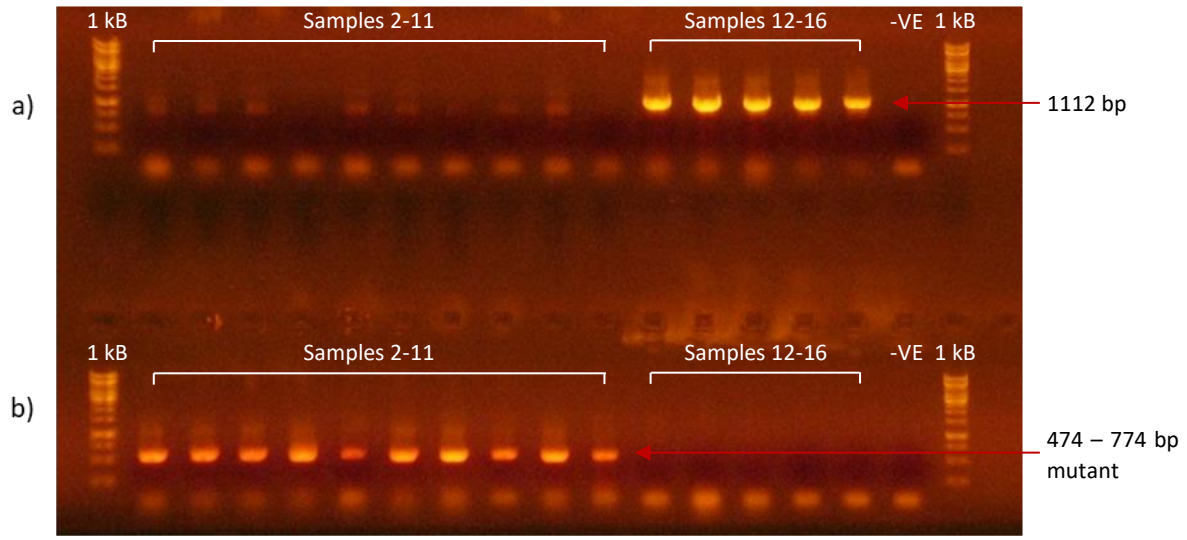

Figure 5.8 – Confirmation of mutant lines. An example of a genotyping gel. Gel a) is with primers designed to amplify a fragment of the *PSKR2* gene. Lanes 1 and 18 are 1kB DNA ladder, lanes 2 to 11 contain PCR amplification from genomic DNA (gDNA) from 10 *pskr2* sample plants, lanes 12 to 16 Col-0 gDNA as a positive control and lane 17 contains water as a negative control. 1112 base pair (bp) amplicon is highlighted in samples 12 to 16. Gel b) is using insertion specific primers for *PSKR2*, with the same lane layout as gel a). A 474 to 774 bp amplicon is highlighted in samples 2 to 11. All plants tested were homozygous for the insertion and 5 Col-0 plants.

5.5.3 – Growth analysis and phenotypic observations for *gck1* and *pskr2*

Germination assays can assess seed viability and rates determine and indicate continuous plant production. Signalling pathways are interlinked and to determine the impact of the genes on the plants as a whole and the effect of ABA, seed germination was observed. ABA promotes seed dormancy, in Table 5.2, gene expression decreased, under the presence of ABA (Rodríguez-Gacio et al., 2009). Figure 5.9 A shows the effect of increasing ABA concentration on seed germination. Both *pskr2* and *gck1* are affected by high levels of ABA application, *pskr2* more than *gck1*. B was the end point data for 3, 5 and 10 µM ABA. Under 0, 1 and 3 µM ABA after 8 days post sterilisation and plating there is a 100 % germination from 40 seeds for all genotypes (see Figure 5.9). At 5 µM this is reduced for both mutant lines, *gck1* to 75 % and pskr2 to 50 % germination. This is reduced by a further 25 % for both at 10 µM ABA and Col-0 was reduced to 75 % germination. The germination assay was repeated two more times and produced similar results. Gene expression on eFP browser showed that both *GCK1* and *PSKR2* had relatively high gene expression in the seed coat and early germination stages. *PSKR2* (13.76 to 41.40) was higher than *GCK1* (5.37 to 11.43). Seed dormancy enhanced by ABA application was affected in mutants, when genes were knocked out or down, they have a hypersensitivity to ABA.

In more mature plants there are other factors which can affect a plant's stomatal conductance. These include: rosette leaf area (see Figure 5.10), stomatal density (see Figure 5.12) and stomatal complex size (see Figure 5.13).

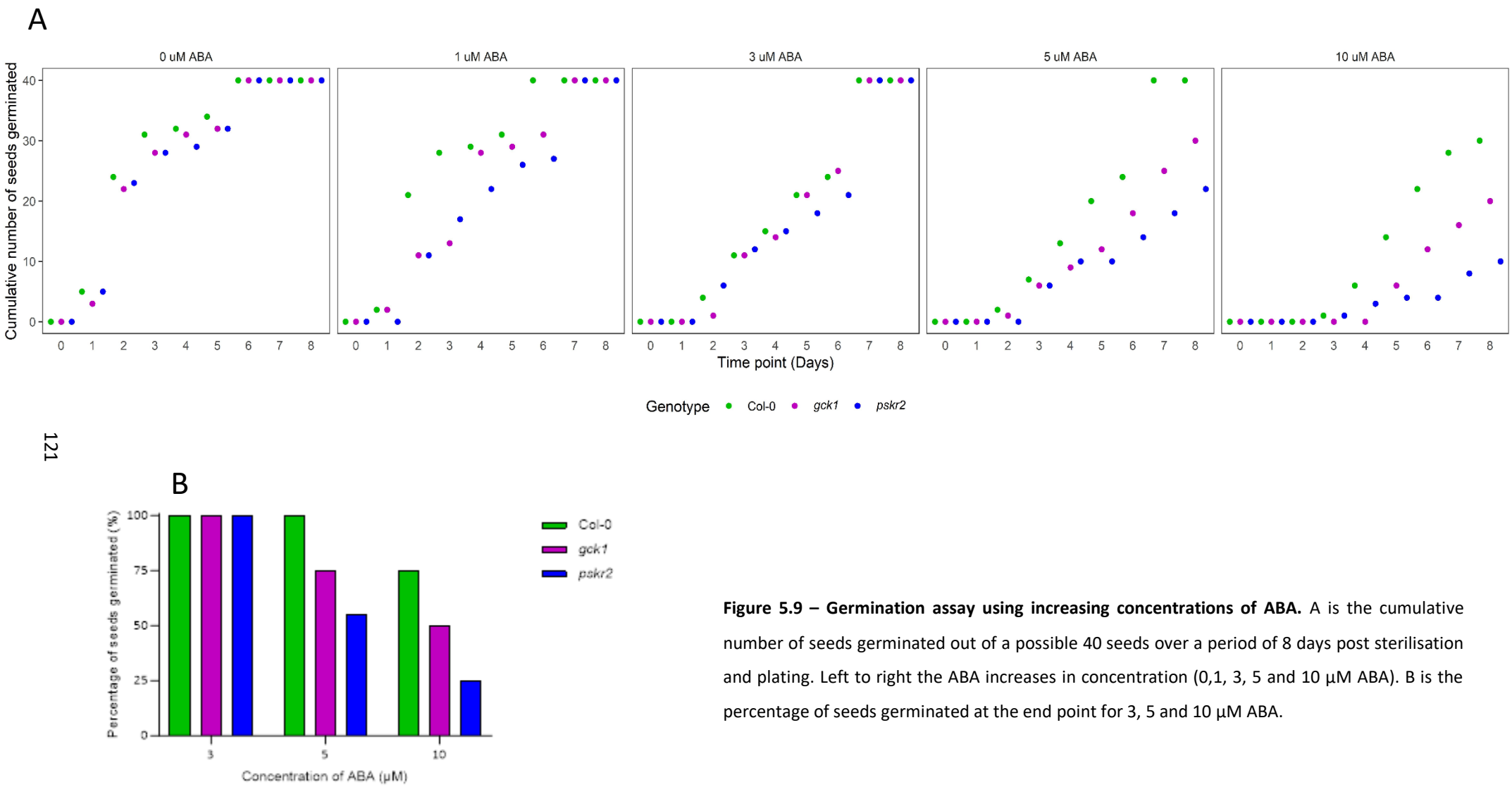

Figure 5.9 – Germination assay using increasing concentrations of ABA. A is the cumulative number of seeds germinated out of a possible 40 seeds over a period of 8 days post sterilisation and plating. Left to right the ABA increases in concentration (0,1, 3, 5 and 10 µM ABA). B is the percentage of seeds germinated at the end point for 3, 5 and 10 µM ABA.

Rosette leaf area of 6 weeks post germination mature plants was measured (see Figure 5.10). The *gck1* plants by eye looked slightly smaller than *pskr2* and Col-0. Overall mean does look slightly smaller for *gck1* but is not significantly different from Col-0 and *pskr2*. Any effects seen under gas exchange is unlikely to be due to rosette leaf area.

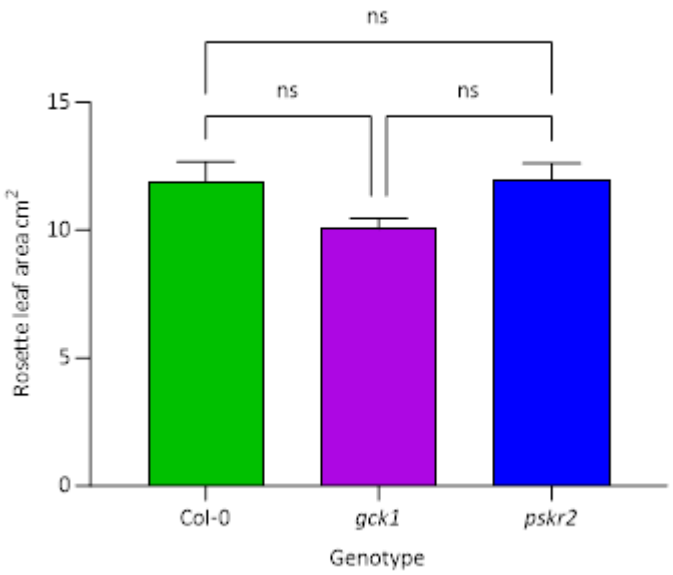

Figure 5.10 – Rosette leaf area. One way ANOVA was performed. Data is mean ± SEM and ns is not significant (n = 15).

There are different approaches to view water loss. Most involve long or short-term drought and whole plant analysis. For screening purposes, a high through-put approach was adopted; fresh weight loss of excised leaf material over time (drying at ambient conditions) was used as a proxy for water loss. The faster the leaves dried out, the higher the cumulative percentage water loss. Figure 5.11 shows that there was an initial sharp loss of water in the first 30 minutes for all lines, followed by continual loss at a lower rate. Overall *gck1* lost water at the fastest rate, followed by *pskr2* and finally Col-0. After 150 minutes the 3 genotypes visually start to separate, small error bars are present.

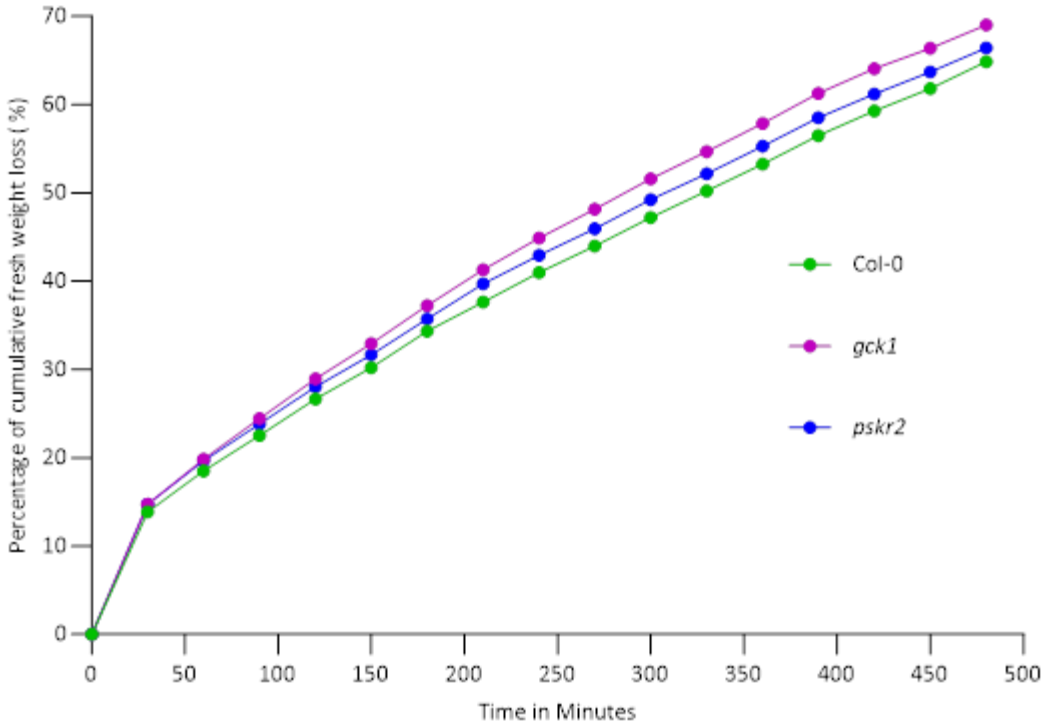

Figure 5.11 – *gck1* loses the highest amount of water compared to *pskr2* and Col-0. Cumulative percentage weight loss from detached leaves. Points are mean and error bars are ± SE (present, just very small). (n=15-17). *gck* loses significantly more weight (water vapour) than *pskr2* and Col-0.

5.5.4 – There is a significant difference in stomatal density between *gck1* and both *pskr2* and Col-0 on abaxial leaf surface and no difference in stomatal size

To assess if knocking out *GCK1* or *PSKR2* had any impact on stomatal development, stomatal density was measured in Col-0 and mutants *gck1* and *pskr2* grown under identical conditions (see Figure 5.12). The abaxial stomatal density of *gck1* plants was significantly lower than *pskr2* and Col-0. There was no significant difference between any of the genotypes for adaxial stomatal density. The ratio between stomatal density and epidermal pavement cell density is denoted by stomatal index. In abaxial stomatal index, both *gck1* and *pskr2* have a significantly higher ratio than Col-0. They have more epidermal pavement cells than stomata. In adaxial stomatal index there is no significant difference between the three genotypes.

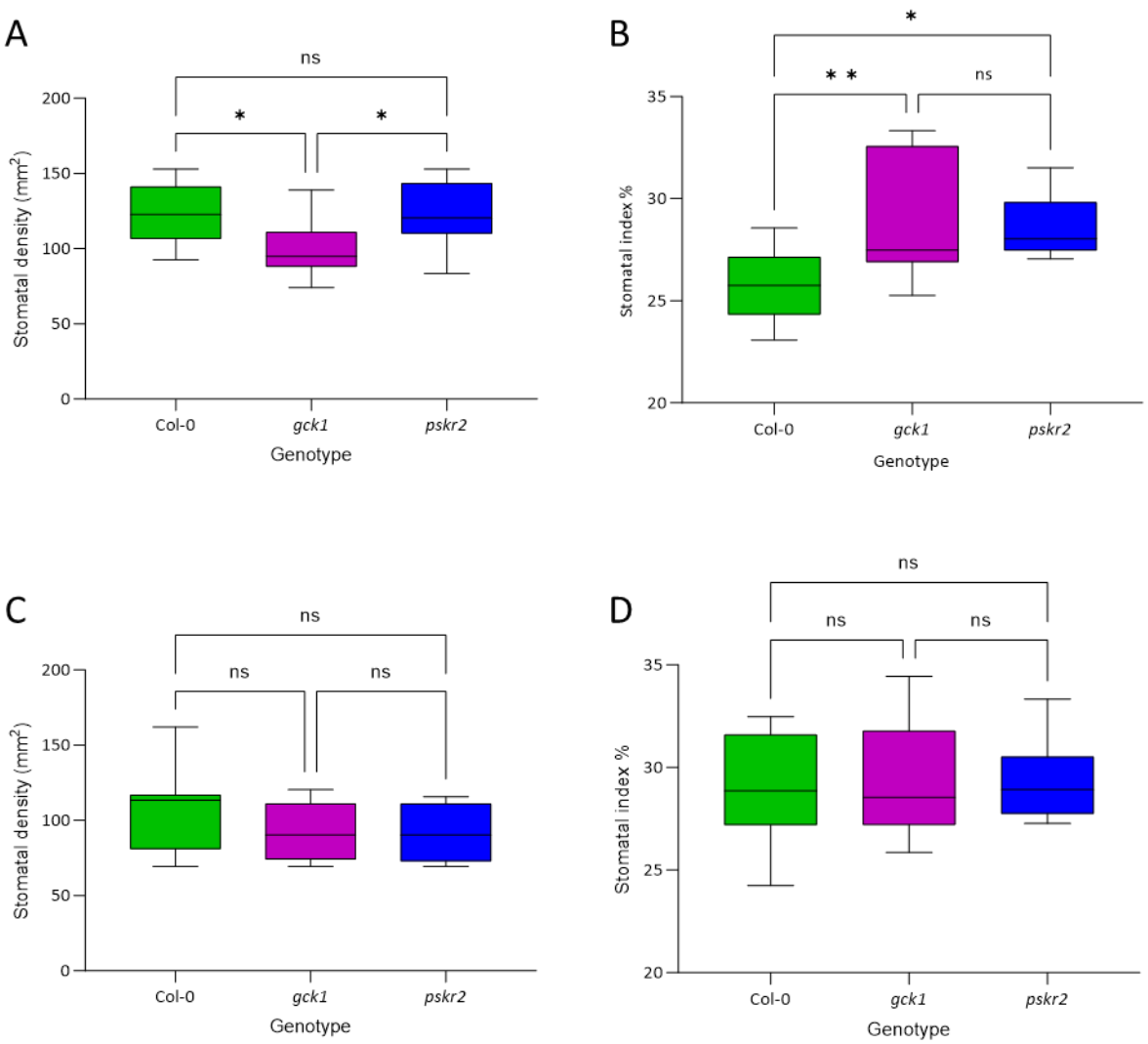

Figure 5.12 – There are slight differences in abaxial stomatal densities. Leaf 6 epidermal impression data. A and C are stomatal density for abaxial and adaxial (respectively) side of the leaf, B and D are stomatal index for abaxial and adaxial side of the leaf (respectively). One way ANOVA followed by post hoc Tukey tests were performed. Significant difference is denoted by an asterix, one asterix is $p<0.05$ and two asterixis $p<0.01$ and ns is not significant. (n = 10).

Stomatal size can also have an effect on stomatal responses; smaller stomata can potentially close faster and a smaller stomatal pore results in less area from which to lose water. Plants were grown under normal growth conditions and impressions were taken from leaves and imaged at X 40 magnification to obtain stomatal complex size. Figure 5.13 shows the spread of data for 40 stomatal complexes. There is no significant difference between any of the three genotypes. There is a spread of data of 200 μm^2. Smaller stomata would lose water slower than larger stomata as the stomatal pore area would be smaller resulting in less area to lose water from. However, from Figure 5.13 and

analysing complex areas from epidermal peel bioassays, there is no significant difference in sizes between the three genotypes.

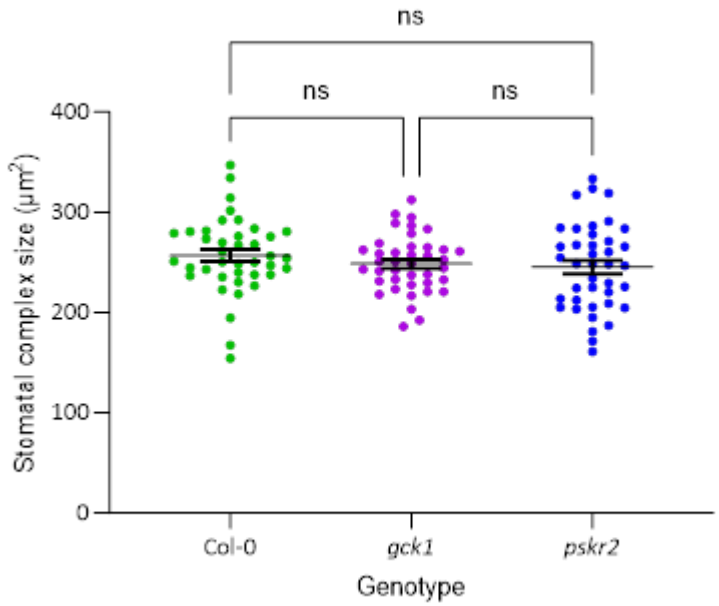

Figure 5.13 – Stomatal complex size. One way ANOVA was performed. Individual points were plotted and lines are mean ± SEM, ns is not significant (n=40).

5.5.5 – *PSKR2* and *GCK1* are potential targets for novel stomatal regulation under whole plant gas exchange analysis

IRGA was performed on verified homozygous mutant lines of *pskr2* and *gck1*. The conditions tested by IRGA were responses to high CO_2 (800 ppm) (see Figure 5.14), low CO_2 (100 ppm) (see Figure 5.16), ABA (5 µM) (Figure 5.18) and red/blue light and darkness (see Figure 5.17). To see if a particular stress caused a response in whole plants, they were acclimatised to ambient conditions before treatment began. For 3 batches of plants grown under the same conditions with staggered growth, the data were pooled for analysis.

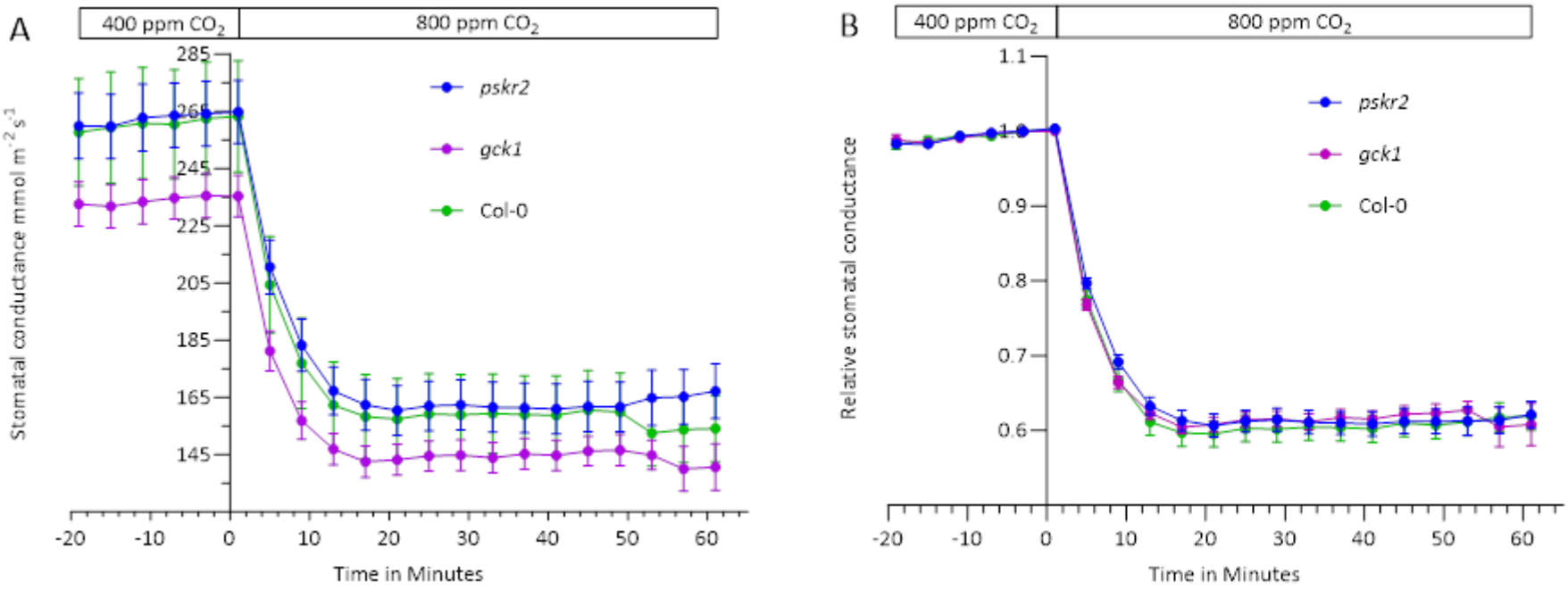

Figure 5.14 – Time course of stomatal conductance during exposure to 400 ppm and then to 800 ppm CO_2. (A) Mean change in stomatal conductance (the absolute steady state levels) and (B) shows the relative (normalised) values (normalised to starting conductance). Error bars are ± SEM (n = 15-17).

IRGA showed that after exposure to high CO_2, stomatal conductance fell rapidly in the first 10 minutes followed by a further, shallower drop until it started to level off in all plant genotypes. The starting conductance for *gck1* was lower than *pskr2* and Col-0, for absolute values (see Figures 5.6 and 5.7).

When the same data for the high CO_2 experiment (see Figure 5.14 B) were normalised to the starting level of conductance, the trend remained the same as seen for the actual values. The results showed that all genotypes reduced stomatal conductance at a similar rate. This indicated that *gck1* had constitutively lower stomatal conductance, but their guard cells remained responsive to a high CO_2 signal.

The starting conductance levels were under 400 ppm CO_2 before levels were changed to 800 ppm were specifically compared. The pre-treatment stomatal conductance of *gck1* is significantly lower than both *pskr2* and Col-0. This can be seen in Figure 5.15, where there was no significant difference between *pskr2* and Col-0 mutants. The steady state stomatal conductance was measured for all treatments and *gck1* was consistently significantly different to both *pskr2* and Col-0.

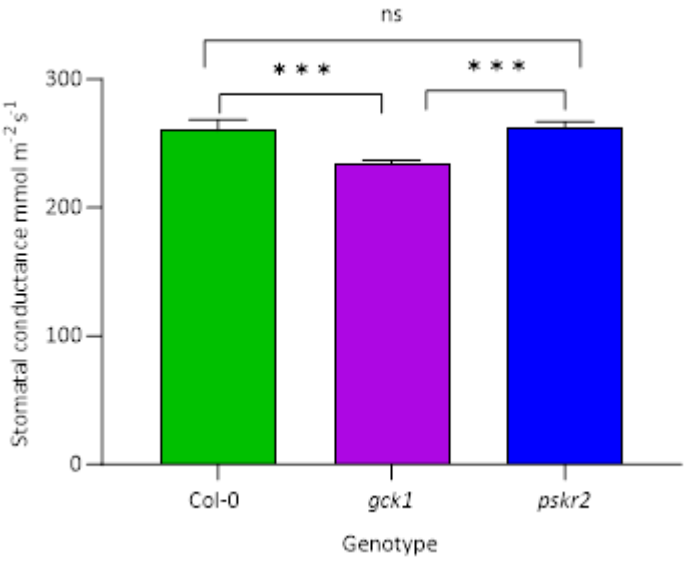

Figure 5.15 – Steady state stomatal conductance at 400 ppm CO_2. Mean stomatal conductance over a 20 minute period after acclimatisation with readings every 4 minutes. One way ANOVA with unequal variance followed by post hoc Tukey tests were performed. Error bars are ± SEM and significant difference is denoted by 3 asterixis $p<0.001$ (n = 15-17). There is a significant difference between *gck1* and both *pskr2* and Col-0. There was no significant difference between *pskr2* and Col-0.

Under ambient CO_2 levels (400 ppm) the steady state stomatal conductance of *gck1* was again lower than *pskr2* and Col-0 and there was a significant difference between the values ($p<0.05$). Figure 5.16, when the CO_2 concentration was lowered to 100 ppm the stomatal conductance increased in all

genotypes, first quite sharply then gradually starts to level off. The conductance levels of *gck1* remained lower than Col-0 and *pskr2* throughout the time course but the differences were not significant.

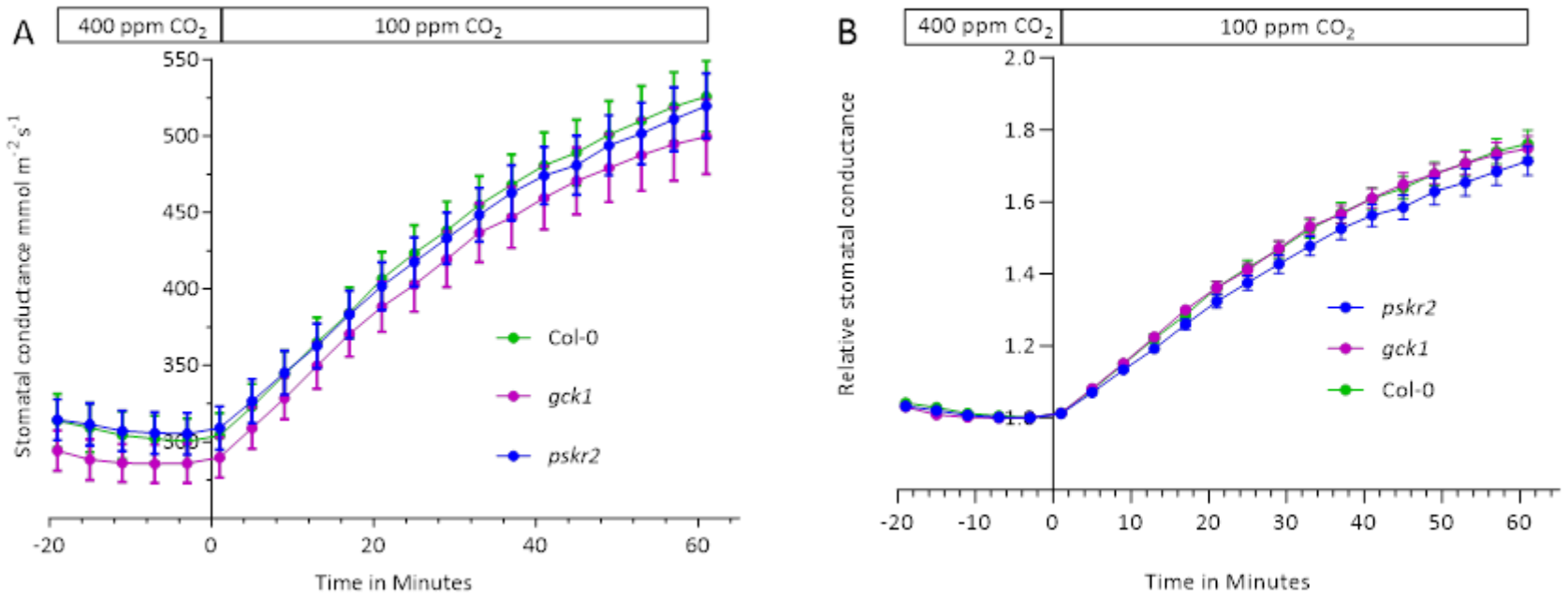

Figure 5.16 – Time course of stomatal conductance during exposure to 400 ppm CO_2 and then to 100 ppm CO_2. (A) Mean change in stomatal conductance during exposure to 400 ppm CO_2 and then 100 ppm. (B) relative (normalised) values for same data set. Error bars are ± SEM (n = 15-17).

The gas exchange data was normalised (see Figure 5.16 B) to equalise the mean values at the start of the experiment. This revealed that *pskr2* conductance rose more slowly than Col-0 on exposure to sub ambient CO_2 and did not reach the same maximal level within the 60 minute exposure period. Although visually different, due to the spread of data not significantly different. *gck1* mutant gas exchange kinetics were again similar to Col-0.

Studies have shown that there are differences in stomatal conductance based on the wavelength of light used. The addition of blue light on top of red light in particular can increase photosynthesis and therefore will exhibit higher stomatal conductance measurements (Matrosova et al., 2015; Inoue and Kinoshita, 2017b; Horak, 2021; Hosotani et al., 2021). Red light has also been linked to responses stomatal responses. There are different forms of red light (red (640 nm) and far red (730 nm)) each with varying effects on plant growth and health. Plants require both red and blue light for optimal photosynthetic ability. Under darkness stomatal conductance should reduce due to no light hitting PSII creating energy for photosynthesis and plants detecting no light resulting in night time response (Pridgeon and Hetherington, 2021). Under light stomata are open, transpiration occurs and stomatal conductance increases. During the photoperiod for the plant, photosynthetic levels change. At the start of daylight, plants are in the early stages of photosynthesis. During this period, the levels of photosynthetic pigments such as chlorophyll are initially low as the plant transitions from the night phase to the day phase. As sunlight increases, plants begin to activate their photosynthetic machinery, gradually increasing the production of energy-rich compounds like glucose. The levels then reach a steady state for most of the day, fluctuating depending on light source available (which is less of a problem under controlled environments compared to natural variation). Towards the end of the photoperiod, photosynthetic rates start to decrease as plants start to transition into night time (little or no photosynthesis and more closed stomata).

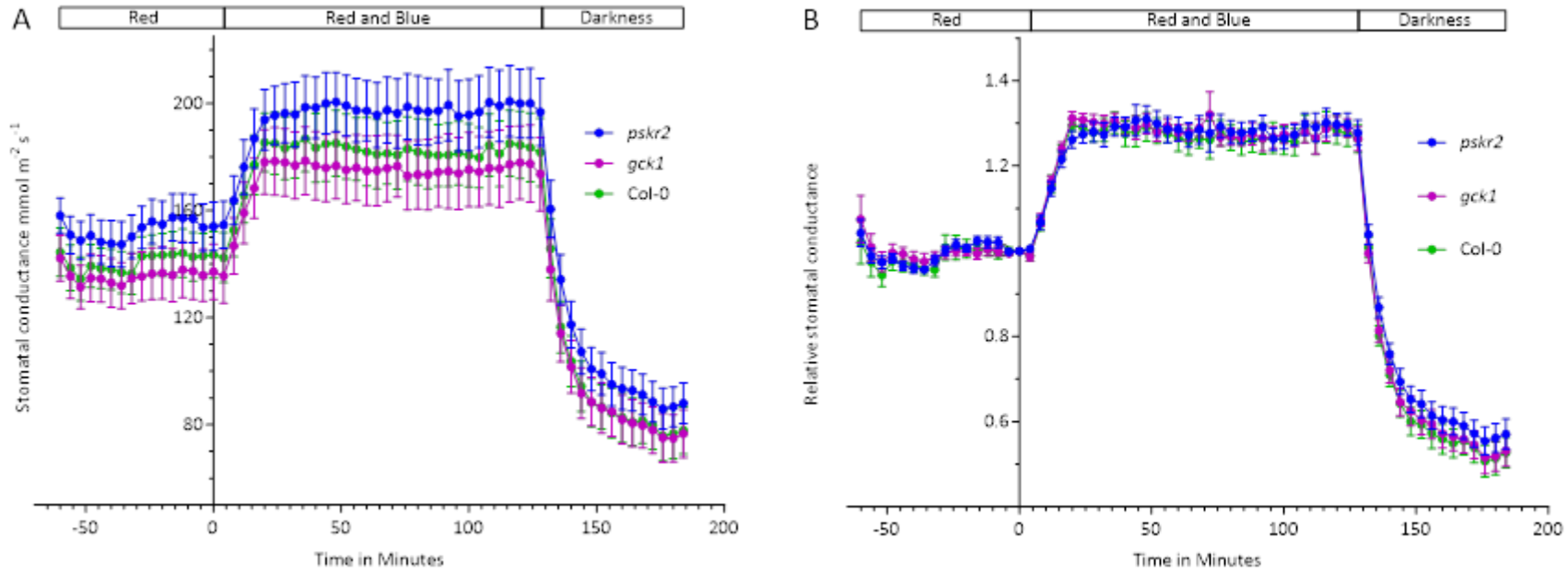

Figure 5.17 – Time course of stomatal conductance during exposure to varying lights. (A) Mean change in stomatal conductance on exposure to red light, followed by the addition of blue light after an hour and finally darkness after 2 hours of red and blue light. (B) Relative stomatal conductance normalised to steady state. Plants were acclimatised and chambers calibrated before measuring started. Due to the method of measurement taking, a reference is taken alongside the samples in a blank chamber (normalisation is at point 0). Error bars are ± SEM (n = 15-17).

Figure 5.17 shows stomatal conductance of plants measured during exposure to red light, followed by the addition of blue light for 2 hours and finally darkness for 1 hour (all at 400 ppm CO_2). Under red light all stomatal conductance values were steady with no significant differences between the three genotypes for steady state conductance. When blue light was added all 3 genotypes increased their stomatal conductance and then levelled off. On the introduction of darkness there was a steep decline in conductance to begin with and then it levelled off towards the end consistent with resting night time conductance levels.

Figure 5.17 B shows IRGA analysis during red/blue/darkness treatment to compare stomatal opening and closing response. Data was normalised to gs at the start of the experiment (point 0 after acclimatisation under red light). The normalised data shows that stomatal conductance increased rapidly after blue light was added and it decreased when plants were exposed to darkness. There were no significant differences in the magnitude of stomatal conductances between the *pskr2* and *gck1* mutants and their background control, although *pskr2* maintained consistently higher stomatal conductance during the dark period. Pre-treatment stomatal conductance variance, as compared with both high and low CO_2 graphs, *gck1* appears to have a lower starting stomatal conductance which was significantly different compared to *pskr2* but there were no significant differences between Col-0 and either mutant.

In this experiment the leaves were sprayed with a solution containing ABA to investigate the magnitude and speed of the stomatal response in the mutants and also to investigate how quickly plants recover from the stress.

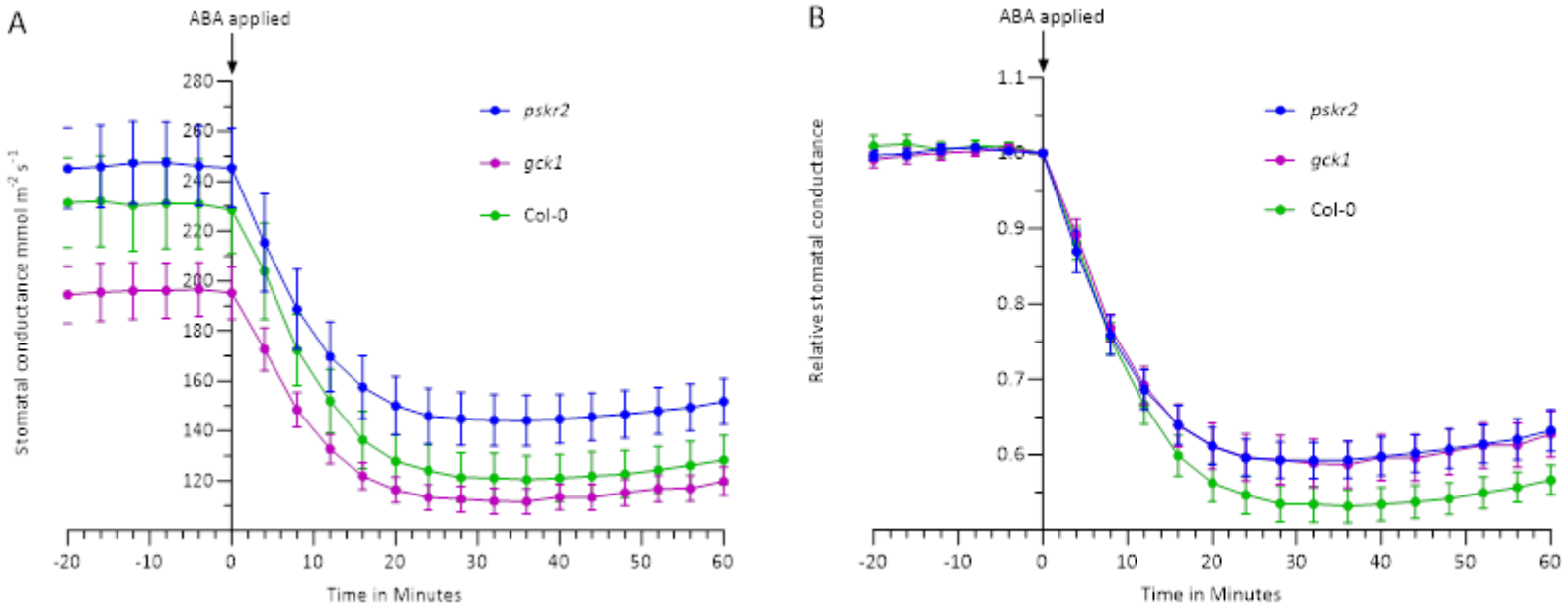

Figure 5.18 – Time course of stomatal conductance after exposure to ABA. (A) Mean change in stomatal conductance after exposure to 5 µM ABA (Sprayed at time point 0 minutes). (B) relative change in stomatal conductance after exposure to 5 µM ABA (normalised to time point 0 minutes). Error bars are ± SEM (n = 15-17).

Before ABA treatment *gck1* stomatal conductance levels were significantly lower than Col-0 and *pskr2* ($p<0.001$). Conductance levels for all three genotypes drop after ABA application, *pskr2* does not drop as much as the others and starts to recover earlier under absolute values (Figure 5.18 A).

Normalised data in Figure 5.18 B followed the same pattern as the actual. To investigate whether the magnitude of the ABA response was affected in the mutants, the data was normalised to pre-ABA application values. It also appears that both mutant lines have a weaker response to ABA in comparison to wild type (Col-0) conductance and dropped on ABA application. This may be because *gck1* stomatal conductance had already reached a minimum value. *pskr2* may not be able to close as much.

5.5.6 – The role of *GCK1* and *PSKR2* in stomatal responses and plant physiology

To investigate stomatal responses to abiotic stresses, epidermal peel bioassays were performed. The effect of increasing ABA concentration on stomatal pore area is shown (see Figure 5.19 (A)). As concentration of ABA increases, stomatal pore aperture decreases for all genotypes with no significant differences seen between the genotypes. End point effects are seen via bioassay, not fast systemic responses.

Under low CO_2 in Figure 5.19 B there is no difference between the 3 genotypes under ambient or low CO_2, but the low CO_2 response is seen. As CO_2 is decreased, stomatal aperture area increases allowing more gas exchange and as shown in Figure 5.16, higher stomatal conductance.

Bioassay data were pooled from 3 consecutive days, 40 stomata per genotype and treatment were measured per day. Plants grown under the same growth conditions. The whole experiment was repeated again and showed similar results.

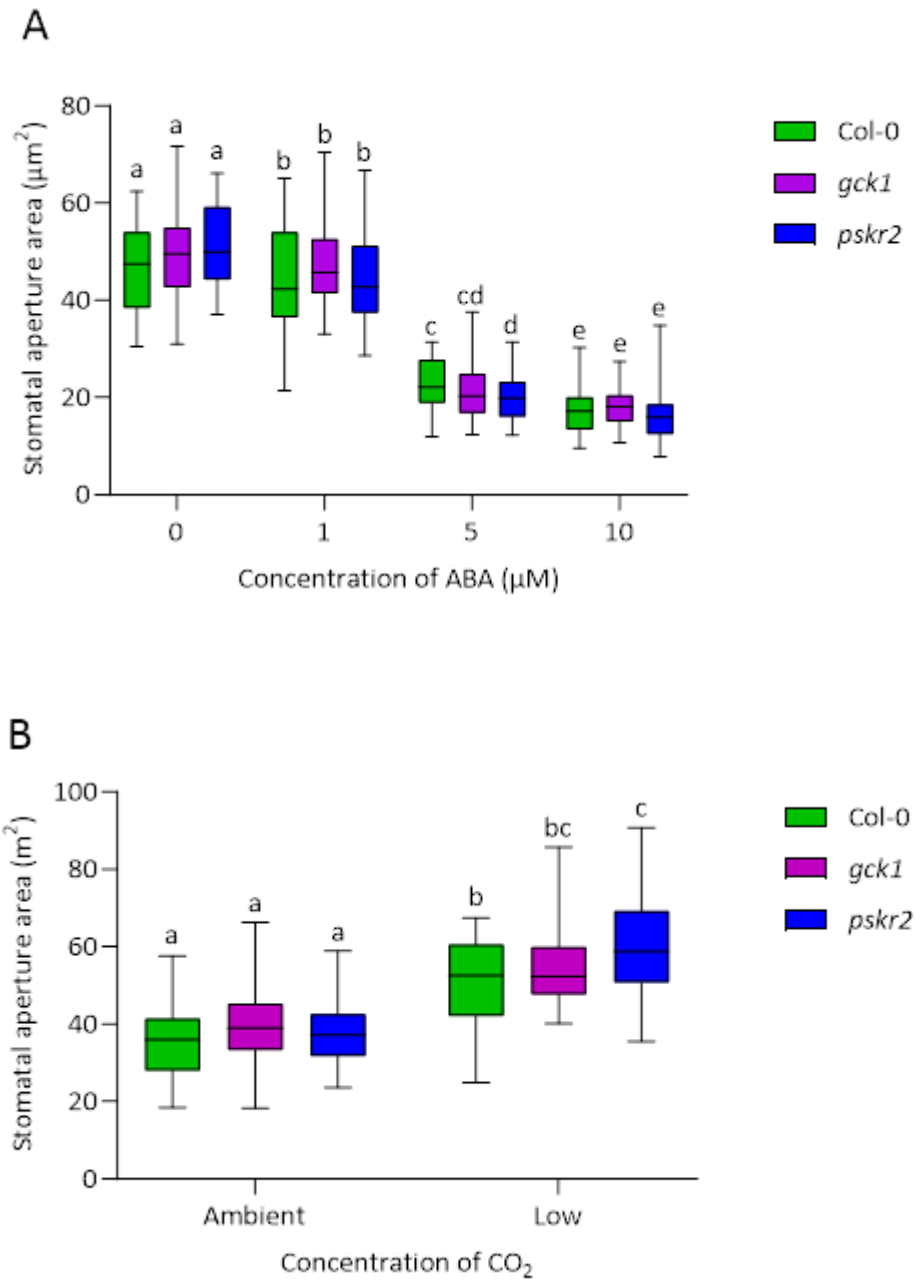

Figure 5.19 – Epidermal peel bioassays on mutant lines and Col-0. (A) Application of increasing concentrations of ABA (0, 1, 5 and 10 µM). (B) Application of either ambient (~500 ppm) or low CO_2. Standard box plot and whisker diagram, where boxes represent interquartile range and whiskers were minimum and maximum values. Two way ANOVA was performed with Geisser – Greenhouse correction followed by multiple comparison Tukey tests for (A). Letters above diagrams represent significant differences ($P < 0.001$ between ABA treatments $P < 0.05$ c and d under ABA treatment) (n = 120). Two – way ANOVA was performed (B) followed by post Hoc Tukey tests. Letters above diagrams denote significant differences, between treatment $P < 0.001$ and between genotype $P < 0.05$ (n = 120).

Bioassays are a snapshot and end point after exposure to a stimulus. Fast systemic responses to ABA were observed using IRGA, as shown in Figure 5.18. The ABA response for all genotypes is presented in Figure 5.19 A. Additionally, fast systemic responses to ABA were observed using dynamic thermal imaging, as illustrated in Figure 5.20. After the initial drop in temperature due to spraying, the ABA treated plants increased in leaf temperature followed by a second dip then a sharp increase in temperature until it started to level off about 30 minutes after treatment (approximately 90 minutes on the graph). Col-0 has a higher temperature compared to *gck1* and *pskr2* but overall no significant difference. Under mock treatment *pskr2* is higher and *gck1* is lower than Col-0, which inferred that *pskr2* stomatal pores were slightly more closed and *gck1* were slightly more open. Under ABA, *gck1* and pskr2 were lower than Col-0, stomata not as closed.

Dynamic thermal imaging (ABA)

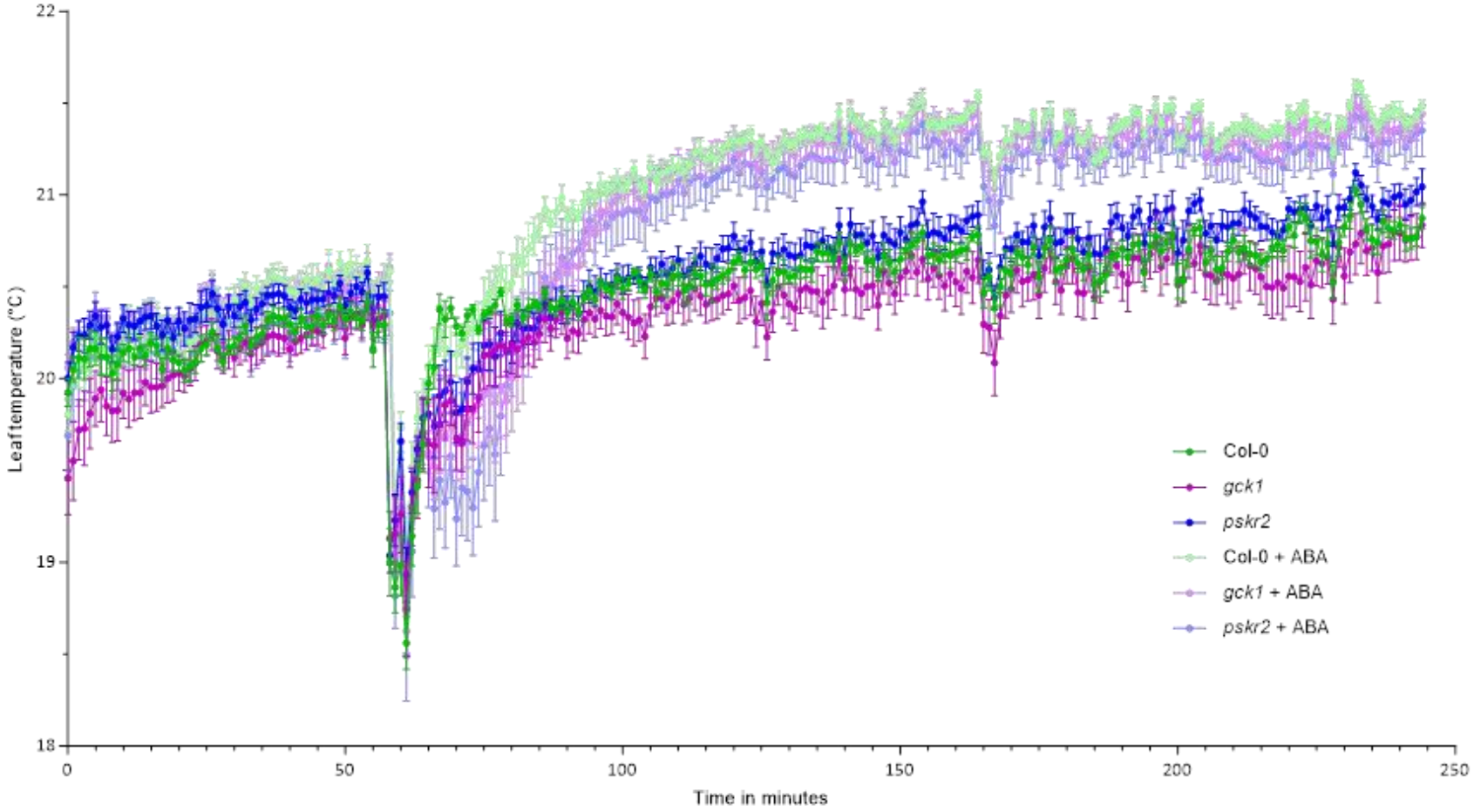

Figure 5.20 – Dynamic thermal imaging of kinase mutants treated with and without 5 µM ABA. The first hour is of acclimatisation for the plants, followed by a dip in temperature where plants were sprayed with either a mock solution or a solution containing 5 µM ABA. Error bars are ± SE (n = 6).

5.6 – Discussion

This Chapter aims to identify potential novel stomatal regulators and to analyse them to determine if they were linked to a particular abiotic stress using a range of phenotypic experiments (see Section 5.3).

5.6.1 – Growth analysis reveals differences between *gck1* and *pskr2* compared to Col-0

ABA signalling promotes seed dormancy (Rodríguez-Gacio et al., 2009; Sanz et al., 2015). Germination assays performed under increasing concentrations of ABA revealed that as ABA concentration increased, germination rate decreases for all genotypes. With both mutants, *gck1* and *pskr2,* germination rates were reduced more, suggesting a hypersensitivity to ABA with *pskr2* being more sensitive than *gck1*. Under 5 µM ABA there is a 25 % decrease between seeds germinated from Col-0 and *gck1* and a 50 % decrease between Col-0 and *pskr2*. Using the eFP browser, it was revealed that both *GCK1* and *PSKR2* are expressed in the seed coat. The expression was higher for *PSKR2* (ranged 92.93 – 41.40 for absolute expression values) compared to *GCK1* (ranged from 32.09 to 13.78) which correlates to the differences seen.

If rosette leaf area is low, then a) there is less area from which to lose water and b) potentially a lower stomatal number or density resulting in less area for gas exchange and therefore a lower stomatal conductance. Under drought conditions, stomata close to reduce water loss, if they cannot close as much or are slower at closing, plants will lose water faster. Water loss can be viewed as a proxy by fresh weight loss (see Figure 5.11). The faster the mass decreases, the faster plants lose water.

Phenotypically, overall although *gck1* plants looked slightly smaller by eye and the overall mean was lower than *pskr2* and Col-0, there was no significant differences in rosette leaf area. The fresh weight loss assay revealed that both mutants can lose water more readily than the control (Col-0) which suggested a difference in stomatal density or stomatal size (Lawson and Blatt, 2014). It could also be linked to stomatal pore size and opening. There was a significant difference in stomatal density for *gck1* compared to both pskr2 and Col-0 for the abaxial side of the leaf, but no difference between mutants and Col-0 for the adaxial side of the leaf. This suggested that there may be independent regulation of stomatal density on abaxial and adaxial sides of the leaf (Lake et al., 2002). *PSKR1* has many studies regarding roots and has been linked to growth responses. Mutant lines (in particular *pskr1-2* and *pskr1-3*) have been shown to have shorter roots and de-etiolated hypocotyls (Kutschmar et al., 2009; Hartmann et al., 2013; Ladwig et al., 2015). As *PSKR2* is linked to *PSKR1* it was thought that similar results would be observed. That was not seen in rosette leaf areas. For the stomatal index of abaxial leaves the mutants had a higher ratio indicating that they had more epidermal pavement

cells compared to stomata and to Col-0. Again, this is not seen for the adaxial side of the leaf, where Col-0 has a higher ratio in adaxial than in abaxial, which is expected. Generally, less stomata are on the adaxial side of the leaf in *Arabidopsis* due to more shading and higher humidity on the lower leaf surface (LU et al., 1993; Goh et al., 1995; Willmer and Fricker, 1996). It is only a small effect and due to one T-DNA line, other lines would need to be studied to see whether it is an actual effect or if it is due to a background mutation. A larger sample size would also be beneficial.

5.6.2 – *PSKR2* and *GCK1* are potential targets for novel stomatal regulation under whole plant gas exchange analysis

Based on the whole plant gas exchange experiments, the *gck1* mutant line appears to have reduced stomatal conductance in the light or at low CO_2 levels. This suggests that *gck1* may have a regulatory mechanism that limits gas exchange under these conditions, possibly to conserve water or to optimise photosynthetic efficiency. Moreover, *gck1* can further reduce stomatal conductance to minimal levels in darkness, or when exposed to elevated CO_2 levels, or ABA. This behaviour indicates a strong regulatory response to environmental and hormonal signals, which might be an adaptive mechanism to prevent water loss during unfavourable conditions such as high CO_2 or drought stress, indicated by the presence of ABA (Hetherington and Woodward, 2003; Nilson and Assmann, 2007; Chaves et al., 2009; Kollist et al., 2014; Lawson and Matthews, 2020). The findings suggest that either a) it has fewer stomata (slightly fewer on abaxial but not adaxial side of the leaf compared to Col-0 and *pskr2*), b) it has smaller stomata (there was no significant differences in stomatal complex size (see Figure 5.13), or c) that the stomatal pore cannot open to the same extent (epidermal peel bioassay data reveals that they can under 0 µM ABA and low CO_2). Combined with the fresh weight loss assay data, where *gck1* loses water more readily than *pskr2* and Col-0, it suggests that the lower stomatal conductance explanation may be more complicated and that factors beyond stomatal function and development might be involved.

In the gas exchange experiments, *gck1* consistently exhibited lower stomatal conductance compared to Col-0 and *pskr2* across all conditions tested. This difference in conductance is interesting, especially since the rosette leaf area is not significantly different across the genotypes (despite physically looking smaller). This suggests that the overall size and potential photosynthetic capacity of the leaves were comparable. Additionally, the changes in stomatal density were not large enough to account for the observed differences in conductance, indicating that other factors must be influencing the stomatal behaviour in *gck1*.

Several studies have shown that stomatal conductance is not solely dependent on stomatal density but also on the functionality and regulation of the stomata. For example, Lawson and Matthews (2020) highlighted that stomatal conductance is governed by complex signalling pathways involving environmental and endogenous signals, including light, CO2 concentration and hormonal regulation by abscisic acid (ABA). Kollist et al. (2019) also discussed the role of ion channels and guard cell metabolism in regulating stomatal aperture, which could be altered in *gck1*, leading to reduced conductance despite similar stomatal density.

In conclusion, the lower stomatal conductance observed in *gck1* under all conditions likely results from intrinsic differences in stomatal regulation mechanisms rather than differences in leaf area or stomatal density. Further investigation into the molecular and physiological pathways affecting stomatal behaviour in *gck1* could provide deeper insights into the specific factors contributing to its reduced conductance. There may be a background mutation or something beyond stomatal function and development involved. More independent T-DNA lines would need to be investigated in order to draw any firmer conclusions.

PSKR1 has been identified as being involved in the regulation of a plant's defence responses and its response to wounding, as well as contributing to mature leaf cell longevity. This suggests that *PSKR1* and potentially its homolog *PSKR2,* may be involved downstream of the ion channel pump control (see Figure 5.1) in guard cells, resulting in a broader influence on stomatal aperture dynamics (Loivamäki et al., 2010; Mosher et al., 2012; Hasanuzzaman and Fujita, 2022).

PSKs are small peptide hormones that play critical roles in many plant processes, including growth, development and stress responses. PSKR1, a receptor for PSKs, has been indicated to be involved in signalling pathways that regulate these physiological responses. Hartmann et al., (2013) demonstrated that PSKR1 is integral to a plant's ability to respond and defend against pathogens. It was also indicated that the plant's response to wounding further highlighted its role in adaptation to stress. Igarashi et al., (2012) also found that PSK signalling delays senescence in Arabidopsis leaves, which implied that PSKR1 can influence cellular processes involved in cell viability under certain conditions.

The suggested roles indicate that PSKR1 and potentially PSKR2 impact stomatal conductance indirectly through its regulatory effects on ion channels in guard cells. Ion channels are essential for controlling the movement of ions like potassium and chloride, which are crucial for stomatal opening and closing (Schroeder et al., 2001). By altering ion channel activity, PSKR1 could affect the turgor pressure in guard cells, leading to changes in stomatal aperture.

Recent studies suggested that peptide hormone signaling, including PSKs, might intersect with abscisic acid (ABA) signaling, a major regulator of stomatal closure during drought stress. This intersection could provide a mechanism for PSKR1 to influence stomatal responses under various environmental conditions.

In conclusion, PSKR1, and potentially PSKR2, are likely to play significant roles in the broader regulation of stomatal aperture changes through their downstream effects on ion channel activity and interaction with other hormonal pathways. Further research into these mechanisms could provide deeper insights into how plants integrate multiple signals to fine-tune their stomatal responses.

5.6.3 – The roles of *GCK1* and *PSKR2* in stomatal function and plant physiology

The ABA epidermal peel bioassay to investigate stomatal aperture changes was performed on Col-0, *gck1* and *pskr2.* Results indicated that stomata in all lines were open in 0 and 1 µM ABA. As expected, stomatal pores were relatively closed under 5 µM and even more closed under 10 µM consistent with a typical ABA response, which was corroborated by the thermal imaging data (Lefebvre et al., 2002; Cutler et al., 2010).

The ABA response is present in all lines; however, differences emerge during the initial response phase. Under bioassay conditions, the overall ABA response was observed but not the rapid systemic responses. Rapid systemic signals, which travel within seconds to minutes after stress application, are critical for triggering defence responses, including stomatal aperture changes. These fast responses which were detectable via IRGA were not observed in the bioassay (Choi et al., 2016).

This suggests that, while the mutant lines can exhibit stomatal opening and closing similar to Col-0, and impairment may be due to the fast systemic signalling rather than the guard cells ability to move. The guard cells in *pskr2* and *gck1* can open and close, indicating that their movement is not restricted.

In the low CO_2 bioassay, stomata were observed to be more open under low CO_2 conditions compared to ambient CO_2. This response correlates with the expected physiological response where stomata open to maximise CO_2 uptake when its availability is limited (Lawson and Blatt, 2014).

The thermal imaging experiment, which involved the application of ABA, initially showed results consistent with the IRGA experiment. At ABA application, leaf temperatures dropped, with mutant plants displaying a higher initial leaf temperature drop compared to Col-0. This suggests that the mutants are less sensitive to ABA and may not be able to shut as quickly as Col-0. Towards the end of the thermal imaging experiment, both the mock treated and ABA treated samples began to reach similar temperatures. This return to a higher temperature indicates more closed stomatal pores, corresponding with the IRGA data where, under normalisation, Col-0 has a lower stomatal

conductance compared to both mutants after ABA application (Lefebvre et al., 2002; Cutler et al., 2010).

These observations suggest that the ABA signalling pathway for stomatal closure has been slightly disrupted and mutants are less sensitive to ABA which is opposite to the germination assay where seeds appeared to be hypersensitive to ABA application. This indicates that different control mechanisms are involved in these responses, which may not be limited to stomatal development and function but extend to more complex interactions within the plant (Cutler et al., 2010; Chater et al., 2015a). Both bioassays and thermal imaging have their limitations, which include the number of plants tested, daylength and ambient temperature fluctuations which could influence the results.

5.7 – Future work

In this Chapter, one mutant line for *GCK1* and *PSKR2* was analysed. Confirmation of phenotypes observed in independent knock-down or knock-out lines is required. The generation of RNAi or CRISPR-CAS9 mutants or identifying further independent T-DNA insertion lines is needed to achieve this (Bortesi and Fischer, 2015).

Ideally, more lines from the list of identified genes need to be investigated to determine if more are potential stomatal regulators. High-throughput screening of these lines, using techniques such as thermal imaging and IRGA, could help to identify these key genetic components in stress response pathways (Lefebvre et al., 2002; Hartmann et al., 2013). Additional growth and development analysis experiments should be performed to assess how these genes influence overall plant growth and morphology. These include phenotyping under various environmental conditions, such as nutrient availability, abiotic and biotic stresses, which can provide insights into the broader functional roles of *GCK1* and *PSKR2*. The interaction between growth regulation and stress response can reveal how these genes contribute to plant adaptability and survival (Igarashi et al., 2012).

The current experiments provided a snapshot of the physiological responses at specific time points. To gain a more comprehensive understanding, it is important to conduct prolonged exposure experiments, such as extended drought or salt stress treatments. These experiments can reveal the dynamic changes in stomatal behaviour and overall plant physiology over time, offering clues about the long-term roles of *GCK1* and *PSKR2* in stress resilience (Chater et al., 2015b).

Ultimately, expanding the scope of experiments and validating the findings across multiple lines and conditions will provide deeper insights into the function of *GCK1* and *PSKR2*. This will help to identify their roles not only in stomatal regulation but also in broader aspects of plant growth and stress

responses. Understanding these pathways can contribute to the development of crops with improved resilience to environmental changes.

Chapter 6 – General discussion

A growing population, climate change and a need to reduce nitrogen fertiliser usage are global challenges that drive the research presented in this thesis. Nitrogen is a vital nutrient for plants, essential for many physiological processes. In many modern farming systems crops primarily obtain nitrogen through the application of nitrogen containing fertilisers, most typically in the form of nitrate or ammonia. However, there are some nitrogen cycles naturally between the atmosphere, soils and plants, such as legumes host nitrogen fixing bacteria in their root nodules and processes driven by bacteria and fungi. For example, most plants have a symbiotic relationship with rhizobia in the soil (Savci, 2012; Sinclair and Rufty, 2012; Li et al., 2017).

This thesis focused on nitrate, examining its uptake and assimilation into plants, as well as its role in stress responses, particularly in relation to stomatal behaviour. The research aimed to elucidate the influence of nitrate availability and environmental stimuli on seed germination and stomatal behaviour (Rohilla and Yadav, 2019; Tang et al., 2022).

6.1 – Summary of findings

6.1.1 – Chapter 3

In Chapter 3, the hypothesis centred on understanding how nitrate reductase activity, specifically in the Arabidopsis *nia1* and *nia2* single mutant knockout/knockdown lines, influences plant growth and stress responses. The experiments revealed that mutations in *NIA1* and *NIA2* which encode the two plant nitrate reductase isoforms, impacted plant growth, with noticeable differences in seed germination and sensitivity to ABA (Figures 3.5, 3.7 and 3.8). Contrary to expectations, the single mutants exhibited less inhibition by ABA during germination compared to wild type (Col-0) controls, whereas the double *nia1nia2* mutant showed increased sensitivity. This surprising outcome suggests that in the single mutants, there may be a compensatory mechanism where the remaining functional NR enzyme, or other pathways, exhibit higher activity or perhaps where unknown alterations in ABA signalling pathways, potentially caused by the T-DNA insertion, affect other genes (Wilkinson and Crawford, 1993; Desikan et al., 2002; Zhao et al., 2016; Zhang et al., 2018b; Olas and Wahl, 2019).

Further analysis revealed that NIA1 contains predicted SUMOylation sites, with the main predicted site being altered in the mutant lines. SUMOylation, a post-translational modification, is known to affect gene transcription and translation of many other proteins. The study found that disrupting the main predicted NIA1 SUMOylation site, led to enhanced plant growth, with plants growing faster and becoming larger than the Col-0 control. Despite no significant differences in stomatal complex sizes (Figure 3.20) or density (Figure 3.19), these plants displayed increased NR enzyme activity (Figure 3.21)

and better recovery from drought conditions. This suggests that SUMOylation significantly influences NR protein stability or activity and consequently, plant growth. However, it is possible that other transcription factors or regulatory mechanisms are contributing to these observed effects (Kim, et al., 2011; Soo Park et al., 2011; Elrouby, 2015; Costa-Broseta et al., 2021).

To further investigate the role of NR and its regulatory role in plant physiology, more experimental work would need to be performed. One interesting approach would be to use stable-isotope-labelled nitrogen (^{15}N) to measure nitrate uptake levels in the mutant lines compared to control, of particular interest is the SUMOylation mutants. This would help to determine if the potentially increased NR activity in the SUMOylation *NIA1* mutant or the *NIA1* single knockout (Figure 3.21) correlates to a higher nitrate uptake and reduced nitrogen wastage, providing valuable insights for improving agricultural efficiency. Additionally, protein level analysis using western blotting and mass spectrometry could confirm if the enhanced NR enzyme activity observed in the mutant lines is due to higher protein abundance or other regulatory mechanisms, such as changes in SUMOylation affecting *NIA1* expression (Sechley et al., 1991; Putz et al., 2011; Yu et al., 2019).

It would also be interesting to investigate the ABA signalling pathway in *nia1* and *nia2* mutants to see if altered seed germination and stress responses are linked to disruptions in these pathways. Transcriptomic analyses and targeted mutagenesis could help pinpoint specific genetic changes contributing to these phenotypes. Additionally, a comprehensive phenotypic analysis of plants with disrupted *NIA1* sumoylation would provide a deeper understanding of how this post-translational modification influences growth traits, stress resilience, and overall plant development. Together, these experiments could address unanswered questions and pave the way for strategies to enhance crop growth and stress tolerance, with important implications for sustainable agriculture (Holman et al., 2009; Rodríguez-Gacio et al., 2009; Soo Park et al., 2011; Signorelli and Considine, 2018; Zhang et al., 2018b; Costa-Broseta et al., 2021).

In conclusion, while NR is critical, redundancy exists, where one *NIA* can be compensated for by another. Previous studies have shown that when both are missing growth is significantly impacted. Interestingly, this study found that plants can exhibit improved growth when gene regulation potentially by SUMOylation is affected, although this may be influenced by a variety of other factors (Wilkinson and Crawford, 1991).

6.1.2 – Chapter 4

The research in this chapter aimed to develop methods (utilising dynamic thermal imaging) to observe whole plant responses to abiotic stress, with a focus on nitrate availability and stomatal behaviour. Initial experiments using Arabidopsis mutants and barley helped to develop a technique to monitor fast systemic responses to stress. Although exogenous nitrate did not enhance ABA-induced stomatal closure, the importance of endogenous nitrate for stomatal responses was highlighted (Figures 4.4 and 4.5) (Hõrak et al., 2020). This finding aligns with the literature that emphasises the complex role of nitrate in plant stress responses (Guo et al., 2017; Tang et al., 2022). However, more work is needed to confirm the mild phenotypes observed in the N-end rule pathway mutant (*prt1-1*), where PRT1 is upstream of NR in the protein degradation pathway, particularly by utilising more independent lines and lower ABA concentrations (Potuschak et al., 1998; Wilkinson and Davies, 2002; Stary et al., 2003; Zhao et al., 2009; Till et al., 2019).

Studies on Arabidopsis mutants, including *nia* and *NIA1SDM* lines, provided insights into the role of NR under salt stress conditions. The *NIA1SDM* lines demonstrated enhanced root growth (Figure 4.7) under moderate salt conditions, suggesting a role for NR in promoting root adaptation to stress. The variability observed in the *nia2* mutant response raised questions about this phenotype, which requires further validation with additional mutant lines. These findings add to the current understanding of the role of NR in plants, which has so far predominantly focused on *NIA1's* involvement in stress responses (Guo et al., 2017; Tang et al., 2022). Additionally, several Arabidopsis *EPF* mutants, which have altered stomatal densities, did not show significant differences in salt tolerance (Figure 4.8), contrary to expectations based on previous studies that highlighted *EPF's* role in stomatal regulation (Hepworth et al., 2015). This suggests that the impact of stomatal density on salt tolerance may be more context-dependent, varying with plant developmental stage and environmental conditions (Dow et al., 2014).

Studies with rice *EPF* mutants under prolonged salt stress also showed only minor improvements in recovery, after stress imposition with no significant effects on growth or tiller number (Figures 4.10, 4.11, 4.12 and 4.14), challenging the initial hypothesis that reduced stomatal density would enhance salt tolerance in crops. Pot size and growth conditions might have influenced these outcomes, indicating the need for alternative experimental setups, such as hydroponics, to control environmental factors and nutrient availability better. Although hydroponic systems were not successfully optimised for Arabidopsis, their successful application in barley demonstrates its potential for future studies on larger crops (Conn et al., 2013; Hepworth et al., 2015; HUANG et al., 2021; Caine et al., 2023).

6.1.3 – Chapter 5

In this chapter, the hypothesis focused on identifying novel guard cell abiotic stress regulators, particularly kinases and phosphatases, given the role of post-translational modifications in stomatal responses suggested by results from Chapters 3 and 4. Using a combination of a literature search, microarray data analysis and the eFP browser, several potential candidate Arabidopsis genes highly expressed in guard cells were identified. From the top 10 candidate genes, *PSKR2* and *GCK1* putative kinases emerged as promising due to the availability of mutant lines and their expression profiles (*pskr2* and *gck1*) (Kaufmann et al., 2021).

Phenotypic characterisation revealed that seed germination in both mutants was more sensitive to increasing levels of ABA (Figure 5.9). Additionally, detached leaves from these mutants lost water faster compared to Col-0 and slight but significant differences in abaxial stomatal index were observed (Figure 5.11 and Figure 5.12). However, stomatal density and stomatal complex size or leaf area remained consistent across the lines. This suggests a hypersensitivity to ABA in mutant lines, which may be growth stage dependent, which would help to explain the fast water loss (Leonhardt et al., 2004; Rodríguez-Gacio et al., 2009).

To assess whole plant stomatal responses, gas exchange analysis was utilised (using a custom built gas exchange system), looking at a range of abiotic stresses. Differences in stomatal conductance were observed for *gck1* under light (Figure 5.17) or at low CO_2 (Figure 5.16) conditions, but again no significant differences were found in stomatal density or stomatal complex sizes. Stomatal aperture movement was also not impaired in epidermal strip bioassay experiments (Figure 5.19), indicating that the guard cell function is intact. However, *gck1* exhibited a higher rate of water loss than *pskr2* and Col-0, which suggests that the explanation may be more complicated and may be due to developmental factors as well as stomatal movements in intact plants (Hõrak et al., 2017).

To draw any conclusions, more independent mutant lines need to be tested, to ensure that the observed results seen were not due to background mutations. With the systems used, there are also limitations in terms of: a) number of plants, b) daylength and c) ambient temperature fluctuations. Some of these issues could be resolved using controlled environment chambers.

In conclusion, *GCK1* and *PSKR2* are potential regulators of stomatal responses, particularly in relation to ABA sensitivity and water loss. However, their roles may be more important in whole plants than in isolated epidermis. It is possible that PSKR2, in particular, may be involved downstream of the ion channel pump control for stomatal closure. Further analysis, including more precise molecular studies is required to validate these findings and provide further information to confirm the mechanisms underlying their involvement in stomatal responses to environmental stresses (Chater et al., 2014).

6.2 – Future work

The work outlined in this thesis increases the current knowledge about the influence of nitrate availability and environmental stimuli on seed germination and stomatal behaviour. Our understanding of stomatal regulation and nitrogen assimilation is also enhanced. However, further work needs to be undertaken before these areas are fully understood. The following section includes recommendations, improvements and suggestions for future investigation on the influence of nitrate availability and environmental stimuli on seed germination and stomatal behaviour.

One of the key findings of this thesis is the high degree of redundancy observed between the two Arabidopsis *NIA* genes. When one gene is disrupted, the other compensates, enabling the plant to maintain its function. This suggests that *NIA* genes play an important role in nitrate assimilation and exploring additional independent mutant lines could provide deeper insights into this redundancy. Developing an experimental system, which enables both shoots and roots to be observed under varying nitrate concentrations could further elucidate the spatial dynamics of nitrate assimilation (Santos-Filho et al., 2014; Tang et al., 2022).

Another significant area of focus is the identification of potential stomatal regulators, *PSKR2* and *GCK1.* The thermal imaging screening techniques developed here could be used to explore this further, together with prolonged stress exposure to plants. This could help to identify additional potential stomatal regulators, providing further information function and phenotype. The Arabidopsis stomatal regulatory genes *OST1* and *HT1* were both identified by temperature changes using thermal imaging (Lefebvre et al., 2002; Hashimoto-Sugimoto et al., 2016; Hõrak et al., 2016). The generation of RNAi lines, CRISPR-Cas9 mutants or the identification of further independent T-DNA lines would aid the confirmatory process for the roles of the *PSKR2* and *GCK1* genes in stomatal behaviour (Jammes et al., 2009; Bortesi and Fischer, 2015).

To build on these findings, future research could incorporate growth and development-based experiments to assess the impact of any stomatal regulatory genes, providing information into their broader function. *PSKR2* and *GCK1* would be good candidates for these experiments and more detailed molecular experiments need to be performed, including transcript abundance. Understanding their role in plant growth and stress responses could provide critical insights into how plants adapt to environmental changes (Igarashi et al., 2012; Hartmann et al., 2013).

Some experiments were time limited, which was a limitation of this work. Undertaking further prolonged studies into long-term drought or salt stress has the potential to offer greater insight into plant stress responses over time. These studies would be especially relevant given the increasing

frequency and intensity of abiotic stresses due to climate change (Ciríaco et al.; Hirt and Shinozaki, 2004; IPCC, 2023).

Undertaking experiments on both Arabidopsis and crop plants, where they are subjected to multiple stresses simultaneously, would provide a deeper and more environmentally relevant understanding on plant adaptation mechanisms under changing environmental conditions. Techniques developed in this study such as dynamic thermal imaging and hydroponics could be used in these investigations to provide comprehensive insights into plant responses (Tocquin et al., 2003; Hõrak et al., 2017; Hõrak et al., 2019; Hõrak et al., 2020). Utilising hydroponic systems to evaluate the impact of abiotic stresses on crop plants would significantly enhance our understanding of nitrate assimilation and its broader impact on plant growth and development. This approach would be particularly valuable in efforts to improve crop resilience and sustainability (Saux et al., 1987; Conn et al., 2013; Tang et al., 2022).

In conclusion, these recommendations, improvements and suggestions would help to contribute to our understanding of plant nutrient use and responses to abiotic stresses, environmental stimuli and ultimately enhance crop resilience and help to ensure global food security.

6.3 – Concluding remarks

The world's population is increasing and the climate is becoming less stable, pressuring the global food supply chain and restricting the availability of arable farmland. If the huge challenge of increased future food production is going to be met, then sustainable land use and improved crop breeding strategies are critically important. Overall, the research conducted in this thesis helps to address these critical global challenges and makes a significant contribution to the fields of plant biology and plant biochemistry through comprehensive investigations into a) nitrate assimilation, b) stomatal regulation and c) stress responses in plants (IPCC, 2023).

References

Abràmoff MD, Magalhães PJ, Ram SJ (2004) Image processing with imageJ. Biophotonics Int **11**: 36–41

Aluko OO, Kant S, Adedire OM, Li C, Yuan G, Liu H, Wang Q (2023) Unlocking the potentials of nitrate transporters at improving plant nitrogen use efficiency. Front Plant Sci. doi: 10.3389/fpls.2023.1074839

Arc E, Galland M, Godin B, Cueff G, Rajjou L (2013) Nitric oxide implication in the control of seed dormancy and germination. Front Plant Sci **4**: 346

Ashraf M, Harris PJC (2013) Photosynthesis under stressful environments: An overview. Photosynthetica **51**: 163–190

Bachmair A, Finley D, Varshavsky A (1986) In vivo half-life of a protein is a function of its amino-terminal residue. Science (80-) **234**: 179–186

Bahrun A, Jensen CR, Asch F, Mogensen VO (2002) Drought-induced changes in xylem pH, ionic composition, and ABA concentration act as early signals in field-grown maize (Zea mays L.). J Exp Bot **53**: 251–63

Balmant KM, Zhang T, Chen S (2016) Protein phosphorylation and redox modification in stomatal guard cells. Front Physiol. doi: 10.3389/fphys.2016.00026

Bauer H, Ache P, Lautner S, Fromm J, Hartung W, Al-Rasheid KAS, Sonnewald S, Sonnewald U, Kneitz S, Lachmann N, et al (2013) The Stomatal Response to Reduced Relative Humidity Requires Guard Cell-Autonomous ABA Synthesis. Curr Biol **23**: 53–57

Bemis SM, Lee JS, Shpak ED, Torii KU (2013) Regulation of floral patterning and organ identity by arabidopsis erecta-family receptor kinase genes. J Exp Bot **64**: 5323–5333

Bertolino LT, Caine RS, Gray JE (2019) Impact of stomatal density and morphology on water-use efficiency in a changing world. Front Plant Sci. doi: 10.3389/fpls.2019.00225

Bertolino LT, Caine RS, Zoulias N, Yin X, Chater CCC, Biswal A, Quick WP, Gray JE (2022) Stomatal Development and Gene Expression in Rice Florets. **63**: 1679–1694

Bethke PC, Libourel IGL, Aoyama N, Chung Y-Y, Still DW, Jones RL (2007) The Arabidopsis aleurone layer responds to nitric oxide, gibberellin, and abscisic acid and is sufficient and necessary for seed dormancy. Plant Physiol **143**: 1173–88

Bista DR, Heckathorn SA, Jayawardena DM, Mishra S, Boldt JK (2018) Effects of Drought on Nutrient Uptake and the Levels of Nutrient-Uptake Proteins in Roots of Drought-Sensitive and -Tolerant Grasses. Plants (Basel, Switzerland). doi: 10.3390/plants7020028

Bloom AJ (2015) The increasing importance of distinguishing among plant nitrogen sources. Curr Opin Plant Biol **25**: 10–16

Bortesi L, Fischer R (2015) The CRISPR/Cas9 system for plant genome editing and beyond. Biotechnol Adv **33**: 41–52

Brandt B, Munemasa S, Wang C, Nguyen D, Yong T, Yang PG, Poretsky E, Belknap TF, Waadt R, Alemán F, et al (2016) Calcium specificity signaling mechanisms in abscisic acid signal transduction in Arabidopsis guard cells. Plant Sci **252**: 282–289

Bright J, Desikan R, Hancock JT, Weir IS, Neill SJ (2006a) ABA-induced NO generation and stomatal closure in Arabidopsis are dependent on H2O2 synthesis. Plant J. doi: 10.1111/j.1365-313X.2005.02615.x

Bright J, Desikan R, Hancock JT, Weir IS, Neill SJ (2006b) ABA-induced NO generation and stomatal closure in Arabidopsis are dependent on H_2O_2 synthesis. Plant J **45**: 113–122

Bucher M, Kossmann J (2007) Chapter 15 - Molecular Physiology of the Mineral Nutrition of the Potato. *In* D Vreugdenhil, J Bradshaw, C Gebhardt, F Govers, DKL Mackerron, MA Taylor, HABT-PB and B Ross, eds,Elsevier Science B.V., Amsterdam, pp 311–329

Büntgen U, Tegel W, Nicolussi K, McCormick M, Frank D, Trouet V, Kaplan JO, Herzig F, Heussner KU, Wanner H, et al (2011) 2500 years of European climate variability and human susceptibility. Science (80-) **331**: 578–582

Bürgmann H, Widmer F, Von Sigler W, Zeyer J (2004) New Molecular Screening Tools for Analysis of Free-Living Diazotrophs in Soil. Appl Environ Microbiol **70**: 240–247

Caine RS, Harrison EL, Sloan J, Flis PM, Fischer S, Khan MS, Nguyen PT, Nguyen LT, Gray JE, Croft H, et al (2023) The influences of stomatal size and density on rice abiotic stress resilience. doi: 10.1111/nph.18704

Caine RS, Yin X, Sloan J, Harrison EL, Mohammed U, Fulton T, Biswal AK, Dionora J, Chater CC, Coe RA, et al (2019) Rice with reduced stomatal density conserves water and has improved drought tolerance under future climate conditions. New Phytol **221**: 371–384

Canales J, Contreras-López O, Álvarez JM, Gutiérrez RA (2017) Nitrate induction of root hair density

is mediated by TGA1/TGA4 and CPC transcription factors in Arabidopsis thaliana. Plant J **92**: 305–316

Casson S, Gray JE (2008) Influence of environmental factors on stomatal development. New Phytol **178**: 9–23

Casson SA, Hetherington AM (2010) Environmental regulation of stomatal development. Curr Opin Plant Biol **13**: 90–95

Castro, P. H., Tavares, R. M., Bejarano, E. R., & Azevedo H (2012) SUMO, a heavyweight player in plant abiotic stress responses. Cell Mol Life Sci **69**: 3269–3283

Chamizo-Ampudia A, Sanz-Luque E, Llamas A, Galvan A, Fernandez E (2017) Nitrate Reductase Regulates Plant Nitric Oxide Homeostasis. Trends Plant Sci **22**: 163–174

Champion A, Kreis M, Mockaitis K, Picaud A, Henry Y (2004) Arabidopsis kinome: After the casting. Funct Integr Genomics **4**: 163–187

Chater C, Peng K, Movahedi M, Dunn JA, Walker HJ, Liang Y-K, McLachlan DH, Casson S, Isner JC, Wilson I, et al (2015a) Elevated CO2-Induced Responses in Stomata Require ABA and ABA Signaling. Curr Biol **25**: 2709–2716

Chater C, Peng K, Movahedi M, Dunn JA, Walker HJ, Liang Y-K, McLachlan DH, Casson S, Isner JC, Wilson I, et al (2015b) Elevated CO2-Induced Responses in Stomata Require ABA and ABA Signaling. Curr Biol **25**: 2709–2716

Chater CCC, Oliver J, Casson S, Gray JE (2014) Putting the brakes on: Abscisic acid as a central environmental regulator of stomatal development. New Phytol **202**: 376–391

Chaves MM, Flexas J, Pinheiro C (2009) Photosynthesis under drought and salt stress: regulation mechanisms from whole plant to cell. Ann Bot **103**: 551–560

Chislock MF. DE. ZRA& WAE (2013) Eutrophication: Causes, Consequences, and Controls in Aquatic Ecosystems. Nat. Educ. Knowl. 4:

Choi W-G, Hilleary R, Swanson SJ, Kim S-H, Gilroy S (2016) Rapid, Long-Distance Electrical and Calcium Signaling in Plants. Annu Rev Plant Biol **67**: 287–307

Ciríaco E, Silva D, Rejane @bullet, Mansur J, Nogueira C, Almeida M, Bandeira De Albuquerque M Drought Stress and Plant Nutrition.

Clark L, Sue-Ob K, Mukkawar V, Jones AR, Sadanandom A (2022) Understanding SUMO-mediated

adaptive responses in plants to improve crop productivity. Essays Biochem **66**: 155–168

Conn SJ, Hocking B, Dayod M, Xu B, Athman A, Henderson S, Aukett L, Conn V, Shearer MK, Fuentes S, et al (2013) Protocol: Optimising hydroponic growth systems for nutritional and physiological analysis of Arabidopsis thaliana and other plants. Plant Methods. doi: 10.1186/1746-4811-9-4

Costa-Broseta Á, Castillo M, León J (2021) Post-translational modifications of nitrate reductases autoregulates nitric oxide biosynthesis in arabidopsis. Int J Mol Sci **22**: 1–13

Crawford NM (1995) Nitrate: Nutrient and Signal for Plant Growth. Plant Cell Online **7**: 859–868

Cutler SR, Rodriguez PL, Finkelstein RR, Abrams SR (2010) Abscisic acid: Emergence of a core signaling network. Annu Rev Plant Biol **61**: 651–679

Debouba M, Dguimi HM, Ghorbel M, Gouia H, Suzuki A (2013) Expression pattern of genes encoding nitrate and ammonium assimilating enzymes in Arabidopsis thaliana exposed to short term NaCl stress. J Plant Physiol. doi: 10.1016/j.jplph.2012.09.011

Debouba M, Maâroufi-Dghimi H, Suzuki A, Ghorbel MH, Gouia H (2007) Changes in Growth and Activity of Enzymes Involved in Nitrate Reduction and Ammonium Assimilation in Tomato Seedlings in Response to NaCl Stress. Ann Bot **99**: 1143–1151

DEFRA (2022) Agri-climate report.

Delledonne M (2005) NO news is good news for plants. Curr Opin Plant Biol **8**: 390–396

Dellero Y (2020) Manipulating Amino Acid Metabolism to Improve Crop Nitrogen Use Efficiency for a Sustainable Agriculture. Front Plant Sci. doi: 10.3389/fpls.2020.602548

Desikan R, Cheung MK, Bright J, Henson D, Hancock JT, Neill SJ (2004) ABA, hydrogen peroxide and nitric oxide signalling in stomatal guard cells. J Exp Bot. doi: 10.1093/jxb/erh033

Desikan R, Griffiths R, Hancock J, Neill S (2002) A new role for an old enzyme: nitrate reductase-mediated nitric oxide generation is required for abscisic acid-induced stomatal closure in Arabidopsis thaliana. Proc Natl Acad Sci U S A **99**: 16314–8

Desikan R, Last K, Harrett-Williams R, Tagliavia C, Harter K, Hooley R, Hancock JT, Neill SJ (2006) Ethylene-induced stomatal closure in Arabidopsis occurs via AtrbohF-mediated hydrogen peroxide synthesis. Plant J **47**: 907–916

Dharmasiri N, Dharmasiri S, Weijers D, Lechner E, Yamada M, Hobbie L, Ehrismann JS, Jürgens G, Estelle M (2005) Plant development is regulated by a family of auxin receptor F box proteins.

Dev Cell **9**: 109–119

Dietrich P, Hedrich R (1998) Anions permeate and gate GCAC1, a voltage-dependent guard cell anion channel. Plant J **15**: 479–487

Dissmeyer N, Schnittger A (2011) The age of protein kinases. Methods Mol Biol **779**: 7–52

Dixon R, Kahn D (2004) Genetic regulation of biological nitrogen fixation. Nat Rev Micro **2**: 621–631

Doheny-Adams T, Hunt L, Franks PJ, Beerling DJ, Gray JE (2012) Genetic manipulation of stomatal density influences stomatal size, plant growth and tolerance to restricted water supply across a growth carbon dioxide gradient. Philos Trans R Soc B Biol Sci **367**: 547–555

Dow GJ, Bergmann DC, Berry JA (2014) An integrated model of stomatal development and leaf physiology. New Phytol **201**: 1218–1226

Ellis JR (1993) CHAPTER 7 - PLANT TISSUE CULTURE AND GENETIC TRANSFORMATION. *In* RRD CROY, ed, Plant Mol. Biol. Labfax. Academic Press, San Diego, pp 253–285

Elrouby N (2015) Analysis of Small Ubiquitin-Like Modifier (SUMO) Targets Reflects the Essential Nature of Protein SUMOylation and Provides Insight to Elucidate the Role of SUMO in Plant Development. Plant Physiol **169**: 1006–17

Fageria, N. K., Baligar, V. C., & Li YC (2008) The role of nutrient efficient plants in improving crop yields in the twenty-first century. J Plant Nutr **31**: 1121–1157

Fan X, Tang Z, Tan Y, Zhang Y, Luo B, Yang M, Lian X, Shen Q, Miller AJ, Xu G (2016) Overexpression of a pH-sensitive nitrate transporter in rice increases crop yields. Proc Natl Acad Sci U S A **113**: 7118–23

Fehér A (2015) Somatic embryogenesis — Stress-induced remodeling of plant cell fate. Biochim Biophys Acta - Gene Regul Mech **1849**: 385–402

Flores P, Botella MÁ, Cerdá A, Martínez V (2004) Influence of nitrate level on nitrate assimilation in tomato (Lycopersicon esculentum) plants under saline stress. Can J Bot **82**: 207–213

Flütsch S, Santelia D (2021) Mesophyll-derived sugars are positive regulators of light-driven stomatal opening. New Phytol **230**: 1754–1760

Flütsch S, Wang Y, Takemiya A, Vialet-Chabrand SRM, Klejchová M, Nigro A, Hills A, Lawson T, Blatt MR, Santelia D (2020) Guard cell starch degradation yields glucose for rapid stomatal opening in Arabidopsis. Plant Cell **32**: 2325–2344

Forde BG (1999) Nitrate transporters in plants: structure, function and regulation.

Franks PJ, Casson S (2014) Connecting stomatal development and physiology. New Phytol **201**: 1079–1082

Franks PJ, W. Doheny-Adams T, Britton-Harper ZJ, Gray JE (2015) Increasing water-use efficiency directly through genetic manipulation of stomatal density. New Phytol **207**: 188–195

Garzón M, Eifler K, Faust A, Scheel H, Hofmann K, Koncz C, Yephremov A, Bachmair A (2007) PRT6/At5g02310 encodes an Arabidopsis ubiquitin ligase of the N-end rule pathway with arginine specificity and is not the CER3 locus. FEBS Lett **581**: 3189–3196

Gibbs D, Vicente Conde J, Berckhan S, Mendiondo, Guillermina M, Prasad G, Holdsworth, Michael J (2015) Group VII Ethylene Response Factors co-ordinate oxygen and nitric oxide signal transduction and stress responses in plants. Plant Physiol **1**: pp.00338.2015

Gibbs DJ, Bacardit J, Bachmair A, Holdsworth MJ (2014a) The eukaryotic N-end rule pathway: Conserved mechanisms and diverse functions. Trends Cell Biol **24**: 603–611

Gibbs DJ, Bailey M, Tedds HM, Holdsworth MJ (2016) From start to finish: amino-terminal protein modifications as degradation signals in plants. New Phytol. doi: 10.1111/nph.14105

Gibbs DJ, Lee SC, Isa NM, Gramuglia S, Fukao T, Bassel GW, Correia CS, Corbineau F, Theodoulou FL, Bailey-Serres J, et al (2011a) Homeostatic response to hypoxia is regulated by the N-end rule pathway in plants. Nature **479**: 415–8

Gibbs DJ, Lee SC, Md Isa N, Gramuglia S, Fukao T, Bassel GW, Correia CS, Corbineau F, Theodoulou FL, Bailey-Serres J, et al (2011b) Homeostatic response to hypoxia is regulated by the N-end rule pathway in plants. Nature **479**: 415–418

Gibbs DJ, MdIsa N, Movahedi M, Lozano-Juste J, Mendiondo GM, Berckhan S, Marín-delaRosa N, VicenteConde J, SousaCorreia C, Pearce SP, et al (2014b) Nitric Oxide Sensing in Plants Is Mediated by Proteolytic Control of Group VII ERF Transcription Factors. Mol Cell **53**: 369–379

Giller KE, Beare MH, Lavelle P, Izac A-MN, Swift MJ (1997) Agricultural intensification, soil biodiversity and agroecosystem function. Appl Soil Ecol **6**: 3–16

Gong Y, Alassimone J, Muroyama A, Amador G, Varnau R, Liu A, Bergmann DC (2021) The Arabidopsis stomatal polarity protein BASL mediates distinct processes before and after cell division to coordinate cell size and fate asymmetries. Development. doi: 10.1242/dev.199919

Graciet E, Wellmer F (2010) The plant N-end rule pathway: Structure and functions. Trends Plant Sci

15: 447–453

Gruffman L, Jämtgård S, Näsholm T, Rennenberg H (2014) Plant nitrogen status and co-occurrence of organic and inorganic nitrogen sources influence root uptake by Scots pine seedlings. Tree Physiol. doi: 10.1093/treephys/tpt121

Guo F, Young J, Crawford NM (2003) The Nitrate Transporter AtNRT1 . 1 (CHL1) Functions in Stomatal Opening and Contributes to Drought Susceptibility in Arabidopsis. **15**: 107–117

Guo FQ, Crawford NM (2005) Arabidopsis nitric oxide synthase1 is targeted to mitochondria and protects against oxidative damage and dark-induced senescence. Plant Cell **17**: 3436–3450

Guo JS, Zhou Q, Li XJ, Yu BJ, Luo QY (2017) Enhancing NO3- supply confers NaCl tolerance by adjusting Cl- uptake and transport in G. max & G. soja. J Soil Sci Plant Nutr **17**: 194–204

Gupta, K. J., Fernie, A. R., Kaiser, W. M., & van Dongen JT (2011) On the origins of nitric oxide. Trends Plant Sci **16**: 160–168

Hachez C, Ohashi-Ito K, Dong J, Bergmann DC (2011) Differentiation of Arabidopsis Guard Cells: Analysis of the Networks Incorporating the Basic Helix-Loop-Helix Transcription Factor, FAMA 1[C][W][OA]. Plant Physiol Ò **155**: 1458–1472

Han ML, Lv QY, Zhang J, Wang T, Zhang CX, Tan RJ, Wang YL, Zhong LY, Gao YQ, Chao ZF, et al (2022) Decreasing nitrogen assimilation under drought stress by suppressing DST-mediated activation of Nitrate Reductase 1.2 in rice. Mol Plant **15**: 167–178

Han S-K, Torii KU (2016) Lineage-specific stem cells, signals and asymmetries during stomatal development. Development **143**: 1259–1270

Hansen G, Wright M (1999) Recent advances in the transformation of plants. Trends Plant Sci **4**: 226–231

Hara K, Kajita R, Torii KU, Bergmann DC, Kakimoto T (2007) The secretory peptide gene *EPF1* enforces the stomatal one-cell-spacing rule. Genes Dev **21**: 1720–1725

Hara K, Yokoo T, Kajita R, Onishi T, Yahata S, Peterson KM, Torii KU, Kakimoto T (2009) Epidermal Cell Density is Autoregulated via a Secretory Peptide, EPIDERMAL PATTERNING FACTOR 2 in Arabidopsis Leaves. Plant Cell Physiol **50**: 1019–1031

Hartmann J, Dahlke RI, Sauter M (2013) Phytosulfokine control of growth occurs in the epidermis, is likely to be non-cell autonomous and is dependent on brassinosteroids. Plant J **73**: 579–590

Hasanuzzaman M, Fujita M (2022) Plant Responses and Tolerance to Salt Stress: Physiological and Molecular Interventions. Int J Mol Sci **23**: 1–6

Hashimoto-Sugimoto M, Negi J, Monda K, Higaki T, Isogai Y, Nakano T, Hasezawa S, Iba K (2016) Dominant and recessive mutations in the Raf-like kinase HT1 gene completely disrupt stomatal responses to CO2 in Arabidopsis. J Exp Bot **67**: 3251–61

Hawkesford, M. J., & De Kok LJ (2006) Managing sulphur metabolism in plants. Plant Cell Environ **29**: 382–395

Hawkesford MJ (2014) Reducing the reliance on nitrogen fertilizer for wheat production. J Cereal Sci **59**: 276–283

Hepworth C, Doheny-Adams T, Hunt L, Cameron DD, Gray JE (2015) Manipulating stomatal density enhances drought tolerance without deleterious effect on nutrient uptake. New Phytol **208**: 336–341

Hepworth C, Turner C, Landim MG, Cameron D, Gray JE (2016) Balancing Water Uptake and Loss through the Coordinated Regulation of Stomatal and Root Development. 1–10

Hetherington AM, Woodward FI (2003) The role of stomata in sensing and driving environmental change. Nature **424**: 901–908

Hirel, B., Le Gouis, J., Ney, B., & Gallais A (2007) The challenge of improving nitrogen use efficiency in crop plants: towards a more central role for genetic variability and quantitative genetics within integrated approaches. J Exp Bot **58**: 2369–2387

Hirt H, Shinozaki K (2004) Plant responses to abiotic stress. Springer

Hoagland DR, Arnon DI (1950) The Water-Culture Method for Growing Plants without Soil.

Holdsworth MJ, Abbas M, Berckhan S, Rooney DJ, Gibbs DJ, Conde JV, Alabadı D (2015) Oxygen Sensing Coordinates Photomorphogenesis to Facilitate Seedling Survival Report Oxygen Sensing Coordinates Photomorphogenesis to Facilitate Seedling Survival. 1483–1488

Holman TJ, Jones PD, Russell L, Medhurst A, Ubeda Tomás S, Talloji P, Marquez J, Schmuths H, Tung S-A, Taylor I, et al (2009) The N-end rule pathway promotes seed germination and establishment through removal of ABA sensitivity in Arabidopsis. Proc Natl Acad Sci U S A **106**: 4549–54

Hõrak H, Fountain L, Dunn JA, Landymore J, Gray JE (2021) Leaf temperature responses to ABA and dead bacteria in wheat and Arabidopsis. Plant Signal Behav 1899471

Hõrak H, Fountain L, Dunn JA, Landymore J, Gray JE (2020) Dynamic thermal imaging confirms local but not fast systemic ABA responses. Plant Cell Environ. doi: 10.1111/pce.13973

Hõrak H, Fountain L, Dunn JA, Landymore J, Gray JE (2019) Dynamic thermal imaging provides robust temporal and spatial resolution of ABA-induced stomatal closure in intact plants.

Hõrak H, Kollist H, Merilo E (2017) Fern stomatal responses to ABA and CO2 depend on species and growth conditions. Plant Physiol **174**: 672–679

Hõrak H, Sierla M, Tõldsepp K, Wang C, Wang YS, Nuhkat M, Valk E, Pechter P, Merilo E, Salojärvi J, et al (2016) A dominant mutation in the ht1 kinase uncovers roles of MAP kinases and GHR1 in CO2-induced stomatal closure. Plant Cell **28**: 2493–2509

Horrer D, Flütsch S, Pazmino D, Matthews JSA, Thalmann M, Nigro A, Leonhardt N, Lawson T, Santelia D (2016) Blue light induces a distinct starch degradation pathway in guard cells for stomatal opening. Curr Biol **26**: 362–370

Hu H, Boisson-dernier A, Israelsson-nordström M, Xue S, Ries A, Godoski J, Kuhn JM, Julian I (2010) Carbonic Anhydrases are Upstream Regulators in Guard Cells of. Nat Cell Biol **12**: 1–18

HUANG G, DING C, MA Y, WANG Y, ZHOU Z, ZHENG S, WANG X (2021) Rice (Oryza sativa L.) seedlings enriched with zinc or manganese: Their impacts on cadmium accumulation and expression of related genes. Pedosphere **31**: 849–858

Hughes J, Hepworth C, Dutton C, Dunn JA, Hunt L, Stephens J, Waugh R, Cameron DD, Gray JE (2017) Reducing Stomatal Density in Barley Improves Drought Tolerance without Impacting on Yield 1 [CC-BY]. **174**: 776–787

Hunt L, Bailey KJ, Gray JE (2010) The signalling peptide EPFL9 is a positive regulator of stomatal development. New Phytol **186**: 609–614

Hunt L, Gray JE (2009) The Signaling Peptide EPF2 Controls Asymmetric Cell Divisions during Stomatal Development. Curr Biol **19**: 864–869

Igarashi D, Tsuda K, Katagiri F (2012) The peptide growth factor, phytosulfokine, attenuates pattern-triggered immunity. Plant J **71**: 194–204

Ikeuchi M, Sugimoto K, Iwase A (2013) Plant Callus: Mechanisms of Induction and Repression. Plant Cell **25**: 3159–3173

IPCC (2023) Climate change 2023: Synthesis Report. Contribution of Working Groups I, II and III to the Sixth Assessment Report of the Intergovernmental Panel on Climate Change.

Jakobson L, Vaahtera L, Tõldsepp K, Nuhkat M, Wang C, Wang YS, Hõrak H, Valk E, Pechter P, Sindarovska Y, et al (2016) Natural Variation in Arabidopsis Cvi-0 Accession Reveals an Important Role of MPK12 in Guard Cell CO2Signaling. PLoS Biol **14**: 1–25

Jammes F, Song C, Shin D, Munemasa S, Takeda K, Gu D, Cho D, Lee S, Giordo R, Sritubtim S, et al (2009) MAP kinases MPK9 and MPK12 are preferentially expressed in guard cells and positively regulate ROS-mediated ABA signaling. Proc Natl Acad Sci **106**: 20520–20525

Jaworski EG (1971) Nitrate reductase assay in intact plant tissues. Biochem Biophys Res Commun. doi: 10.1016/S0006-291X(71)80010-4

Jones HG (1999) Use of thermography for quantitative studies of spatial and temporal variation of stomatal conductance over leaf surfaces. Plant Cell Environ **22**: 1043–1055

Kalcsits LA, Guy RD (2013) Whole-plant and organ-level nitrogen isotope discrimination indicates modification of partitioning of assimilation, fluxes and allocation of nitrogen in knockout lines of Arabidopsis thaliana. Physiol Plant. doi: 10.1111/ppl.12038

Kaufmann C, Stührwohldt N, Sauter M, Sauter M (2021) Tyrosylprotein sulfotransferase-dependent and -independent regulation of root development and signaling by PSK LRR receptor kinases in Arabidopsis. J Exp Bot **72**: 5508–5521

Khasanova A, James JJ, Drenovsky RE (2013) Impacts of drought on plant water relations and nitrogen nutrition in dryland perennial grasses.

Kim, T. H., Bohmer, M., Hu, H., Nishimura, N., & Schroeder JI (2011) Guard Cell Signal Transduction Network. Annu Rev Plant Biol 561–591

Kolbert Z, Ortega L, Erdei L (2010) Involvement of nitrate reductase (NR) in osmotic stress-induced NO generation of Arabidopsis thaliana L. roots. J Plant Physiol. doi: 10.1016/j.jplph.2009.08.013

Kollist H, Nuhkat M, Roelfsema MRG (2014) Closing gaps: Linking elements that control stomatal movement. New Phytol. doi: 10.1111/nph.12832

Konishi M, Yanagisawa S (2011) The regulatory region controlling the nitrate-responsive expression of a nitrate reductase gene, NIA1, in Arabidopsis. Plant Cell Physiol. doi: 10.1093/pcp/pcr033

Konishi M, Yanagisawa S (2013) Arabidopsis NIN-like transcription factors have a central role in nitrate signalling. Nat Commun **4**: 1617

Konstantis N, Koskorellos K, Balou A, Paravolidaki A, Garantziotis G, Koulopoulou CE, Koulopoulos A, Zervoudakis G (2022) The Effect of Leaf Wounding on Basil Plants of Different Developmental

Stages. 1–15

Krapp A (2015) Plant nitrogen assimilation and its regulation: a complex puzzle with missing pieces. Curr Opin Plant Biol **25**: 115–122

Krapp A, David LC, Chardin C, Girin T, Marmagne A, Leprince AS, Chaillou S, Ferrario-Méry S, Meyer C, Daniel-Vedele F (2014) Nitrate transport and signalling in Arabidopsis. J Exp Bot. doi: 10.1093/jxb/eru001

Kuhn JM, Boisson-Dernier A, Dizon MB, Maktabi MH, Schroeder JI (2006) The protein phosphatase AtPP2CA negatively regulates abscisic acid signal transduction in arabidopsis, and effects of abh1 on AtPP2CA mRNA. Plant Physiol **140**: 127–139

Kumari S, Sharma N, Raghuram N (2021) Meta-Analysis of Yield-Related and N-Responsive Genes Reveals Chromosomal Hotspots, Key Processes and Candidate Genes for Nitrogen-Use Efficiency in Rice. Front Plant Sci **12**: 627955

Kusumi K, Hirotsuka S, Kumamaru T, Iba K (2012) Increased leaf photosynthesis caused by elevated stomatal conductance in a rice mutant deficient in SLAC1, a guard cell anion channel protein. J Exp Bot **63**: 5635–5644

Lake JA, Woodward FI, Quick WP (2002) Long-distance CO2 signalling in plants. J Exp Bot **53**: 183–193

Lamattina L, García-Mata C, Graziano M, Pagnussat G (2003) NITRIC OXIDE : The Versatility of an Extensive Signal Molecule. Annu Rev Plant Biol **54**: 109–136

Lawson T, Blatt MR (2014) Stomatal Size, Speed, and Responsiveness Impact on Photosynthesis and Water Use Efficiency. Plant Physiol **164**: 1556–1570

Lawson T, Matthews J (2020) Guard Cell Metabolism and Stomatal Function. Annu Rev Plant Biol **71**: 273–302

Lawson T, Vialet-Chabrand S (2019) Speedy stomata, photosynthesis and plant water use efficiency. New Phytol **221**: 93–98

Le QT, Truong HA, Nguyen DT, Yang S, Xiong L, Lee H (2023) Enhanced growth performance of abi5 plants under high salt and nitrate is associated with reduced nitric oxide levels. J Plant Physiol **286**: 154000

Lea, P. J., & Azevedo RA (2006) Nitrogen use efficiency. 1. Uptake of nitrogen from the soil. Ann Appl Biol **149**: 243–247

Lee JS, Kuroha T, Hnilova M, Khatayevich D, Kanaoka MM, Mcabee JM, Sarikaya M, Tamerler C, Torii KU (2012) Direct interaction of ligand-receptor pairs specifying stomatal patterning. Genes Dev **26**: 126–136

Lee YJ, Lee WJ, Le QT, Hong SW, Lee H (2021) Growth Performance Can Be Increased Under High Nitrate and High Salt Stress Through Enhanced Nitrate Reductase Activity in Arabidopsis Anthocyanin Over-Producing Mutant Plants. Front Plant Sci. doi: 10.3389/fpls.2021.644455

Lefebvre Â, Sotta B, Merlot S, Mustilli A, Genty B, North H (2002) Use of infrared thermal imaging to isolate Arabidopsis mutants defective in stomatal regulation. doi: 10.1046/j.1365-313X.2002.01322.x

Lehti-Shiu MD, Shiu SH (2012) Diversity, classification and function of the plant protein kinase superfamily. Philos Trans R Soc B Biol Sci **367**: 2619–2639

Leonhardt N, Kwak JM, Robert N, Waner D, Leonhardt G, Schroeder JI (2004) Microarray expression analyses of Arabidopsis guard cells and isolation of a recessive abscisic acid hypersensitive protein phosphatase 2C mutant. Plant Cell **16**: 596–615

Leyser HMO, Furner IJ (1992) Characterisation of three shoot apical meristem mutants of Arabidopsis thaliana. Development **116**: 397–403

Li H, Hu B, Chu C (2017) Nitrogen use efficiency in crops: Lessons from Arabidopsis and rice. J Exp Bot **68**: 2477–2488

Li SX, Wang ZH, Stewart BA (2013) Responses of Crop Plants to Ammonium and Nitrate N. Adv Agron. doi: 10.1016/B978-0-12-405942-9.00005-0

Li Y, Xu S, Wang Z, He L, Xu K, Wang G (2018) Glucose triggers stomatal closure mediated by basal signaling through HXK1 and PYR/RCAR receptors in Arabidopsis. J Exp Bot **69**: 1471–1484

Licausi F, Kosmacz M, Weits DA, Giuntoli B, Giorgi FM, Voesenek LACJ, Perata P, Van Dongen JT (2011) Oxygen sensing in plants is mediated by an N-end rule pathway for protein destabilization. Nature **479**: 419–422

Lim SL, Flütsch S, Liu J, Distefano L, Santelia D, Lim BL (2022) Arabidopsis guard cell chloroplasts import cytosolic ATP for starch turnover and stomatal opening. Nat Commun. doi: 10.1038/s41467-022-28263-2

Linkohr BI, Williamson LC, Fitter AH, Leyser HMO (2002) Nitrate and phosphate availability and distribution have different effects on root system architecture of Arabidopsis. Plant J **29**: 751–

760

Liu C, Duan N, Chen X, Li H, Zhao X, Duo P, Wang J, Li Q (2022) Metabolic Pathways Involved in the Drought Stress Response of Nitraria tangutorum as Revealed by Transcriptome Analysis. Forests. doi: 10.3390/f13040509

Liu RX, Li HL, Rui L, Liu GD, Wang T, Wang XF, Li LG, Zhang Z, You CX (2023) An apple NITRATE REDUCTASE 2 gene positively regulates nitrogen utilization and abiotic stress tolerance in Arabidopsis and apple callus. Plant Physiol Biochem **196**: 23–32

Liu Y, Ye N, Liu R, Chen M, Zhang J (2010) H2O2 mediates the regulation of ABA catabolism and GA biosynthesis in Arabidopsis seed dormancy and germination. J Exp Bot **61**: 2979–90

Lopez-Molina L, Mongrand S, Chua NH (2001) A postgermination developmental arrest checkpoint is mediated by abscisic acid and requires the ABI5 transcription factor in Arabidopsis. Proc Natl Acad Sci U S A **98**: 4782–7

Lozano-Juste J, León J (2010) Enhanced Abscisic Acid-Mediated Responses in nia1nia2noa1-2 Triple mutant impaired in NIA/NR- and AtNOA1-dependent nitric oxide biosynthesis in Arabidopsis. Plant Physiol **152**: 891–903

LU Z, QUIÑONES MA, ZEIGER E (1993) Abaxial and adaxial stomata from Pima cotton (Gossypium barbadense L.) differ in their pigment content and sensitivity to light quality. Plant Cell Environ **16**: 851–858

M€uller HM, Sch€afer N, Bauer H, Geiger D, Lautner S, Fromm J, Riederer M, Bueno A, Nussbaumer T, Mayer K, et al (2017) The desert plant Phoenix dactylifera closes stomata via nitrate-regulated SLAC1 anion channel. New Phytol **216**: 150–162

MacRobbie EA (1998) Signal transduction and ion channels in guard cells. Philos Trans R Soc Lond B Biol Sci **353**: 1475–88

Mandal VK, Jangam AP, Chakraborty N, Raghuram N (2022) Nitrate-responsive transcriptome analysis reveals additional genes/processes and associated traits viz. height, tillering, heading date, stomatal density and yield in japonica rice. Planta **255**: 42

Manik SMN, Shi S, Mao J, Dong L, Su Y, Wang Q, Liu H (2015) The Calcium Sensor CBL-CIPK Is Involved in Plant's Response to Abiotic Stresses. Int J Genomics **2015**: 493191

De Marchi R, Sorel M, Mooney B, Fudal I, Goslin K, Kwaśniewska K, Ryan PT, Pfalz M, Kroymann J, Pollmann S, et al (2016) The N-end rule pathway regulates pathogen responses in plants. doi:

10.1038/srep26020

Mcainsh MR, Brownlee C, Hetherington AM (1991) Partial Inhibition of ABA-Induced Stomatal Closure by Calcium-Channel Blockers.

Medeiros DB, Perez Souza L, Antunes WC, Araújo WL, Daloso DM, Fernie AR (2018) Sucrose breakdown within guard cells provides substrates for glycolysis and glutamine biosynthesis during light-induced stomatal opening. Plant J **94**: 583–594

Medici A, Krouk G (2014) The primary nitrate response: a multifaceted signalling pathway. J Exp Bot **65**: 5567–76

Medrano H, Tomás M, Martorell S, Flexas J, Hernández E, Rosselló J, Pou A, Escalona J-M, Bota J (2015) From leaf to whole-plant water use efficiency (WUE) in complex canopies: Limitations of leaf WUE as a selection target. Crop J **3**: 220–228

Mendiondo GM, Gibbs DJ, Szurman-Zubrzycka M, Korn A, Marquez J, Szarejko I, Maluszynski M, King J, Axcell B, Smart K, et al (2016) Enhanced waterlogging tolerance in barley by manipulation of expression of the N-end rule pathway E3 ligase PROTEOLYSIS6. Plant Biotechnol J **14**: 40–50

Merilo E, Laanemets K, Hu H, Xue S, Jakobson L, Tulva I, Gonzalez-Guzman M, Rodriguez PL, Schroeder JI, Broschè M, et al (2013) PYR/RCAR receptors contribute to ozone-, reduced air humidity-, darkness-, and CO2-induced stomatal regulation. Plant Physiol **162**: 1652–1668

Meyer S, Genty B Mapping Intercellular CO 2 Mole Fraction (C i) in Rosa rubiginosa Leaves Fed with Abscisic Acid by Using Chlorophyll Fluorescence Imaging 1 Significance of C i Estimated from Leaf Gas Exchange.

Miller MJ, Vierstra RD (2011) Mass spectrometric identification of SUMO substrates provides insights into heat stress-induced SUMOylation in plants. Plant Signal Behav **6**: 130–133

Misra BB, Acharya BR, Granot D, Assmann SM, Chen S (2015) The guard cell metabolome: functions in stomatal movement and global food security . Front Plant Sci **6**: 334

Mohamed D, Vonapartis E, Corcega DY, Gazzarrini S (2023) ABA guides stomatal proliferation and patterning through the EPF-SPCH signaling pathway in Arabidopsis thaliana. Dev. doi: 10.1242/dev.201258

Moll, R. H., Kamprath, E. J., & Jackson WA (1982) Analysis and interpretation of factors which contribute to efficiency of nitrogen utilization. Agron J **74**: 562–564

Movahedi M, Zoulias N, Casson SA, Sun P, Liang Y-K, Hetherington AM, Gray JE, Chater CCC (2021)

Stomatal responses to carbon dioxide and light require abscisic acid catabolism in Arabidopsis. Interface Focus **11**: 20200036

Muhammad Aslam M, Waseem M, Jakada BH, Okal EJ, Lei Z, Saqib HSA, Yuan W, Xu W, Zhang Q (2022) Mechanisms of Abscisic Acid-Mediated Drought Stress Responses in Plants. Int J Mol Sci. doi: 10.3390/ijms23031084

Munns R, Tester M (2008) Mechanisms of salinity tolerance. Annu Rev Plant Biol **59**: 651–81

Nadeau JA, Sack FD (2002) Control of Stomatal Distribution on the *Arabidopsis* Leaf Surface. Science (80-) **296**: 1697–1700

Nadeau JA, Sack FD, Nadeau JA, Sack FD (2002) Stomatal Development in Arabidopsis. Arab B **1**: 1–28

National Atmospheric Emissions Inventory (2024) Pollutant Information: Nitrous Oxide. Natl. Atmos. Emiss. Invent.,

Negrão S, Schmöckel SM, Tester M (2017) Evaluating physiological responses of plants to salinity stress. Ann Bot **119**: 1–11

Neill S, Barros R, Bright J, Desikan R, Hancock J, Harrison J, Morris P, Riberio D (2007) Nitric oxide, stomatal closure and abiotic stress. Comp Biochem Physiol Part A Mol Integr Physiol **146**: S257

Neill S, Bright J, Desikan R, Hancock J, Harrison J, Wilson I (2008) Nitric oxide evolution and perception. J. Exp. Bot. pp 25–35

Neill SJ, Desikan R, Hancock JT (2003) Nitric oxide signalling in plants. New Phytol **159**: 11–35

Nilson SE, Assmann SM (2007) The Control of Transpiration. Insights from Arabidopsis. Plant Physiol **143**: 19 LP – 27

Nowak MA, Boerlijst MC, Cooke J, Smith JM (1997) A. Linking herbivory and pollination: defoliation and selective fruit abortion in. **275**: 0–4

Nunes TDG, Zhang D, Raissig MT (2020) Form, development and function of grass stomata. Plant J **101**: 780–799

Olas JJ, Wahl V (2019) Tissue-specific NIA1 and NIA2 expression in Arabidopsis thaliana . Plant Signal Behav 1–5

Orr CH, James A, Leifert C, Cooper JM, Cummings SP (2011) Diversity and Activity of Free-Living Nitrogen-Fixing Bacteria and Total Bacteria in Organic and Conventionally Managed Soils. Appl

Environ Microbiol **77**: 911–919

Palavan-Unsal N, Arisan D (2009) Nitric oxide signalling in plants. Bot Rev. doi: 10.1007/s12229-009-9031-2

Pantin F, Blatt MR (2018) Stomatal Response to Humidity: Blurring the Boundary between Active and Passive Movement. Plant Physiol **176**: 485–488

Pantin F, Monnet F, Jannaud D, Costa JM, Renaud J, Muller B, Simonneau T, Genty B (2013a) The dual effect of abscisic acid on stomata. New Phytol **197**: 65–72

Pantin F, Renaud J, Barbier F, Vavasseur A, Le Thiec D, Rose C, Bariac T, Casson S, McLachlan DH, Hetherington AM, et al (2013b) Developmental priming of stomatal sensitivity to abscisic acid by leaf microclimate. Curr Biol **23**: 1805–1811

Papdi C, Pérez-Salamõ I, Joseph MP, Giuntoli B, Bögre L, Koncz C, Szabados L (2015) The low oxygen, oxidative and osmotic stress responses synergistically act through the ethylene response factor VII genes RAP2.12, RAP2.2 and RAP2.3. Plant J **82**: 772–784

Park, H. J., & Yun DJ (2013) New insights into the role of the small ubiquitin-like modifier (SUMO) in plants. Int Rev Cell Mol Biol **300**: 161–209

Park S, Fung P, Nishimura N, Jensen DR, Zhao Y, Lumba S, Santiago J, Rodrigues A, Alfred SE, Bonetta D, et al (2010) Abscisic acid inhibits PP2Cs via the PYR/PYL family of ABA- binding START proteins. Science (80-) **324**: 1068–1071

Pathak, R. R., & Lochab S (2010) Improving nitrogen use efficiency in plants: Technological options. Plant Biotechnol Methods Protoc 365–377

Pei ZM, Kuchitsu K, Ward JM, Schwarz M, Schroeder JI (1997) Differential abscisic acid regulation of guard cell slow anion channels in arabidopsis wild-type and abi1 and abi2 mutants. Plant Cell **9**: 409–423

Peoples MB, Herridge DF, Ladha JK (1995) Biological nitrogen fixation: An efficient source of nitrogen for sustainable agricultural production? Plant Soil **174**: 3–28

Pichaco J, Manandhar A, McAdam SAM (2024) Mechanical advantage makes stomatal opening speed a function of evaporative demand. Plant Physiol **195**: 370–377

Pike CS, Cohen WS, Monroe JD (2002) Nitrate reductase: A model system for the investigation of enzyme induction in eukaryotes. Biochem Mol Biol Educ **30**: 111–116

Potuschak T, Stary S, Schlögelhofer P, Becker F, Nejinskaia V, Bachmair A (1998) PRT1 of Arabidopsis thaliana encodes a component of the plant N-end rule pathway. Proc Natl Acad Sci U S A **95**: 7904–8

Putz B, Drapela T, Wanek W, Schmidt O, Frank T, Zaller JG (2011) A simple method for in situ-labelling with 15N and 13C of grassland plant species by foliar brushing. Methods Ecol Evol **2**: 326–332

Rasehke K (1975) Simultaneous Requirement of Carbon Dioxide and Abscisic Acid for Stomatal Closing in X a n t h i u m s t r u m a r i u m L. * * *. Springer-Verlag

Rashmi I, Roy T, Kartika KS, Pal R, Coumar V, Kala S, Shinoji KC (2020) Organic and Inorganic Fertilizer Contaminants in Agriculture: Impact on Soil and Water Resources BT - Contaminants in Agriculture: Sources, Impacts and Management. *In* M Naeem, AA Ansari, SS Gill, eds,Springer International Publishing, Cham, pp 3–41

Raven JA (2014) Speedy small stomata'. J Exp Bot **65**: 1415–1424

Ray DK, Mueller ND, West PC, Foley JA (2013) Yield Trends Are Insufficient to Double Global Crop Production by 2050. PLoS One **8**: e66428

Rockel P, Strube F, Rockel A, Wildt J, Kaiser WM Regulation of nitric oxide (NO) production by plant nitrate reductase in vivo and in vitro.

Rodríguez-Gacio M del C, Matilla-Vázquez MA, Matilla AJ (2009) Seed dormancy and ABA signaling: the breakthrough goes on. Plant Signal Behav **4**: 1035–1048

Rohilla P, Yadav JP (2019) Acute salt stress differentially modulates nitrate reductase expression in contrasting salt responsive rice cultivars. Protoplasma. doi: 10.1007/s00709-019-01378-y

Sakihama Y, Murakami S, Yamasaki H (2003) Involvement of Nitric Oxide in the Mechanism for Stomatal Opening in Vicia faba Leaves. Biol Plant **46**: 117–119

Salmi ML, Clark G, Roux SJ, Stacey G Current status and proposed roles for nitric oxide as a key mediator of the effects of extracellular nucleotides on plant growth. doi: 10.3389/fpls.2013.00427

Sánchez-Moreiras AM, Graña E, Reigosa MJ, Araniti F (2020) Imaging of Chlorophyll a Fluorescence in Natural Compound-Induced Stress Detection. Front Plant Sci. doi: 10.3389/fpls.2020.583590

Santos-Filho PR, Saviani EE, Salgado I, Oliveira HC (2014) The effect of nitrate assimilation deficiency on the carbon and nitrogen status of Arabidopsis thaliana plants. Amino Acids. doi: 10.1007/s00726-014-1674-6

Sanz L, Albertos P, Mateos I, Sánchez-Vicente I, Lechón T, Fernández-Marcos M, Lorenzo O (2015) Nitric oxide (NO) and phytohormones crosstalk during early plant development. J Exp Bot **66**: 2857–2868

Sanz L, Fernández-Marcos M, Modrego A, Lewis DR, Muday GK, Pollmann S, Dueñas M, Santos-Buelga C, Lorenzo O (2014) Nitric oxide plays a role in stem cell niche homeostasis through its interaction with auxin. Plant Physiol **166**: 1972–1984

Saux C, Lemoine Y, Marion-Poll A, Valadier MH, Deng M, Morot-Gaudry JF (1987) Consequence of Absence of Nitrate Reductase Activity on Photosynthesis in Nicotiana plumbaginifolia Plants. Plant Physiol.

Savci S (2012) Investigation of Effect of Chemical Fertilizers on Environment. APCBEE Procedia **1**: 287–292

Schäfer N, Maierhofer T, Herrmann J, Jørgensen ME, Lind C, von Meyer K, Lautner S, Fromm J, Felder M, Hetherington AM, et al (2018) A Tandem Amino Acid Residue Motif in Guard Cell SLAC1 Anion Channel of Grasses Allows for the Control of Stomatal Aperture by Nitrate. Curr Biol **28**: 1370-1379.e5

Schindelin, J., Arganda-Carreras, I., Frise E et al. (2012) Fiji: an open-source platform for biological-image analysis. Nat Methods **9**: 676–682

Schroeder JI, Kwak JM, Allen GJ (2001) Guard cell abscisic acid signalling and engineering drought hardiness in plants. Nature **410**: 327–30

Sechley KA, Oaks A, Bewley JD (1991) Enzymes of Nitrogen Assimilation Undergo Seasonal Fluctuations in the Roots of the Persistent Weedy Perennial Cichorium intybus'. Plant Physiol **97**: 322–329

Seligman K, Saviani EE, Oliveira HC, Pinto-Maglio CAF, Salgado I (2008) Floral transition and nitric oxide emission during flower development in Arabidopsis thaliana is affected in nitrate reductase-deficient plants. Plant Cell Physiol. doi: 10.1093/pcp/pcn089

Shagun Khandelwal The Nitrogen cycle. Biol. Discuss., http://www.biologydiscussion.com/nitrogen-fixation/nitrogen-fixation-in-plants/23870

Shatil-Cohen A, Attia Z, Moshelion M (2011) Bundle-sheath cell regulation of xylem-mesophyll water transport via aquaporins under drought stress: A target of xylem-borne ABA? Plant J **67**: 72–80

Shpak ED, McAbee JM, Pillitteri LJ, Torii KU (2005) Stomatal Patterning and Differentiation by

Synergistic Interactions of Receptor Kinases. Science (80-) **309**: 290–293

Sierla M, Hõrak H, Overmyer K, Waszczak C, Yarmolinsky D, Maierhofer T, Vainonen JP, Salojärvi J, Denessiouk K, Laanemets K, et al (2018) The receptor-like pseudokinase GHR1 is required for stomatal closure. Plant Cell **30**: 2813–2837

Signorelli S, Considine MJ (2018) Nitric oxide enables germination by a four-pronged attack on ABA-induced seed dormancy. Front Plant Sci. doi: 10.3389/fpls.2018.00296

DE SILVA DLR, HETHERINGTON AM, MANSFIELD TA (1985) Synergism Between Calcium Ions and Abscisic Acid in Preventing Stomatal Opening. New Phytol **100**: 473–482

Sinclair TR, Rufty TW (2012) Nitrogen and water resources commonly limit crop yield increases, not necessarily plant genetics. Glob Food Sec **1**: 94–98

Sirichandra C, Wasilewska A, Vlad F, Valon C, Leung J (2009) The guard cell as a single-cell model towards understanding drought tolerance and abscisic acid action. J Exp Bot **60**: 1439–1463

Soltani F, Heidari S, Azizi M, Hadian J (2014) Influence of Ca(NO3)2 and KNO3 Application on Biomass, Yield, Oil and Mineral Contents of Tarragon in "Ray" Region. J Agric Sci **7**: 19–29

Soo Park B, Tae Song J, Soo Seo H (2011) Arabidopsis nitrate reductase activity is stimulated by the E3 SUMO ligase AtSIZ1. doi: 10.1038/ncomms1408

Srivastava AK, Zhang C, Yates G, Bailey M, Brown A, Sadanandom A (2016) SUMO Is a critical regulator of salt stress responses in rice. Plant Physiol **170**: 2378–2391

Stary S, Yin X, Potuschak T, Schlögelhofer P, Nizhynska V, Bachmair A (2003) PRT1 of Arabidopsis is a ubiquitin protein ligase of the plant N-end rule pathway with specificity for aromatic amino-terminal residues. Plant Physiol **133**: 1360–6

Sugimoto K, Meyerowitz EM (2013) Regeneration in Arabidopsis Tissue Culture. *In* I De Smet, ed, Plant Organog. Methods Protoc. Humana Press, Totowa, NJ, pp 265–275

Sussmilch FC, Schultz J, Hedrich R, Roelfsema MRG (2019) Acquiring Control: The Evolution of Stomatal Signalling Pathways. Trends Plant Sci **24**: 342–351

Tameshige T, Ikematsu S, Torii KU, Uchida N, Etchells P (2017) Stem development through vascular tissues: EPFL-ERECTA family signaling that bounces in and out of phloem. J Exp Bot **68**: 45–53

Tang X, Peng Y, Li Z, Guo H, Xia X, Li B, Yin W (2022) The Regulation of Nitrate Reductases in Response to Abiotic Stress in Arabidopsis. Int J Mol Sci. doi: 10.3390/ijms23031202

Terrile MC, París R, Calderõn-Villalobos LIA, Iglesias MJ, Lamattina L, Estelle M, Casalongué CA (2012) Nitric oxide influences auxin signaling through S-nitrosylation of the Arabidopsis TRANSPORT INHIBITOR RESPONSE 1 auxin receptor. Plant J **70**: 492–500

Thirkell TJ, Cameron DD, Hodge A (2016) Resolving the 'nitrogen paradox' of arbuscular mycorrhizas: fertilization with organic matter brings considerable benefits for plant nutrition and growth. Plant Cell Environ **39**: 1683–1690

Thorpe TA (2007) History of plant tissue culture. Mol Biotechnol **37**: 169–80

Tian W, Hou C, Ren Z, Pan Y, Jia J, Zhang H, Bai F, Zhang P, Zhu H, He Y, et al (2015) A molecular pathway for CO2 response In Arabidopsis guard cells. Nat Commun. doi: 10.1038/ncomms7057

Till CJ, Vicente J, Zhang H, Oszvald M, Deery MJ, Pastor V, Lilley KS, Ray R V., Theodoulou FL, Holdsworth MJ (2019) The Arabidopsis thaliana N-recognin E3 ligase PROTEOLYSIS1 influences the immune response. Plant Direct. doi: 10.1002/pld3.194

Tocquin P, Corbesier L, Havelange A, Pieltain A, Kurtem E, Bernier G, Perilleux C (2003) A novel high efficiency, low maintenance, hydroponic system for synchronous growth and flowering of Arabidopsis thaliana. BMC Plant Biol **3**: 2

Tõldsepp K, Zhang J, Takahashi Y, Sindarovska Y, Hõrak H, Ceciliato PHO, Koolmeister K, Wang YS, Vaahtera L, Jakobson L, et al (2018) Mitogen-activated protein kinases MPK4 and MPK12 are key components mediating CO2-induced stomatal movements. Plant J **96**: 1018–1035

Torii KU (2012) Mix-and-match: ligand–receptor pairs in stomatal development and beyond. Trends Plant Sci **17**: 711–719

Torii KU (2015) Stomatal differentiation: The beginning and the end. Curr Opin Plant Biol **28**: 16–22

Torii KU (2021) Stomatal development in the context of epidermal tissues. Ann Bot **128**: 137–148

Ullrich W.R. (2002) Salinity and Nitrogen Nutrition - Chapter 11. Läuchli A, Lüttge U Salin Environ - Plants - Mol 229–248

United Nations D of E and SA, Population Division (2009) World Population Prospects: The 2008 Revision, Highlights. 2009; Working Paper No ESA/P/WP.210, 1-107.

Uraji M, Katagiri T, Okuma E, Ye W, Hossain MA, Masuda C, Miura A, Nakamura Y, Mori IC, Shinozaki K, et al (2012) Cooperative function of PLDδ and PLDα1 in abscisic acid-induced stomatal closure in arabidopsis. Plant Physiol **159**: 450–460

Vazquez MM, Casalongué CA, París R (2019) Nitrate reductase mediates nitric oxide-dependent gravitropic response in Arabidopsis thaliana roots. Plant Signal Behav. doi: 10.1080/15592324.2019.1578631

Vicente J, Mendiondo GM, Movahedi M, Peirats-Llobet M, Juan Y ting, Shen Y yen, Dambire C, Smart K, Rodriguez PL, Charng Y yung, et al (2017) The Cys-Arg/N-End Rule Pathway Is a General Sensor of Abiotic Stress in Flowering Plants. Curr Biol **27**: 3183-3190.e4

Viger M, Rodriguez-Acosta M, Rae AM, Morison JIL, Taylor G (2013) Toward improved drought tolerance in bioenergy crops: QTL for carbon isotope composition and stomatal conductance in Populus. Food Energy Secur **2**: 220–236

Vosyka, O., Kottke, N., Balcke, G. U., Clemens, S., & Dietz KJ (2020) Nitric oxide interferes with SUMOylation patterning during heavy metal exposure in Arabidopsis thaliana. Front Plant Sci **11**: 785

Waldie T, Leyser O (2018) Cytokinin targets auxin transport to promote shoot branching. Plant Physiol **177**: 803–818

Wang, Y., & Wu WH (2013) Potassium transport and signaling in higher plants. Annu Rev Plant Biol **64**: 451–476

Wang H-H, Huang J-J, Bi Y-R (2010) Nitrate reductase-dependent nitric oxide production is involved in aluminum tolerance in red kidney bean roots. Plant Sci **179**: 281–288

Wang R, Tischner R, Gutiérrez RA, Hoffman M, Xing X, Chen M, Coruzzi G, Crawford NM Genomic Analysis of the Nitrate Response Using a Nitrate Reductase-Null Mutant of Arabidopsis 1[w]. doi: 10.1104/pp.104.044610

Wang W, Feng B, Zhou J, Tang D (2020) Plant immune signaling: Advancing on two frontiers. J Integr Plant Biol **62**: 2–24

Webb AA, Larman MG, Montgomery LT, Taylor JE, Hetherington AM (2001) The role of calcium in ABA-induced gene expression and stomatal movements. Plant J **26**: 351–62

Weigel, D., & Glazebrook J (2002) Arabidopsis: A Laboratory Manual. Cold Spring Harbor Laboratory Press.

Wendehenne, D., Durner, J., & Klessig DF (2004) Nitric oxide: a new player in plant signalling and defence responses. Curr Opin Plant Biol **7**: 449–455

Wheeler T, von Braun J (2013) Climate Change Impacts on Global Food Security. Science (80-) **341**:

508 LP – 513

Wilkinson JQ, Crawford NM (1991) Identification of the Arabidopsis CHL3 gene as the nitrate reductase structural gene NIA2. Plant Cell **3**: 461–71

Wilkinson JQ, Crawford NM (1993) Identification and characterization of a chlorate-resistant mutant of Arabidopsis thaliana with mutations in both nitrate reductase structural genes NIA1 and NIA2. MGG Mol Gen Genet. doi: 10.1007/BF00281630

Wilkinson S, Davies WJ (2002) ABA-based chemical signalling: the co-ordination of responses to stress in plants. Plant Cell Environ **25**: 195–210

WILSON ID, NEILL SJ, HANCOCK JT (2008) Nitric oxide synthesis and signalling in plants. Plant Cell Environ **31**: 622–631

Xie X, Wang Y, Williamson L, Holroyd GH, Tagliavia C, Murchie E, Theobald J, Knight MR, Davies WJ, Leyser HMO, et al (2006) The Identification of Genes Involved in the Stomatal Response to Reduced Atmospheric Relative Humidity. Curr Biol **16**: 882–887

Xu, G., Fan, X., & Miller AJ (2012) Plant nitrogen assimilation and use efficiency. Annu Rev Plant Biol **63**: 153–182

Xu J, Xing X, Tian Y, Peng R, Xue Y, Zhao W (2015) Transgenic Arabidopsis Plants Expressing Tomato Glutathione S-Transferase Showed Enhanced Resistance to Salt and Drought Stress. 1–16

Xu N, Cheng L, Kong Y, Chen G, Zhao L, Liu F (2024) Functional analyses of the NRT2 family of nitrate transporters in Arabidopsis. Front Plant Sci. doi: 10.3389/fpls.2024.1351998

Yamamoto Y, Negi J, Wang C, Isogai Y, Schroeder JI, Iba K (2015) The transmembrane region of guard cell SLAC1 channels perceives CO2 signals via an ABA-independent pathway in arabidopsis. Plant Cell **28**: 557–567

Yang J, Li C, Kong D, Guo F, Wei H (2020) Light-Mediated Signaling and Metabolic Changes Coordinate Stomatal Opening and Closure. Front Plant Sci. doi: 10.3389/fpls.2020.601478

Yarwood CE (1946) DETACHED LEAF CULTURE.

Yoshida R, Umezawa T, Mizoguchi T, Takahashi S, Takahashi F, Shinozaki K (2006) The regulatory domain of SRK2E/OST1/SnRK2.6 interacts with ABI1 and integrates abscisic acid (ABA) and osmotic stress signals controlling stomatal closure in Arabidopsis. J Biol Chem **281**: 5310–5318

Yu H, Chaimbault P, Clarot I, Chen Z, Leroy P (2019) Labeling nitrogen species with the stable isotope

15N for their measurement by separative methods coupled with mass spectrometry: A review. Talanta **191**: 491–503

Yu X, Sukumaran S, Márton L (1998) Differential Expression of the Arabidopsis Nia1 and Nia2 Genes 1 Cytokinin-Induced Nitrate Reductase Activity Is Correlated With Increased Nia1 Transcription and mRNA Levels.

Zhang G Bin, Meng S, Gong JM (2018a) The expected and unexpected roles of nitrate transporters in plant abiotic stress resistance and their regulation. Int J Mol Sci. doi: 10.3390/ijms19113535

Zhang H, Gannon L, Jones PD, Rundle CA, Hassall KL, Gibbs DJ, Holdsworth MJ, Theodoulou FL (2018b) Genetic interactions between ABA signalling and the Arg / N-end rule pathway during Arabidopsis seedling establishment. Sci Rep 1–12

Zhang H, Zhao Y, Zhu J (2020) Review Thriving under Stress : How Plants Balance Growth and the Stress Response. Dev Cell **55**: 529–543

Zhao C, Cai S, Wang Y, Chen Z-H (2016) Loss of nitrate reductases NIA1 and NIA2 impairs stomatal closure by altering genes of core ABA signaling components in Arabidopsis. Plant Signal Behav **11**: e1183088

Zhao J, Zhang W, da Silva JAT, Liu X, Duan J (2021) Rice histone deacetylase HDA704 positively regulates drought and salt tolerance by controlling stomatal aperture and density. Planta **254**: 79

Zhao M-G, Chen L, Zhang L-L, Zhang W-H (2009) Nitric Reductase-Dependent Nitric Oxide Production Is Involved in Cold Acclimation and Freezing Tolerance in Arabidopsis. PLANT Physiol **151**: 755–767

Zhao M-G, Tian Q-Y, Zhang W-H Nitric Oxide Synthase-Dependent Nitric Oxide Production Is Associated with Salt Tolerance in Arabidopsis 1[OA]. doi: 10.1104/pp.107.096842

Zhou Y, Zhao D, Shuang L, Xiao D, Xuan Y, Duan Y, Chen L, Wang Y, Liu X, Fan H, et al (2020) Transcriptome Analysis of Rice Roots in Response to Root-Knot Nematode Infection. Int J Mol Sci **21**: 848

Zoulias N, Harrison EL, Casson SA, Gray JE (2018) Molecular control of stomatal development. Biochem J **475**: 441–454

Zoulias N, Rowe J, Thomson EE, Dabrowska M, Sutherland H, Degen GE, Johnson MP, Sedelnikova SE, Hulmes GE, Hettema EH, et al (2021) Inhibition of Arabidopsis stomatal development by

plastoquinone oxidation. Curr Biol **31**: 5622-5632.e7

Zulawski M, Schulze G, Braginets R, Hartmann S, Schulze WX (2014) The Arabidopsis Kinome: phylogeny and evolutionary insights into functional diversification. BMC Genomics **15**: 548